

# Gold potential of the Nuuk region based on multi-parameter spatial modelling of known gold showings

Interim report 2004

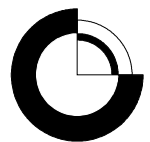
Bo Møller Nielsen, Thorkild M. Rasmussen  
& Agneta Steenfelt



# **Gold potential of the Nuuk region based on multi-parameter spatial modelling of known gold showings**

Interim report 2004

Bo Møller Nielsen, Thorkild M. Rasmussen  
& Agneta Steenfelt



# Contents

<b>Abstract</b>	<b>5</b>
<b>Introduction</b>	<b>6</b>
<b>Study area</b>	<b>7</b>
<b>Outline of geology and known gold showings</b>	<b>8</b>
<b>Statistical approach</b>	<b>9</b>
Selection of data .....	9
Preparation of data.....	9
Pixelation.....	10
Masking data to model area .....	11
Construction of mineral showings groups .....	12
Determination of data signatures .....	12
Likelihood ratio .....	12
Joint likelihood ratio.....	13
Construction of gold potential maps.....	13
<b>Description of input data</b>	<b>14</b>
Gold showings .....	14
Assigning occurrences to pixels .....	15
Geochemical and geophysical data themes.....	16
Geochemical stream sediment data .....	16
Selection of elements .....	17
Gridding (pixelation) .....	21
Regional aeromagnetic data .....	22
<b>Data signatures of gold showings</b>	<b>23</b>
Geochemical signatures.....	23
Aeromagnetic signatures .....	24
<b>Gold potential map</b>	<b>26</b>
<b>Preliminary evaluation of the statistical methods and results</b>	<b>27</b>
Data and methodology .....	27
Grouping of gold showings.....	27
Interpolation .....	27
Pixel size .....	27
Cross-validation .....	28

Comments on favourable areas.....	28
Areas with known gold showings .....	28
Bjørneøen southeast (area A).....	28
Storø west (area C).....	28
Ivisaartoq (area H) .....	29
Isukasia (area K).....	29
New areas without known gold showings .....	30
Bjørneøen north-east (area B) .....	30
Storø east (area D) .....	30
Sermitsiaq (area E) .....	30
Qooqqut (area F).....	30
Ilulialik (area G) .....	30
Ujarassuit Nunaat (area I) .....	31
Northwest of the lake Tussaap Tasia (area J).....	31
North of Alaangua (area L).....	31
Spatial distribution of favourable areas.....	31
<b>Conclusions</b>	<b>34</b>
<b>Recommendations</b>	<b>35</b>
<b>Acknowledgements</b>	<b>37</b>
<b>References</b>	<b>38</b>
<b>Appendix A. Localities with gold-bearing rock samples (above 100 ppb Au)</b>	<b>40</b>
<b>Appendix B. Data</b>	<b>49</b>
<b>Appendix C. Empirical distribution functions</b>	<b>65</b>
<b>Appendix D. Predictive potential map for Au showings in the Nuuk region</b>	<b>153</b>

## Abstract

This report documents the first phase of a statistical multi-parameter spatial analysis of geochemical, geophysical, lithological and topographical data covering a c. 13 700 km<sup>2</sup> region north and east of Nuuk. The investigation in 2004 was carried out jointly between the Geological Survey of Denmark and Greenland and the Bureau of Minerals and Petroleum, government of Greenland with the objective of identifying areas with a high potential for gold mineralisation.

An inventory of localities with gold bearing rock samples in the study area has been made and all information has been stored in a database. Forty-five localities have been identified from which one or more rock samples have yielded gold concentrations above 1 ppm. These localities, termed gold showings, are all hosted by rocks within the greenstone belts of the Nuuk region.

Twenty-nine geochemical and geophysical parameters have been gridded using 200 m x 200 m cells (pixels), and the gold showings are assigned to pixels of the same grid. For each of the parameters, the signal derived at pixels with gold showings was compared with the variation at pixels without showings (the background). Thirteen of the parameters exhibited a statistically significant signal over gold showings, and nine of these were used to calculate a nine-parameter combined signature characterising cells with gold showings.

The final step of the analysis is the construction of a gold potential map, in which the nine-parameter signature at each pixel is ranked and coloured according to the similarity with the nine-parameter signature of the gold showings. In other words, the gold potential map illustrates the predicted favourability for the presence of a gold showing, similar to the known showings, within each pixel.

Almost all of the known gold showings lie within areas ranked as most favourable in the gold potential map, but in addition, two larger and five smaller areas were classified as favourable. With one exception, the favourable areas lie within a 50 km wide and 160 km long NNE-trending tract. The gold potential map presented here is preliminary, and before a more reliable identification of gold potential areas can be achieved, the methodology needs refining and more data sets need to be included. At this stage, however, it is concluded that although some of the favourable areas in the present gold potential map might turn out to reflect artefacts in the interpolation procedure, at least three are regarded as interesting targets for gold exploration because they occur in lithologies resembling those hosting the known gold showings.

# **Introduction**

The Nuuk region contains a number of Archaean greenstone belts, several of which are known to host gold mineralisation. Gold showings have been recognised at a number of discrete localities, and two of these are currently targets for commercial exploration.

The Bureau of Minerals and Petroleum (BMP), government of Greenland, and the Geological Survey of Denmark and Greenland (GEUS) have initiated several projects to investigate the origin and economic potential of the gold mineralisation in the Nuuk region. The studies undertaken include lithology, structure, mineralogy and geochronology aiming at an improved understanding of the greenstone belts, their original depositional environment and plate-tectonic setting, their evolution, the timing of tectonic events, and the character and timing of different phases of hydrothermal alteration.

This report presents preliminary results from one of these projects. The project objective is to determine multi-parameter data signatures for areas with known gold showings using available digital geoscientific and topographic data, and then identify the same signatures outside these areas. The work conducted in 2004 represents the initial phase of the project in which the methodology is applied using regional geochemical and geophysical data. The methods are described, and a preliminary gold potential map for the Nuuk region is presented and discussed. Finally, the report contains recommendations for the continuation of the project.

## Study area

The statistical analysis is performed for data covering the Nuuk region, here defined as the ice-free land between 64°N and 65°23'N. The region contains the capital Nuuk and the large fjord system north-east and east of Nuuk (Fig. 1).

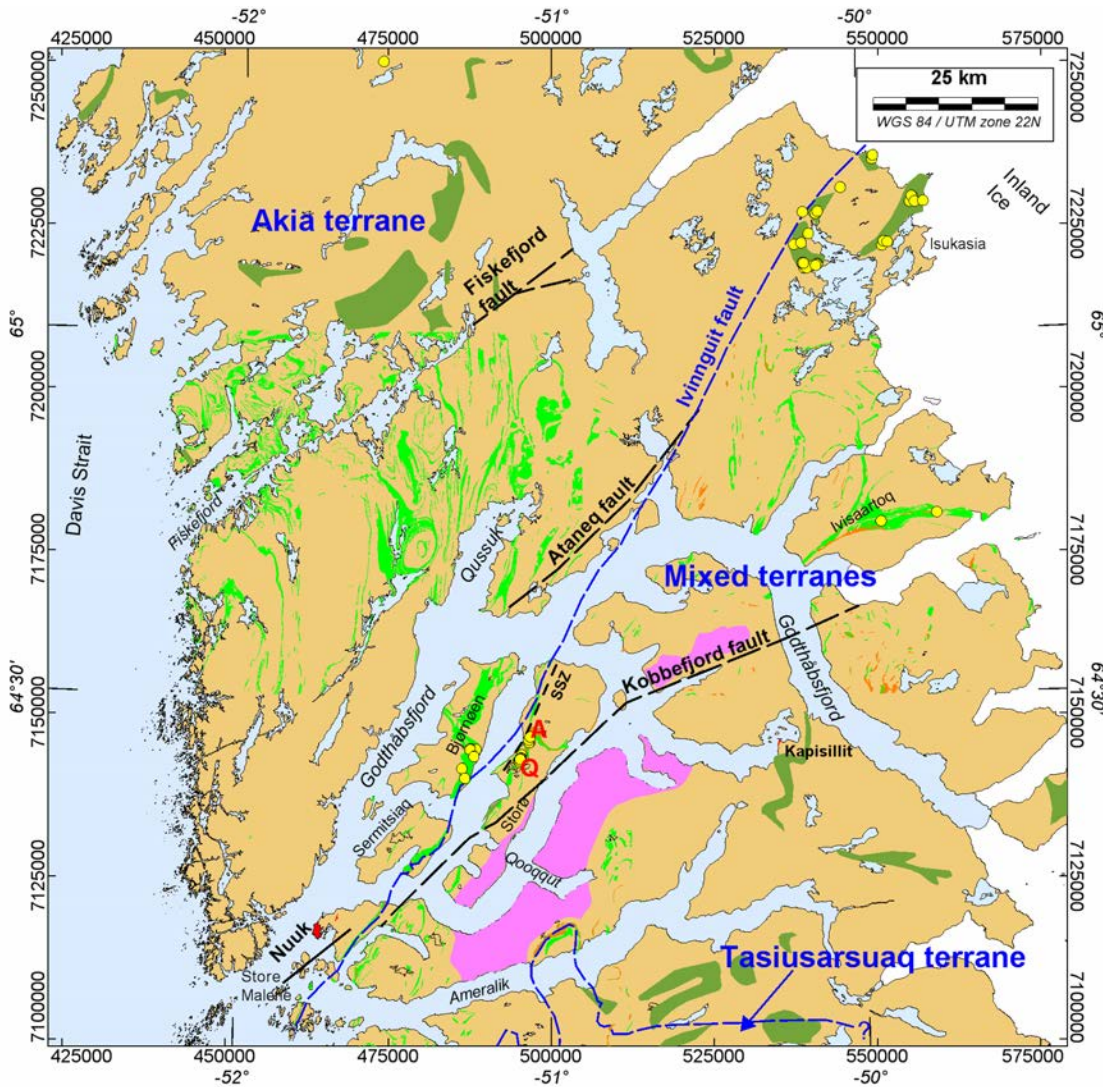


**Figure 1.** Map of the study area showing the distribution of supracrustal rock units in the Nuuk region together with the Qôrquut granite (pink), major terrane boundaries (blue), faults and location of gold showings (yellow dots). The letters Q and A mark the commercial gold prospects, Qingaaq and Aappalaartoq. Used abbreviation: SSZ, Storø shear zone. The outline of supracrustal rocks are from digital versions of the 1:100 000 scale geological maps, Fiskefjord (Garde 1989), Qôrquut (McGregor 1983), and Ivisaartoq (Chadwick & Coe 1988). Amphibolite rock units are shown in light green, metasedimentary rocks in light orange-brown. Outside these three map sheets the supracrustal units are taken from a digital version of the 1:2 500 000 map of Greenland (Escher & Pulvertaft 1995) and are shown in olive green. Gneisses are shown in brown. Misfits between geological features and the coastline in the map are due to different topographical bases. The topographical base used here is a new 1:100 000 base prepared digitally by the Photogeological Laboratory at GEUS from aerial photographs (Hollis et al. 2004).

## Outline of geology and known gold showings

The Nuuk region comprises an intricate assemblage of sections of different continents, terranes, representing different age records within early to late Archaean time. Between the larger Akia terrane to the north and the Tasiussarsuaq terrane to the south, four smaller terranes have been recognised (Friend & Nutman 2005). In a general sense these can be regarded as a series of terranes that have been amalgamated via NW-directed thrusting during the middle to late Archaean, along tectonic boundaries that are now also deformed by later tectonism. Each of the terranes contains greenstone belts intercalated with tonalitic to granodioritic gneiss. The greenstone belts represent remnants of Archaean volcanic and associated magmatic rocks including subordinate chemical and clastic sediments. They were once thought to be dismembered parts of the same supracrustal sequence, but are now known to belong to distinct age groups and probably represent several unrelated belts, occurring both within and between the terranes (see Hollis *et al.* 2004). Recent accounts of the lithology and structure of the greenstone belts are published in Appel *et al.* (2003) and Hollis *et al.* (2004) and these reports contain comprehensive references to earlier and recent work in the area.

The metamorphic grade in the greenstone belts varies from lower to upper amphibolite facies. The most common rock type is amphibolite of tholeiitic to komatiitic composition, but amphibolite of andesitic composition has also been recognised in some belts. Bodies of gabbro and ultramafic rock are commonly associated with the amphibolite. Less common metasedimentary rocks are dominated by garnet-biotite schists. Local enrichment in tourmaline, scheelite or sulphides characterises some of the belts. Current studies, field observations and chemistry (Hollis *et al.* 2004) suggest that the greenstone belts contain rocks formed in oceanic as well as in continental volcanic arc environments.

Several of the greenstone belts are hosts to gold mineralisation, and gold showings have been recognised at a number of discrete localities as shown in Fig. 1, two of which, Qinggaaq and Aappalaartoq, are currently targets for commercial exploration (NunaMinerals 2003) (license number 2002/07 – NunaMinerals A/S). In view of the evidence that the individual gold-hosting greenstone belts may be unrelated, an intriguing question is if all gold showings in the Nuuk region were formed during the same event after the assembling of the terranes. Presently, there are few age constraints on the formation of the gold showings. However, the location of many gold showings in the neighbourhood of regional scale tectonic structures (Fig. 1) (Appel *et al.* 2003; Dave Collar in NunaMinerals 2003) has encouraged the possibility that one or more of the structures have acted as passageways for mineralising fluids. A gold showing is in this report defined as a predefined 200 m × 200 m area in which one or more analysed rock samples has yielded 1 ppm Au or more.

Elevated gold concentrations are most commonly encountered in sulphide-bearing rocks exhibiting quartz veining, silification, carbonatisation or other signs of hydrothermal alteration. Elevated concentrations of one or more of the As, Sb, Ag, Cu, Mo, W, Rb, Cs have been recorded in the auriferous samples, but the suite of associated elements appear to vary among individual gold showings, see Appel *et al.* (2003) and Hollis *et al.* (2004).

## **Statistical approach**

The methods applied to produce a prediction map for gold mineralisation is a robust statistical procedure described by Chung & Keating (2002). The procedure involves spatial analysis of a number of data themes to identify the multi-parameter signature of known gold showings. The results of the analysis are tested quantitatively by cross-validation techniques and justified qualitatively by expert knowledge (e.g. a geologist). The procedure includes not only the determination of quantitative data signatures of the gold showings and the construction of a predictive gold potential map; it also addresses the grouping of gold showings, the probability for making new gold discoveries and the construction of input to conversion of the results to economic terms. The procedure involves a number of statistical tools, such as empirical distribution functions, likelihood ratio functions, joint likelihood ratio functions, ordered statistics and Bayes' conditional probability formulae (Bernardo & Smith 2000). The procedure requires that all data are in digital form and are referred to a common co-ordinate system.

The main steps in the procedure are shown in Fig. 2. Descriptions of some of the functions are given in later sections. In the initial stage of the present project steps 1, 3 and 4 were performed in this work. The remaining steps will be undertaken during future studies.

### **Selection of data**

The principal parameter is the distribution of known gold showings within the study area. The data ideally include a large number of different parameters measured in areas of gold showings, such as lithological, structural, geochemical, geophysical, topographical data. At this initial stage of the investigation we have chosen as input data a number of available digital data covering the Nuuk region, namely regional geochemical and geophysical data. Lithological data are presently not available in digital form for the entire area. The acquisition and treatment of the data are described in later sections.

### **Preparation of data**

The data comprise two types. Gold showings are discrete point data, while the geochemical and geophysical data themes are continuous in the sense that they are represented by a surface based on interpolated values in a regular grid. Continuous refers in this context to the results produced by the interpolation procedure – in reality these data are also discrete data points. Firstly, the original data are sampled data with a non-uniform sampling distance and secondly the results from the interpolation are sampled into a regular grid. It is assumed that the interpolated data functions are sufficiently smooth that they are fully described by the sampled values. If the data density is considered insufficient to produce reliable interpolated results these areas are excluded from the spatial analysis.

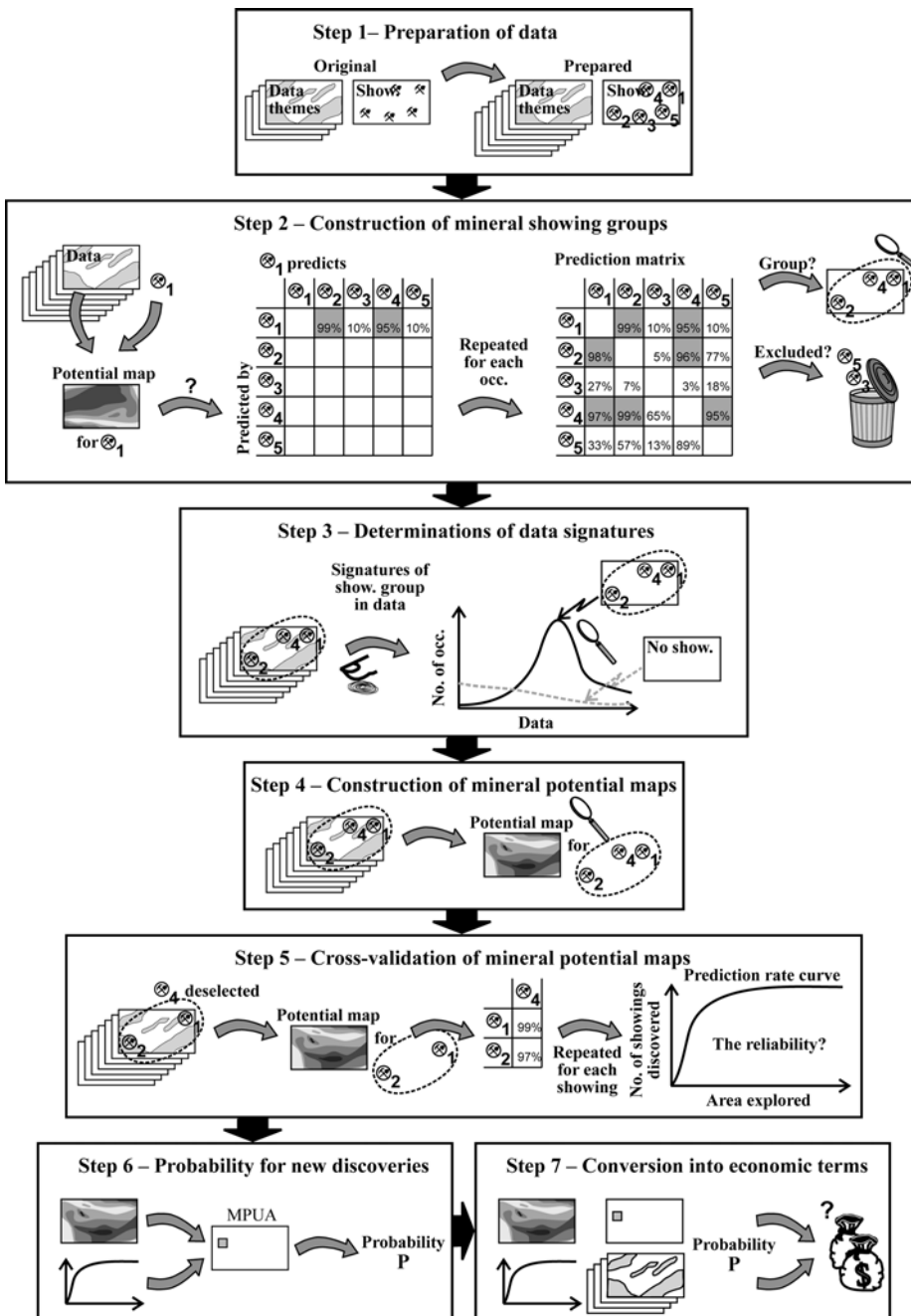


**Figure 2.** Steps in the cross-validated procedure for probabilistic analysis for multi-parameter modelling of geoscientific data types. The abbreviation show. refers to showings.

## Pixelation

Both types of data, gold showings as well as geochemical and geophysical data, must be represented in grids that are equal in size and sampling interval. Each grid cell is termed a pixel, and the value within a pixel is a pixel value. In the case of gold showings, a pixel value will either be 1 (a showing) or 0 (no showing). For the other data themes, the assignment of a value to a particular pixel is done by interpolation between data points for the

variable. In the analysis presented in this report, the pixel size is 200 m x 200 m. The choice of pixel size is discussed in a later section.

## Masking data to model area

The area selected for the statistical analysis, here termed the model area, is defined as the surface containing valid data for all input data, and representing land surface excluding ice caps and large lakes in the 1:100 000 scale topographical map. All input data themes are clipped according to this area.

The masking process used to produce the model area has been: Firstly, only pixels with valid values for all kinds of input data were included. Secondly, data are excluded sea-wards from the outer coastline where islands smaller than 0.5 km<sup>2</sup> are omitted. After this, pixels covered by the Inland Ice or local ice caps are excluded from the study area. Similarly, pixels covered by lakes larger than 5 km<sup>2</sup> are excluded. The resulting study area covers 13 687 km<sup>2</sup> (or 342182 pixels) and is shown in Fig. 3.

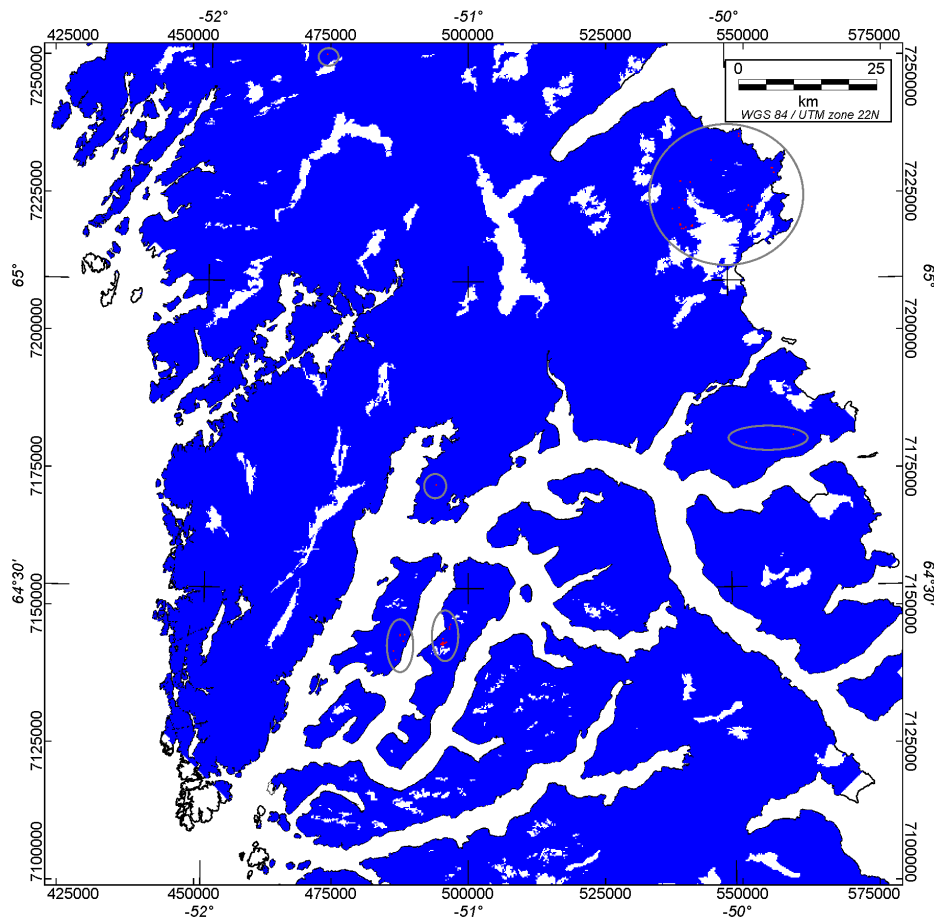


**Figure 3.** The established model area for the statistical analysis is shown by blue colour. Very small red squares indicate the forty-five gold showings used in the statistical analysis. A gold showing is defined as an 200 m x 200 m area in which one or more analysed rock samples has yielded 1 ppm Au or more. As the pixels are very small at the scale used here, grey ovals are used to indicate where they are.

## Construction of mineral showings groups

In the present modelling, all gold showings are treated as one group; hence this step has been omitted. Grouping of gold showings is an important exercise to conduct in the continuation of the project.

## Determination of data signatures

For each data theme the values acquired in pixels with gold showings need to be compared with values for pixels without showings (the 'background signature'). The tool for this comparison is the construction of empirical distribution functions for each of the two pixel groups in a diagram where pixel values are ordered across their range. The original "raw" distribution functions are convolved with a kernel function (Parzen 1962; Scott 1992; Silverman 1986). The shape of the kernel, and especially the bandwidth of the kernel function, determines the shape of the distribution function. The wider the kernel (a large bandwidth), the smoother the distribution function. The bandwidth is also denoted the spread parameter. The final distribution function is found iteratively. The function should not be too 'rough' and not over-smoothed with multi-modalities concealed. The effect of bandwidth is illustrated in the diagrams in Appendix C.

For each data theme, the distribution functions relating to pixels with known showings may be matched with the one for pixels without showings – the background signature – and the significance of the difference can be evaluated. The ratio between the two empirical distribution functions for a specific data theme is called the empirical likelihood ratio function. This ratio ranges from 0 to infinity. To display and evaluate the calculated ratios, they are normalised using the following function: *likelihood ratio* / (1 + *likelihood ratio*). The two distribution functions show the same signature when the normalised likelihood ratio is 0.5. If the normalised ratio is well above 0.7, the empirical distribution function of the showings is said to be significantly different from the background signature.

## Likelihood ratio

The formalised idea of the likelihood function was introduced in Chung *et al.* (2002). Consider a point  $p$  with  $m$  pixel values  $c_1, \dots, c_m$  in the entire study area  $\mathbf{A}$  consisting of two sub-areas, one area  $\mathbf{M}$  with stochastic events present and the remaining area  $\overline{\mathbf{M}}$  where no event is present. Let  $f\{c_1, \dots, c_m | \mathbf{M}\}$  and  $f\{c_1, \dots, c_m | \overline{\mathbf{M}}\}$  be the multivariate frequency distribution functions based on pixels from  $\mathbf{M}$ , and from  $\overline{\mathbf{M}}$ , respectively. Then the likelihood ratio at  $p$  is defined as

$$\lambda_p(c_1, \dots, c_m) = \frac{f\{c_1, \dots, c_m | \mathbf{M}\}}{f\{c_1, \dots, c_m | \overline{\mathbf{M}}\}} \quad [1]$$

$\lambda_p(c_1, \dots, c_m)$  is estimated for every pixel. According to the model, the pixel with the largest estimate is to be considered as the pixel most likely containing ‘event present’. Both discriminant analysis and Bayesian methods can be used to estimate  $\lambda_p(c_1, \dots, c_m)$ . In the current work, only Bayesian methods have been utilised.

### **Joint likelihood ratio**

The joint data signature for pixels with gold showings is the combination of signatures for all individual data themes. This signature is obtained by means of the joint likelihood ratio. It results from the product of the individual likelihood ratios for the variables (geoscientific data themes). In this project, the calculation of joint likelihood ratio has been delimited to include only data themes with significant signatures in pixels with gold showings.

### **Construction of gold potential maps**

When the joint likelihood ratio has been calculated for each pixel, the joint likelihood ratio values are ranked into 200 prediction classes and normalised so that the maximum value is 100%. The gold potential map displays these normalised prediction classes in different colours thereby illustrating the predicted likelihood for the presence of a gold showing within each pixel. Prediction classes greater than 99% correspond to 1% of the entire model area. Areas outlined as favourable according to the prediction classes in the presented analysis will be discussed later in a separate section.

# Description of input data

## Gold showings

Information about sample localities and analytical data has been extracted (September 2004) from the GEUS database GEUSGREEN (Tukiainen & Christensen 2001) and from a scrutiny of all available data reported by exploration companies working in the Nuuk region and adjacent areas (from c. 63°30'N to 65°30'N). The latter include all reports mentioned in Appel *et al.* (2003) and two additional reports on data from Bjørneøen (Skyseth 1998; Smith 1998).

A database has been made containing a record for every locality where rock samples yielding gold concentrations above 50 ppb have been collected. The record holds information about sample type (grab, composite or chip channel samples etc.), rock type, sample site, sample locality, other analytical data and source of information. In total, 525 localities have yielded rock samples with concentrations above 50 ppb Au; 130 of these localities have more than 1 ppm Au. A table containing all the compiled localities with rock samples yielding more than 100 ppb Au (348 localities) is available in Appendix A.

The highest Au concentration reported from the Nuuk region is 106 ppm in a sample of dolomite collected at Isukasia in 1998 within a shear zone cutting a sequence of mafic and ultramafic rocks (pers. com. P. Appel, GEUS). Localities with reported concentrations above 100 ppb are shown in Fig. 4. The accuracy of the location of gold showings used in GIS applications is important and not always satisfactory. Therefore, it is appropriate to evaluate and rank the location data derived from company reports according to their quality, see Appendix A.

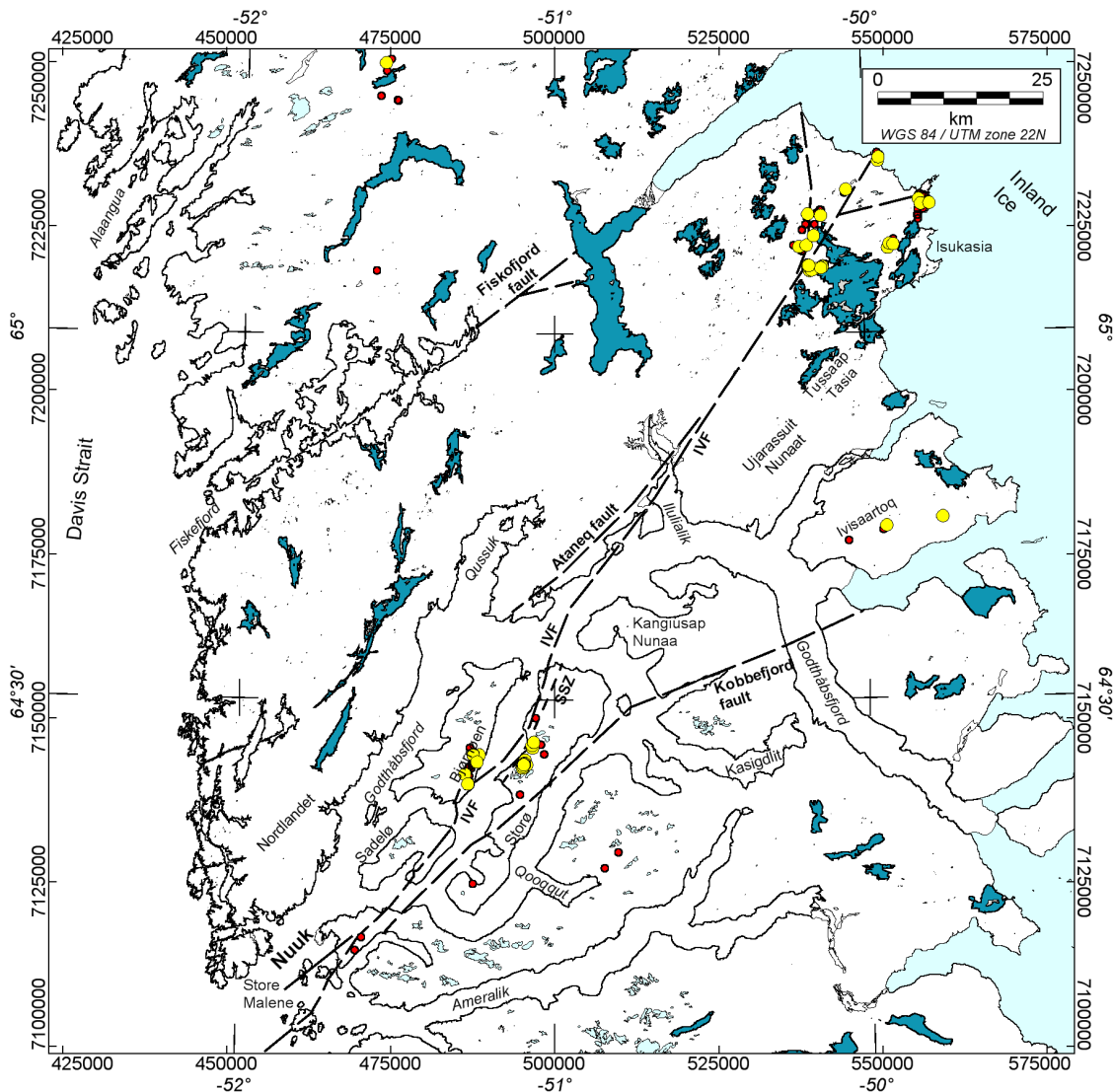


**Figure 4.** Distribution of rock samples with analytical results above or equal to 100 ppb Au indicated by small red dots. Samples with Au above or equal to 1 ppm are indicated by larger yellow dots. Used abbreviations: IVF, Ivinnguit fault; SSZ, Storø shear zone.

### Assigning occurrences to pixels

Gold showings in the statistical modelling are a pixel containing one or more localities with rock samples with Au concentration above 1 ppm (see Appendix A). Results from localities were floats have been collected with more than 1 ppm Au were not included in the construction of showings. Forty-five gold showings within the model area have been defined in this way (Fig. 3). A few gold showings plot within ice caps or lakes; they obviously have erroneous location data, and they are not included in the present spatial analysis. However, if their location can be corrected after inspection of old locality maps and descriptions, they should be included in the next phase of the study.

## **Geochemical and geophysical data themes**

Regional geochemical and geophysical surveys are available as digital data (Appel *et al.* 2003; Steenfelt 2001a). The geochemical data are derived from low-density stream sediment surveys and the geophysical data from aeromagnetic surveys.

### **Geochemical stream sediment data**

Stream sediment samples have been collected from the study area during several campaigns and analysed in batches (Fig. 5, Table 1). The analytical data from these campaigns were used in a compilation of stream sediment data for the entire West and South Greenland presented as a geochemical atlas containing element distribution maps as contoured grid images (Steenfelt 2001a). The compilation of analytical data involved quality control and calibration of data from different campaigns and analytical batches to ensure that the resulting data set is consistent (Steenfelt 1999, 2001b). However, the sampling and compilation of data for the geochemical atlas were designed to outline the large-scale chemical variation, and although the consistency of the data is advantageous, the low sampling density is not ideal for the present study. See Fig. 6 for location of stream sediment data.

Stream sediment samples at higher density were collected in specific areas for uranium and tungsten mineral prospecting purposes (Appel 1989, 1990, 1994; Appel & Garde 1987). Only a few of the samples from these campaigns were included in the “atlas” data set; the remaining samples have only been analysed for a limited number of elements.

For the purpose of the present study, data obtained within the area limited by latitudes 63°30'N and 65°30'N have been selected from the atlas database. New grids have been produced from the selected data using the procedure described below. The new grids were purposely produced to cover a larger area than the actual study area (64°N to 65°15'N) to avoid marginal errors in the grids.

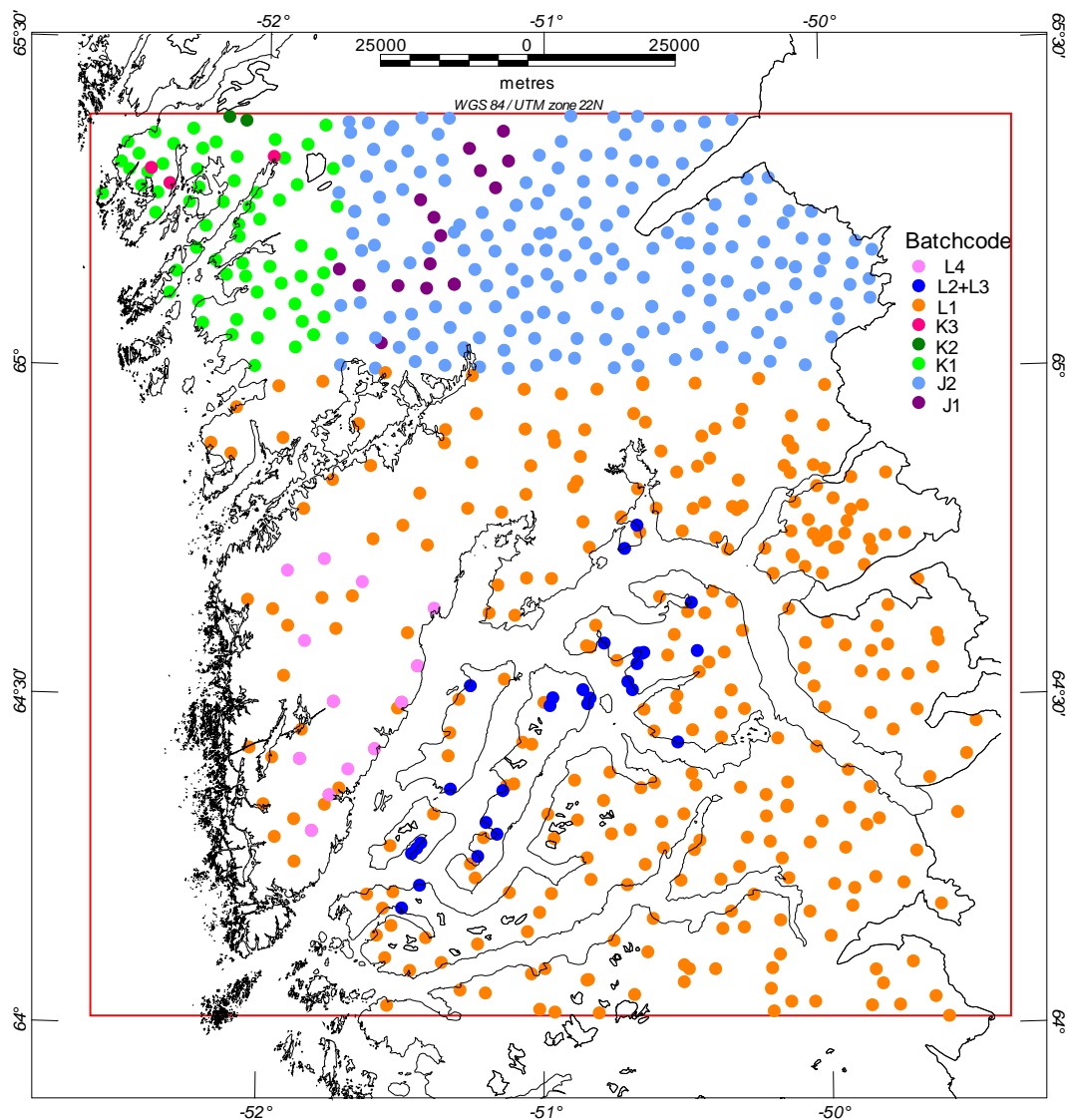


**Figure 5.** Distribution of low-density stream sediment sample localities and colour coding reflecting sample batches analysed as indicated in Table 1.

### Selection of elements

Table 1 shows that the study area comprises data derived from a number of analytical methods. The quality control and data corrections conducted as part of the data compilation for the atlas revealed that some element data from the present study area are not sufficiently reliable to justify their use in the present study. Further, a number of element variations are redundant and hence only one representative, the most reliable, has been chosen for this study. Table 2 presents the available elements and those selected for the present study. Main statistical parameters for the analytical data of the selected elements are given in Table 3.

**Table 1.** Analytical treatment of the less than 0.1 mm grain size fraction of stream sediment samples collected at low density in the Nuuk region.

Batch code	Major elements	Non-calibratable trace elements by INA and DNC				Calibratable trace elements by INA	
		As,Au,Br,Cs, Mo,Sb,Ta,W	Nd,Lu	U	Eu,Yb	Ce,Co,Hf,La,Sc,Sm,Th	
J1, J2	GGU XRF*	Act INA	Act INA	Risø DNC	Act INA	Act INA	
I4, K1, K2	GGU XRF	Act INA	Act INA	Act INA	Act INA	Act INA	
K3	GGU XRF	Act INA	Act INA	Risø DNC	Act INA	Act INA	
L1	GGU XRF*	Act INA	Act INA	B-C INA	Act INA	Act INA	
L2, L3	GGU XRF	Act INA	Act INA	Risø DNC	Act INA	Act INA	
L4	GGU XRF	Act INA	Act INA	Act INA	Act INA	Act INA	

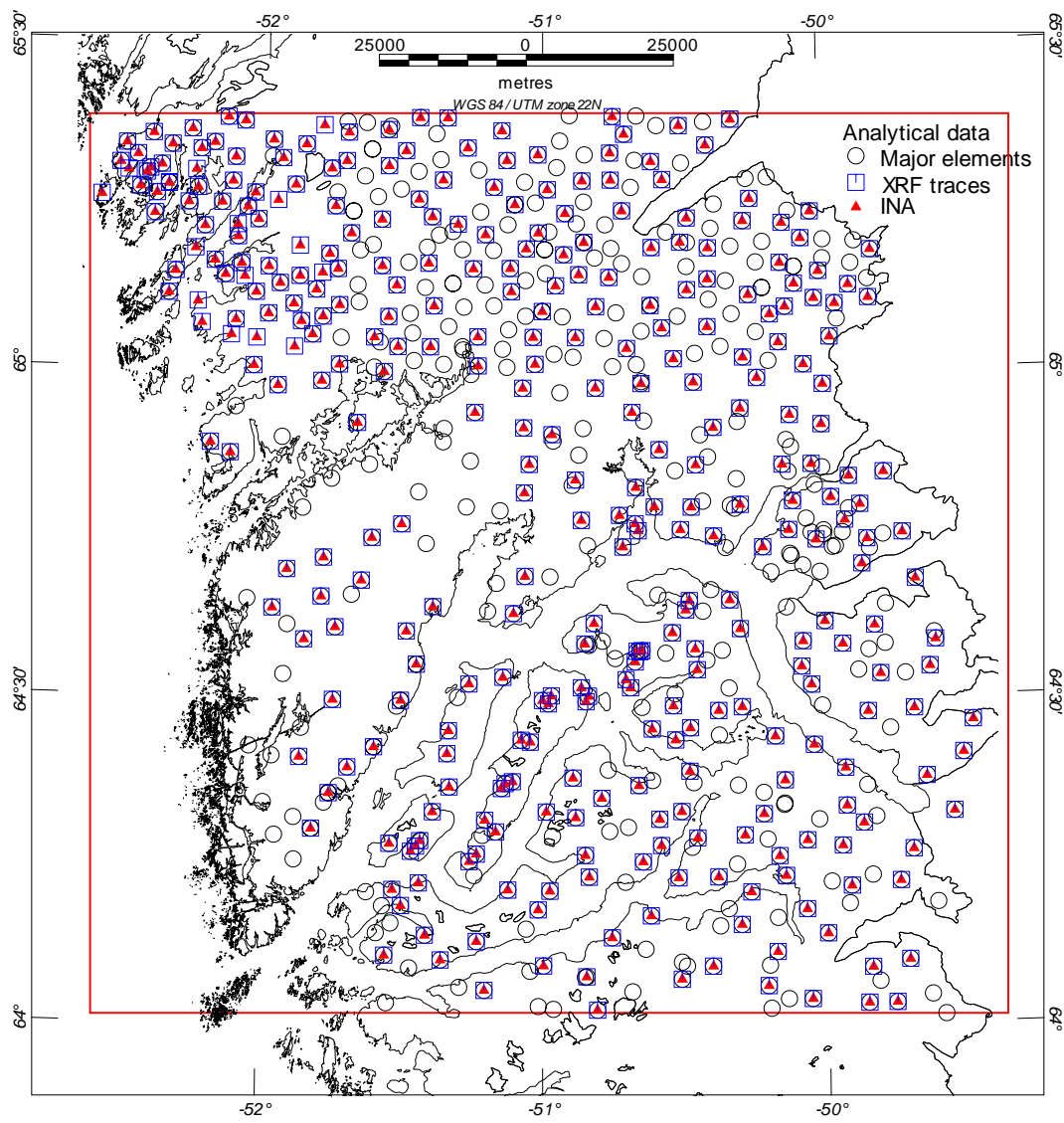
  

Batch code	Calibratable trace elements mainly by XRF							
	Ba,Cr	Ni,Sr	V	Rb,Zn,Zr	Nb	Y	Ga	Cu
J1, J2	GGU XRF*	GGU XRF*	GGU XRF*	Risø XRF*	Risø XRF*	Risø XRF*	Risø XRF*	Risø XRF*
I4, K1, K2	Act XRF	Act XRF	Act XRF	Act XRF	Act XRF	Act XRF	Act XRF	GGU AAS
K3	GGU XRF	GGU XRF	GGU XRF	GGU XRF	Risø XRF*	Risø XRF*	Risø XRF*	GGU AAS
L1	GGU XRF*	GGU XRF*	GGU XRF*	GGU XRF*	GGU XRF (poor)	Act ICP	no data	Act ICP
L2, L3	GGU XRF	GGU XRF	GGU XRF	GGU XRF	Risø XRF*	Risø XRF*	Risø XRF*	GGU AAS
L4	Act XRF	Act XRF	Act XRF	Act XRF	Act XRF	Act XRF	Act XRF	Act XRF

\* analysed without standards

Laboratories: GGU (Geological Survey of Greenland); Act (Activation Laboratories Ltd.); Risø (Risø National Laboratory); B-C (Bondar-Clegg and Co. Ltd.).

Methods: XRF (X-ray Fluorescence Spectrometry); DNC (Delayed Neutron Counting); INA (Instrumental Neutron Activation); ICP (Inductively Coupled Plasma Emission Spectrometry); AAS (Atomic Absorption Spectrometry).



**Figure 6.** Coverage of data derived from different analytical treatments of the 0.1 mm fraction of stream sediment samples within the Nuuk region. For analytical methods, see Table 1.

**Table 2.** Quality of analytical data for stream sediment samples collected in the Nuuk region.  
Gridded data for chemical elements in bold characters are used in the statistical analysis.

Available data		Precision	Comments
<b>Silicon oxide</b>	$\text{SiO}_2$	high	
<b>Titanium oxide</b>	$\text{TiO}_2$	high	
<b>Aluminium oxide</b>	$\text{Al}_2\text{O}_3$	high	
<b>Iron oxide</b>	$\text{Fe}_2\text{O}_3$	high	
<b>Manganese oxide</b>	$\text{MnO}$	high	
<b>Magnesium oxide</b>	$\text{MgO}$	high	
<b>Calcium oxide</b>	$\text{CaO}$	high	
<b>Sodium oxide</b>	$\text{Na}_2\text{O}$	high	
<b>Potassium oxide</b>	$\text{K}_2\text{O}$	high	
<b>Phosphorus oxide</b>	$\text{P}_2\text{O}_5$	medium	
<b>Arsenic</b>	As	unknown	
<b>Gold</b>	Au	unknown	
Barium	Ba	variable, some data not calibratable	
Bromine	Br	high	not considered relevant
Cerium	Ce	medium to low	Redundant to La
Cobalt	Co	medium	Redundant to Ni
Chromium	Cr	high	Combined with Ni
<b>Caesium</b>	Cs	unknown	
<b>Copper</b>	Cu	high	
Europium	Eu	low	
Gallium	Ga	low	
Hafnium	Hf	medium	Combined with Zr
<b>Lanthanum</b>	La	medium	
Lutetium	Lu	low	
Molybdenum	Mo	unknown	Very few concentrations above detection limit
Niobium	Nb	low or unknown	
Neodymium	Nd	low	
<b>Nickel</b>	Ni	high	
<b>Rubidium</b>	Rb	medium	
<b>Antimony</b>	Sb	unknown	
Scandium	Sc	medium	Some problems with calibration
Samarium	Sm	low	
<b>Strontrium</b>	Sr	high	
Tantalum	Ta	unknown	Very few concentrations above detection limit
Terbium	Tb	unknown	Very few concentrations above detection limit
<b>Thorium</b>	Th	medium	
<b>Uranium</b>	U	high	
<b>Vanadium</b>	V	medium	
Tungsten	W	unknown	Very few concentrations above detection limit
Yttrium	Y	low to unknown	
Ytterbium	Yb	low	Some problems with calibration
<b>Zinc</b>	Zn	high	
<b>Zirconium</b>	Zr	medium	Combined with Hf

**Table 3.** Number of available analytical data points and major statistical parameters for selected elements determined in stream sediment samples collected in the Nuuk region. For location see Fig. 6.

unit	det.lim.	No of analyses		Min.	Mean	Max.
		Total	>det.lim.			
SiO <sub>2</sub>	%	0.01	789	all	35.83	65.68
TiO <sub>2</sub>	%	0.01	789	all	0.16	0.57
Al <sub>2</sub> O <sub>3</sub>	%	0.01	789	all	7.63	14.85
Fe <sub>2</sub> O <sub>3</sub>	%	0.01	789	all	0.74	5.40
MnO	%	0.01	789	all	0.03	0.09
MgO	%	0.01	789	all	0.77	2.70
CaO	%	0.01	789	all	2.28	4.63
Na <sub>2</sub> O	%	0.01	789	all	0.13	3.65
K <sub>2</sub> O	%	0.01	789	all	0.46	1.56
P <sub>2</sub> O <sub>5</sub>	%	0.01	789	all	0.02	0.22
As	ppm	2	532	88	0.5	0.96
Au	ppb	5	532	122	0	3.56
Cs	ppm	2	532	154	0.5	1.14
Cu	ppm	5	614	607	5	31
La	ppm	1	532	all	7	46
Ni/Mg	ppm		758	all	3	21
Ni+Cr	ppm		763	all	20	265
Rb	ppm	10	763	757	1	41
Sb	ppm	0.2	532	104	0.1	0.2
Sr	ppm	50	763	all	107	318
Th	ppm	0.5	532	all	1	7.41
U	ppm	0.1	677	606	0.15	5.23
V	ppm	40	763	all	42	83.92
Zn	ppm	20	763	762	1	57.89
Zr (Hf)	ppm	50	804	802	4	398.75
						2358

### Gridding (pixelation)

Prior to gridding, measured concentrations below the lower detection limit (d.l.) of the analytical method have been assigned values equal to half the d.l., except for Au where zero was maintained as minimum (Table 3). The gridding has been performed using the Geosoft software, which offers three different gridding methods. A number of test-runs using different methods, cell sizes and range of influence revealed that when the cell size is very small in relation to the distance between samples, the minimum curvature method appears to give the most reliable results. For reasons given in the former section on pixelation a 200-m cell size has been chosen for this study, and a blanking distance of 10,000 m was used. Appendix B contains contoured and masked images illustrating the produced grids. Inevitably, grids based on elements for which measured concentrations are largely below the detection limit (As, Au, Cs and Sb, Table 3), contain many cells with values below d.l. The calculated variation at such low levels is nonsensical in relation to the true geochemical variation, and grids for these elements have been modified, so that all cell values below d.l. are given the d.l. value (Fig. B2, B3, B5 and B15 in Appendix B).

## **Regional aeromagnetic data**

The magnetic data used in the analysis are from the regional aeromagnetic surveys carried out in the joint GEUS and BMP 'Aeromag 1998' project. Data descriptions and interpretations are found in Appel *et al.* (2003).

The survey was flown with a N-S oriented line spacing of 500 m and nominal altitude above ground of 300 m. Orthogonal tie-lines were flown with a mutual separation of 5000 m. The sampling interval along the lines is approximately 7 m. The data were gridded with a 200 m sampling interval.

In addition to the total magnetic field, a number of derived parameters have been calculated. These are first vertical derivative, horizontal derivatives in four different directions, the amplitude of the horizontal gradient vector and the analytic signal.

Although the derivatives are calculated from the total magnetic field, and as such do not include any additional information, the anomalies expressed by the derivatives are sharper and the attenuated signal enhances short wavelength responses from shallow or subcropping structures. Thereby, they reflect lithological boundaries and faults more clearly than the total magnetic field, which may be advantageous when the data are used in the statistical analysis.

# Data signatures of gold showings

When interpreting the results of the statistical analysis, it is important to keep in mind that the data signatures of showings and the gold potential map do not only reflect the locality of auriferous samples, but also the rocks and overburden within the 200 m x 200 m pixel surrounding these samples.

## Geochemical signatures

Significant enrichment in areas (pixels) with gold showings was found for the elements and ratio: As, Au, Cs, Rb, Th, U and the Ni/Mg ratio. Table 4 documents the degree of enrichment by listing the ranges of element variation found in within and outside pixels with gold showings.

**Table 4.** Overview over the most characteristic signatures for the analysed stream sediment geochemistry data. Red asterisk indicates the data used in the predictive statistical analysis presented in this report.

Geochemical element Regional stream sediment data from GEUS	Range for data signature of gold showings	Range for data signature of background	Significance and remarks
As*	22– 42 ppm As	Below 3 ppm As (modified As grid)	Highly significant
Au*	40–100 ppb Au and 140–220 ppb Au	Below 20–30 ppb Au (modified Au grid)	Highly significant. A bi-modal distribution is observed.
Cs*	3.5–5 ppm Cs and 5.8–6 ppm Cs	Below 2.3 ppm Cs (modified Cs grid)	Highly significant. A bi-modal distribution is observed with the higher range belonging to a small part of the gold showings.
Rb*	60–75 ppm Rb	10–50 ppm Rb	Moderately significant. Some overlap with the background signature exists.
Th*	15–17.5 ppm Th	3–13 ppm Th	Little significance. A bi-modal, or multi-modal distribution is observed. Overlap with the background signature exists.
U*	80–150 ppm U	0–25 ppm U	Highly significant. Some overlap with the background signature exists.
Ni/Mg ratio*	Ratio 30–43	Ratio between 1–35	Moderately significant. Overlap with the background signature exists.

The following elements have no distinct enrichment in pixels with gold showings: Al<sub>2</sub>O<sub>3</sub>, CaO, Fe<sub>2</sub>O<sub>3</sub>, K<sub>2</sub>O, La, MgO, Na<sub>2</sub>O, P<sub>2</sub>O<sub>5</sub>, Sb, SiO<sub>2</sub>, TiO<sub>2</sub>, V, Zr, Zn and Ni + Cr, see Table 5.

**Table 5.** Data variation recorded in pixels with and without gold showings, respectively, for elements showing insignificant signature related to gold showings.

Geochemical element	Range for data signature in pixels with gold showings	Range for background signature	Significance and remarks
$\text{Al}_2\text{O}_3$	Bimodal, 13.5–14.5 % and 15.5–16.5 %	12.5–17 %	Insignificant
$\text{CaO}$	Not different from the background	3–7 %	Insignificant
$\text{Fe}_2\text{O}_3$	Bimodal, 6.5–8.5 % and 10.5–12 %	2–11 %	Insignificant
$\text{K}_2\text{O}$	Not different from the background	0.5–2.5 %	Insignificant
$\text{La}$	Bimodal, 55–75 ppm and 10–15 ppm	15–100 ppm	Insignificant, though the lower range shows a significant signature
$\text{MgO}$	Not different from background	1–7 %	Insignificant
$\text{Na}_2\text{O}$	2.8–3.5 %	3–4.5 %	Insignificant
$\text{P}_2\text{O}_5$	Not different from the background	0–0.5 %	Insignificant
$\text{Sb}$	Not different from the background	0.2–0.6 ppm	Insignificant
$\text{SiO}_2$	Not different from the background	55.0–72 %	Insignificant
$\text{TiO}_2$	Not different from the background	0.3–1.2 %	Insignificant
$\text{V}$	Not different from the background	50–150 ppm	Insignificant
$\text{Zn}$	Not different from the background	20–120 ppm	Insignificant. A shift towards higher Zn values compared to the background signature is observed for the gold showings.
$\text{Zr}$	175–375 ppm	125–1050 ppm	Insignificant
$\text{Ni} + \text{Cr}$	500–700 ppm	80–1200 ppm	Insignificant. A shift towards higher ratios compared to the background signature is observed for the gold showings.

## Aeromagnetic signatures

Both the vertical gradient of the total magnetic field intensity (VG-TMI) and the amplitude of the horizontal gradient of TMI (Amp-Hor-Grad-TMI) show distinct differences in data variation within and outside pixels with gold showings. Maxima in the Amp-Hor-Grad-TMI will tend to be located over abrupt changes in the magnetisation. Thus, this data set emphasises similar structures as the VG-TMI. Horizontal gradients (Hor-Grads-TMI) in different directions also have characteristic signatures for the gold showings. Since the Amp-Hor-Grad-TMI contains information from Hor-Grads-TMI in two orthogonal directions, the individual horizontal gradient data are not included in the construction of a predictive mineral potential map. Total magnetic field intensity (TMI) itself yields no significant data signature for the gold showings. The range of the significant aeromagnetic signatures for the gold showings and the background are given in Table 6.

**Table 6.** Overview over the variation in processed aeromagnetic data within and outside pixels with gold showings. Red asterisk indicates the data used in the predictive statistical analysis presented in this report.

Aeromagnetic data - Regional aeromagnetic data from GEUS	Range for data sig- natures found to be characteristic for gold showings	Range for back- ground signature	Significance and remarks
<b>VG-TMI*</b>	-0.35 – -0.55 nT/m and 0.45 – 0.75 nT/m	-0.3 – 0.4 nT/m	Highly significant. Bi-modal distribution.
<b>Amp-Hor-Grad_TMI*</b>	0.45 – 1.0 nT/m	0.0 – 0.4 nT/m	Highly significant
<b>Hor-Grad-North</b>	-3.6 – 2.9 nT/m and -1.2 – -0.7 nT/m	-0.5 – 0.5 nT/m	Highly significant
<b>Hor-Grad-Northwest</b>	-3.6 – -2.7 nT/m and -1.4 – -0.6 nT/m	-0.5 – 0.5 nT/m	Highly significant
<b>Hor-Grad-East</b>	0.4 – 0.7 nT/m	-0.3 – 0.4 nT/m	Highly significant – though the characteristic data signature is only for a limited number of the showings.
<b>Hor-Grad-Southeast</b>	-1.6 – -1.3 nT/m, -0.9 – -0.5 nT/m and 0.3 – 0.6 nT/m	-0.4 – 0.4 nT/m	High significant – though the characteristic data signature is only for a limited number of the showings.
<b>TMI</b>	-400 – 400 nT	-400 – 800 nT	Insignificant

## Gold potential map

A predictive potential map for the gold showings was constructed as described in a previous section using data with statistically significant signatures relating to pixels with gold showings (see Table 4 and 6). The map is preliminary in nature as it is based on a limited set of input data, but it does illustrate the capacity of the method. More data and evaluation of data is warranted before the method can be regarded fully developed, and before a reliable and verified result can be obtained.

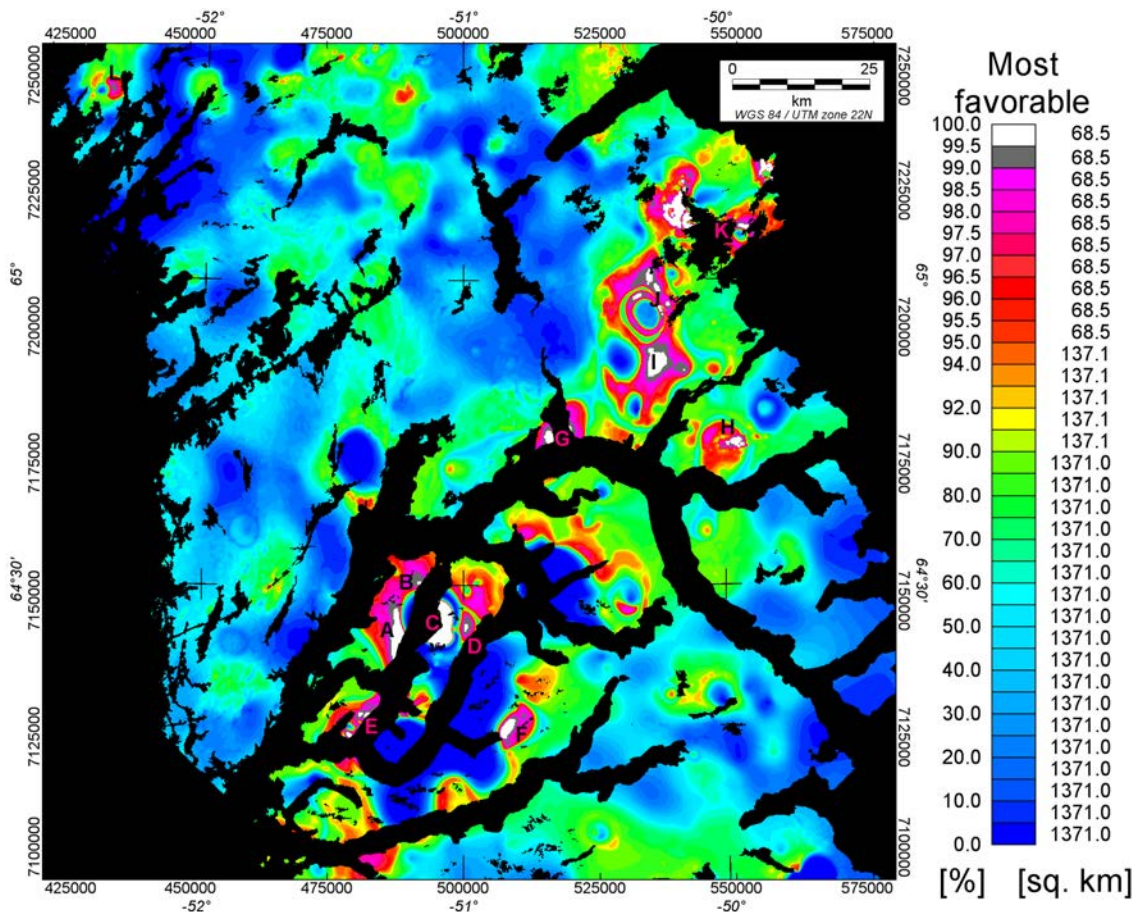


**Figure 7.** Predictive potential map for gold showings for the model area based on 45 known gold showings and 12 different regional geoscientific data themes: seven geochemical and five geophysical (Table 4 and 6). Individual areas of highest probability for gold (shown in white) are marked with letters. The white areas represent the 68.5 km<sup>2</sup> most favourable area, grey colouring the next 68.5 km<sup>2</sup> most favourable area. Areas outlined as favourable are discussed in a later section. An enlarged version of the map is included in Appendix D in order to facilitate more detailed studies.

# Preliminary evaluation of the statistical methods and results

## Data and methodology

### Grouping of gold showings

For simplicity, all gold showings have been treated as one group in this work. However, the fact that some empirical distribution functions exhibit more than one peak indicates that the gold showings fall into more than one group. This will be analysed in the continuation of the project.

### Interpolation

The input data used in the construction of the mineral potential map are all interpolated spatially and sampled into a regular grid. The original sampling density of the magnetic field is sufficiently high to ensure that most field variations are properly described by the grid values. By contrast, interpolation of geochemical data is a much more difficult task. Among the reasons for these difficulties is that geochemical anomalies are not necessarily continuous variations and the initial sampling density is insufficient to describe the actual variations. Most probably the grids of interpolated geochemical data are overly smoothed representations of the true variations. The problems involved in the interpolation of the input data create some spurious anomalies in the final map of the mineral potential. Some concentric circular anomalies in the anomaly map with adjacent high and low values can safely be regarded as an artefact related to the interpolation procedure. The results of the statistical analysis must be viewed critically. These should be considered as input to an interpretation of the gold showings in the region, which also include an evaluation of the data and other sources of both qualitative and quantitative information. Furthermore, it is important to keep in mind, that the results so far only outline different potentials for gold showings; the probability for new discoveries has not been estimated.

### Pixel size

Choosing an appropriate pixel size is difficult because of the small size of the target and the variable resolutions provided by the input data themes. The geochemical data has the lowest resolution with up to 10 km between data points. The aeromagnetic data has a line spacing of 500 m and 7-m interval between data points along lines. The gold showings themselves are hosted in structures commonly less than 5 m wide and 100 m long. A large pixel size, e.g. 5 km x 5 km, would ensure a high degree of reliability in the signal of each pixel, but target areas with favourable gold signal would be unreasonably large for follow-

up. In addition, a larger pixel size would imply that significant features in high-resolution data, such as the magnetic data, are weakened or completely removed. A very small pixel size increases the number of pixels with values that are far from real data points and therefore more or less fictitious.

The pixel size we have chosen (200 m x 200 m) is a compromise allowing us to perform the analysis and to give us a preliminary result. In the next phase of the project, we will examine the effect of changing pixel size as well as different interpolation algorithms.

## Cross-validation

The reliability of the results should always be evaluated by cross-validation when a prediction is carried out. Several statistical techniques are available for this. One approach is to test if an omitted showing can be predicted by the remaining showings.

## Comments on favourable areas

The areas outlined as having the highest probability of hosting gold showings (yellow transparent colouring in Fig. 8, here termed favourable areas) cover 137 km<sup>2</sup> in total. It is not surprising that areas immediately surrounding known gold showings are predicted as favourable, i.e. the areas marked A, C, H, and K in Fig. 8. A more interesting result is that seven other areas, i.e. B, D, E, F, G, I and J are identified as favourable areas. All areas are commented in the following.

## Areas with known gold showings

### Bjørneøen southeast (area A)

Nunaoil A/S has investigated several scattered gold bearing localities in this area (max 4 ppm Au, Skyseth 1998; Smith 1998). The gold mineralised rocks are found locally in two rusty siliceous, garnitiferous, graphitic and pyritic mica schist bands, up to 8 m thick, mostly conformable with the foliation in the enclosing amphibolites. The ore minerals comprise pyrite, together with pyrrhotite, minor chalcopyrite and traces of native copper occurs disseminated, typically with 5–10 vol. per cent (description based on fieldwork by the first author and B. Thomassen, GEUS, pers. com. 2004). Greenstone units on Bjørneøen further to the southwest are not outlined as favourable. Noticeably, Nunaoil A/S has also investigated this area in detail and has not found any gold mineralisation. A local and small Pb-Zn mineral showing is located here.

### Storø west (area C)

The showings at these two places have been investigated in detail by Nunaoil A/S and Nu-naMinerals A/S (Dunnells 1995; Era-Maptec 1995; Grahl-Madsen 1994; Skyseth 1997;

Skytseth 1998; Smith 1998; Trepka-Bloch 1995). NunaMinerals A/S is presently undertaking an exploration and diamond drilling-programme at these localities.

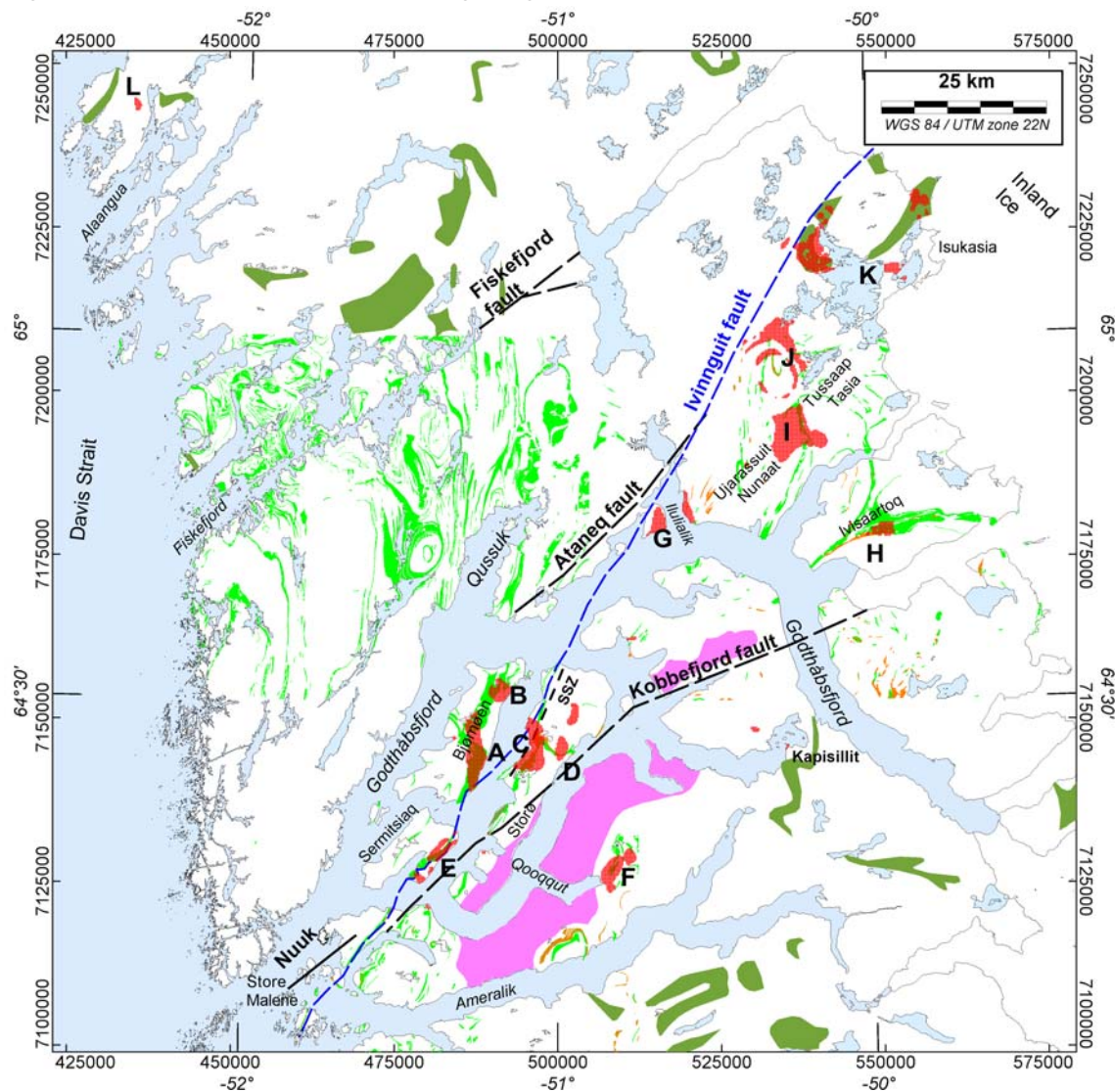


**Figure 8.** Predictive potential map for gold showings for the model area with the outlined 1 percent most favourable area ( $137 \text{ km}^2$ ) for gold showings (Fig. 7) shown in transparent red on top of the simplified geology (see Fig. 1 for colour explanation). However, all gneisses have been coloured white (shown in brown in Fig. 1) in order to enhance the potential areas. The predicted potential areas are based on the same data as Fig. 7. Only lakes above  $5 \text{ km}^2$  are shown.

### Ivisaartoq (area H)

Several gold showings have been located in mafic metavolcanic rocks at Ivisaartoq (Appel et al. 2003; Downes & Gardinev 1986, and pers. com. P. Appel, GEUS, 2004).

### Isukasia (area K)

One large and a few small areas outlined as favourable within the Isua Greenstone Belt coincide with well-known gold showings. However, one favourable area located just south

of the southern part of the Isua greenstone belt (to the right of **K** in Fig. 7 and 8) falls outside known greenstone units and known gold mineralisation.

## New areas without known gold showings

### **Bjørneøen north-east (area B)**

A small favourable area (**B** in Fig. 7 and 8) lies near the coast towards north-east of Bjørneøen. The area is situated just east of the greenstone belt that is a continuation of the gold bearing rocks on southern Bjørneøen, and thus a gold potential appears likely.

### **Storø east (area D)**

A small area indicated as favourable for gold showings is located east of the large area around the known showings (north of **D** in Fig. 7 and 8). Their location is not far from the Kobbefjord fault, but on the other hand they are outside the Storø greenstone belt, and a close inspection of the data structure for these areas is advised.

### **Sermitsiaq (area E)**

Four small areas are outlined as favourable for gold showings at the southern peninsula of Sermitsiaq. The two southern areas are located within gneiss, whereas the northern areas are located partly in gneiss and partly in greenstone units (Hollis *et al.* 2004). Gold concentrations in the range of 0.1 ppm have been recorded in rock samples from this part of Sermitsiaq (Dunnells 1995 and pers. com. H. Stendal, GEUS); one of these localities is located right in the middle of the northernmost of the four favourable areas. Recent geological mapping has indicated that the greenstone belt on Sermitsiaq can be correlated with the gold mineralised Bjørneøen greenstone belt (Hollis *et al.* 2004).

### **Qooqqut (area F)**

An area outlined as favourable is situated near a greenstone belt east of the inner part of the fjord Qooqqut (**F** in Fig. 7 and 8). Nunaoil A/S reports three rock samples from this area with gold values above 200 ppb (Dunnells 1995). One sample is from a silicified amphibolite with 5 vol.% pyrrhotite at contact with a N–S trending pegmatite contained 210 ppb Au. One sample is from a rusty stained silicate facies iron formation and quartz veins with traces of pyrite and contained 210 ppb Au. The third sample is silicified calc-silicate altered amphibolite with disseminated pyrrhotite that contained 380 ppb Au. The favourable area at Qooqqut is located within mapped amphibolite units with a high content of ultramafic rock bodies (McGregor 1983).

### **Ilulialik (area G)**

Two favourable areas are located at the inlet to the Ilulialik fjord arm at the south-orientated branch of the Godthåbsfjord (**G** in Fig. 7 and 8). The western area is located partly on the eastern side of a large anorthosite body within Nûk gneisses with inclusions of amphibolites

(Chadwick & Coe 1988). The eastern area is located in Nûk gneisses with metasedimentary constituents (Chadwick & Coe 1988).

#### **Ujarassuit Nunaat (area I)**

One large and one much smaller area to the east are outlined as favourable at Ujarassuit Nunaat (**I** in Fig. 7 and 8). The area covers a greenstone unit that is correlated with gold bearing greenstone units at Ivisaartoq (Friend & Nutman 2005).

#### **Northwest of the lake Tussaap Tasia (area J)**

Several small favourable areas are located northwest of the lake Tussaap Tasia (**J** in Fig. 7 and 8). These areas are located within the same terrane as the gold bearing Isua Greenstone Belt.

#### **North of Alaangua (area L)**

The small isolated area in the northwestern corner of the study area just north of the inner part of the fjord Alaangua (**L** in Fig. 7 and 8) is the only of the favourable areas that lies far away from the terrane boundaries and faults. Amphibolite sequences are indicated on the geological map just south of the area (Allaart 1982).

### **Spatial distribution of favourable areas**

The spatial distribution of favourable areas suggests the existence of a regional tract favourable for gold showings. This is particularly obvious in a map showing areas with above 90% probability of hosting gold showings (Fig. 9 and 10). The NNE-trending tract of favourable areas across the Nuuk region also embraces the known gold showings as well as geochemical gold anomalies, and the entire zone or tract has previously been suggested to have a potential for gold mineralisation (e.g. Appel *et al.* 2003; Hollis *et al.* 2004; NunaMinerals 2003).

The NNE-trend is common to the general orientation of greenstone belts in this area and to the regional faults as well as to the distribution patterns of most of the individual geochemical and geophysical data themes with characteristic signatures over gold showings (Appendix B and C).

Although the NNE-trend has been recognised as a qualitative feature possibly reflecting the distribution of gold mineralisation, the multi-parameter modelling presented in Fig. 9 can be considered a first approach toward a quantitative definition of a ‘favourable gold tract’. However, the model needs careful evaluation before it can be established with certainty whether the ‘tract’ reflects properties related to the gold showings themselves or to their surroundings environment (the rocks of the greenstone belts).

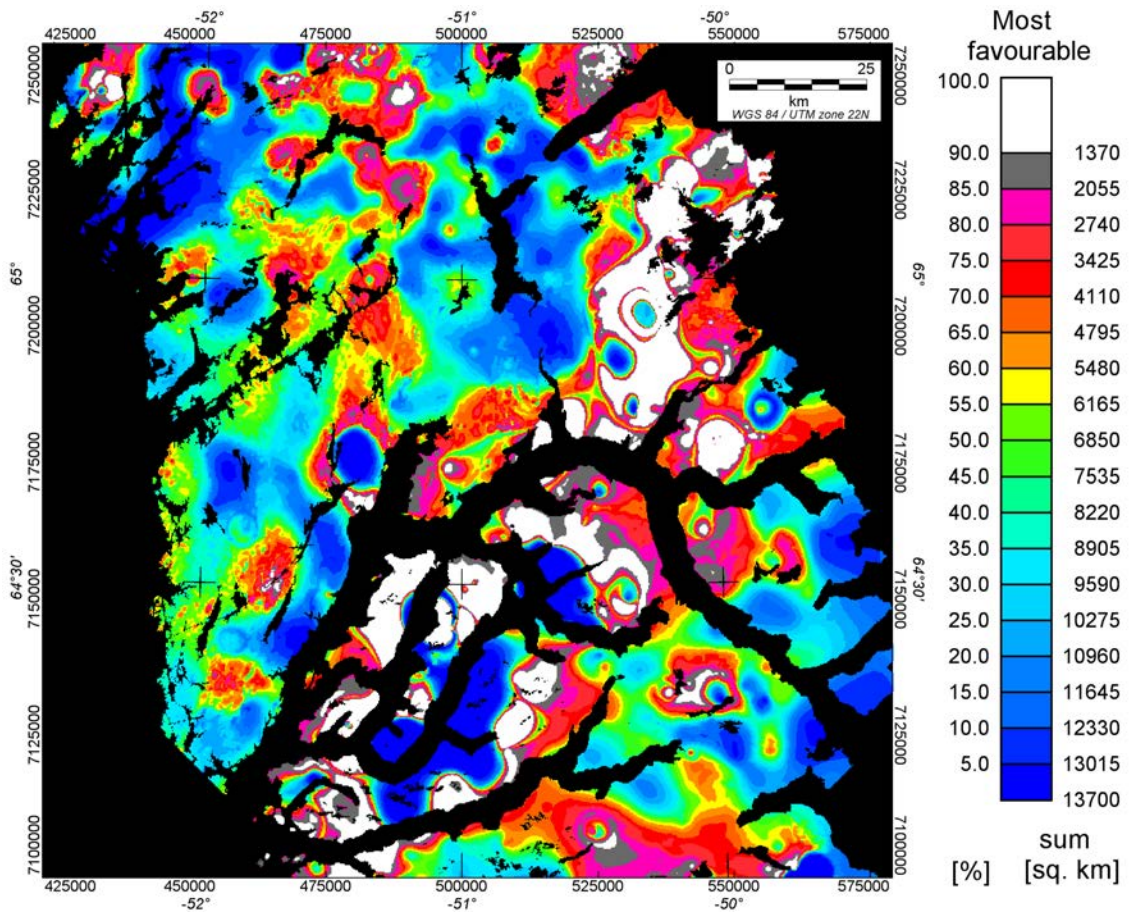


**Figure 9.** Predictive potential map for gold showings for the model area with the 10% most favourable area ( $1370 \text{ km}^2$ ) in white colour. The map is based on 45 known gold showings and 9 geoscientific input data themes: 7 geochemical components from fine fraction regional stream sediment geochemistry, and 2 from regional aeromagnetic data (see Table 4 and 6).

The gold tract is characterised by a sharp northern boundary, which in the western part of the Nuuk region follows the Godthåbsfjord and in the eastern part is sub-parallel the course of the regional faults.

Areas covered by the Qôrput granite complex and areas mapped as being dominated by granite sheets and pegmatites belonging to the complex (McGregor 1983) are all outlined as having a low favourability for gold showings. These areas are excluded from the tract presented in Fig. 10.

The southern boundary of the tract is more irregular and the gold tract stretches more to south than defined in previous work (e.g. Appel *et al.* 2003; Hollis *et al.* 2004; NunaMinerals 2003). However, many of the favourable areas, which are stretching to the south, fall within known greenstone units (Allaart 1982; McGregor 1983).

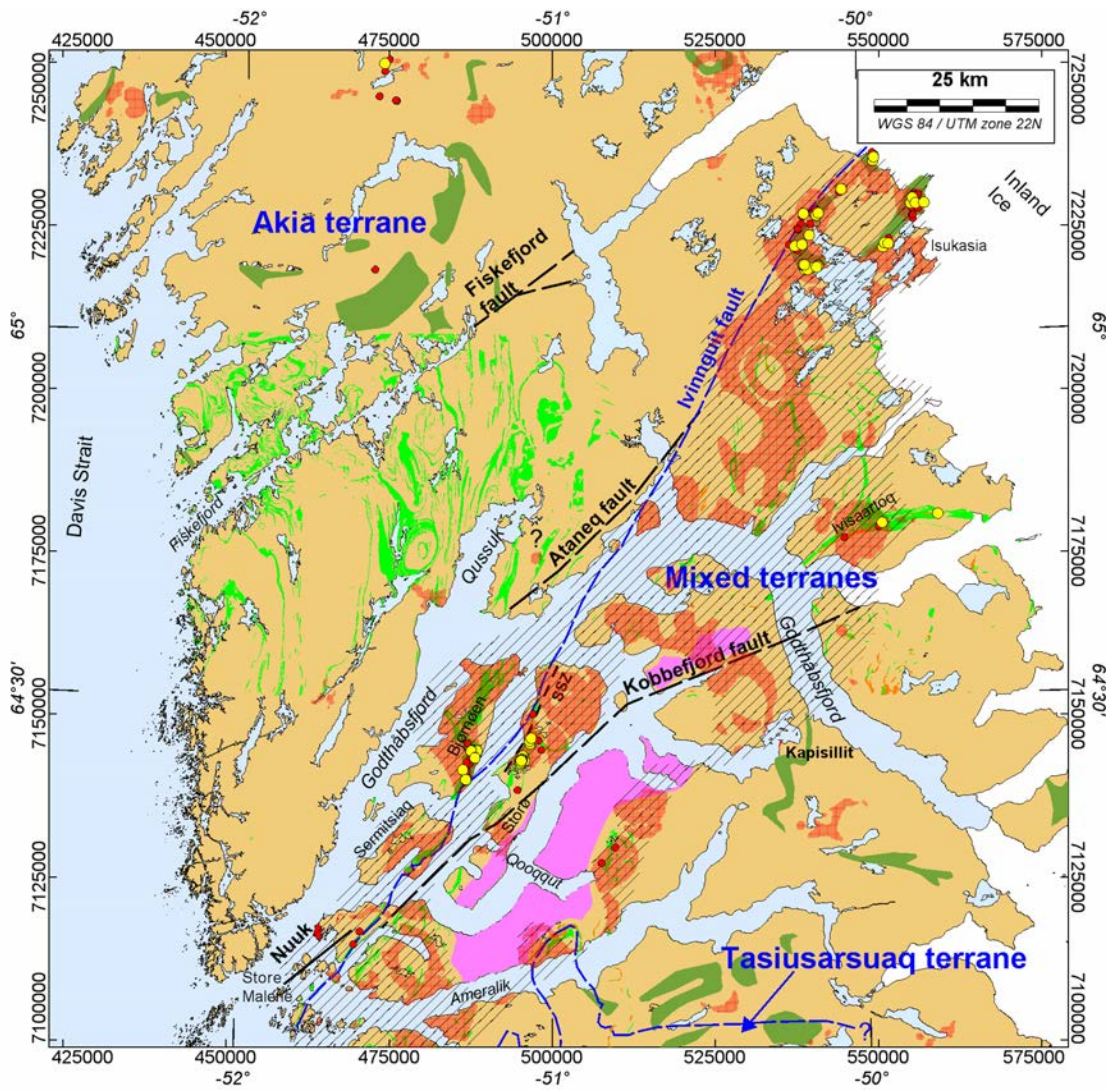


**Figure 10.** Simplified outline of the Nuuk gold tract (hatched area) defined by the 10% most favourable areas (Fig. 9) shown in transparent red on top of the simplified geology of the region (Fig. 1). Distribution of rock samples with analytical results above or equal to 100 ppb Au is indicated by small red dots. Samples with Au above or equal to 1 ppm are indicated by larger yellow dots. Only lakes above 5 km<sup>2</sup> are shown.

## Conclusions

A statistical multi-parameter modelling of geoscientific data that enables identification of data signatures pertaining to gold showings and construction of a gold potential map have been undertaken in the Nuuk region.

Areas containing gold showings proved to have data signatures distinct from the background for 11 out of 29 analysed geochemical and geophysical data sets included in the statistical analysis.

The data ranges of significant signatures for the gold showings are generally characterised by:

- High content of As, Au, Cs, Rb, Th, U, and Ni/Mg ratio in stream sediment geochemistry.
- Large negative and/or positive vertical and horizontal gradients of the total magnetic field intensity, and high positive amplitude of horizontal gradients of the total magnetic field intensity.

Using the combined signature from the nine data sets found to be significant for the known gold showings, the statistical method was able to identify five known and seven new areas as having a high probability of hosting gold showings. Almost all outlined areas fall within mapped greenstone units and gold bearing rock samples have been reported from many of these areas. No rock samples with more than 1 ppm Au have been reported from the new areas. It must be emphasised that the input data behind the favourable areas must be evaluated qualitatively before any follow-up is undertaken.

According to the results of the multi-parameter modelling, illustrated by a gold potential map, a 40 km wide and 160 km long NNE-trending tract is prospective for gold. The tract embraces the main tectonic features within and between the Archaean terranes of the Nuuk region.

# Recommendations

Though interesting results already have been archived through the project, several tasks remain to be done before a fully reliable multi-parameter modelling of gold showings in the Nuuk region has been reached. Considerations on future tasks remaining are given below.

## ***Data input***

More types of geoscientific input data should be included in the statistical analyses; both new input data derived from the types treated so far and from completely new types. Examples of some of the input data, which can be included and tested in future analysis, are given in Table 7.

Furthermore, experiments with the representation of the different input data should be made. For example: so far in the project, the stream sediment geochemistry data have been treated as interpolated and continuous data. However, it can be argued that geochemical stream sediment data should be treated as a non-conservative field; either as discrete point data or as interpolated data obtained from small independent areas with discontinuities at boundaries between adjacent drainage areas. Similarly, the dependence on the predictive results from different gridding techniques and artificial patterns caused uneven sampling of stream sediment geochemistry data should be investigated and minimised.

## ***Grouping of gold showings***

All gold showings in the current work have been treated as one uniform group of showings. This assumption may impact on the resulting predictive potential map. Consequently, it should be tested if it is justified to treat the showings as one group, or if it is required to divide the showings into several groups. Furthermore, it is also likely, that some of the gold showings do not have signatures in common with other showings.

The dissimilarities in signatures among the showings can be tested statistically. Such a test enables a division of showings into different groups and the exclusion of showings that does not have a common signature with other showings.

## ***Probabilistic models***

In the present work, a likelihood ratio model has been used as the probabilistic model; joint likelihood ratio functions from individual likelihood ratio functions for each input data theme at each pixel have been used. These calculations are made according to the Bayesian Theorem (Bayes 1763; Bernardo & Smith 2000) under the assumption of conditional independences (Agterberg *et al.* 1990; Bonham-Carter 1994; Chung *et al.* 2002; Duda *et al.* 1976; Heckerman 1985; Spiegelhalter 1986).

In future work, other probabilistic models such as Fuzzy logic model, weight-of-evidence model, logistic and linear models and Bayesian predictive discriminate model should be utilized and results from the different models should be compared.

### Cross-validation

The reliability of the predictive mineral potential maps should be tested using cross-validation techniques in order to ensure that the results are reliable.

**Table 7.** Overview of input data sets that ought to be considered in future statistical analysis.

Type	Data name	Description
Geological	1:500k Geological Map	Digital geological map at scale 1:500 000 (if/when available)
	1:100k Geological map	Digital geological map at scale 1:100 000 (for selected areas, if/when available)
Geochemical	New data sets derived from regional fine fraction stream sediment data	Besides testing some of the elements and element ratios not included so far, results from principal component analyses and tri-plots could be included. Considering that Ni/Mg ratios are found indicative for gold showings, e.g. the signatures of Cr alone, Cr/Mg ratio and Cr+Ni/Mg ratio should also be tested. The signature of Co and Mn, which can be regarded as indicator elements for metakomatiitic lithologies, should also be investigated.
	Detailed fine fraction stream sediment data	Reported company stream sediment data from exploration activities in the Nuuk region comprise a data set, which is much more detailed than the regional stream sediment data collected by GEUS. Besides including released publicly available data stored at GEUS, the possibility to include non-released data from companies presently active in the Nuuk region should be considered if these companies agree to make their data available.
	Heavy mineral content	Geochemistry of heavy mineral content from stream sediments and possibly also soil samples should be included (the number of samples available is uncertain).
Geophysical	Aero-radiometric radiation	Airborne radiometric data from 1975 and 1976 (Tukiainen et al. 2003).
	Ground radiometric gamma radiation	Measurements of the ground radiometric gamma radiation have been made at almost each locality where GEUS has collected a stream sediment samples.
	New data sets derived from region aeromagnetic data	From further processing of the regional aeromagnetic data new types of information should be extracted.
	Regional gravity data sets	Combined gravity grids of airborne and ground gravity measurements.
Topography	Digital terrain model	A digital terrain model should be made from new 1:100K topography.
Combined geological, structural, morphological and geophysical data	Distance to lineaments	Maps showing the distance to lineaments (lithological boundaries, faults, topographical depressions and linear features in geophysical data)
	Distance to faults	Maps showing the distance to confirmed faults
	Lithodiversity	Maps showing the relative diversity in lithology types

### Probability for making new gold discoveries

It is not sufficient to outline the areas with the highest favourability for gold showings – the probability for actually making a new discovery should also be addressed in order to provide useful results for exploration and decision-making. A probability estimation based on prediction rate curves from cross-validation is given in Chung et al. (2002).

### Conversion into economic terms

In order to provide the public with useful and easily understandable results, a conversion into socio-economic terms should be considered. Mineral potential maps and the probability for making new discoveries can possibly be used as input in socio-economic models.

## Acknowledgements

The reported study is the result of a project jointly financed by the Bureau of Minerals and Petroleum (BMP) and the Geological Survey of Denmark and Greenland (GEUS). The authors wish to thank Else Moberg and Mette Svane Jørgensen at GEUS for their technical support in data preparation. Other colleagues at GEUS working in the Nuuk region and staff at BMP are thanked for providing valuable contributions.

## References

- Agterberg, F.P., Bonham-Carter, G.F. & Wright, D.F. 1990: Statistical pattern integration for mineral exploration. In: Merriam, D.F. (ed.): Computer Applications in Resources Estimation, Prediction and Assessment of Metals and Petroleum, 1–21. New York, U.S.: Pergamon Press.
- Allaart, J.H. 1982: Geological map of Greenland, 1:500 000, Frederikshåb Isblink - Søndre Strømfjord, sheet 2. Copenhagen: Geological Survey of Greenland.
- Appel, P.W.U. 1989: Investigations of heavy mineral concentrates from stream sediment samples collected during the period 1982 to 1986 in the Nuuk area, West Greenland. Rapport Grønlands Geologiske Undersøgelse **89/1**, 17 pp.
- Appel, P.W.U. 1990: Tungsten mineralization in the Nuuk region, West Greenland. Open File Series Grønlands Geologiske Undersøgelse **90/4**, 51 pp.
- Appel, P.W.U. 1994: Strata-bound scheelite in altered Archaean komatiites, West Greenland. Mineralium Deposita **29**, 341–352.
- Appel, P.W.U. & Garde, A.A. 1987: Stratabound scheelite and stratiform tourmalinies in the Archaean Malene supracrustal rocks, southern West Greenland. Bulletin Grønlands Geologiske Undersøgelse **156**, 26 pp.
- Appel, P.W.U., Garde, A.A., Jørgensen, M.S., Moberg, E., Rasmussen, T.M., Schjøth, F. & Steenfelt, A. 2003: Economic potential of the greenstone belts in the Nuuk area. Danmarks og Grønlands Geologiske Undersøgelse Rapport **2003/94**, 137 pp.
- Bayes, T. 1763: Essay towards solving a problem in the doctrine of chances. By the late Rev. Mr. Bayes, F.R.S. communicated by Mr. Price, in a letter to John Canton, A.M.F.R.S. Philosophical Transactions of the Royal Society of London **53**, 370–418.
- Bernardo, J. & Smith, A.F.M. 2000: Bayesian theory, 586 pp. New York, U.S.: Wiley.
- Bonham-Carter, G.F. 1994: Geographic information systems for geoscientists - modelling with GIS, 398 pp. New York: Pergamon.
- Chadwick, B. & Coe, K. 1988: Geological map of Greenland, 1:100 000, Ivisártoq 64 V.2 Nord. Copenhagen: Geological Survey of Greenland.
- Chung, C. & Keating, P.B. 2002: Mineral potential evaluation based on airborne geophysical data. Exploration Geophysics **33**, 28–34.
- Chung, C.F., Fabbri, A.G. & Chi, K.H. 2002: A strategy for sustainable development of non-renewable resources using spatial prediction models. In: Fabbri, A.G. (ed.): Deposit and geoenvironmental models for resource exploitation and environmental security, 101–117. Dordrecht, Netherlands: Kluwer Academic Publishers.
- Downes, M.J. & Gardinev, W.W. 1986: Report of field work - 1985: Greenland tungsten project, 32 pp., 6 app., 25 plates. Kidd Creek Mines Ltd. Exploration division (in archives of the Geological Survey of Denmark and Greenland, GEUS Report file 20036).
- Duda, R.O., Hart, P. & Nilsson, N. 1976: Subjective Bayesian methods for rule-based inference systems. In: Proceedings of the 1976 national Computer conference, 1075–1082.
- Dunnells, D. 1995: Mineral exploration in the Malene concession and Nuuk Fjord region, southern West Greenland: July-August 1995, 30 pp., 5 app., 10 plates. NunaOil A/S (in archives of Geological Survey of Denmark and Greenland, GEUS Report File 21457).
- Era-Maptec 1995: Structural analysis of the Quingat gold prospect, Storø, Nuuk Fjord, West Greenland. Field report prepared for NunaOil A/S., 16 pp. NunaOil A/S (in archives of Geological Survey of Denmark and Greenland, GEUS Report File 21452).
- Escher, J.C. & Pulvertaft, T.C.R. 1995: Geological map of Greenland, 1:2 500 000. Copenhagen, Denmark: Geological Survey of Greenland.
- Friend, C.R.L. & Nutman, A.P. 2005: New pieces to the Archaean terrane jigsaw puzzle in the Nuuk region, southern West Greenland: steps in transforming a simple insight into a complex regional tectonothermal model. Journal Geological Society, London **162**, 147–162.
- Garde, A.A. 1989: Geological map of Greenland, 1:100 000, Fiskefjord 64 V.1 Nord. Copenhagen: Geological Survey of Greenland.

- Grahl-Madsen, L. 1994: Storø gold project, Southwest Greenland 1994. Internal report, 20 pp., 7 app., 16 plates. NunaOil A/S (in archives of Geological Survey of Denmark and Greenland, GEUS Report File 21413).
- Heckerman, D. 1985: Probabilistic interpretation for MYCIN's certainty factors. In: Lemmer, J.F. (ed.): Uncertainty in Artificial Intelligence, 167–196. New York, U.S.: Elsevier.
- Hollis, J.A., van Gool, J.A.M., Steenfelt, A. & Garde, A.A. 2004: Greenstone belts in the central Godthåbsfjord region, southern West Greenland. Danmark og Grønlands Geologiske Undersøgelse Rapport **2004/110**, 110 pp., 1 DVD.
- McGregor, V.R. 1983: Geological map of Greenland, 1:100 000, Qôrqu 64 V.1 Syd. Copenhagen: Geological Survey of Greenland.
- NunaMinerals 2003: Nuuk Fjord. A gold province in West Greenland NunaMinerals A/S Internal report. NunaMinerals A/S (available from NunaMinerals A/S, P.O. Box 790, DK-3900 Nuuk, Greenland).
- Parzen 1962: On estimation of a probability density function and mode. Annals of Mathematical Statistics **33**, 1065–1076.
- Scott, D.W. 1992: Multivariate Density Estimation: Theory, Practice, and Visualization, 336 pp. New York, U.S.: John Wiley & Sons, Inc.
- Silverman, B. 1986: Density estimation in statistics and data analysis, 176 pp. London, U.K.: Chapman and Hall/CRC Press.
- Skyseth, T. 1997: Gold exploration on Storø 1996 South west Greenland, Exploration Licence 13/97 (former 02/92), 14 pp., 12 app., 3 plates. NunaOil A/S [21564 temporary report] (in archives of Geological Survey of Denmark and Greenland, GEUS Report File 21565).
- Skyseth, T. 1998: Gold and base metal exploration on Bjørneø and Sermitsiaq, Nuukfjord, South West Greenland, 1997, 21 pp. NunaOil A/S (in archives of Geological Survey of Denmark and Greenland, GEUS Report File 21648).
- Skytseth, T. 1998: Gold exploration on Storø 1997, South West Greenland, 25 pp., 5 app., 3 plates. NunaOil A/S (in archives of Geological Survey of Denmark and Greenland, GEUS Report File 21601).
- Smith, G.M. 1998: Geology and mineral potential of the Bjørneøen supracrustal belt, Nuukfjord, West Greenland, 13 pp. NunaOil A/S (in archives of Geological Survey of Denmark and Greenland, GEUS Report File 21649).
- Spiegelhalter, D. 1986: A statistical view of uncertainty in expert systems. In: Gale, W. (ed.): Artificial Intelligence and Statistics, 17–56. Reading, UK: Addison Wesley.
- Steenfelt, A. 1999: Compilation of data sets for a geochemical atlas of West and South Greenland based on stream sediment surveys 1977 to 1997. Danmarks og Grønlands Geologiske Undersøgelse Rapport **1999/41**, 33 pp.
- Steenfelt, A. 2001a: Geochemical atlas of Greenland - West and South Greenland. Danmarks og Grønlands Geologiske Undersøgelse Rapport **2001/46**, 39 pp.
- Steenfelt, A. 2001b: Calibration of stream sediment data from West and South Greenland. A supplement to GEUS report 1999/41. Danmarks og Grønlands Geologiske Undersøgelse Rapport **2001/47**, 43 pp.
- Trepka-Bloch 1995: Gold exploration Storø 1995, 19 pp., 8 plates. NunaOil A/S (in archives of Geological Survey of Denmark and Greenland, GEUS Report File 21823).
- Tukiainen, T. & Christensen, L. 2001: GimmeX database relateret til GEUS' nummersystem for geologiske prøver fra Grønland. Danmark og Grønlands Geologiske Undersøgelse Rapport **2001/132**, 28 pp., 1 plate.
- Tukiainen, T., Rasmussen, T.M., Secher, K. & Steenfelt, A. 2003: Restored digital airborne radiometric data from surveys flown in 1975 and 1976 by GGU between 63° and 69°N. Danmarks og Grønlands Geologiske Undersøgelse Rapport **2003/37**, 9 pp., 5 maps.

## Appendix A. Localities with gold-bearing rock samples (above 100 ppb Au)

**Table A1.** Compiled localities with rock samples yielding more than 100 ppb Au. The sources of the localities are given in the column ‘Source’. ‘Original site nomination’ refers to the sample or locality number given in the source. The references of the sources are given in the end of appendix A. GEUSGREEN refers to localities that originate from the GEUS database of that name. This database is used to store sample information from fieldwork conducted by the Survey. The GEUSGREEN data was extracted September 2004. In the column is GEUSGREEN followed by the name of the Survey geologist how have collected the sample. ‘Original site nomination’ refers to the locality or sample number given in the sources. The geographical coordinates are given in datum WGS84 as decimal degrees. The coordinates have been transformed into this form if other datum or UTM were used in the source. The number given in the column ‘Quality of position’ is explained in Table A2.

Original site nomination	Longitude	Latitude	Quality of position	Au [ppb]	Sample type	Source
803	-51.263228	64.409770	6	110	Grab	Downes, M. J. & Gardinev, W. W. 1986
517	-50.059764	64.715649	6	225	Grab	Downes, M. J. & Gardinev, W. W. 1986
539	-49.937710	64.735369	6	1420	Grab	Downes, M. J. & Gardinev, W. W. 1986
130704	-51.069236	64.430777	8	754	Float	Christiansen, O. 1992
130728	-51.067442	64.434805	8	3460	Float	Christiansen, O. 1992
309980	-51.069403	64.437045	8	641	Grab	Christiansen, O. 1992
111358	-51.070007	64.433854	7	46420	Grab	Grahl-Madsen, L. 1994
106920	-51.090346	64.410862	7	36669	Chip	Grahl-Madsen, L. 1994
106921	-51.090346	64.410862	7	32681	Chip	Grahl-Madsen, L. 1994
106916	-51.091299	64.410502	7	32181	Composite grab	Grahl-Madsen, L. 1994
106974	-51.090015	64.411391	7	24205	Chip	Grahl-Madsen, L. 1994
106966	-51.091428	64.411731	7	19611	Scree	Grahl-Madsen, L. 1994
106963	-51.091428	64.411731	7	10697	Scree	Grahl-Madsen, L. 1994
106924	-51.090658	64.411211	7	9497	Chip	Grahl-Madsen, L. 1994
106928	-51.090014	64.411095	7	6563	Scree	Grahl-Madsen, L. 1994
106965	-51.097346	64.407079	7	6274	Scree	Grahl-Madsen, L. 1994
106904	-51.093833	64.417195	7	5649	Scree	Grahl-Madsen, L. 1994
106926	-51.090014	64.411095	7	5275	Chip	Grahl-Madsen, L. 1994
106923	-51.090658	64.411095	7	5148	Chip	Grahl-Madsen, L. 1994
106964	-51.096702	64.406963	7	5056	Scree	Grahl-Madsen, L. 1994
108461	-51.071657	64.437559	7	4980	Grab	Grahl-Madsen, L. 1994
106967	-51.094500	64.412035	7	4614	Chip	Grahl-Madsen, L. 1994
106922	-51.091300	64.410807	7	4177	Chip	Grahl-Madsen, L. 1994
106973	-51.088727	64.410746	7	4177	Composite grab	Grahl-Madsen, L. 1994
304827	-51.269000	64.434200	6	331	Grab	Dunnells, D. 1995
304829	-51.252100	64.427600	6	284	Composite grab	Dunnells, D. 1995
304840	-51.283800	64.398000	6	2363	Grab	Dunnells, D. 1995
305713	-51.109800	64.370300	6	178	Composite grab	Dunnells, D. 1995
305716	-50.843100	64.269700	6	210	Composite grab	Dunnells, D. 1995
305718	-50.800200	64.291400	6	240	Scree	Dunnells, D. 1995
305719	-50.800200	64.291400	6	380	Scree	Dunnells, D. 1995
195302	-50.157073	65.147877	9	112	Composite grab	Bliss, Ian & Palmer, David 1997
195557	-49.812488	65.180751	9	106	Composite grab	Bliss, Ian & Palmer, David 1997

195561	-49.810801	65.173495	9	248	Composite grab	Bliss, Ian & Palmer, David 1997
196162	-50.181773	65.121427	9	127	Grab	Bliss, Ian & Palmer, David 1997
196246	-50.226078	65.119600	9	141	Trench	Bliss, Ian & Palmer, David 1997
196280	-50.182251	65.157843	9	130	Composite grab	Bliss, Ian & Palmer, David 1997
196440	-50.208027	65.117271	9	1050	Composite grab	Bliss, Ian & Palmer, David 1997
196465	-49.915599	65.120295	9	284	Composite grab	Bliss, Ian & Palmer, David 1997
196507	-49.902169	65.126691	9	251	Composite grab	Bliss, Ian & Palmer, David 1997
196534	-49.819837	65.185249	9	139	Composite grab	Bliss, Ian & Palmer, David 1997
197461	-50.205542	65.113723	9	141	Composite grab	Bliss, Ian & Palmer, David 1997
219931	-51.254000	64.423833	9	541	Composite grab	Heilmann, A. 1997
219937	-51.254500	64.425000	9	236	Composite grab	Heilmann, A. 1997
219938	-51.239000	64.424333	9	2910	Composite grab	Heilmann, A. 1997
220214	-51.277333	64.381500	9	189	Composite grab	Heilmann, A. 1997
220229	-51.274167	64.384667	9	661	Composite grab	Heilmann, A. 1997
220231	-51.275833	64.385000	9	592	Composite grab	Heilmann, A. 1997
220232	-51.273833	64.384500	9	153	Composite grab	Heilmann, A. 1997
220239	-51.272833	64.382667	9	585	Composite grab	Heilmann, A. 1997
215365	-49.758140	64.746530	9	3840	Composite grab	Bliss, I. 1998A
219514	-51.101349	64.409902	9	6380	Composite grab	Skyseth, T. 1997
219516	-51.103437	64.408374	9	1790	Composite grab	Skyseth, T. 1997
219517	-51.103567	64.408764	9	286	Composite grab	Skyseth, T. 1997
219518	-51.101953	64.409006	9	111	Composite grab	Skyseth, T. 1997
219519	-51.101446	64.409276	9	7550	Composite grab	Skyseth, T. 1997
219520	-51.099925	64.407414	9	147	Composite grab	Skyseth, T. 1997
219522	-51.095786	64.411989	9	4010	Composite grab	Skyseth, T. 1997
219525	-51.098149	64.411171	9	125	Composite grab	Skyseth, T. 1997
219527	-51.095894	64.411951	9	7340	Composite grab	Skyseth, T. 1997
219528	-51.095848	64.411971	9	795	Composite grab	Skyseth, T. 1997
219551	-51.095720	64.411998	9	3530	Composite grab	Skyseth, T. 1997
219552	-51.095894	64.411951	9	344	Composite grab	Skyseth, T. 1997
219553	-51.095851	64.411933	9	1850	Composite grab	Skyseth, T. 1997
219554	-51.095275	64.412240	9	4390	Composite grab	Skyseth, T. 1997
219556	-51.097011	64.411326	9	214	Composite grab	Skyseth, T. 1997
219558	-51.095371	64.412136	9	18400	Composite grab	Skyseth, T. 1997
219559	-51.095346	64.412140	9	11000	Composite grab	Skyseth, T. 1997
219560	-51.095220	64.412338	9	387	Composite grab	Skyseth, T. 1997
219562	-51.095245	64.412337	9	2230	Composite grab	Skyseth, T. 1997
219565	-51.095062	64.412436	9	100	Composite grab	Skyseth, T. 1997
219570	-51.095708	64.411712	9	257	Composite grab	Skyseth, T. 1997
219572	-51.095730	64.411835	9	651	Composite grab	Skyseth, T. 1997
219636	-51.101430	64.406242	9	4120	Composite grab	Skyseth, T. 1997
220028	-51.033870	64.425507	9	823	Composite grab	Skyseth, T. 1997
220055	-51.065654	64.437086	9	480	Composite grab	Skyseth, T. 1997
220056	-51.065654	64.437086	9	605	Composite grab	Skyseth, T. 1997
220116	-51.043946	64.438549	9	298	Composite grab	Skyseth, T. 1997
221019	-51.069515	64.436923	9	131	Composite grab	Skyseth, T. 1997
221031	-51.069192	64.435961	9	115	Composite grab	Skyseth, T. 1997
221032	-51.069192	64.435961	9	633	Composite grab	Skyseth, T. 1997
221154	-51.093467	64.404461	9	157	Composite grab	Skyseth, T. 1997
221216	-51.060836	64.474956	9	106	Composite grab	Skyseth, T. 1997
222301	-51.097775	64.410991	9	8060	Composite grab	Skyseth, T. 1997

215182	-50.199370	65.111610	9	687	Composite grab	Bliss, I. & Palmer, D. 1998
106201	-50.184689	65.088570	9	401	Chip	Bliss, I. 1998B
106234	-50.186409	65.147881	9	191	Composite grab	Bliss, I. 1998B
106239	-50.212700	65.116669	9	269	Scree	Bliss, I. 1998B
106295	-50.148689	65.163757	9	110	Chip	Bliss, I. 1998B
106323	-50.197281	65.140099	9	539	Grab	Bliss, I. 1998B
106324	-50.197842	65.140587	9	225	Grab	Bliss, I. 1998B
106425	-49.909740	65.121147	9	104	Float	Bliss, I. 1998B
106427	-49.821411	65.166611	9	134	Grab	Bliss, I. 1998B
106454	-49.810040	65.170822	9	426	Grab	Bliss, I. 1998B
106459	-49.813309	65.181351	9	492	Scree	Bliss, I. 1998B
106462	-49.949001	65.233879	9	1559	Grab	Bliss, I. 1998B
106467	-50.148972	65.162560	9	145	Grab	Bliss, I. 1998B
108490	-50.161758	65.089310	9	110	Grab	Bliss, I. 1998B
108751	-50.196941	65.116028	9	480	Chip	Bliss, I. 1998B
108764	-49.920361	65.114662	9	8948	Grab	Bliss, I. 1998B
112111	-49.950142	65.232819	9	541	Composite grab	Bliss, I. 1998B
112112	-50.174679	65.084412	9	3206	Grab	Bliss, I. 1998B
112220	-50.163288	65.086960	9	133	Grab	Bliss, I. 1998B
112221	-50.158531	65.085579	9	398	Grab	Bliss, I. 1998B
112295	-49.915070	65.120438	9	1554	Composite grab	Bliss, I. 1998B
112315	-49.942261	65.241859	9	556	Composite grab	Bliss, I. 1998B
112352	-49.826981	65.174263	9	1693	Float	Bliss, I. 1998B
112358	-49.813709	65.181198	9	226	Scree	Bliss, I. 1998B
112359	-49.819199	65.185822	9	130	Composite grab	Bliss, I. 1998B
112360	-49.819199	65.185822	9	391	Scree	Bliss, I. 1998B
112381	-49.803520	65.167297	9	158	Chip	Bliss, I. 1998B
112388	-49.942829	65.241043	9	221	Chip	Bliss, I. 1998B
112392	-49.951839	65.245293	9	119	Chip	Bliss, I. 1998B
112419	-49.946232	65.238602	9	2887	Chip	Bliss, I. 1998B
112462	-50.140209	65.163033	9	122	Composite grab	Bliss, I. 1998B
112463	-50.135799	65.167442	9	156	Scree	Bliss, I. 1998B
112469	-50.053680	65.195030	9	117	Composite grab	Bliss, I. 1998B
112470	-50.053680	65.195030	9	1359	Composite grab	Bliss, I. 1998B
112471	-50.053680	65.195030	9	241	Composite grab	Bliss, I. 1998B
112474	-50.059891	65.190659	9	283	Composite grab	Bliss, I. 1998B
195302	-50.157073	65.147877	9	112	Composite grab	Bliss, I. 1998B
195557	-49.812488	65.180751	9	106	Composite grab	Bliss, I. 1998B
195561	-49.810801	65.173495	9	248	Composite grab	Bliss, I. 1998B
196162	-50.181773	65.121427	9	127	Grab	Bliss, I. 1998B
196198	-49.823031	65.158809	9	163	Composite grab	Bliss, I. 1998B
196246	-50.226078	65.119600	9	141	Trench	Bliss, I. 1998B
196280	-50.182251	65.157843	9	130	Composite grab	Bliss, I. 1998B
196307	-50.180258	65.090488	9	32200	Composite grab	Bliss, I. 1998B
196308	-50.180956	65.090725	9	401	Composite grab	Bliss, I. 1998B
196309	-50.179842	65.090227	9	215	Composite grab	Bliss, I. 1998B
196369	-50.132953	65.088791	9	258	Composite grab	Bliss, I. 1998B
196440	-50.208027	65.117271	9	1050	Composite grab	Bliss, I. 1998B
196465	-49.915599	65.120295	9	284	Composite grab	Bliss, I. 1998B
196499	-49.820990	65.153646	9	219	Composite grab	Bliss, I. 1998B
196500	-49.820990	65.158646	9	522	Composite grab	Bliss, I. 1998B

196507	-49.902169	65.126691	9	251	Composite grab	Bliss, I. 1998B
196534	-49.819837	65.185249	9	139	Composite grab	Bliss, I. 1998B
196591	-50.152045	65.086271	9	254	Composite grab	Bliss, I. 1998B
196598	-50.156703	65.086870	9	3110	Composite grab	Bliss, I. 1998B
196601	-50.129700	65.090500	9	410	Grab	Bliss, I. 1998B
196619	-50.136501	65.159576	9	2974	Grab	Bliss, I. 1998B
196651	-49.921902	65.118057	9	127	Float	Bliss, I. 1998B
196662	-49.817600	65.180817	9	2500	Grab	Bliss, I. 1998B
196664	-49.821602	65.182152	9	1061	Float	Bliss, I. 1998B
196668	-49.814800	65.187981	9	114	Grab	Bliss, I. 1998B
196671	-49.818600	65.184830	9	153	Grab	Bliss, I. 1998B
196678	-49.818901	65.179199	9	176	Float	Bliss, I. 1998B
196679	-49.820202	65.177849	9	443	Grab	Bliss, I. 1998B
196684	-49.807301	65.185760	9	135	Grab	Bliss, I. 1998B
196685	-49.801899	65.186317	9	252	Grab	Bliss, I. 1998B
196695	-49.811401	65.174377	9	1440	Grab	Bliss, I. 1998B
196806	-49.917198	65.115929	9	51	Chip	Bliss, I. 1998B
196872	-50.132801	65.090363	9	10000	Chip	Bliss, I. 1998B
196873	-50.132500	65.090439	9	3904	Chip	Bliss, I. 1998B
196874	-50.132500	65.090446	9	875	Chip	Bliss, I. 1998B
196876	-50.132301	65.090446	9	333	Chip	Bliss, I. 1998B
196887	-50.131901	65.090500	9	102	Chip	Bliss, I. 1998B
196897	-50.131199	65.090424	9	67	Chip	Bliss, I. 1998B
196917	-50.135300	65.090248	9	130	Chip	Bliss, I. 1998B
196920	-50.129101	65.090599	9	111	Chip	Bliss, I. 1998B
196926	-50.132500	65.090446	9	327	Chip	Bliss, I. 1998B
197301	-50.128799	65.166763	9	146	Float	Bliss, I. 1998B
197304	-50.130001	65.162529	9	9050	Float	Bliss, I. 1998B
197305	-50.138100	65.163963	9	227	Float	Bliss, I. 1998B
197307	-50.141899	65.160141	9	174	Grab	Bliss, I. 1998B
197327	-50.178398	65.161842	9	5161	Grab	Bliss, I. 1998B
197431	-50.138933	65.086535	9	221	Composite grab	Bliss, I. 1998B
197461	-50.205542	65.113723	9	141	Composite grab	Bliss, I. 1998B
215002	-50.180516	65.092108	9	50200	Composite grab	Bliss, I. 1998B
215004	-50.180489	65.092109	9	1020	Composite grab	Bliss, I. 1998B
215006	-50.180107	65.091653	9	2730	Composite grab	Bliss, I. 1998B
215009	-50.180016	65.091562	9	195	Composite grab	Bliss, I. 1998B
215010	-50.179717	65.091179	9	140	Composite grab	Bliss, I. 1998B
215014	-50.181167	65.092520	9	270	Composite grab	Bliss, I. 1998B
215015	-50.181463	65.092731	9	630	Composite grab	Bliss, I. 1998B
215029	-50.167500	65.085000	9	2060	Composite grab	Bliss, I. 1998B
215036	-50.183990	65.119310	9	1130	Composite grab	Bliss, I. 1998B
215182	-50.199370	65.111610	9	687	Composite grab	Bliss, I. 1998B
215212	-50.133884	65.089523	9	2950	Composite grab	Bliss, I. 1998B
215224	-50.134476	65.089670	9	142	Composite grab	Bliss, I. 1998B
215264	-50.133312	65.089395	9	1030	Composite grab	Bliss, I. 1998B
215729	-50.143151	65.087707	9	163	Composite grab	Bliss, I. 1998B
215730	-50.143151	65.087707	9	744	Composite grab	Bliss, I. 1998B
219670	-51.100037	64.408414	10	1230	Grab	Skyseth, T. 1998
221703	-51.096407	64.412161	10	11162	Composite grab	Skyseth, T. 1998
221705	-51.097581	64.410970	10	789	Chip	Skyseth, T. 1998

221706	-51.097542	64.410964	10	182	Chip	Skyseth, T. 1998
221707	-51.097673	64.410966	10	3366	Chip	Skyseth, T. 1998
221708	-51.097668	64.411500	10	1596	Channel	Skyseth, T. 1998
221709	-51.097693	64.411522	10	4168	Channel	Skyseth, T. 1998
221710	-51.097743	64.411569	10	2337	Channel	Skyseth, T. 1998
221711	-51.097841	64.411555	10	3218	Composite grab	Skyseth, T. 1998
221713	-51.097718	64.411546	10	2778	Channel	Skyseth, T. 1998
221717	-51.096562	64.412004	10	879	Channel	Skyseth, T. 1998
221718	-51.096581	64.412007	10	1739	Channel	Skyseth, T. 1998
221719	-51.096612	64.412022	10	604	Channel	Skyseth, T. 1998
221720	-51.096438	64.412099	10	4423	Channel	Skyseth, T. 1998
221721	-51.096447	64.411824	10	573	Trench	Skyseth, T. 1998
221722	-51.096611	64.411840	10	121	Chip	Skyseth, T. 1998
221723	-51.095775	64.412969	10	4460	Trench	Skyseth, T. 1998
221728	-51.097184	64.411815	10	2950	Trench	Skyseth, T. 1998
221729	-51.098108	64.410920	10	3360	Composite grab	Skyseth, T. 1998
221730	-51.098183	64.410912	10	4061	Composite grab	Skyseth, T. 1998
221551	-51.257342	64.424115	9	498	Channel	Skyseth, T. 1998
221552	-51.257363	64.424106	9	819	Channel	Skyseth, T. 1998
221553	-51.257404	64.424079	9	1097	Channel	Skyseth, T. 1998
221554	-51.257446	64.424079	9	160	Channel	Skyseth, T. 1998
221555	-51.257446	64.424088	9	231	Channel	Skyseth, T. 1998
221556	-51.257466	64.424097	9	844	Channel	Skyseth, T. 1998
221557	-51.257446	64.424088	9	290	Channel	Skyseth, T. 1998
221561	-51.257576	64.424743	9	136	Channel	Skyseth, T. 1998
221562	-51.257494	64.424770	9	188:	Channel	Skyseth, T. 1998
221563	-51.257576	64.424743	9	245	Composite grab	Skyseth, T. 1998
221564	-51.257494	64.424833	9	392	Channel	Skyseth, T. 1998
221565	-51.257515	64.424878	9	211	Channel	Skyseth, T. 1998
221567	-51.257729	64.425515	9	644	Channel	Skyseth, T. 1998
221568	-51.257687	64.425524	9	126	Channel	Skyseth, T. 1998
221572	-51.257254	64.423604	9	363	Channel	Skyseth, T. 1998
221573	-51.257233	64.423595	9	2013	Channel	Skyseth, T. 1998
221574	-51.257233	64.423586	9	820	Channel	Skyseth, T. 1998
221575	-51.257192	64.423640	9	1443	Channel	Skyseth, T. 1998
221576	-51.257193	64.423676	9	576	Channel	Skyseth, T. 1998
221579	-51.257193	64.423676	9	232	Channel	Skyseth, T. 1998
221602	-51.257413	64.425039	9	2766	Chip	Skyseth, T. 1998
221603	-51.258741	64.416144	9	217	Grab	Skyseth, T. 1998
221604	-51.258720	64.416144	9	101	Grab	Skyseth, T. 1998
221605	-51.257346	64.422348	9	378	Chip	Skyseth, T. 1998
221614	-51.257318	64.423783	9	523	Chip	Skyseth, T. 1998
221615	-51.257318	64.423783	9	549	Grab	Skyseth, T. 1998
221616	-51.257339	64.423828	9	3988	Chip	Skyseth, T. 1998
221617	-51.257339	64.423828	9	2310	Grab	Skyseth, T. 1998
221618	-51.257277	64.423837	9	362	Chip	Skyseth, T. 1998
221619	-51.257340	64.423891	9	385	Chip	Skyseth, T. 1998
221620	-51.257277	64.423837	9	1160	Grab	Skyseth, T. 1998
221621	-51.257277	64.423837	9	1510	Composite grab	Skyseth, T. 1998
221622	-51.257319	64.423900	9	1090	Composite grab	Skyseth, T. 1998
221623	-51.257319	64.423900	9	834	Composite grab	Skyseth, T. 1998

221624	-51.257319	64.423900	9	1120	Grab	Skyseth, T. 1998
222764	-51.259129	64.415890	9	160	Chip	Skyseth, T. 1998
222765	-51.258354	64.416504	9	218	Chip	Skyseth, T. 1998
222766	-51.257476	64.417559	9	840	Chip	Skyseth, T. 1998
222767	-51.257387	64.417402	9	231	Chip	Skyseth, T. 1998
222787	-51.245618	64.414714	9	3395	Chip	Skyseth, T. 1998
222788	-51.264001	64.406309	9	309	Chip	Skyseth, T. 1998
222797	-51.269568	64.388407	9	523	Chip	Skyseth, T. 1998
222823	-51.275152	64.384125	9	309	Chip	Skyseth, T. 1998
222824	-51.274518	64.384568	9	1399	Chip	Skyseth, T. 1998
222835	-51.258294	64.424933	9	173	Chip	Skyseth, T. 1998
222855	-51.262328	64.412783	9	271	Chip	Skyseth, T. 1998
222860	-51.245613	64.414667	9	493	Chip	Skyseth, T. 1998
222875	-51.244095	64.417339	9	244	Grab	Skyseth, T. 1998
222893	-51.245657	64.414656	9	1453	Channel	Skyseth, T. 1998
222894	-51.245664	64.414596	9	857	Channel	Skyseth, T. 1998
222898	-51.245911	64.414559	9	605	Channel	Skyseth, T. 1998
222907	-51.270743	64.395762	9	109	Chip	Skyseth, T. 1998
222909	-51.272274	64.407936	9	347	Chip	Skyseth, T. 1998
222912	-51.274352	64.384713	9	107	Chip	Skyseth, T. 1998
222922	-51.257326	64.424167	9	185	Chip	Skyseth, T. 1998
222923	-51.257318	64.424177	9	480	Composite grab	Skyseth, T. 1998
222965	-51.245860	64.414470	9	497	Channel	Skyseth, T. 1998
222985	-51.257893	64.426450	9	479	Chip	Skyseth, T. 1998
222988	-51.258102	64.426091	9	116	Chip	Skyseth, T. 1998
222991	-51.258065	64.425977	9	122	Composite grab	Skyseth, T. 1998
222992	-51.258101	64.425989	9	249	Chip	Skyseth, T. 1998
222995	-51.257705	64.424767	9	163	Chip	Skyseth, T. 1998
222996	-51.257707	64.424763	9	242	Chip	Skyseth, T. 1998
222997	-51.257709	64.424761	9	285	Chip	Skyseth, T. 1998
222998	-51.257357	64.424131	9	110	Chip	Skyseth, T. 1998
222999	-51.257349	64.424140	9	144	Composite grab	Skyseth, T. 1998
223000	-51.257338	64.424152	9	105	Composite grab	Skyseth, T. 1998
257419	-51.549129	65.359123	2	120	Grab	GEUSGREEN, K. Secher
257431	-51.555470	65.368561	2	110	Grab	GEUSGREEN, K. Secher
257433	-51.555470	65.368561	2	180	Grab	GEUSGREEN, K. Secher
257441	-51.550961	65.369911	2	170	Grab	GEUSGREEN, K. Secher
257442	-51.550961	65.369911	2	2120	Grab	GEUSGREEN, K. Secher
257447	-51.534840	65.375252	2	100	Grab	GEUSGREEN, K. Secher
257560	-51.510448	65.318428	2	100	Grab	GEUSGREEN, K. Secher
257561	-51.513458	65.319321	2	310	Grab	GEUSGREEN, K. Secher
257575	-51.567322	65.324638	2	170	Grab	GEUSGREEN, K. Secher
257612	-51.576462	65.085960	2	180	Grab	GEUSGREEN, K. Secher
301210	-49.902660	65.119469	2	1180	Grab	GEUSGREEN, P. Appel
329126	-51.627090	64.156799	2	180	Grab	GEUSGREEN, P. Appel
329880	-51.607510	64.174454	2	210	Grab	GEUSGREEN, P. Appel
329891	-51.607510	64.174454	2	130	Grab	GEUSGREEN, P. Appel
329922	-51.607510	64.174454	2	100	Grab	GEUSGREEN, P. Appel
353233	-49.948769	64.730110	2	100	Grab	GEUSGREEN, P. Appel
407804	-51.066669	64.441704	2	12900	Grab	GEUSGREEN, P. Appel
407813	-51.066669	64.441704	2	2010	Grab	GEUSGREEN, P. Appel

407814	-51.066669	64.441704	2	7540	Grab	GEUSGREEN, P. Appel
407815	-51.066669	64.441704	2	180	Grab	GEUSGREEN, P. Appel
407825	-51.066669	64.441704	2	810	Grab	GEUSGREEN, P. Appel
407828	-51.066669	64.441704	2	1950	Grab	GEUSGREEN, P. Appel
407829	-51.066669	64.441704	2	110	Grab	GEUSGREEN, P. Appel
407834	-51.066669	64.441704	2	550	Grab	GEUSGREEN, P. Appel
407843	-49.783333	65.175000	2	8700	Grab	GEUSGREEN, P. Appel
450165	-50.137860	65.088070	2	350	Grab	GEUSGREEN, P. Appel
462734	-49.804400	65.177510	2	210	Grab	GEUSGREEN, P. Appel
462747	-50.137857	65.088067	2	450	Grab	GEUSGREEN, P. Appel
462748	-50.137860	65.088070	2	520	Grab	GEUSGREEN, P. Appel
462749	-50.137860	65.088070	2	1550	Grab	GEUSGREEN, P. Appel
462750	-50.137860	65.088070	2	1170	Grab	GEUSGREEN, P. Appel
462751	-50.137860	65.088070	2	970	Grab	GEUSGREEN, P. Appel
462752	-50.137860	65.088070	2	1940	Grab	GEUSGREEN, P. Appel
462753	-50.137860	65.088070	2	760	Grab	GEUSGREEN, P. Appel
462753	-50.137860	65.088070	2	650	Grab	GEUSGREEN, P. Appel
462754	-50.137860	65.088070	2	5830	Grab	GEUSGREEN, P. Appel
462755	-50.176975	65.091500	2	410	Grab	GEUSGREEN, P. Appel
462756	-50.176970	65.091500	2	21000	Grab	GEUSGREEN, P. Appel
462757	-50.176970	65.091500	2	106000	Grab	GEUSGREEN, P. Appel
462758	-50.176970	65.091500	2	2750	Grab	GEUSGREEN, P. Appel
462759	-50.176970	65.091500	2	51700	Grab	GEUSGREEN, P. Appel
462760	-50.176970	65.091500	2	79950	Grab	GEUSGREEN, P. Appel
462761	-50.176970	65.091500	2	180	Grab	GEUSGREEN, P. Appel
462762	-50.176970	65.091500	2	52500	Grab	GEUSGREEN, P. Appel
462763	-50.176970	65.091500	2	130	Grab	GEUSGREEN, P. Appel
462764	-50.176970	65.091500	2	130	Grab	GEUSGREEN, P. Appel
462766	-50.176970	65.091500	2	460	Grab	GEUSGREEN, P. Appel
462767	-50.176970	65.091500	2	250	Grab	GEUSGREEN, P. Appel
462768	-50.176970	65.091500	2	44300	Grab	GEUSGREEN, P. Appel
462769	-50.176970	65.091500	2	110	Grab	GEUSGREEN, P. Appel
462770	-50.176970	65.091500	2	6970	Grab	GEUSGREEN, P. Appel
465632	-50.139585	65.167412	2	150	Grab	GEUSGREEN, P. Appel
466093	-50.159975	65.132184	2	1150	Grab	GEUSGREEN, P. Appel
477313	-51.107350	64.733233	1	203	Grab	GEUSGREEN, A.A. Garde
477326	-51.092333	64.771733	1	2260	Grab	GEUSGREEN, A.A. Garde
477384	-51.122567	64.669383	1	1430	Grab	GEUSGREEN, A.A. Garde
479720	-51.255350	64.423533	1	248	Grab	GEUSGREEN, D. Frei
493003	-51.091533	64.410420	1	8405	Grab	GEUSGREEN, P. Appel
493004	-51.094419	64.409070	1	3660	Grab	GEUSGREEN, P. Appel
493008	-51.084060	64.412460	1	1870	Grab	GEUSGREEN, P. Appel
493009	-51.084060	64.412460	1	254	Grab	GEUSGREEN, P. Appel
493010	-51.084060	64.412460	1	699	Grab	GEUSGREEN, P. Appel
493029	-49.960005	64.737740	1	479	Grab	GEUSGREEN, P. Appel
493041	-51.092697	64.407640	1	436	Grab	GEUSGREEN, P. Appel
493046	-51.094430	64.408960	1	1140	Grab	GEUSGREEN, P. Appel
493047	-51.094430	64.408960	1	1360	Grab	GEUSGREEN, P. Appel
493048	-51.094430	64.408960	1	251	Grab	GEUSGREEN, P. Appel
493049	-51.094430	64.408960	1	8480	Grab	GEUSGREEN, P. Appel
493050	-51.094430	64.408960	1	3520	Grab	GEUSGREEN, P. Appel

493051	-51.094430	64.408960	1	1670	Grab	GEUSGREEN, P. Appel
493052	-51.094430	64.408960	1	3270	Grab	GEUSGREEN, P. Appel
493054	-51.094430	64.408960	1	4710	Grab	GEUSGREEN, P. Appel
493055	-51.094430	64.408960	1	1690	Grab	GEUSGREEN, P. Appel
493061	-51.094612	64.409200	1	11700	Grab	GEUSGREEN, P. Appel
493062	-51.094612	64.409200	1	6730	Grab	GEUSGREEN, P. Appel
493063	-51.094612	64.409200	1	4940	Grab	GEUSGREEN, P. Appel
493064	-51.094612	64.409200	1	329	Grab	GEUSGREEN, P. Appel
493065	-51.094612	64.409200	1	2460	Grab	GEUSGREEN, P. Appel

**Table A2.** Quality ranking of the coordinates extracted from various sources.

Ranking	Sample locality and reported coordinates...
1	Measured by GPS after May 1, 2000. Coordinates given in the report.
2	Measured by GPS before May 1, 2000. Coordinates given in the report.
3	Probably not measured by GPS, but precise coordinates are given in the report.
4	Measured and determined by the authors of this report from a high-resolution and good map (with corner coordinates). Report published after 1 May, 2000.
5	Measured and determined by the authors of this report from a low-resolution map (with corner coordinates) but good map. Report published after 1 May, 2000.
6	Measured and determined by the authors of this report from a high-resolution map (without corner coordinates) and accurate map. Report from before 1 of May 2000.
7	Measured and determined by the authors from a low-resolution map (without corner coordinates) but inaccurate map. Report from before 1 of May 2000.
8	Measured and determined by the authors of this report from a high or low-resolution map (without corner coordinates) and accurate map, where it is possible to transfer the position of a locality (according to the locality position relative to coastlines, rivers, lakes, etc.) to a new map.
9	Uncertainty if they are measured by GPS or extracted from a map. Coordinates given in the report.
10	Coordinates given in company report, but it is uncertain if they are measured by GPS or extracted from a map. Moreover, the company admits to have problem with their projections of coordinates. Coordinates given in the report.
11	Survey samples. Coordinates from GGU sample database maintained by GEUS.

### References given in appendix A:

- Bliss, I. 1998A: Follow-up on Molybdenite mineralization at Ivisartoq, West Greenland 1997. Internal report, Nunaoil A/S. 6 pp., 3 app., 2 plates (in archives of the Geological Survey of Denmark and Greenland, GEUS Report file 21562).
- Bliss, I. 1998B: Isua data compilation report 1993 - 1997. Internal report, Nunaoil A/S. 7 pp., 6 app. (in archives of the Geological Survey of Denmark and Greenland, GEUS Report file 21575).
- Bliss, I. & Palmer, D. 1998: Isua, 1997 Field report. Internal report, Nunaoil A/S. 11 pp., 3 app., 5 plates (in archives of the Geological Survey of Denmark and Greenland, GEUS Report file 21574).

Bliss, Ian & Palmer, David 1997: Prospecting, mapping and, target evaluation within the Isua supracrustal belt, West Greenland 1996. (Licence 01/93. (Prepared for Nunaoil A/S by ICB Exploration Services). 2 volumes (Copy 3), 34 pp., 5 app., 17 plates (in archives of the Geological Survey of Denmark and Greenland, GEUS Report file 21513).

Christiansen, O. 1992: Mineral exploration on Storø, Nuuk Fiord, southern West Greenland. Internal report, Nunaoil A/S, 17 pp., 1 app. (in archives of the Geological Survey of Denmark and Greenland, GEUS Report file 21029).

Downes, M. J. & Gardinev, W. W. 1986: Report of field work - 1985: Greenland tungsten project. Kidd Creek Mines Ltd. Exploration division. Internal report, Kidd Creek Mines Ltd., 32 pp., 6 app., 25 plates (in archives of the Geological Survey of Denmark and Greenland, GEUS Report file 20036).

Dunnells, D. 1995: Mineral exploration in the Malene concession and Nuuk Fjord region, southern West Greenland: July-August 1995. Internal report, Nunaoil A/S, 30 pp., 5 app., 10 plates (in archives of the Geological Survey of Denmark and Greenland, GEUS Report file 21457).

Grahl-Madsen, L. 1994: Storø gold project, Southwest Greenland 1994. Internal report, Nunaoil A/S, 20 pp., 7 app., 16 plates (in archives of the Geological Survey of Denmark and Greenland, GEUS Report file 21413).

Heilmann, A. 1997: Mineral exploration in the Malene Concession, southern West Greenland, July-September 1996. Licence no. 08/94. Internal report, Nunaoil A/S, 22 pp., 4 app., 4 plates (in archives of the Geological Survey of Denmark and Greenland, GEUS Report file 21514).

Skyseth, T. 1997: Gold Exploration on Storø 1996 South West Greenland, Exploration License 13/97 (former 02/92). Internal report, Nunaoil A/S. 14 pp., 12 app., 3 plates. [21564 temporary report] (in archives of the Geological Survey of Denmark and Greenland, GEUS Report file 21565).

Skyseth, T. 1998: Gold and base metal exploration on Bjørneø and Sermitsiaq, Nuukfjord, South West Greenland, 1997. Internal report, Nunaoil A/S. 31 pp., 15 app. (in archives of the Geological Survey of Denmark and Greenland, GEUS Report file 21648).

## **Appendix B. Data**

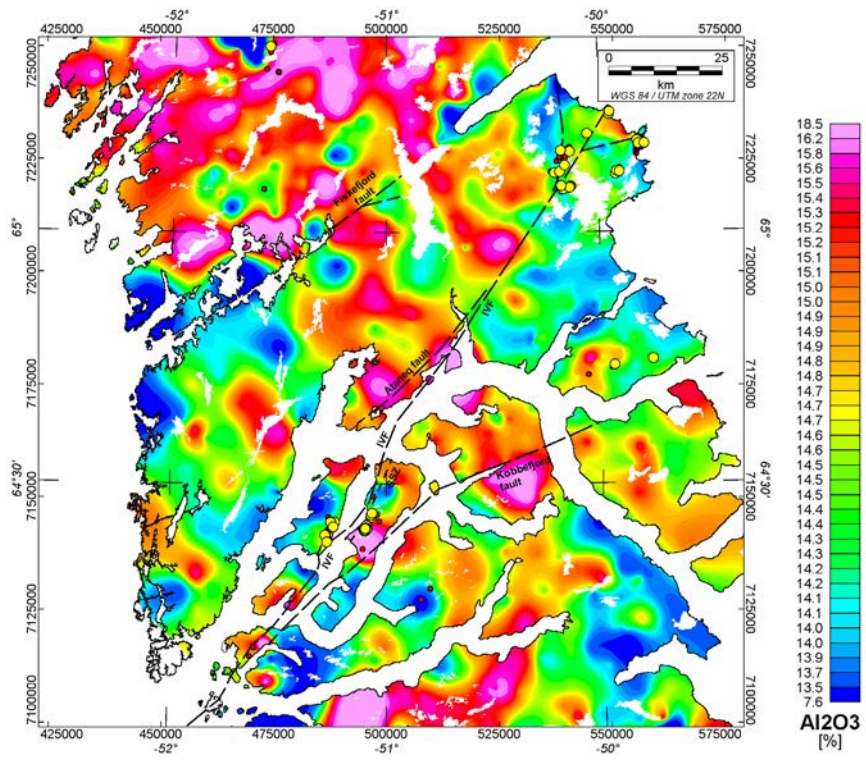


**Figure B1.**  $\text{Al}_2\text{O}_3$  in fine fraction from regional stream sediment samples, 200 m grid cell size.

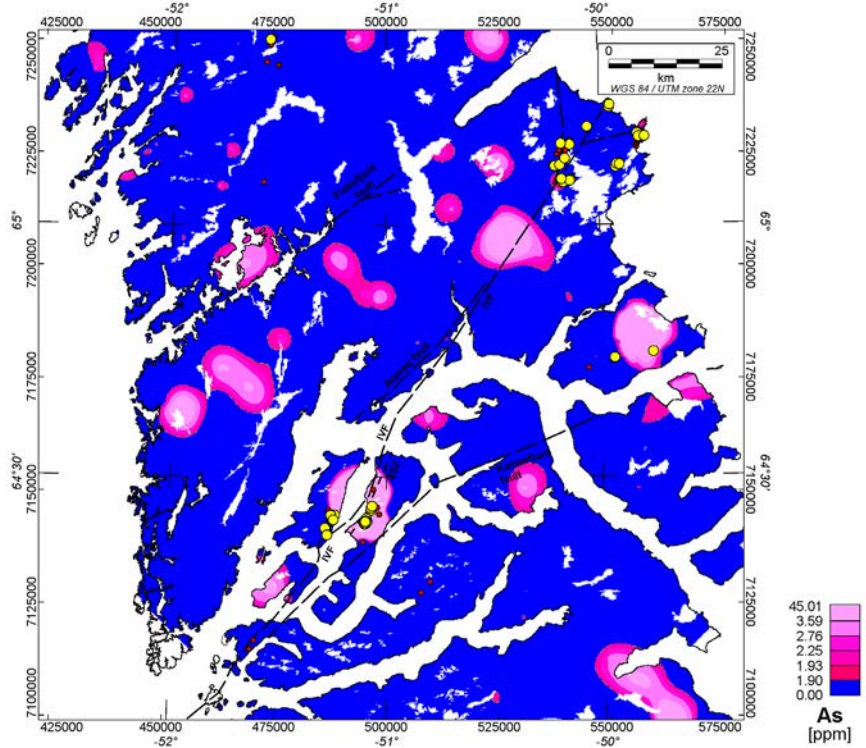


**Figure B2.** As (modified) in fine fraction from regional stream sediment samples, 200 m grid cell size.

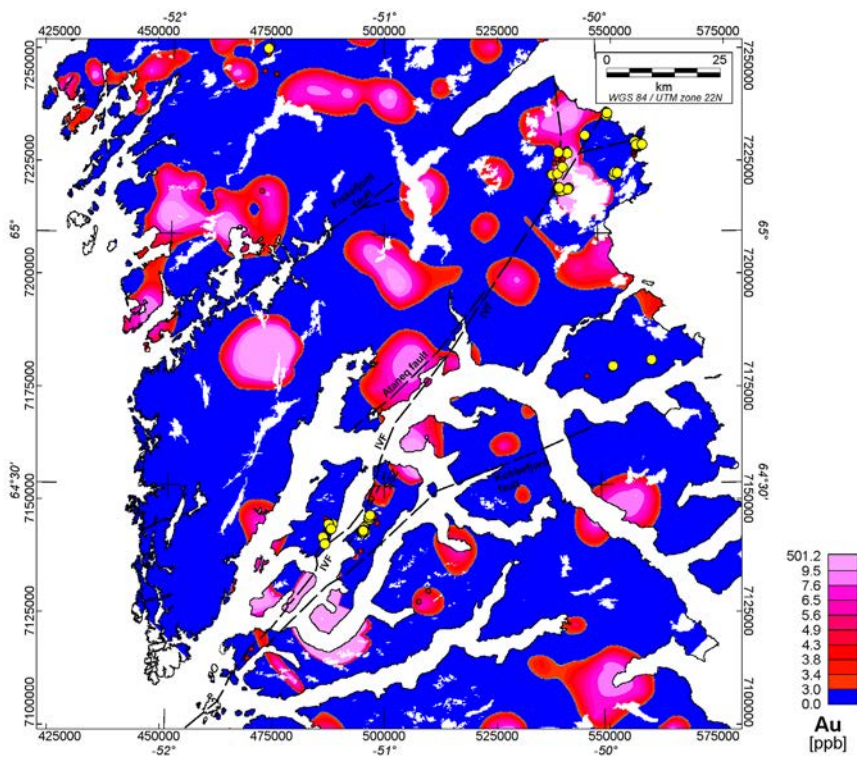


**Figure B3.** Au (modified) in fine fraction from regional stream sediment samples, 200 m grid cell size.

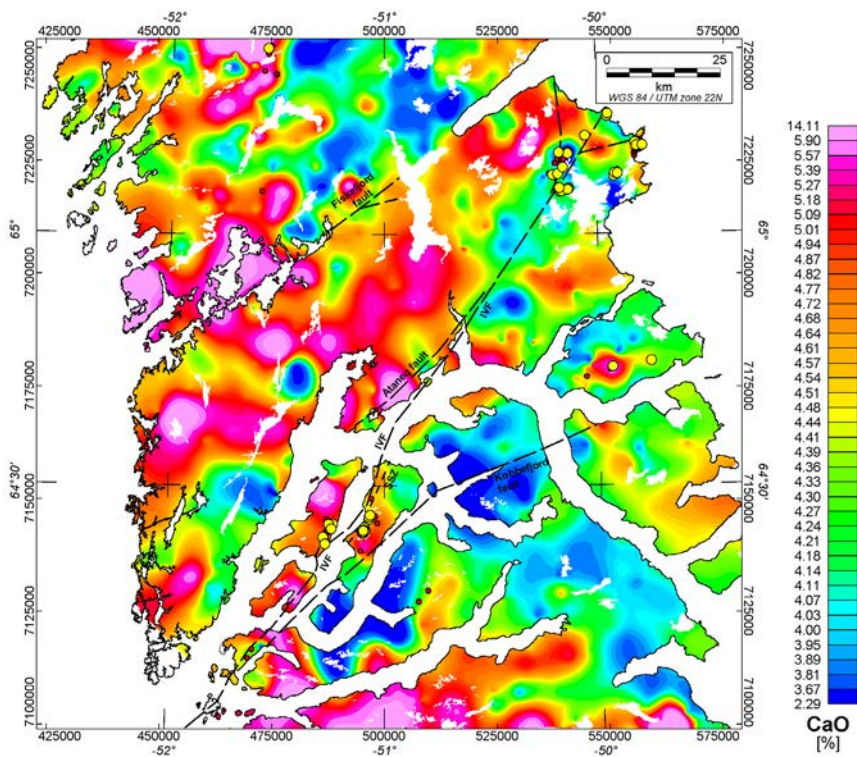


**Figure B4.** CaO in fine fraction from regional stream sediment samples, 200 m grid cell size.

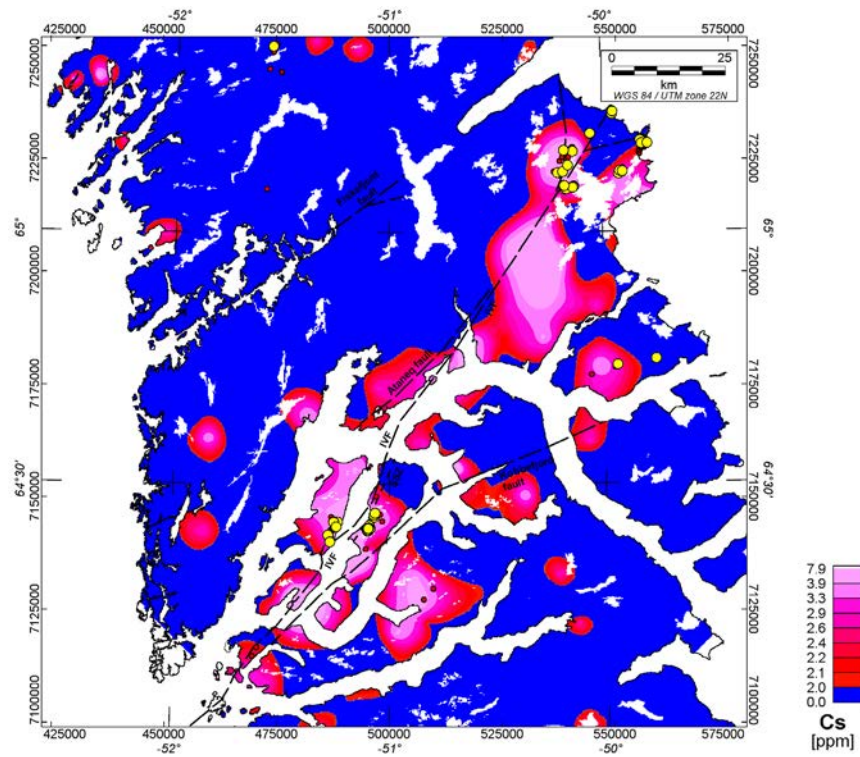


**Figure B5.** Cs (modified) in fine fraction from regional stream sediment samples, 200 m grid cell size.

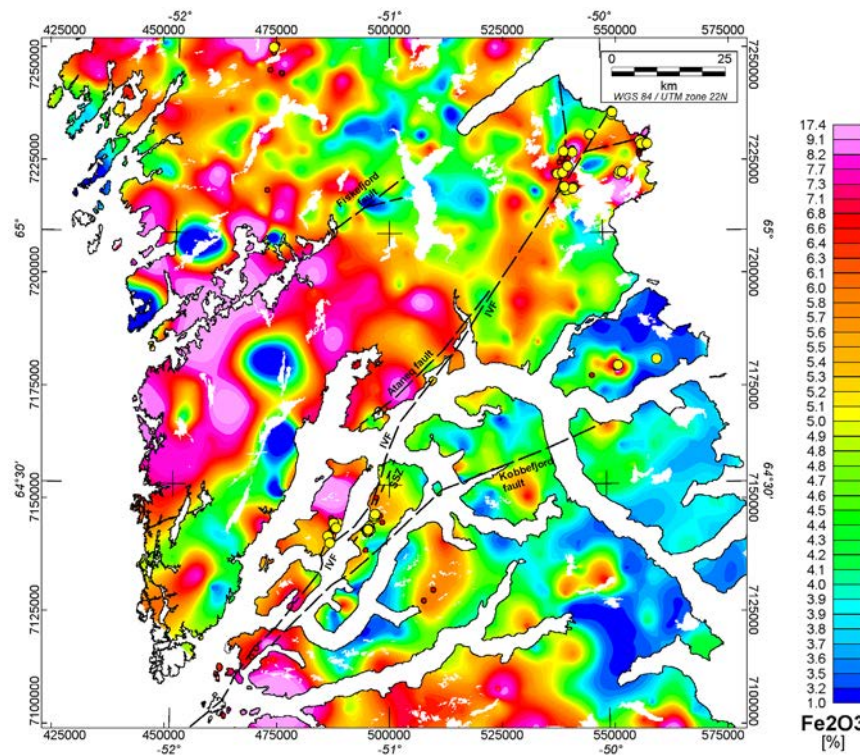


**Figure B6.**  $\text{Fe}_2\text{O}_3$  in fine fraction from regional stream sediment samples, 200 m grid cell size.

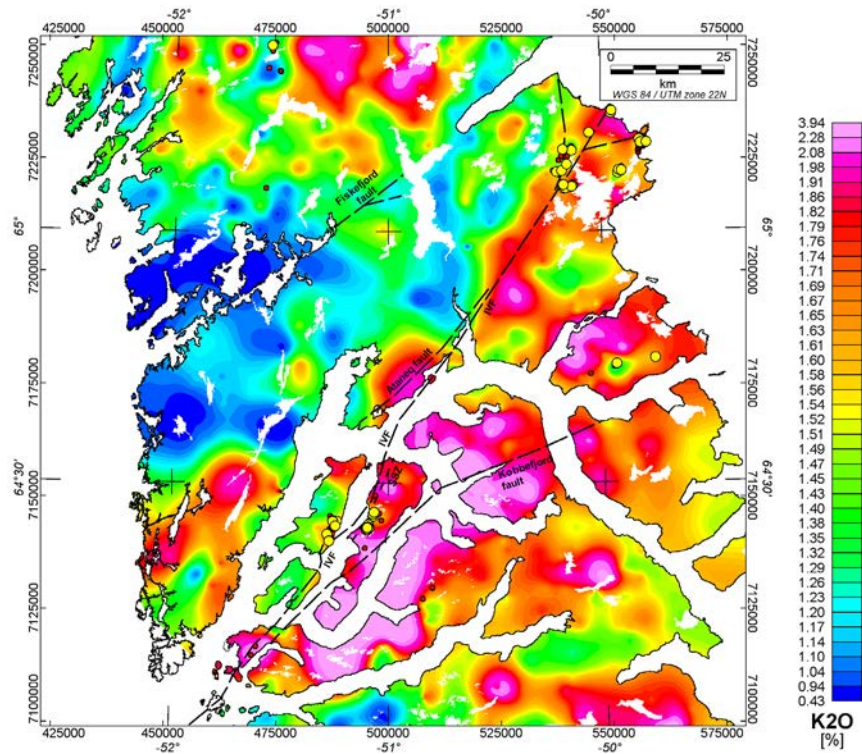


**Figure B7.**  $K_2O$  in fine fraction from regional stream sediment samples, 200 m grid cell size.

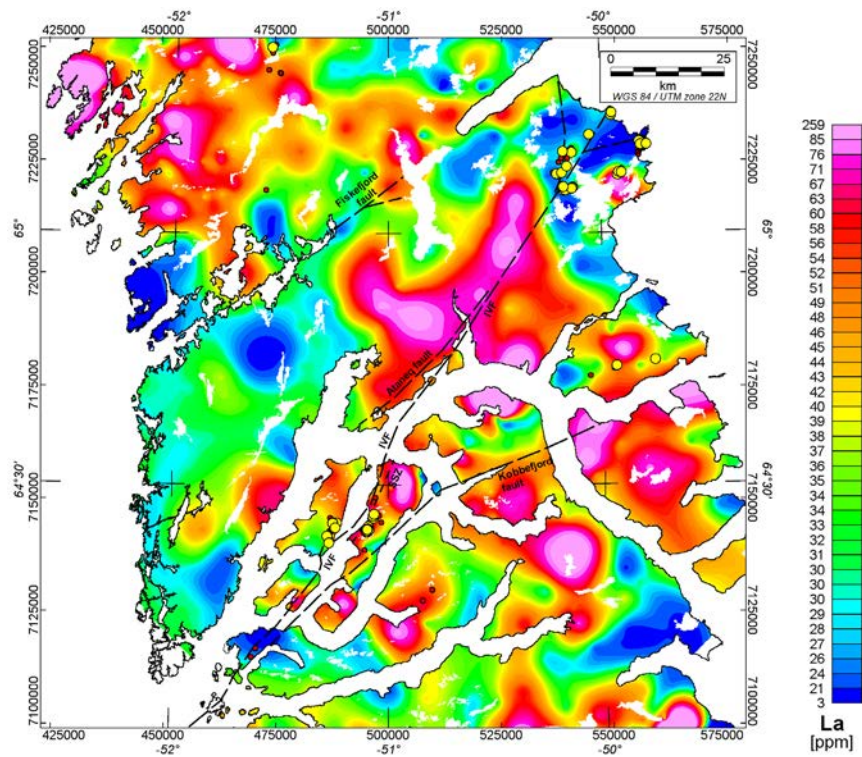


**Figure B8.** La in fine fraction from regional stream sediment samples, 200 m grid cell size.

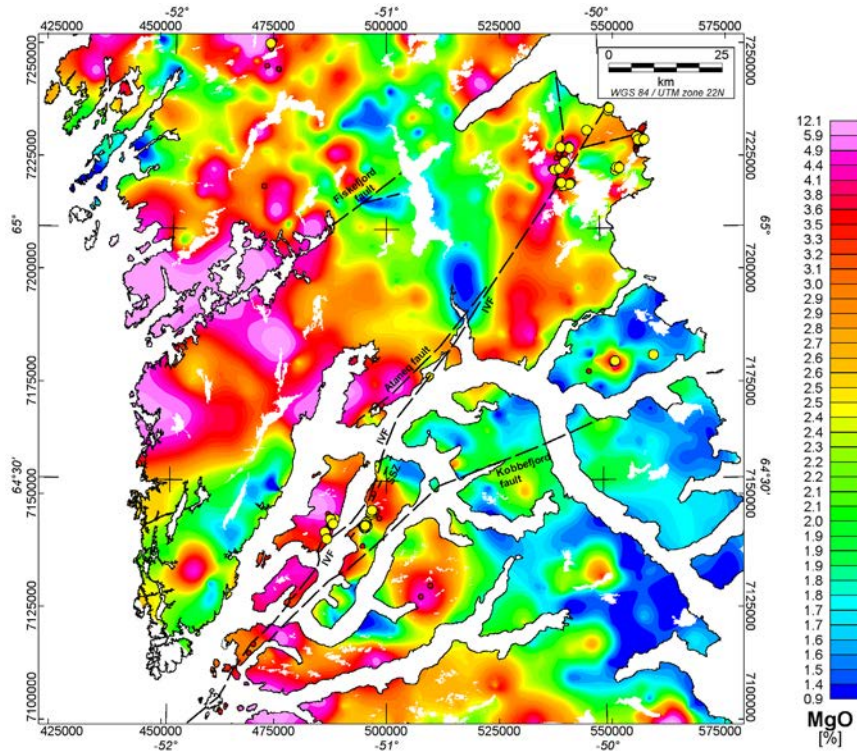


**Figure B9.** MgO in fine fraction from regional stream sediment samples, 200 m grid cell size.

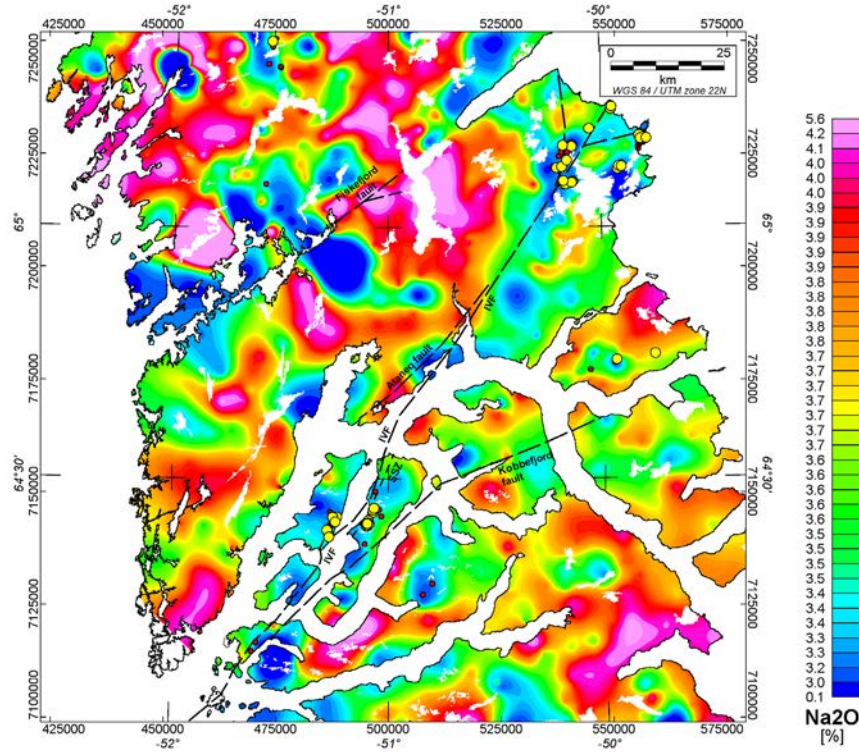


**Figure B10.** Na<sub>2</sub>O in fine fraction from regional stream sediment samples, 200 m grid cell size.

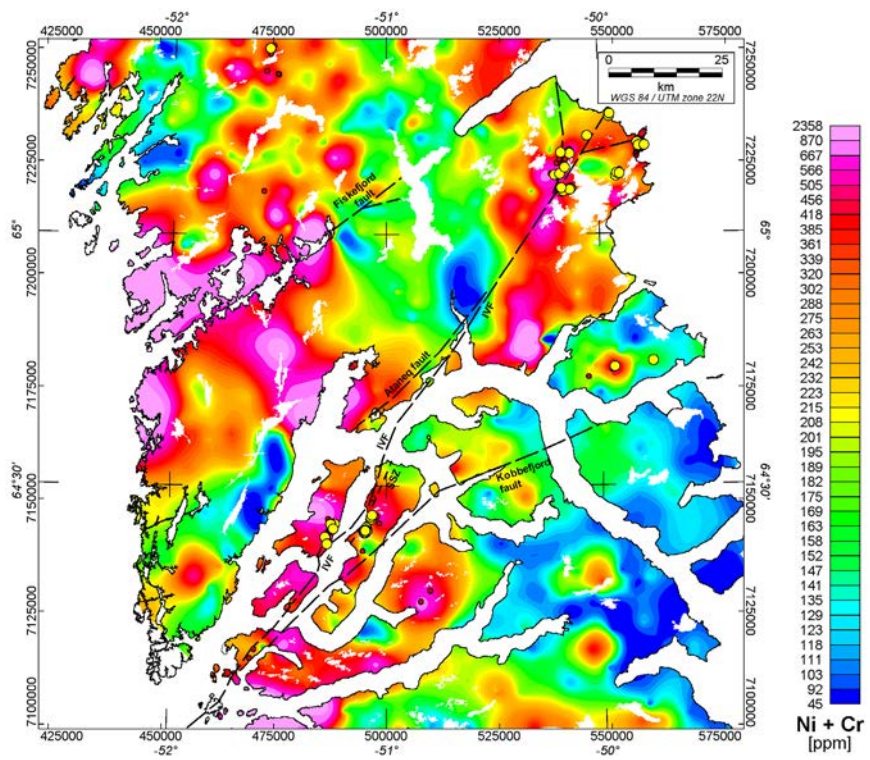


**Figure B11.** *Ni + Cr in fine fraction from regional stream sediment samples, 200 m grid cell size.*

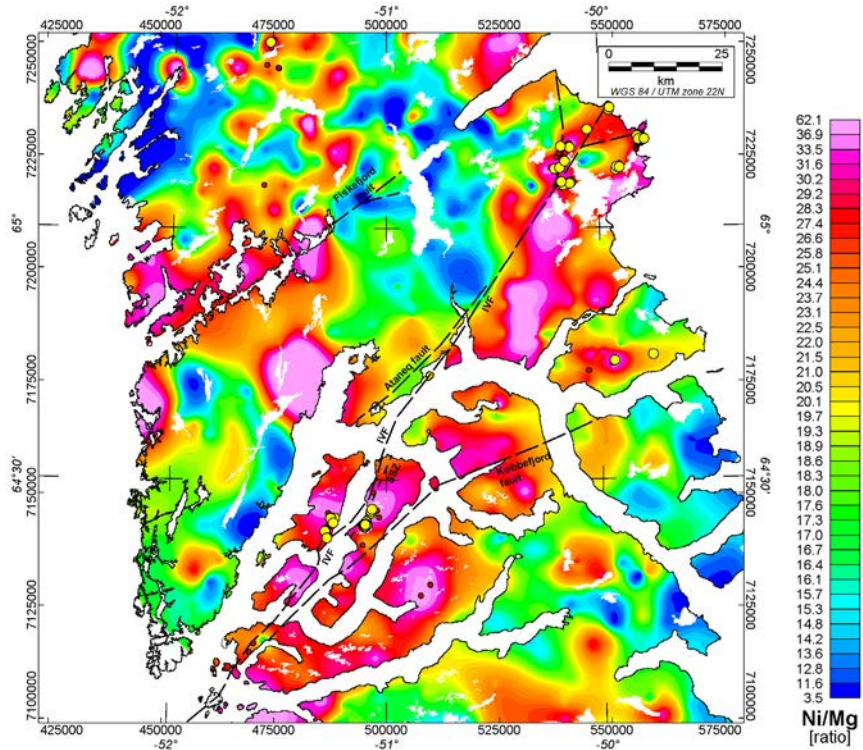


**Figure B12.** *Ni/Mg ratio in fine fraction from regional stream sediment samples, 200 m grid cell size.*

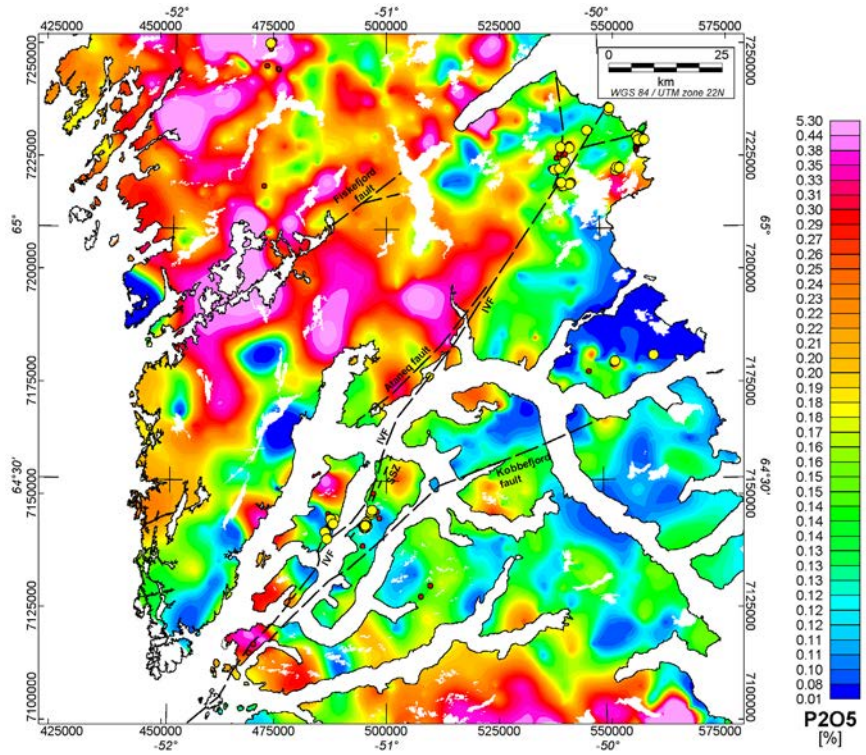


**Figure B13.**  $P_2O_5$  in fine fraction from regional stream sediment samples, 200 m grid cell size.

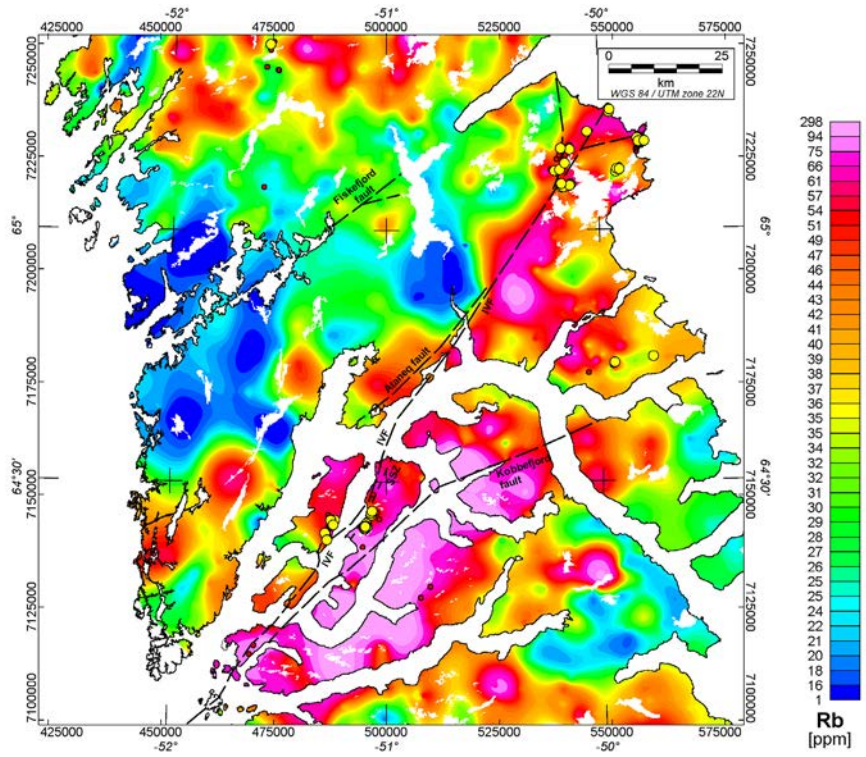


**Figure B14.** Rb in fine fraction from regional stream sediment samples, 200 m grid cell size.

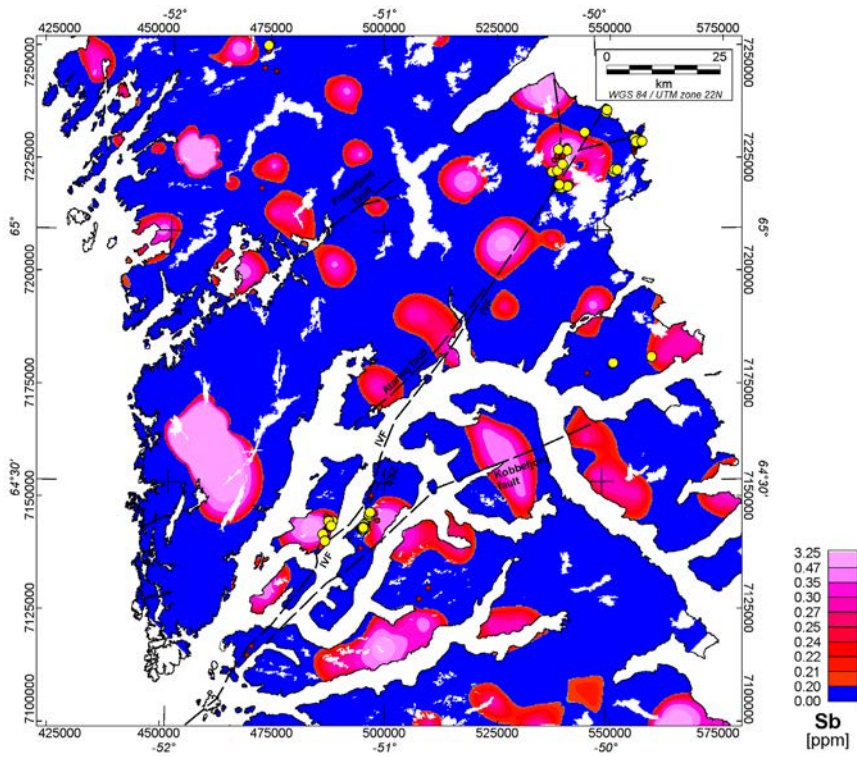


**Figure B15.** Sb (modified) in fine fraction from regional stream sediment samples, 200 m grid cell size.

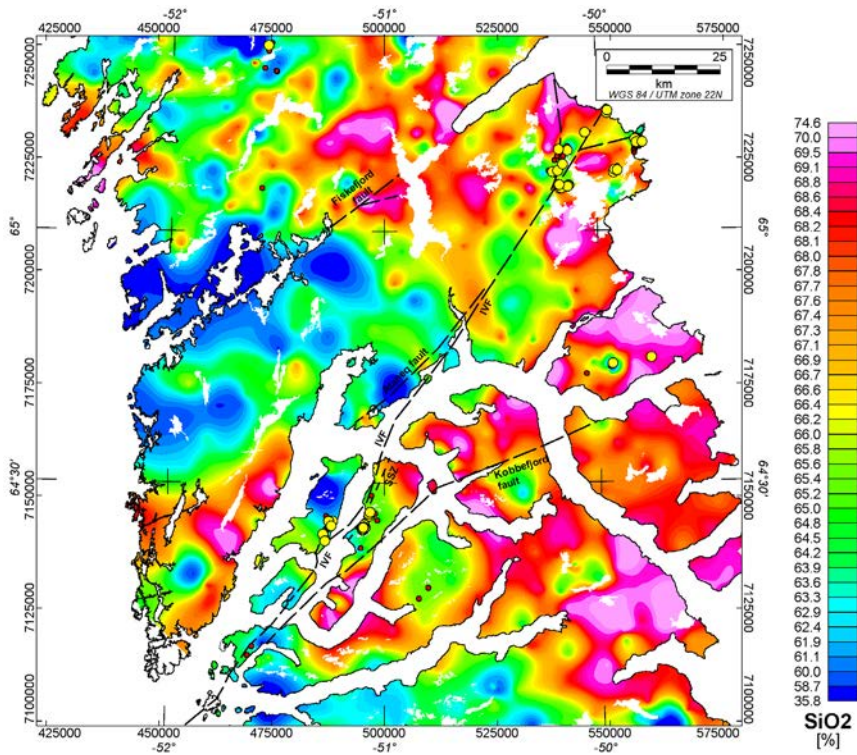


**Figure B16.** SiO<sub>2</sub> in fine fraction from regional stream sediment samples, 200 m grid cell size.

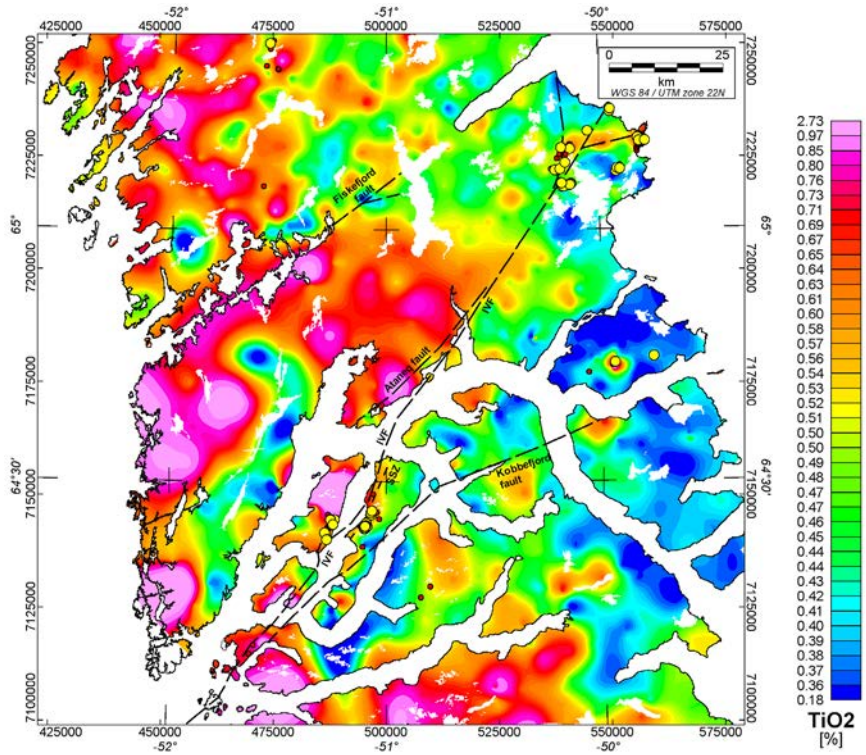


**Figure B17.**  $TiO_2$  in fine fraction from regional stream sediment samples, 200 m grid cell size.

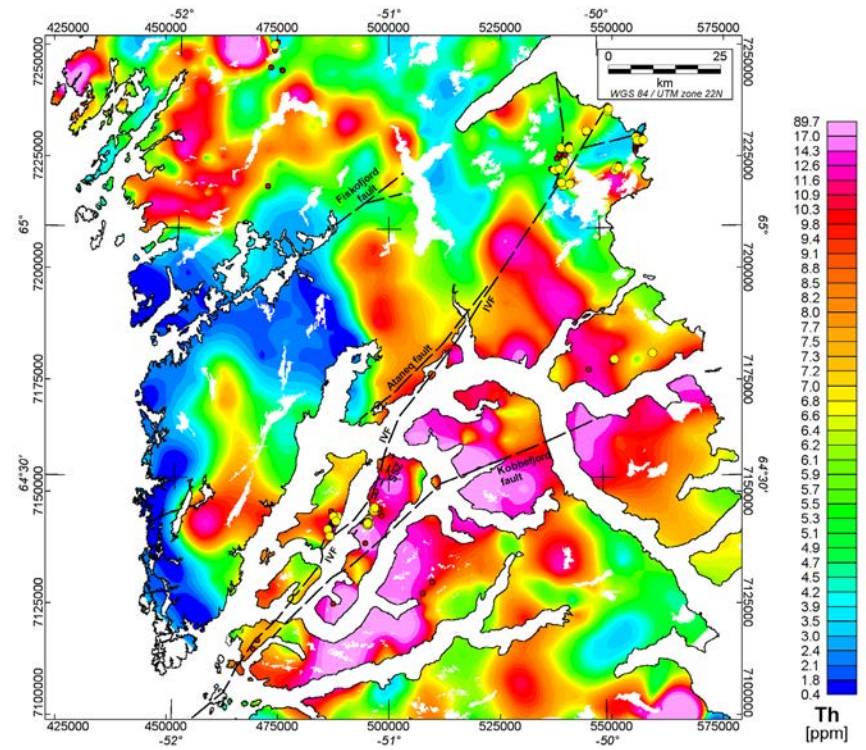


**Figure B18.**  $Th$  in fine fraction from regional stream sediment samples, 200 m grid cell size.

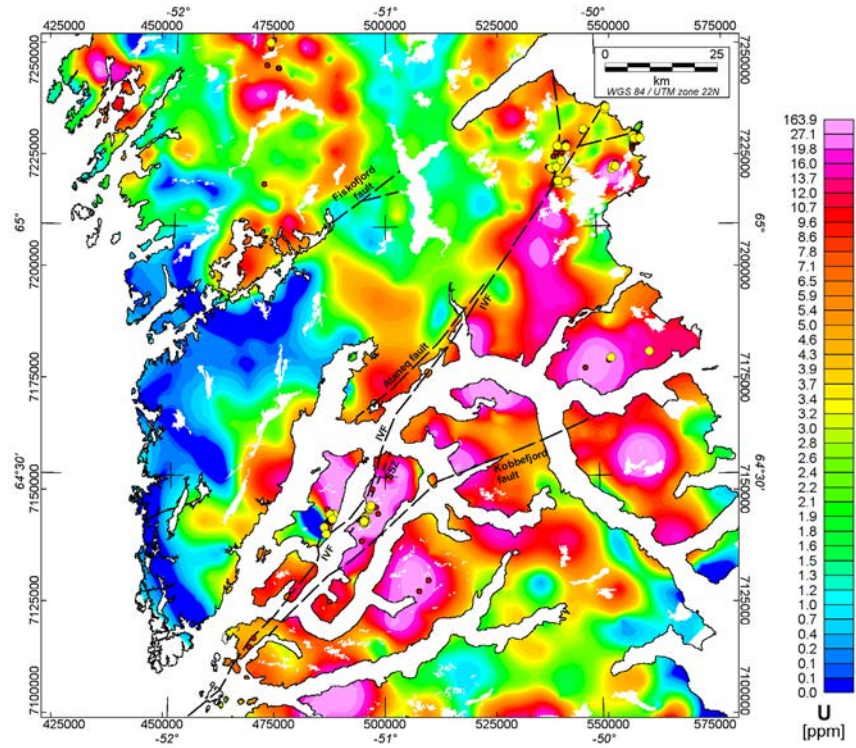


**Figure B19.**  $U$  in fine fraction from regional stream sediment samples, 200 m grid cell size.

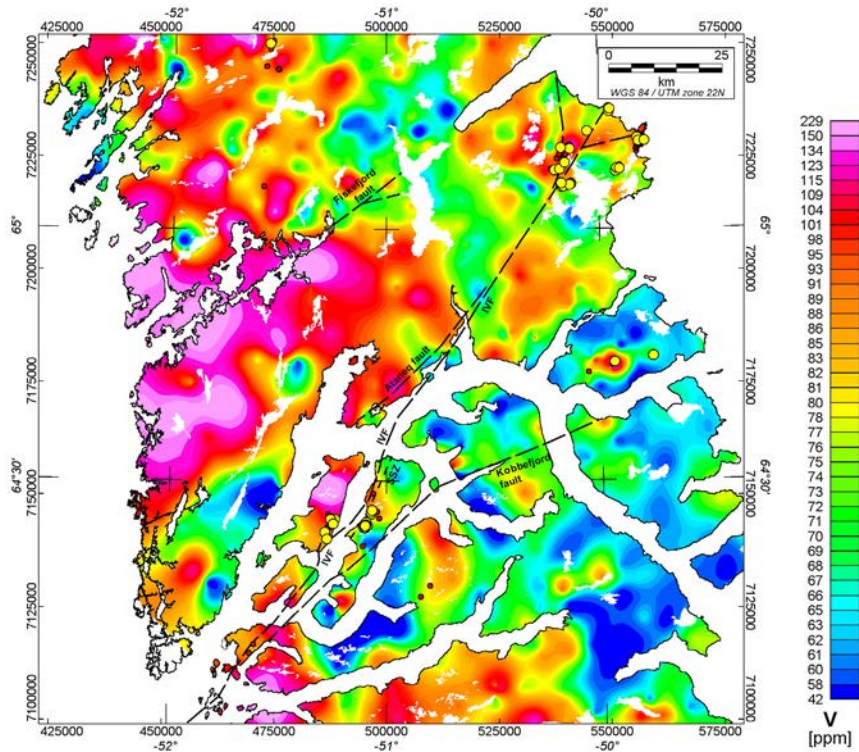


**Figure B20.**  $V$  in fine fraction from regional stream sediment samples, 200 m grid cell size.

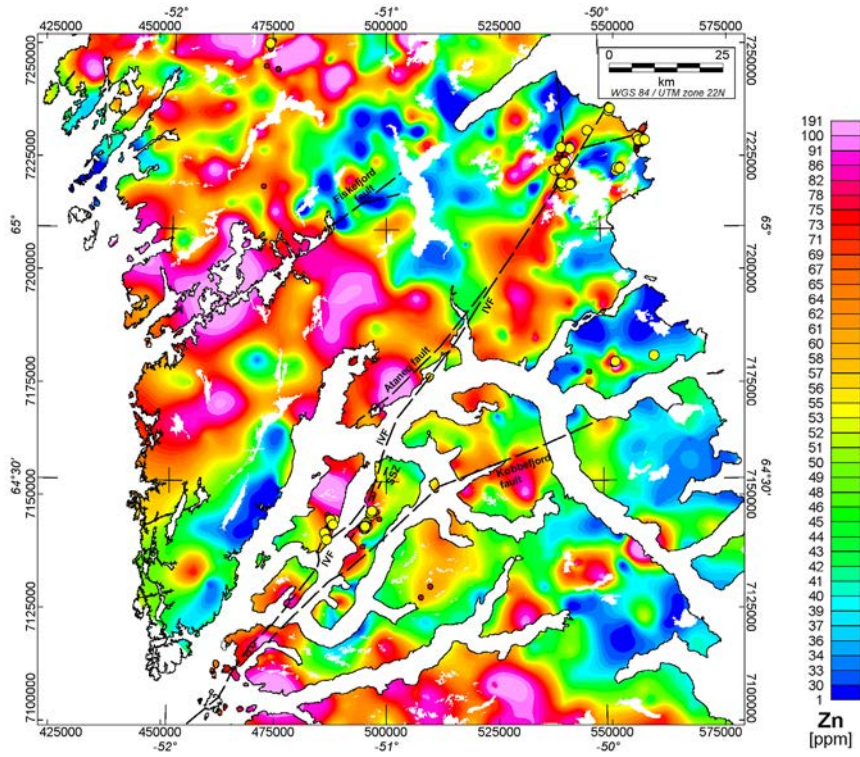


**Figure B21.** Zn in fine fraction from regional stream sediment samples, 200 m grid cell size.

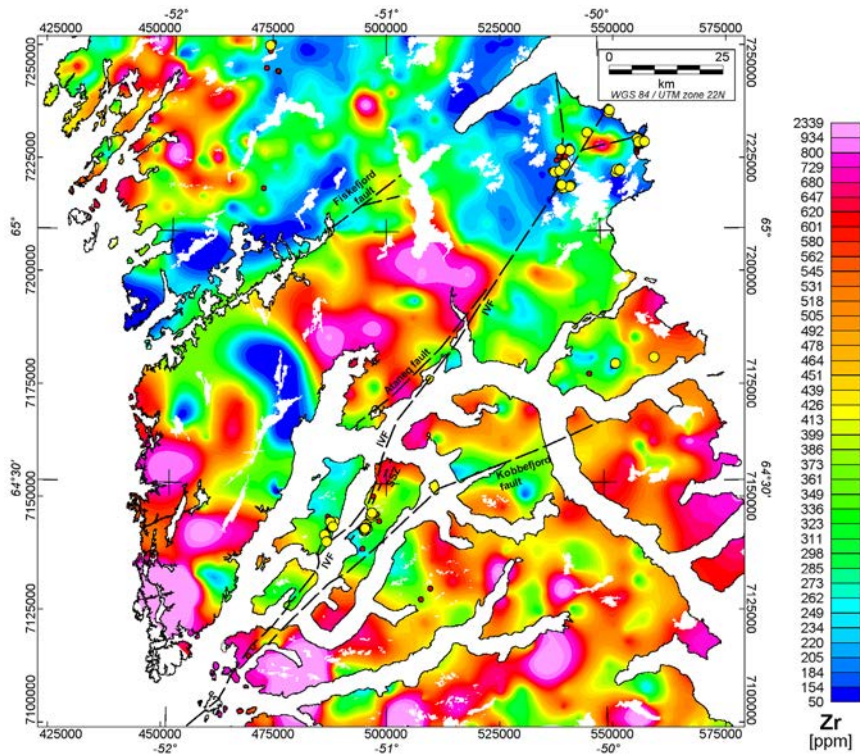


**Figure B22.** Zr in fine fraction from regional stream sediment samples, 200 m grid cell size.

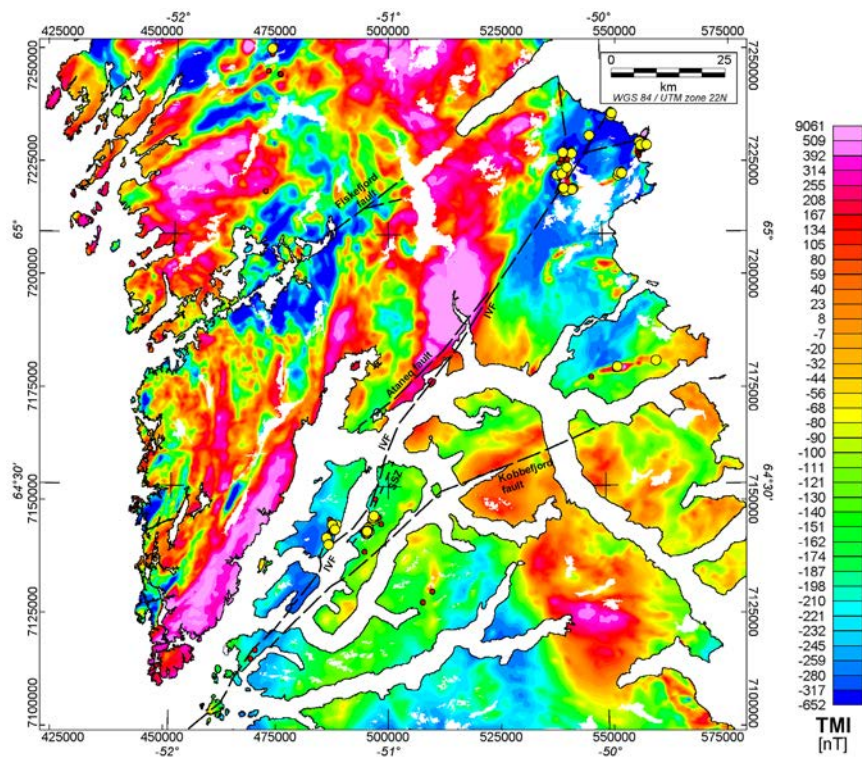


**Figure B23.** Total magnetic field intensity (TMI) from regional aeromagnetic data, 200 m grid cell size.

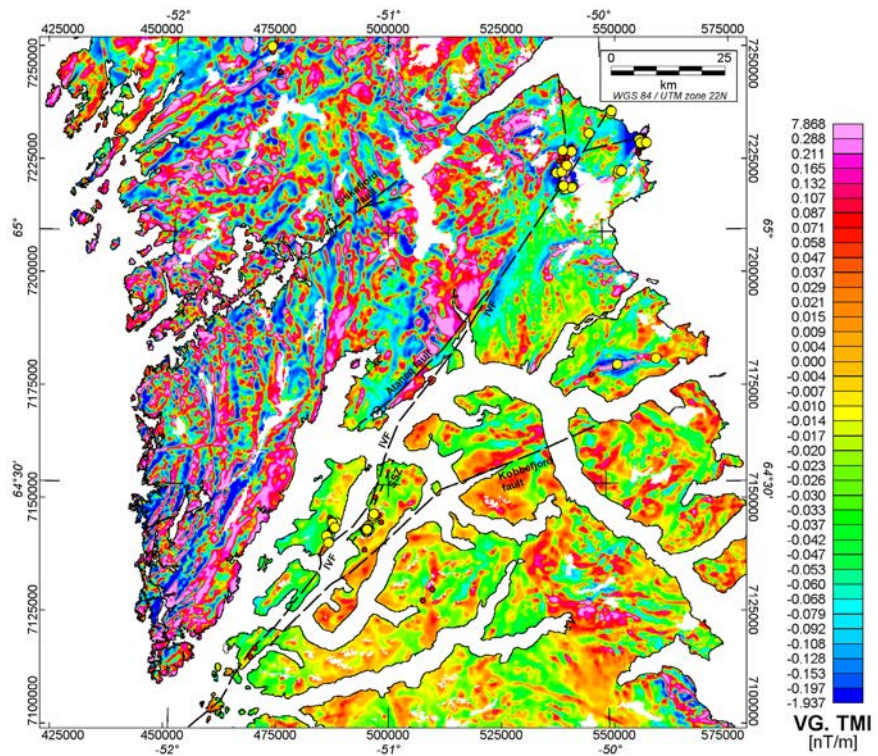


**Figure B24.** Vertical gradient of TMI from regional aeromagnetic data, 200 m grid cell size.

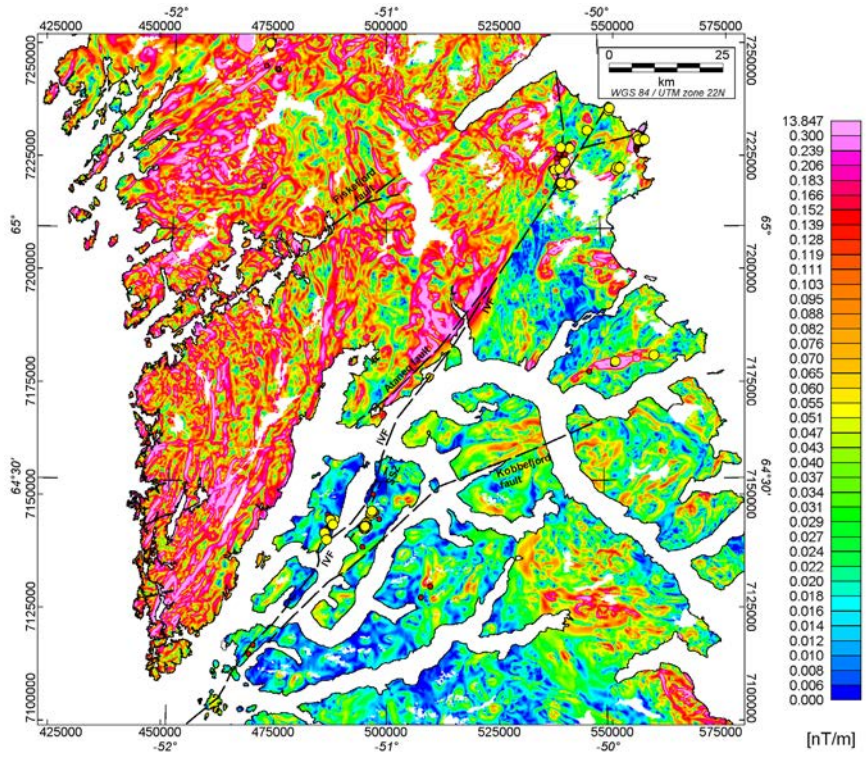


**Figure B25.** Amplitude of horizontal gradient vector of the TMI from regional aeromagnetic data, 200 m grid cell size.

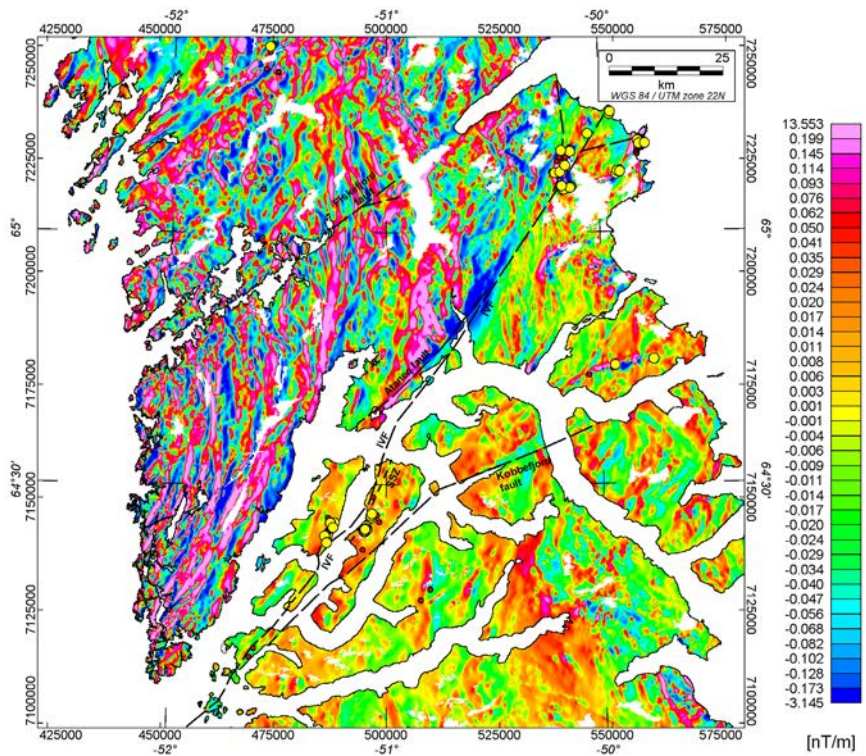


**Figure B26.** Horizontal gradient in east direction of TMI from regional aeromagnetic data, 200 m grid cell size.

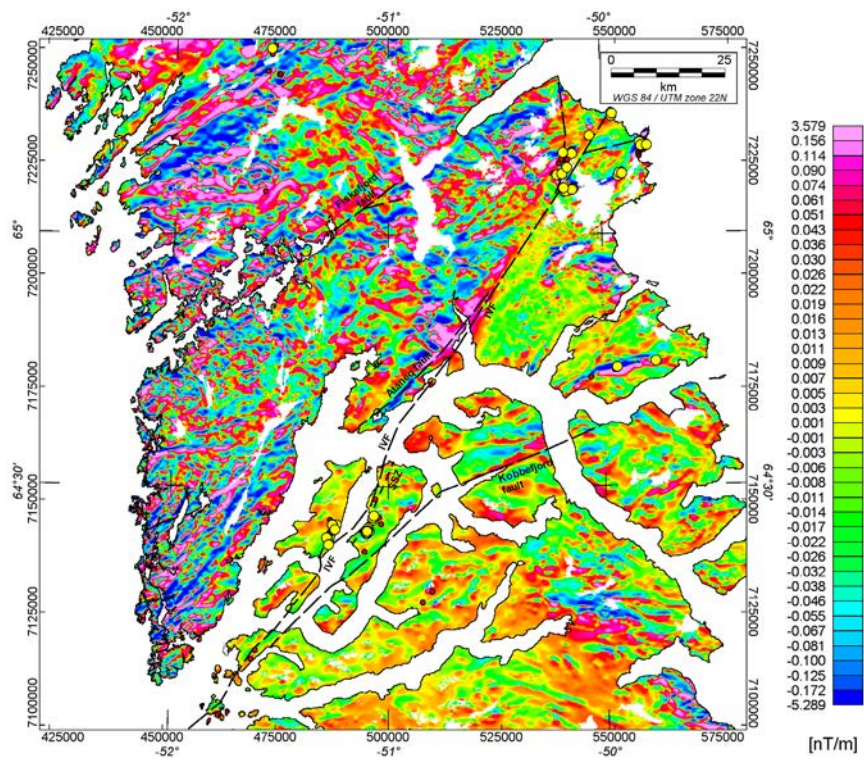


**Figure B27.** Horizontal gradient in north direction of TMI from regional aeromagnetic data, 200 m grid cell size.

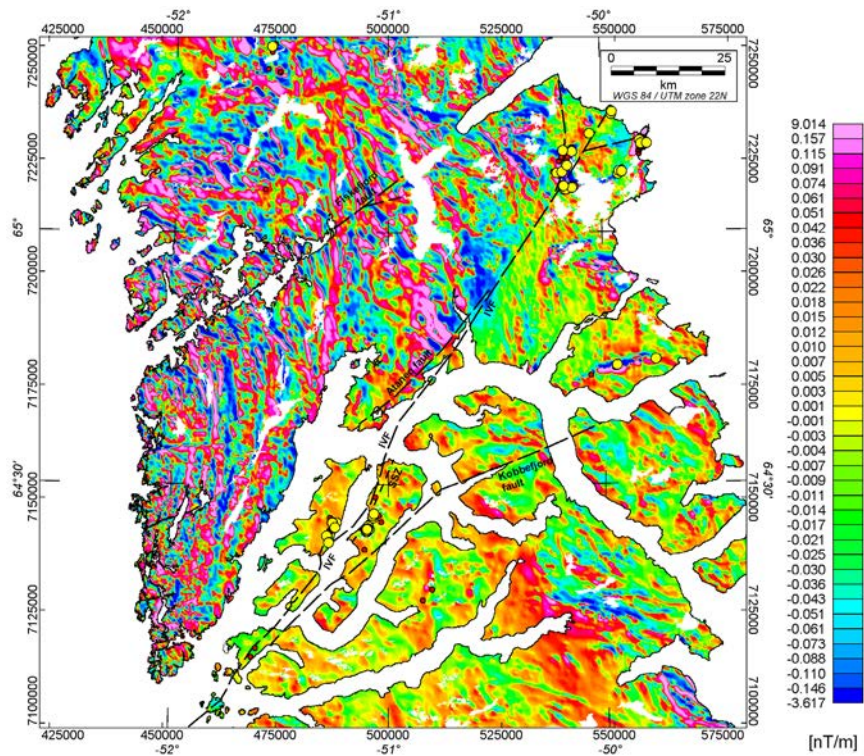


**Figure B28.** Horizontal gradient in northwest direction of TMI from regional aeromagnetic data, 200 m grid cell size.

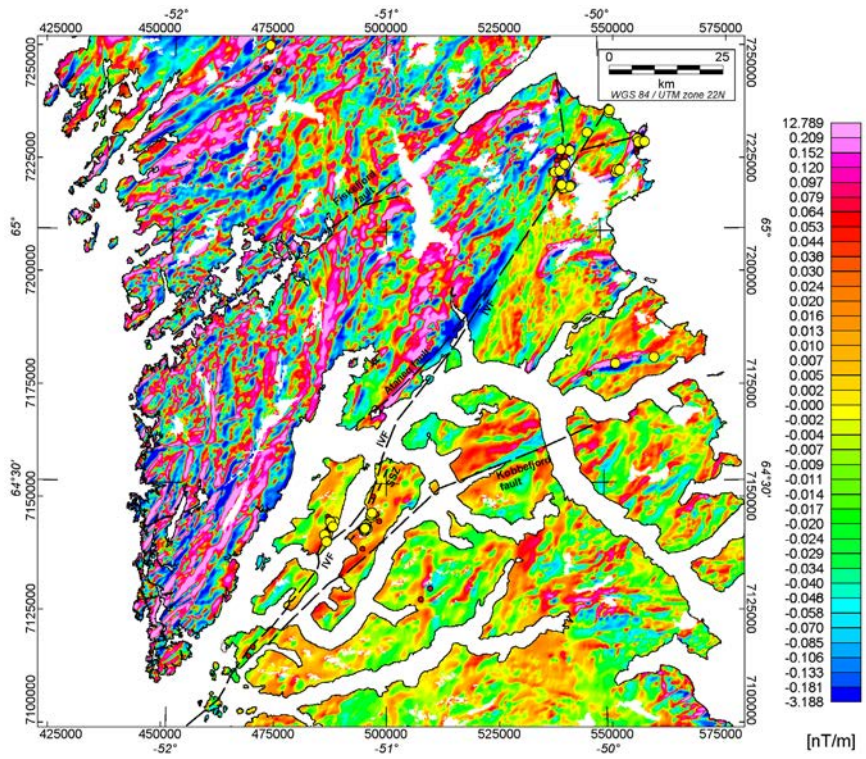


**Figure B29.** Horizontal gradient in southeast direction of TMI from regional aeromagnetic data, 200 m grid cell size.

## **Appendix C. Empirical distribution functions**

$\text{Al}_2\text{O}_3$ , GEUS, minimum curvature, 200 m  
spread parameter 0.5%

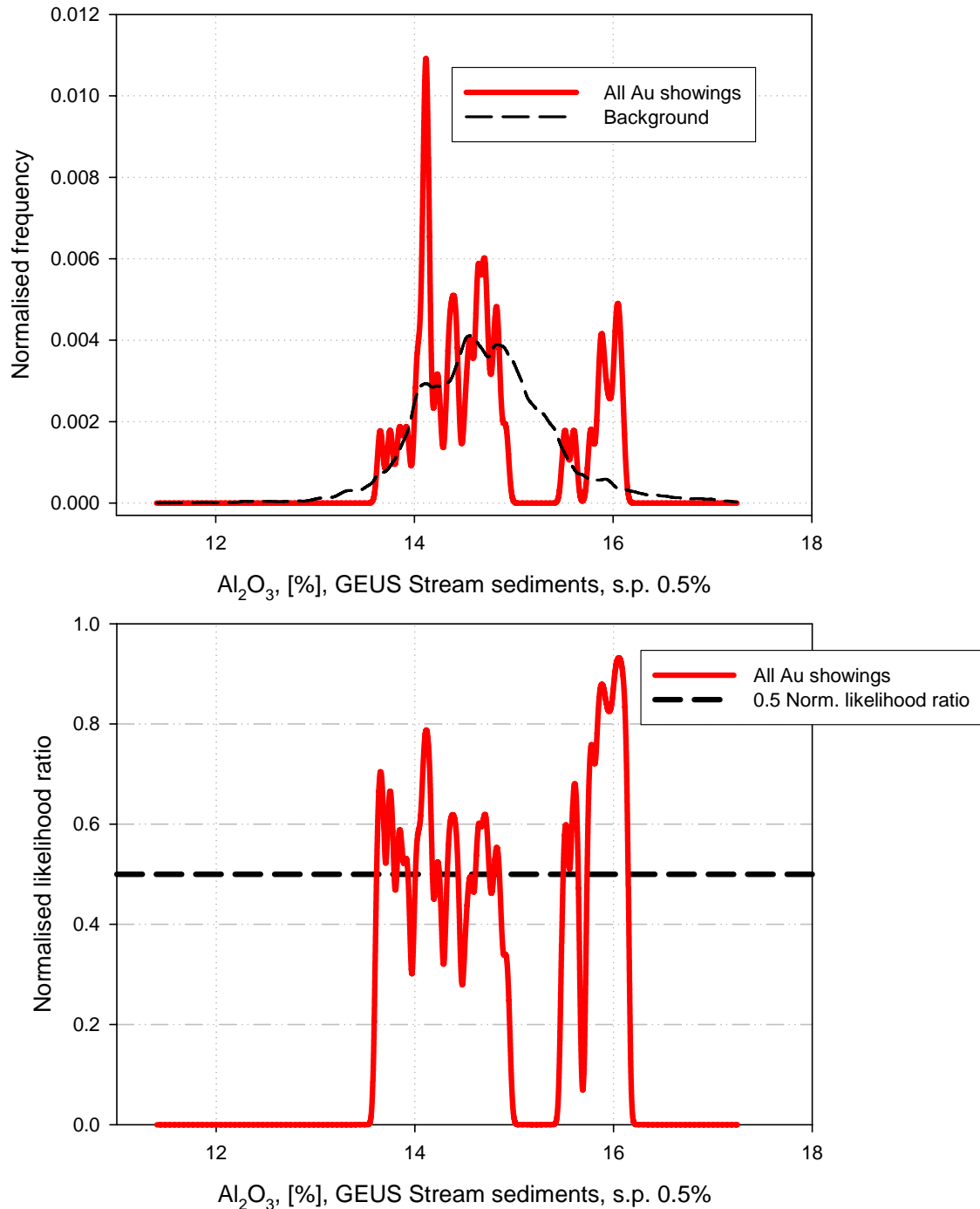


**Figure C1.**  $\text{Al}_2\text{O}_3$ , spread parameter 0.5% - Regional stream sediment geochemistry from GEUS.

$\text{Al}_2\text{O}_3$ , GEUS, minimum curvature, 200 m  
spread parameter 2%

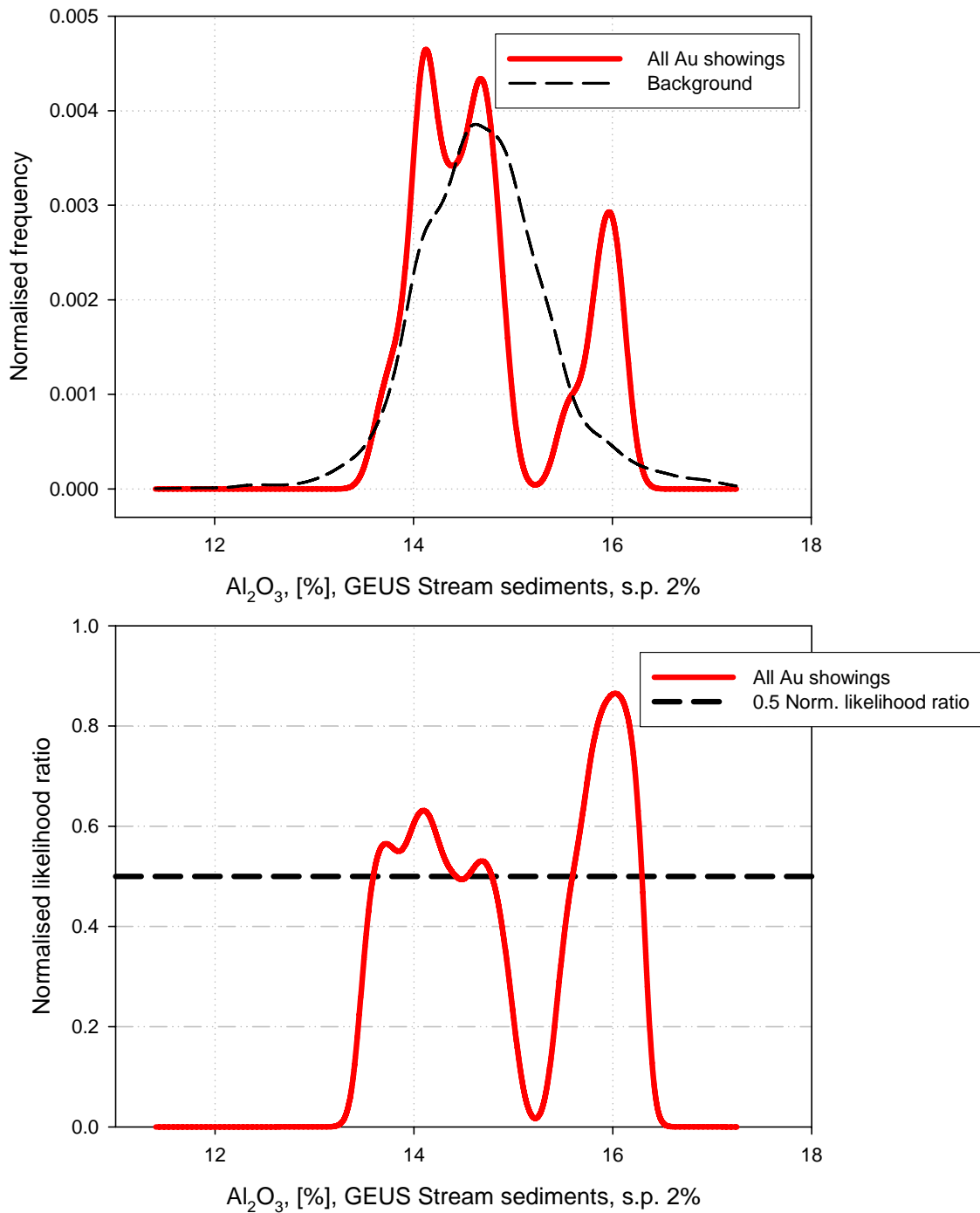


**Figure C2.**  $\text{Al}_2\text{O}_3$ , spread parameter 2% - Regional stream sediment geochemistry from GEUS.

$\text{Al}_2\text{O}_3$ , GEUS, minimum curvature, 200 m  
spread parameter 4%

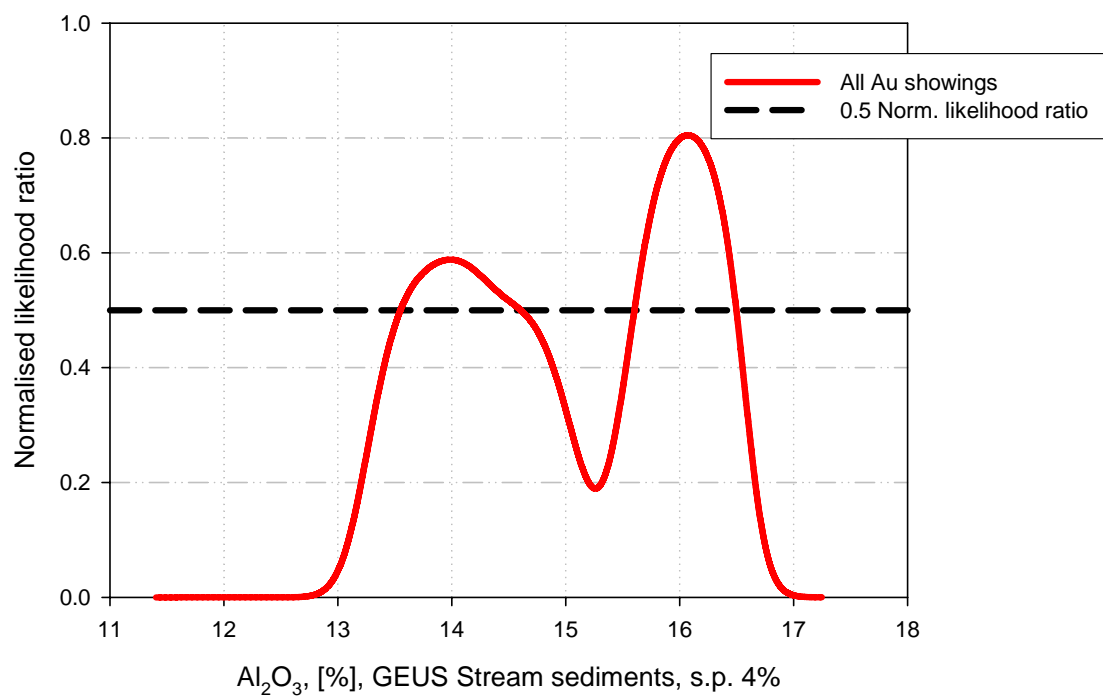
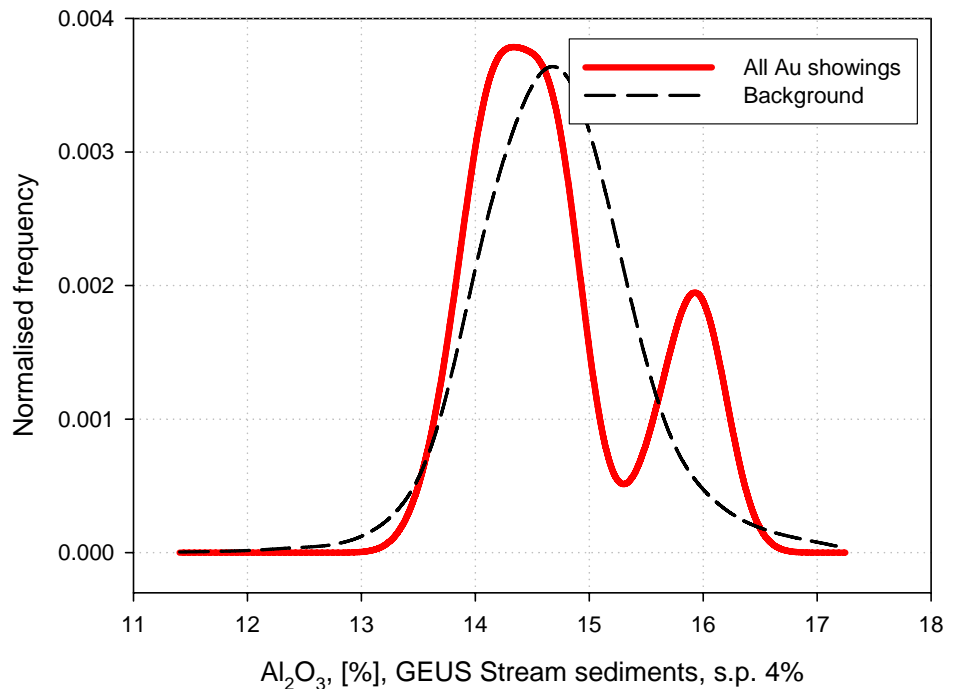


**Figure C3.**  $\text{Al}_2\text{O}_3$ , spread parameter 4% - Regional stream sediment geochemistry from GEUS.

As, GEUS, minimum curvature, modified 200 m  
spread parameter 0.5%

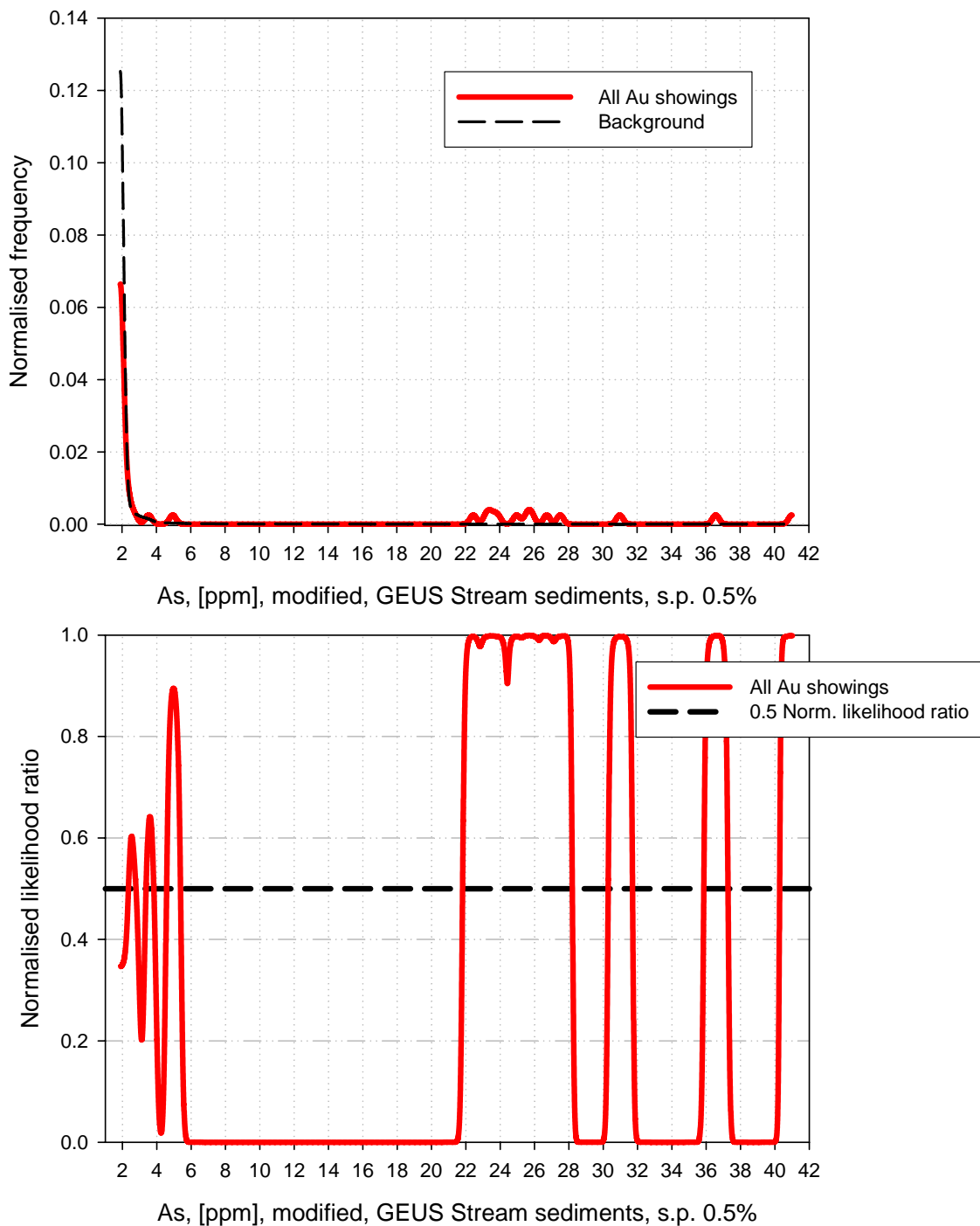


**Figure C4.** As, spread parameter 0.5% - Regional stream sediment geochemistry from GEUS.

As, GEUS, minimum curvature, modified 200 m  
spread parameter 2%

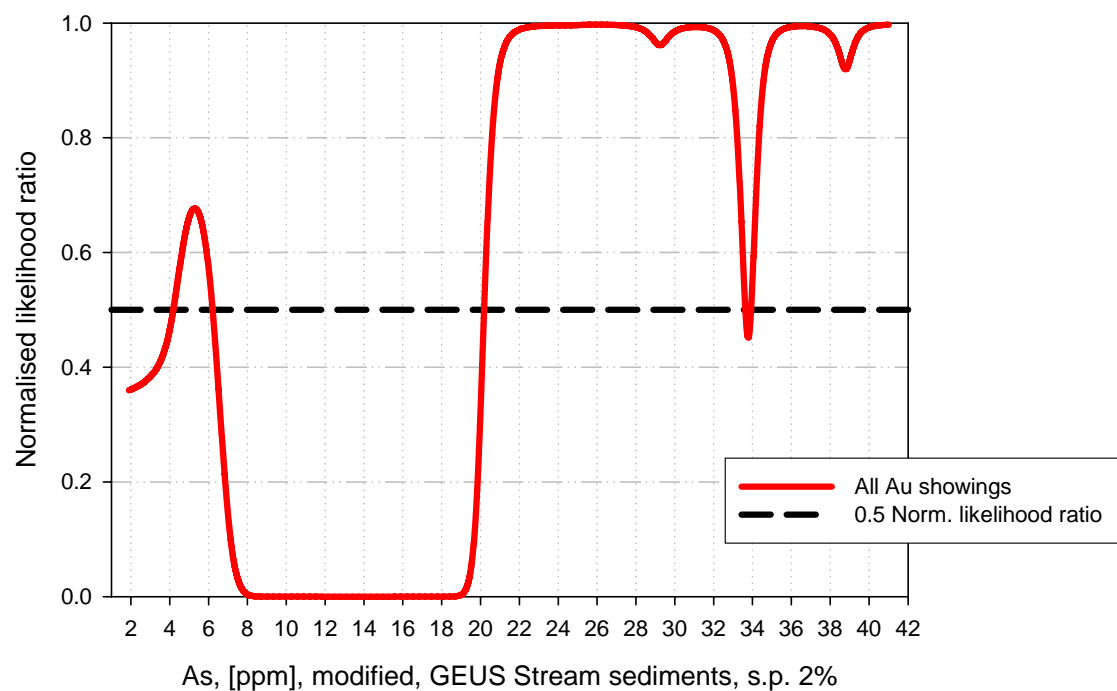
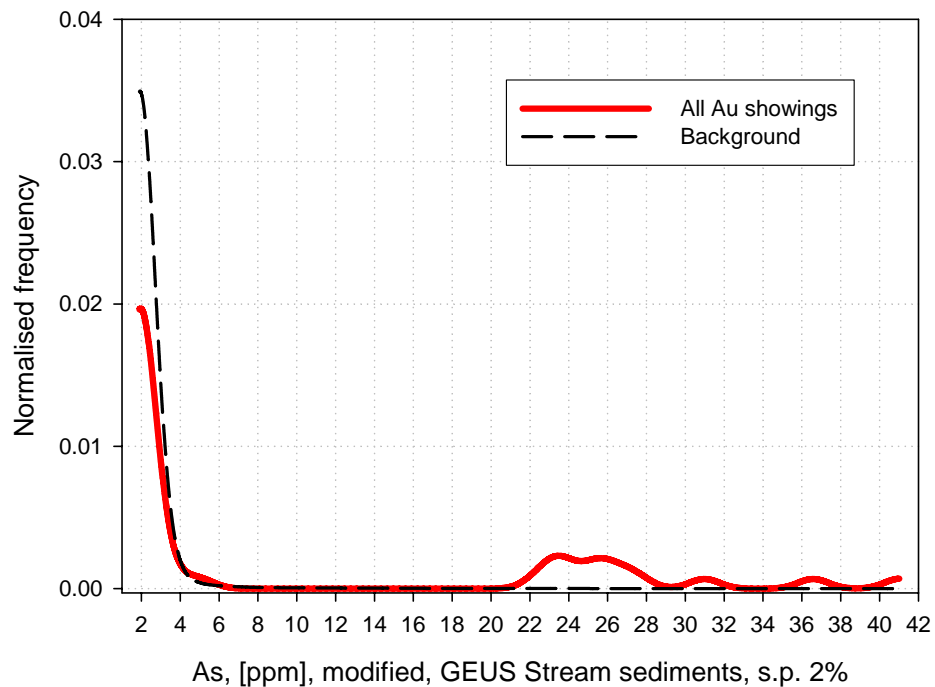


**Figure C5.** As, spread parameter 2% - Regional stream sediment geochemistry from GEUS.

As, GEUS, minimum curvature, modified 200 m  
spread parameter 4%

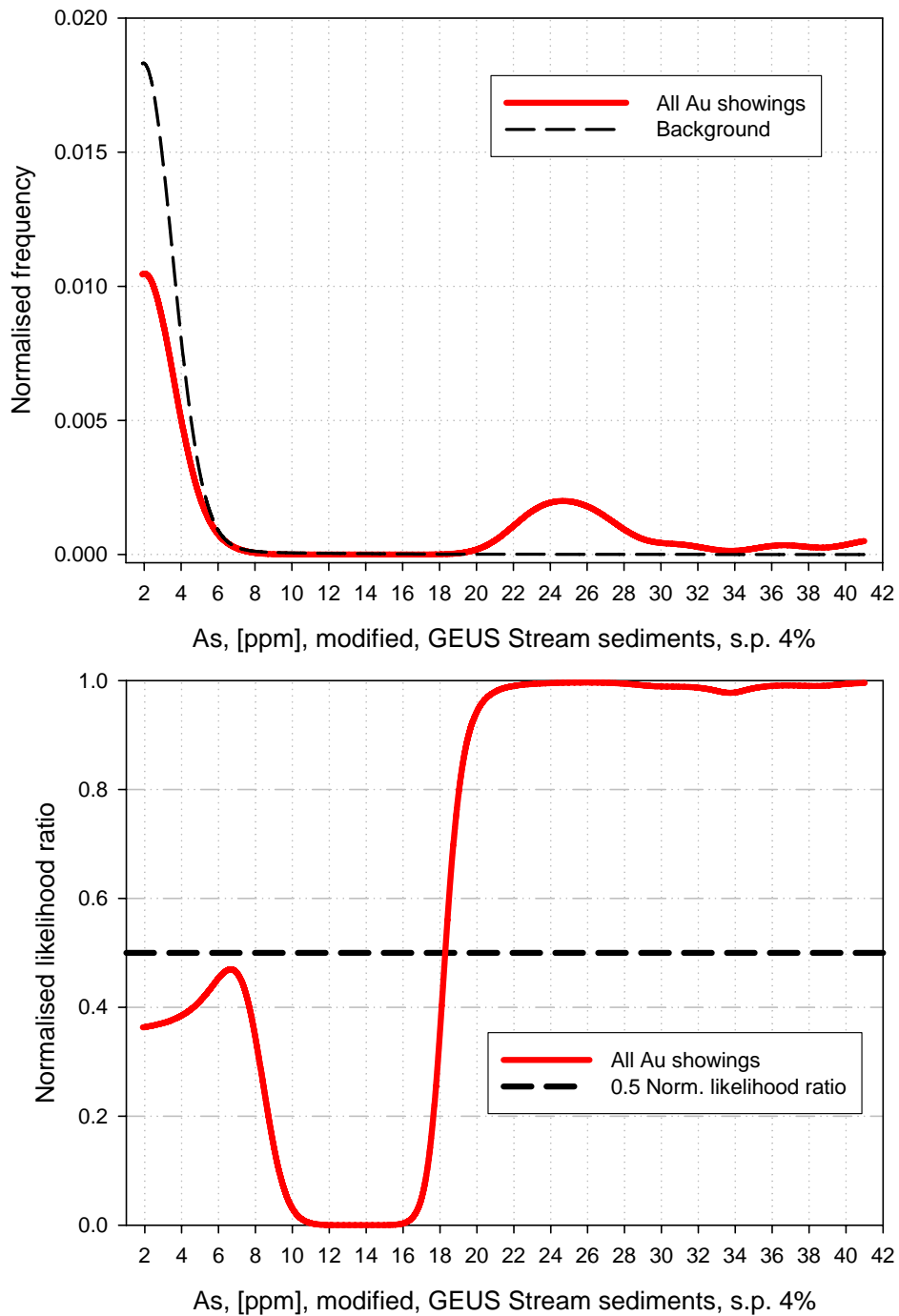


**Figure C6.** As, spread parameter 4% - Regional stream sediment geochemistry from GEUS.

Au, GEUS, minimum curvature, modified 200 m  
spread parameter 0.5%

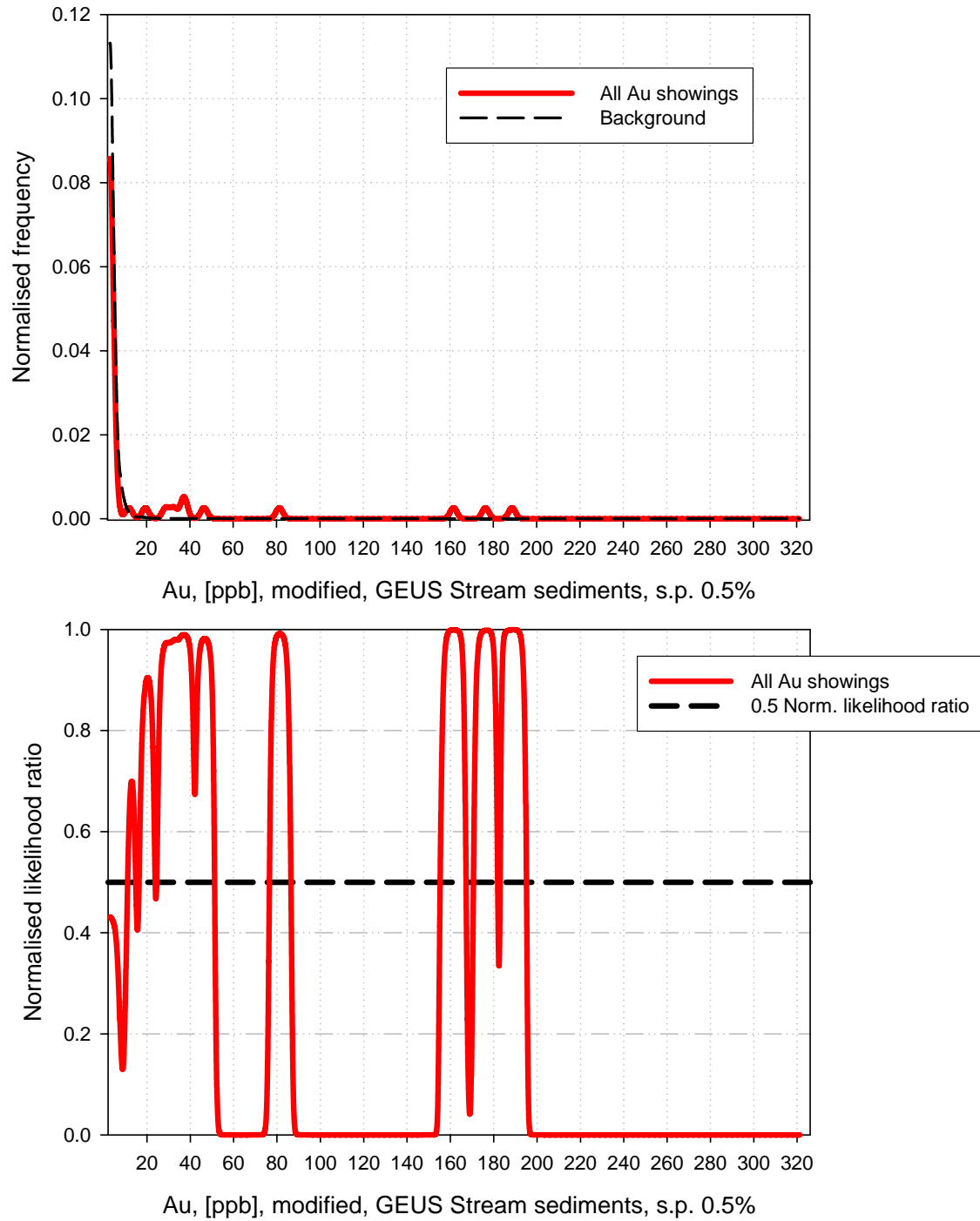
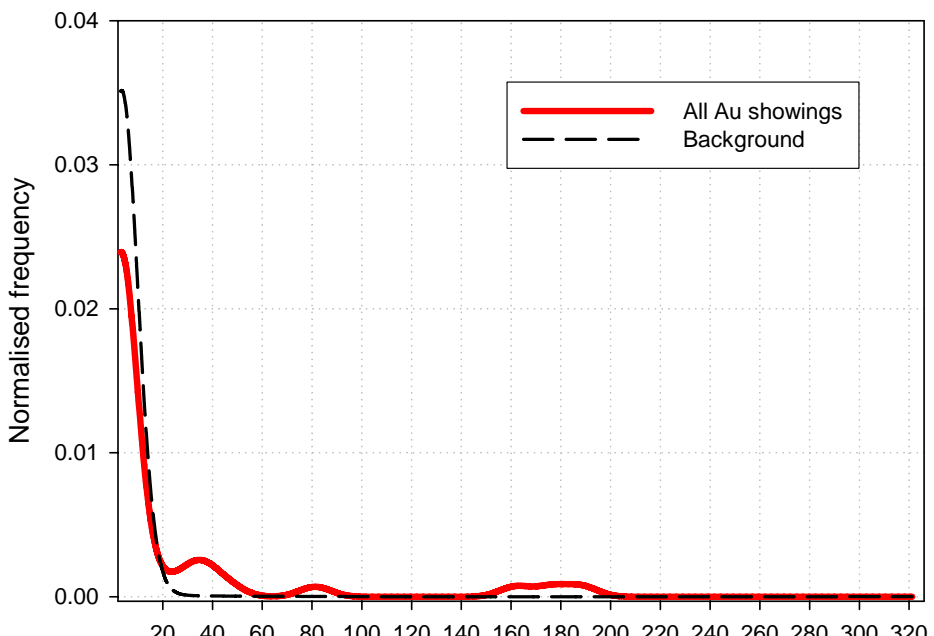


**Figure C7.** Au, spread parameter 0.5% - Regional stream sediment geochemistry from GEUS.

Au, GEUS, minimum curvature, modified, 200 m  
spread parameter 2%



Au, [ppb], modified, GEUS Stream sediments, s.p. 2%

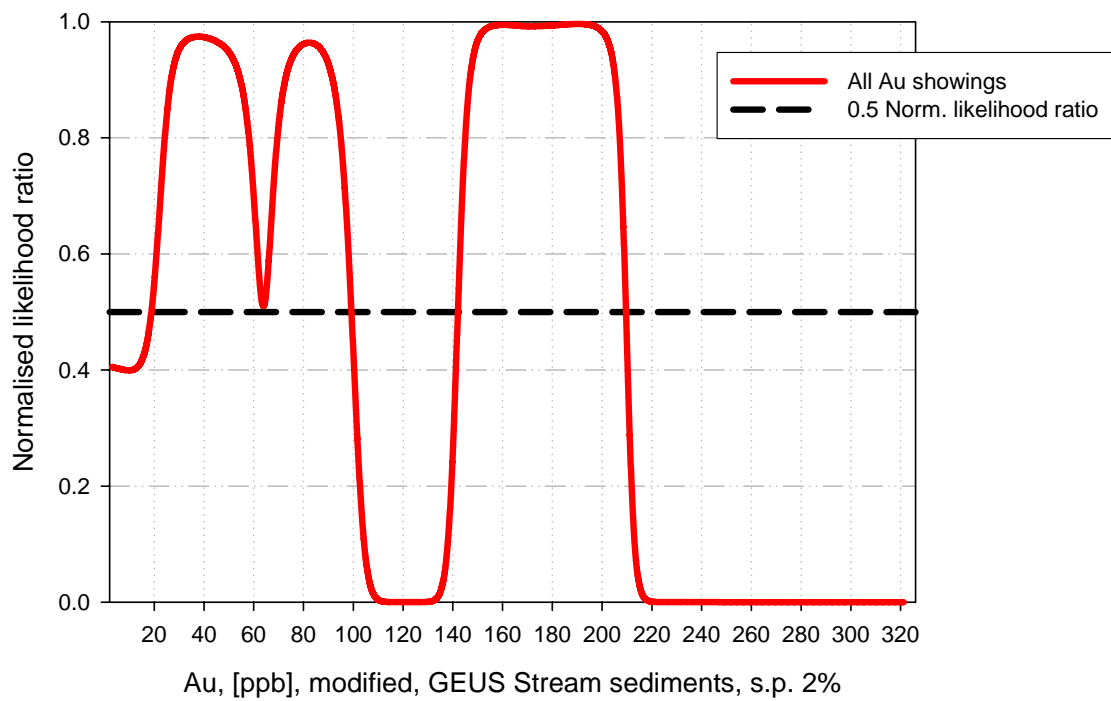
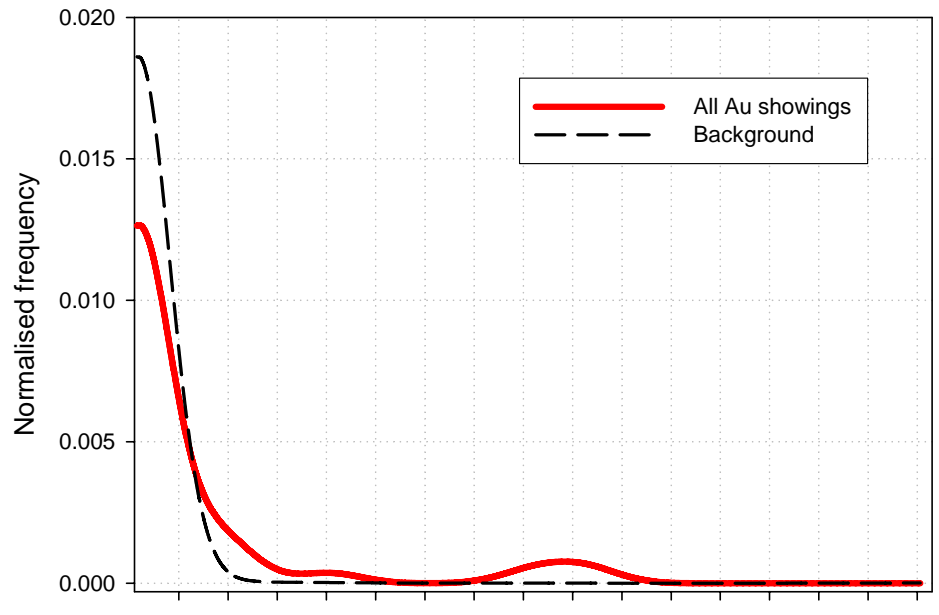


**Figure C8.** Au, spread parameter 2% - Regional stream sediment geochemistry from GEUS.

Au, GEUS, minimum curvature, modified, 200 m  
spread parameter 4%



Au, [ppb], modified, GEUS Stream sediments, s.p. 4%

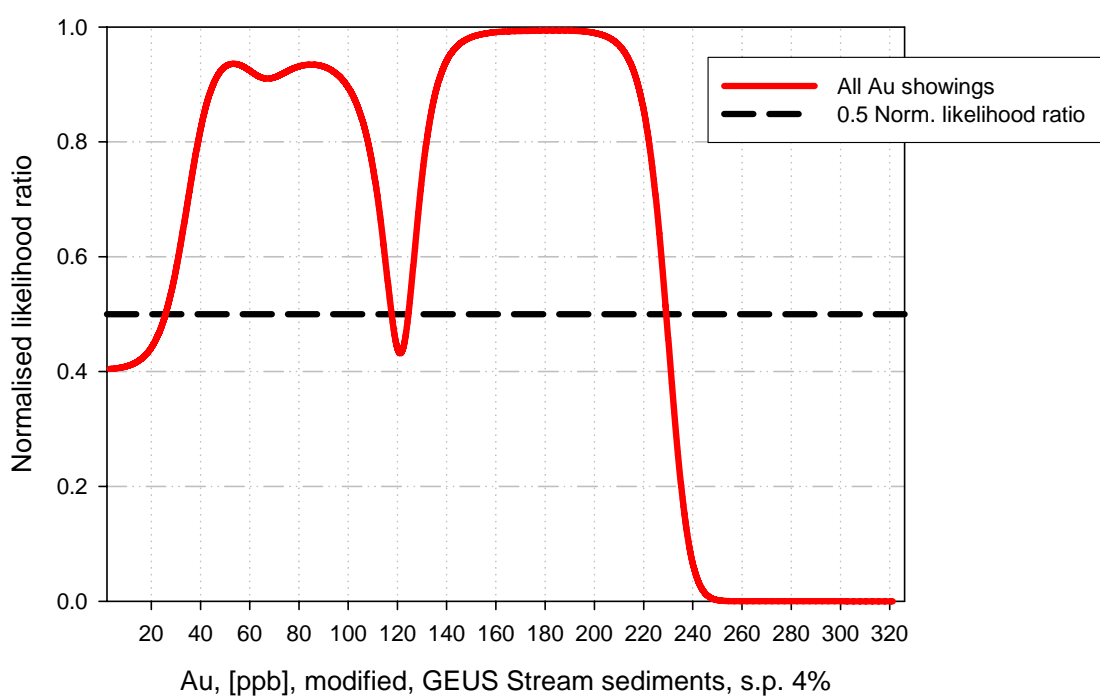


**Figure C9.** Au, spread parameter 4% - Regional stream sediment geochemistry from GEUS.

CaO, GEUS, minimum curvature, 200 m  
spread parameter 0.5%

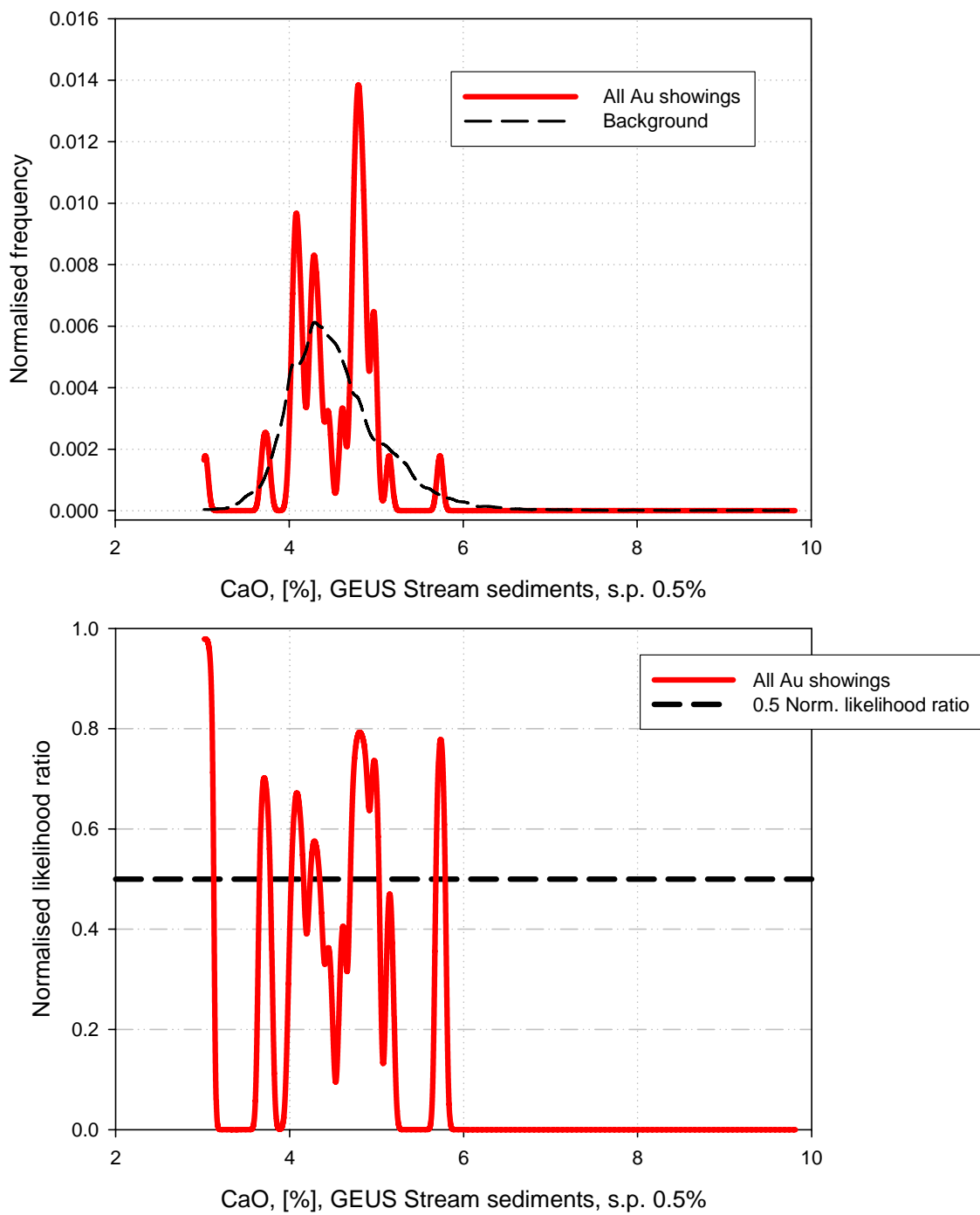


**Figure C10.** CaO, spread parameter 0.5% - Regional stream sediment geochemistry from GEUS.

CaO, GEUS, minimum curvature, 200 m  
spread parameter 2%

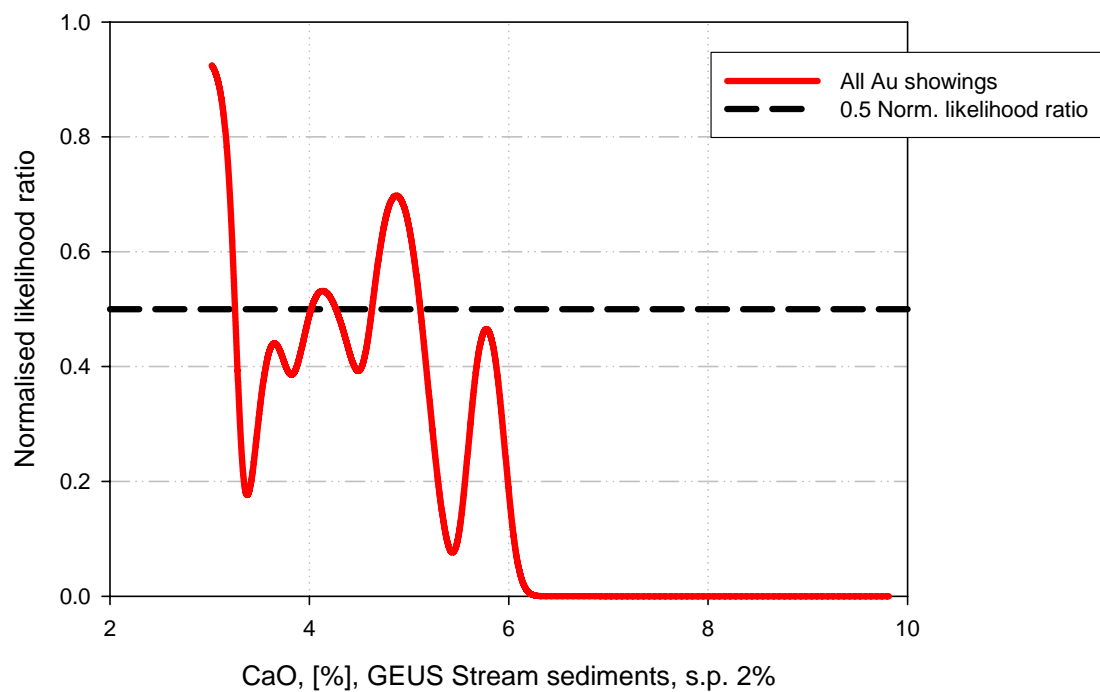
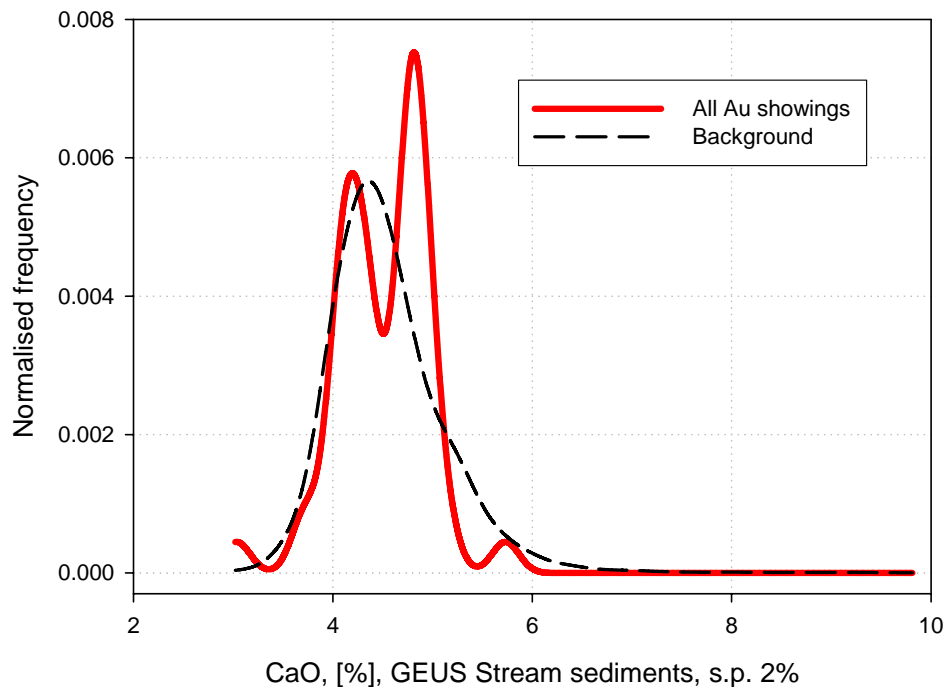


**Figure C11.** CaO, spread parameter 2% - Regional stream sediment geochemistry from GEUS.

CaO, GEUS, minimum curvature, 200 m  
spread parameter 4%

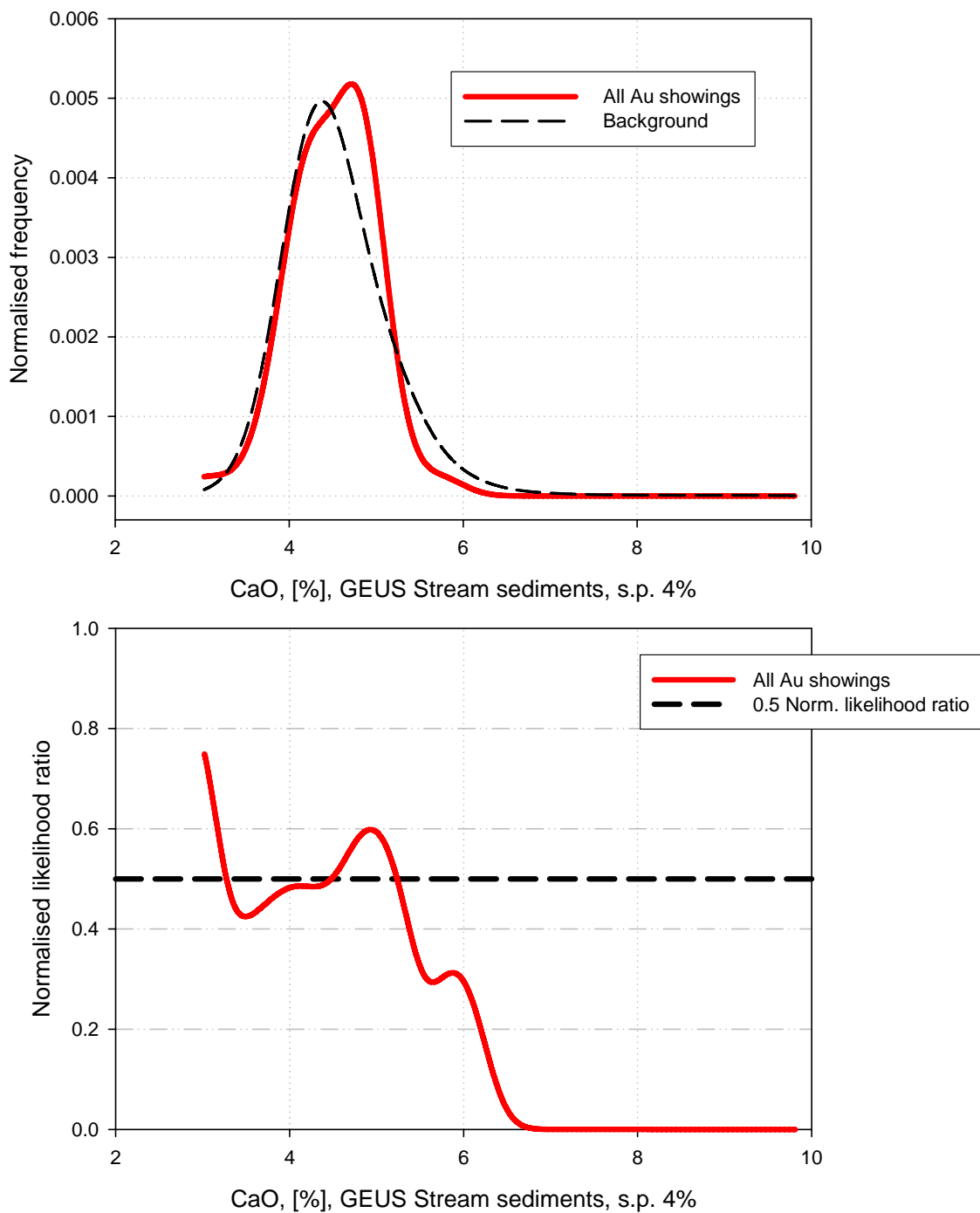


**Figure C12.** CaO, spread parameter 4% - Regional stream sediment geochemistry from GEUS.

Cs, GEUS, minimum curvature, modified 200 m  
spread parameter 0.5%

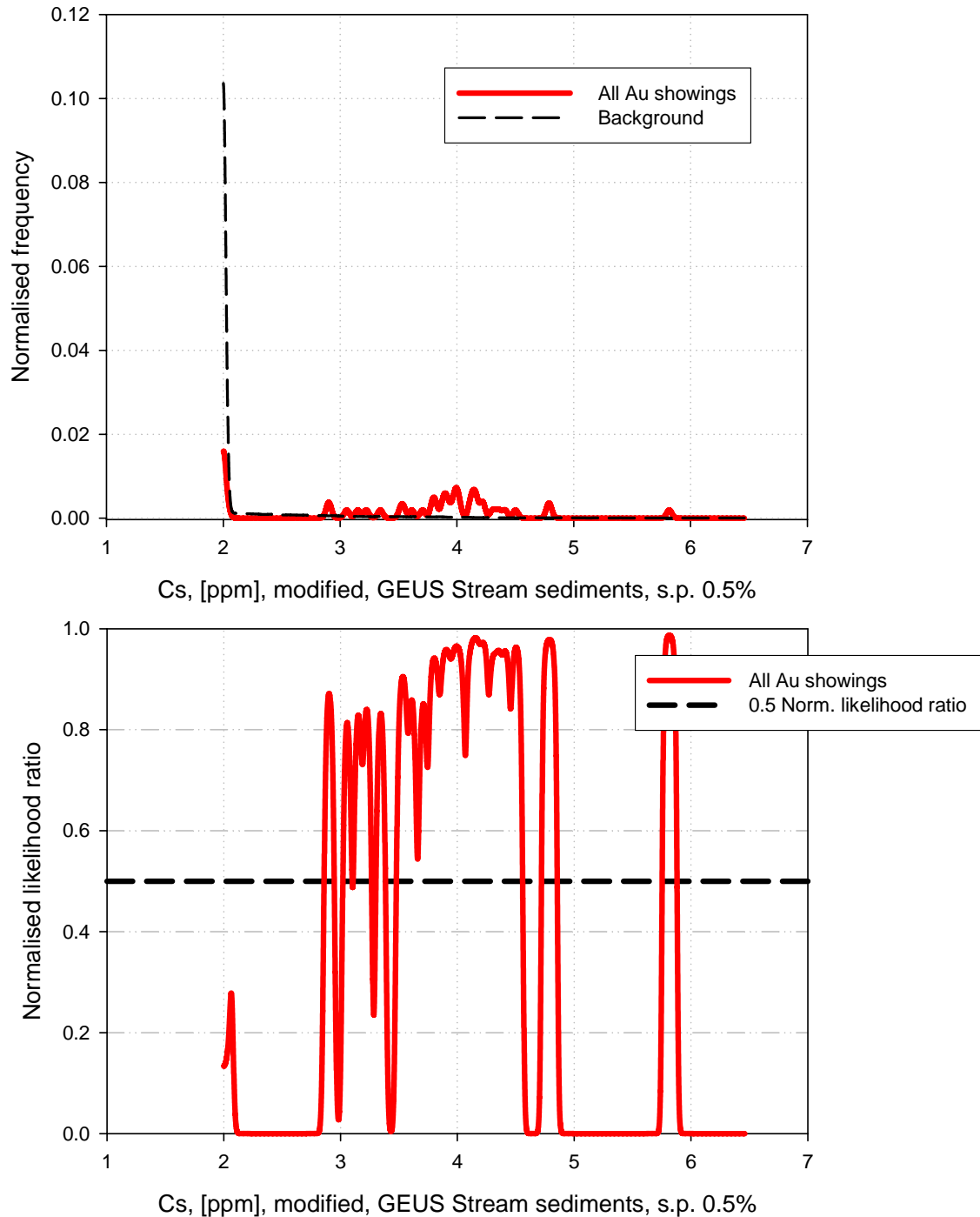


**Figure C13.** Cs, spread parameter 0.5% - Regional stream sediment geochemistry from GEUS.

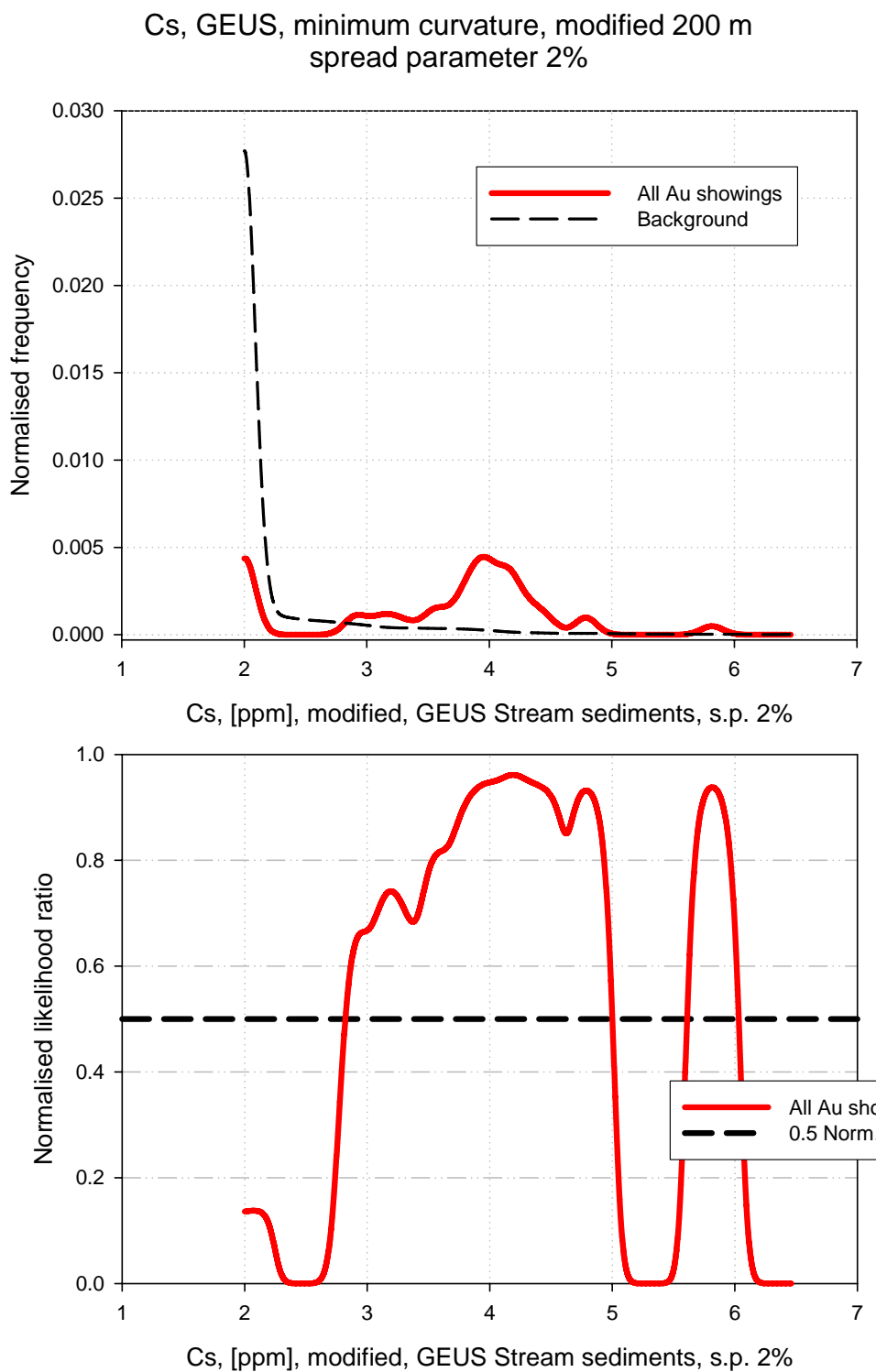


**Figure C14.** Cs, spread parameter 2% - Regional stream sediment geochemistry from GEUS.

Cs, GEUS, minimum curvature, modified 200 m  
spread parameter 4%

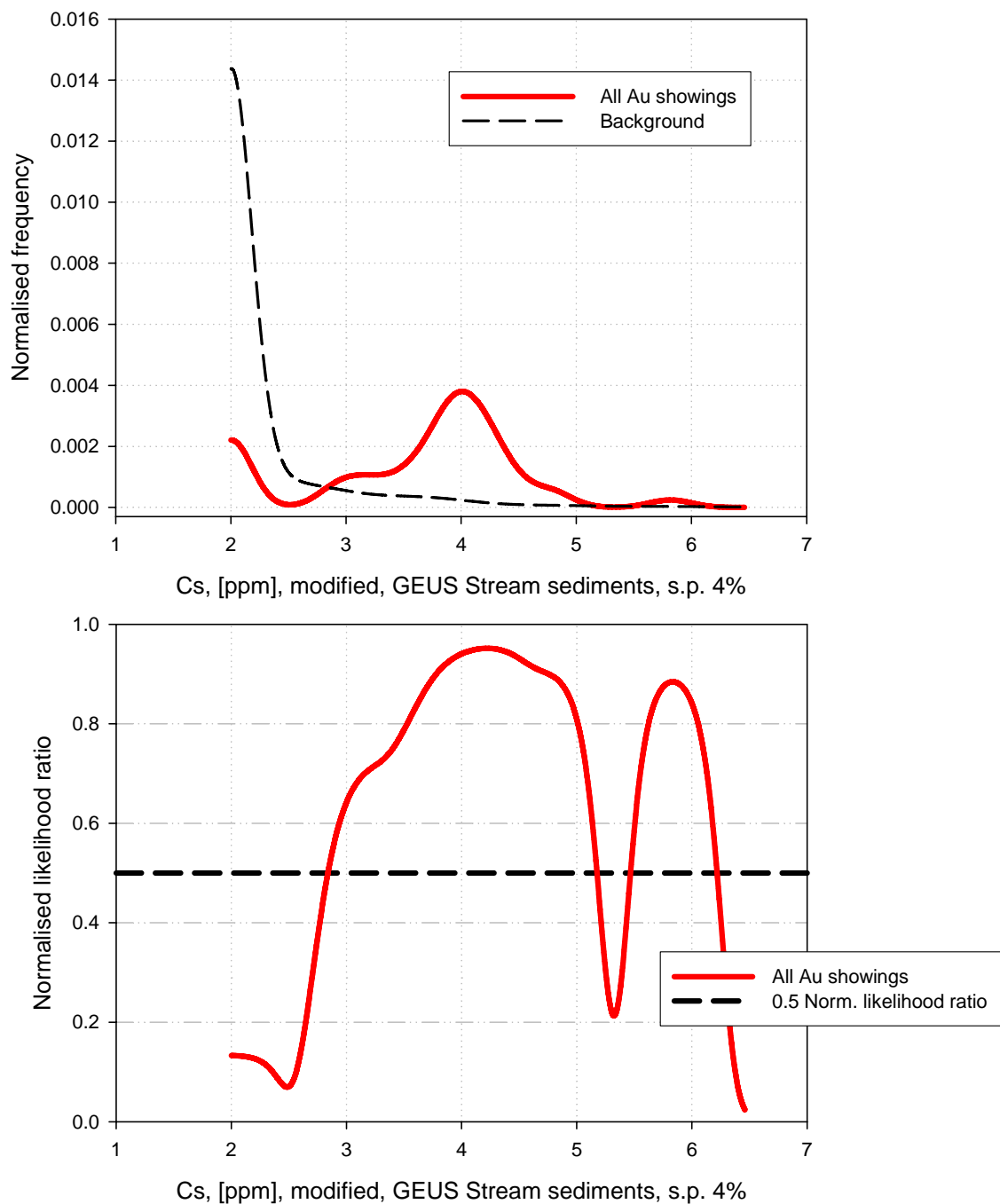


**Figure C15.** Cs, spread parameter 4% - Regional stream sediment geochemistry from GEUS.

$\text{Fe}_2\text{O}_3$ , GEUS, minimum curvature, 200 m  
spread parameter 0.5%

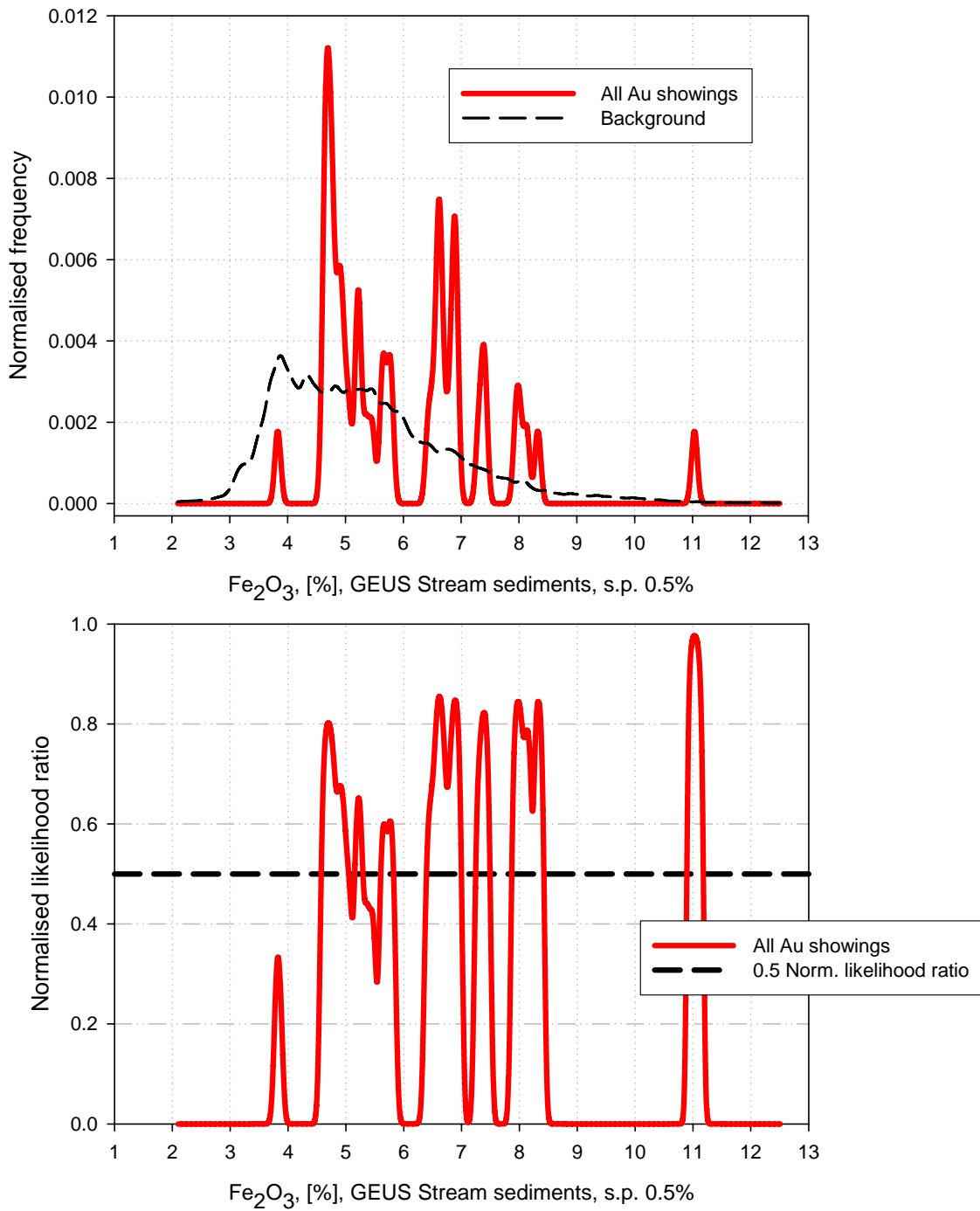


**Figure C16.**  $\text{Fe}_2\text{O}_3$ , spread parameter 0.5% - Regional stream sediment geochemistry from GEUS.

$\text{Fe}_2\text{O}_3$ , GEUS, minimum curvature, 200 m  
spread parameter 2%

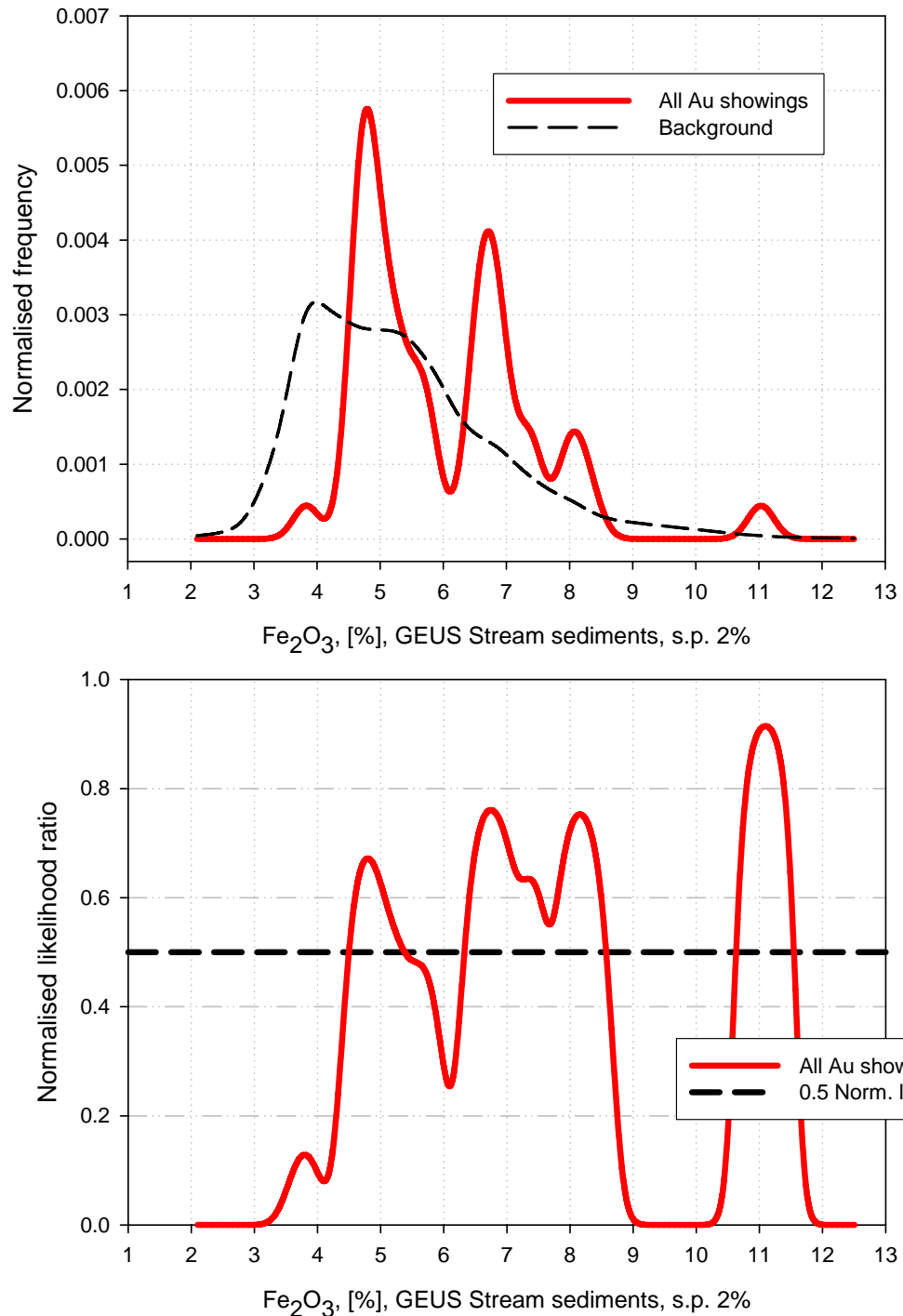


**Figure C17.**  $\text{Fe}_2\text{O}_3$ , spread parameter 2% - Regional stream sediment geochemistry from GEUS.

$\text{Fe}_2\text{O}_3$ , GEUS, minimum curvature, 200 m  
spread parameter 4%

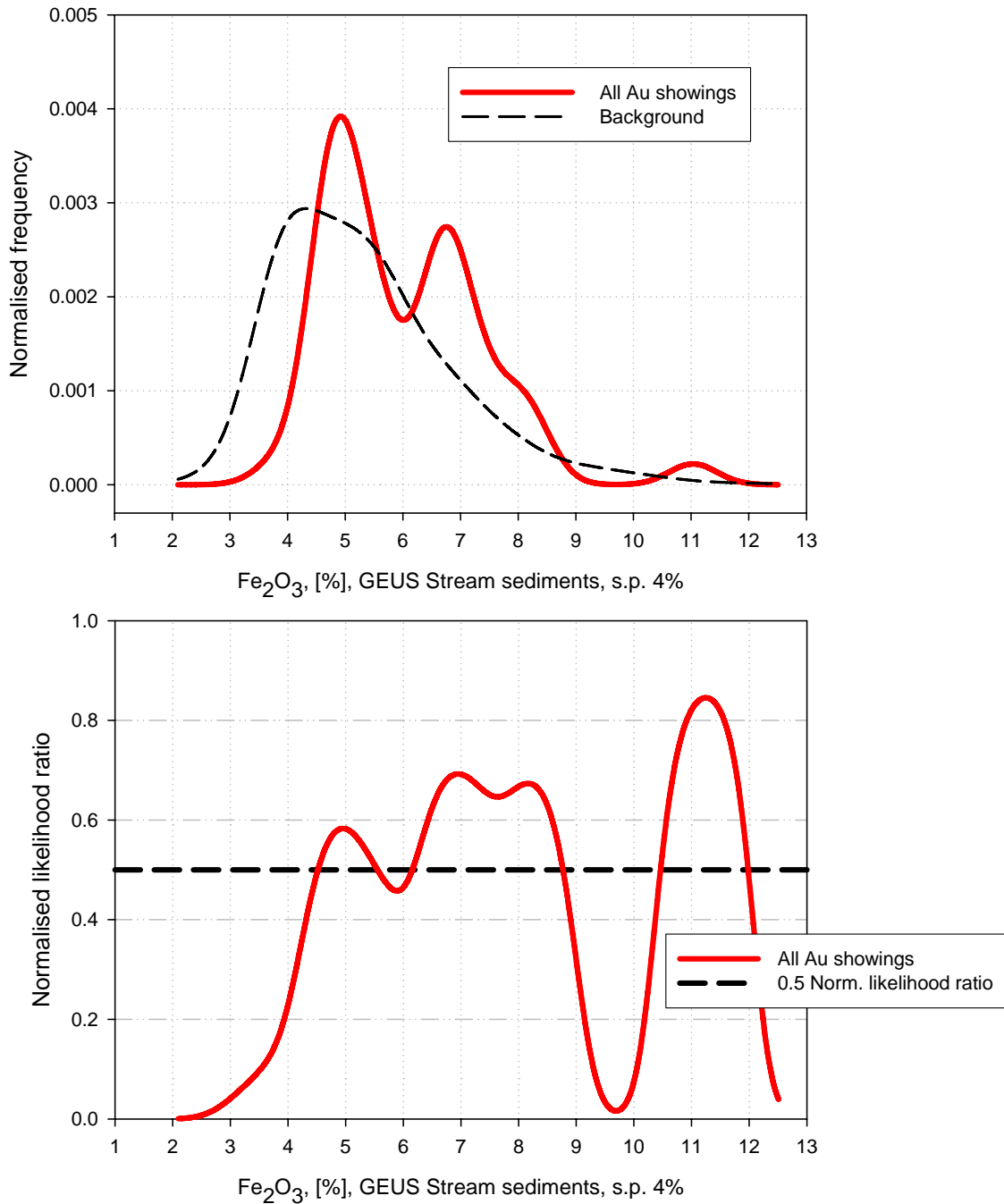


**Figure C18.**  $\text{Fe}_2\text{O}_3$ , spread parameter 4% - Regional stream sediment geochemistry from GEUS.

$K_2O$ , GEUS, minimum curvature, 200 m  
spread parameter 0.5%

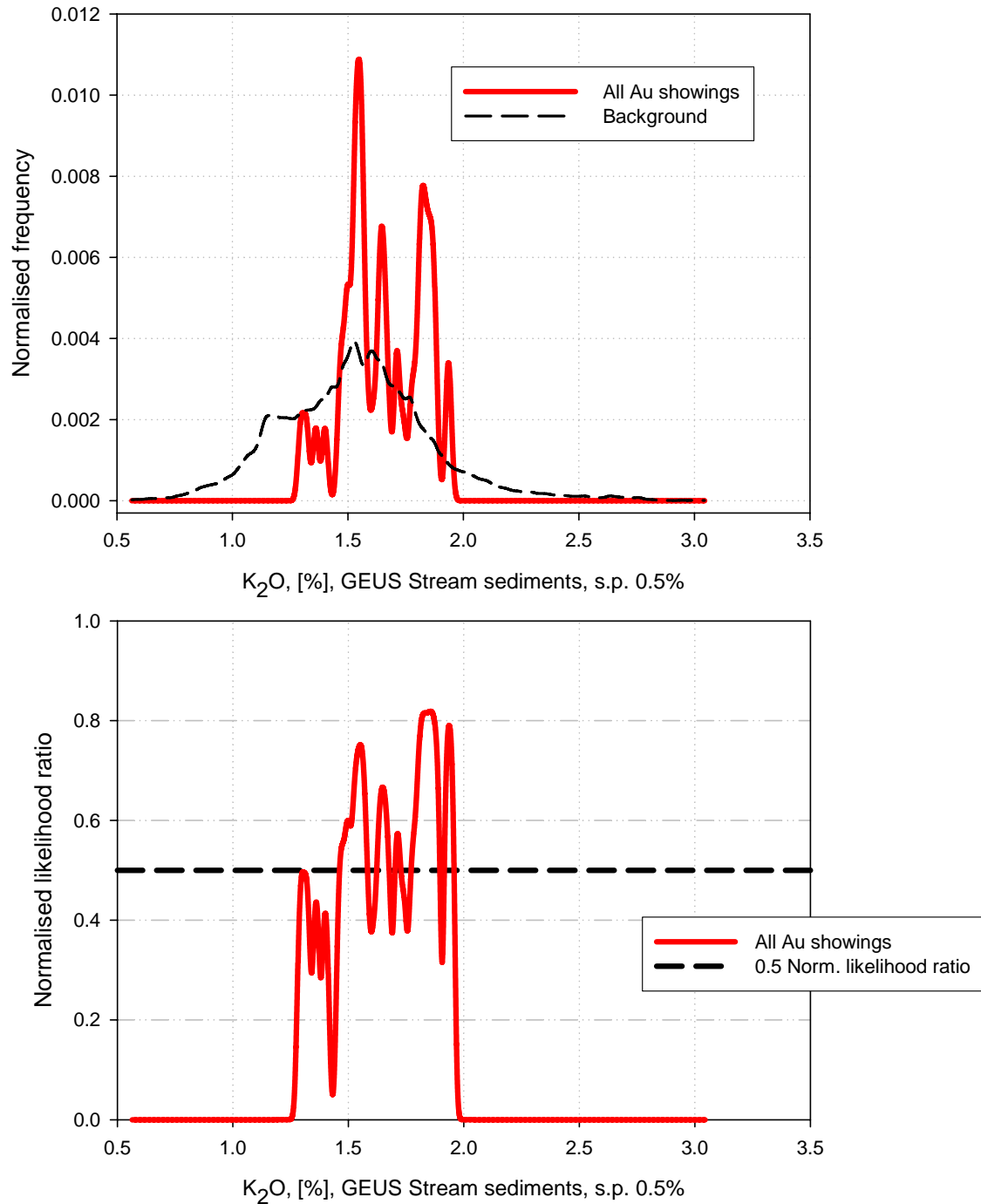


**Figure C19.**  $K_2O$ , spread parameter 0.5% - Regional stream sediment geochemistry from GEUS.

$K_2O$ , GEUS, minimum curvature, 200 m  
spread parameter 2%

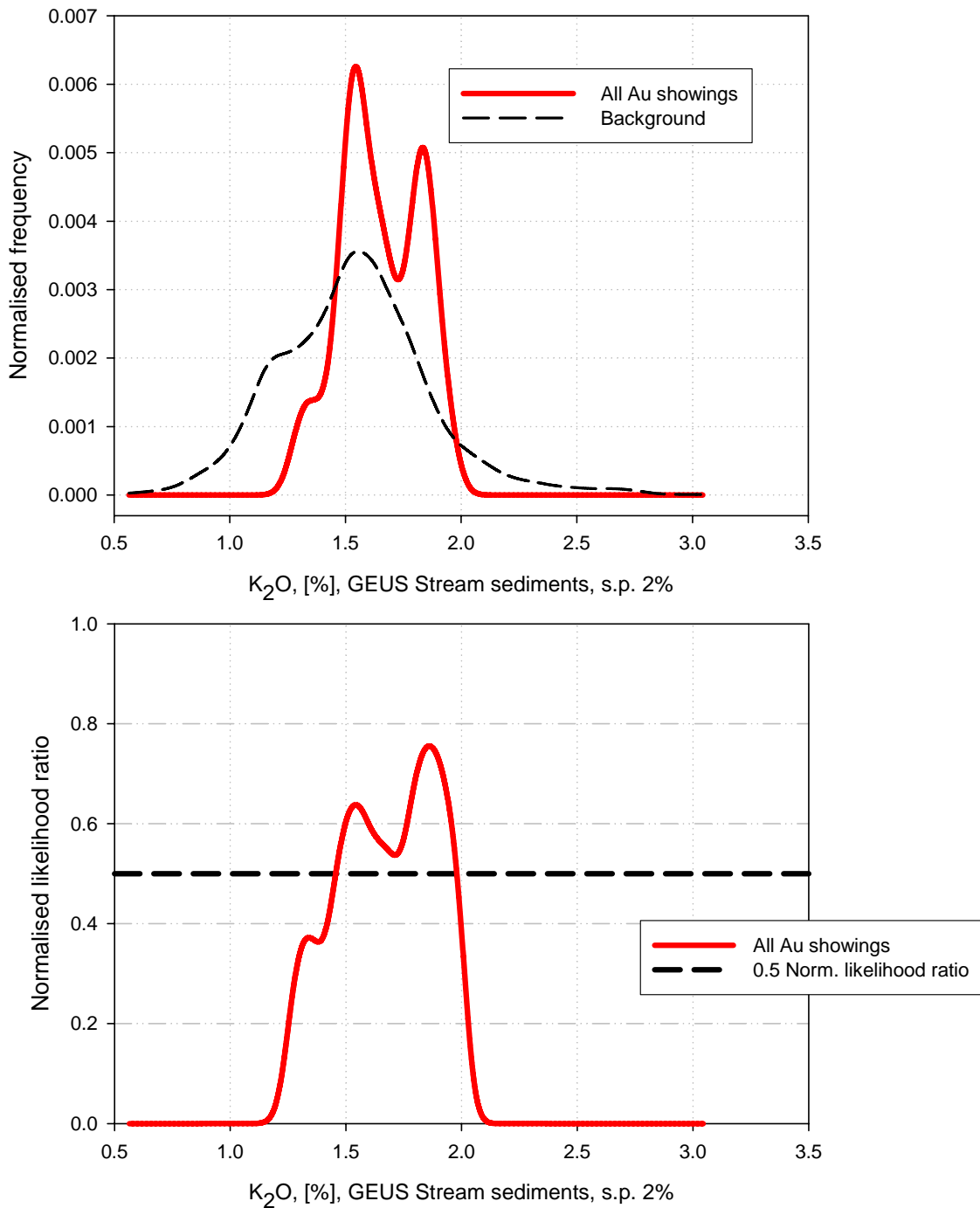


**Figure C20.**  $K_2O$ , spread parameter 2% - Regional stream sediment geochemistry from GEUS.

$K_2O$ , GEUS, minimum curvature, 200 m  
spread parameter 4%

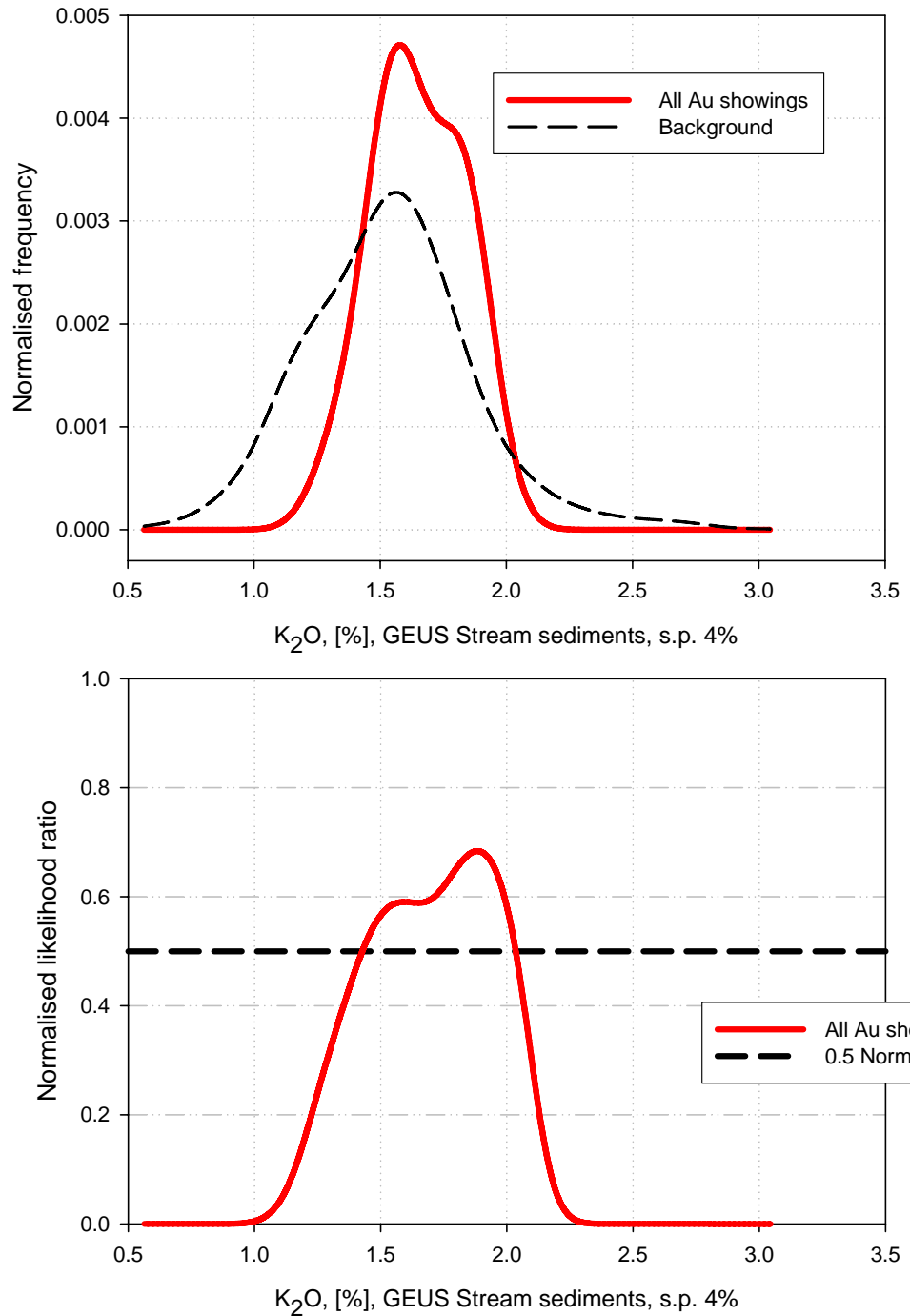


**Figure C21.**  $K_2O$ , spread parameter 4% - Regional stream sediment geochemistry from GEUS.

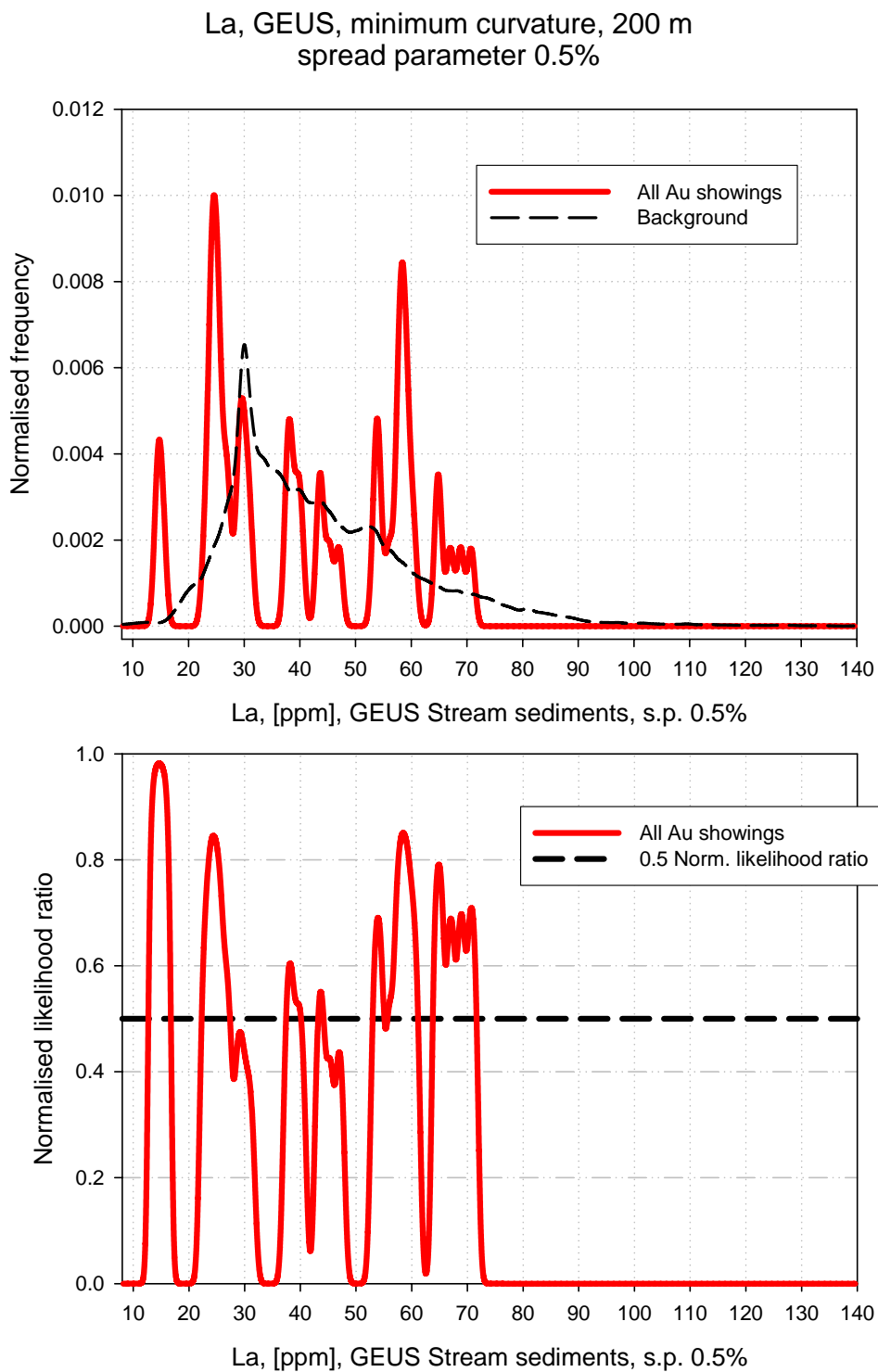


**Figure C22.** *La, spread parameter 0.5% - Regional stream sediment geochemistry from GEUS.*

La, GEUS, minimum curvature, 200 m  
spread parameter 2%

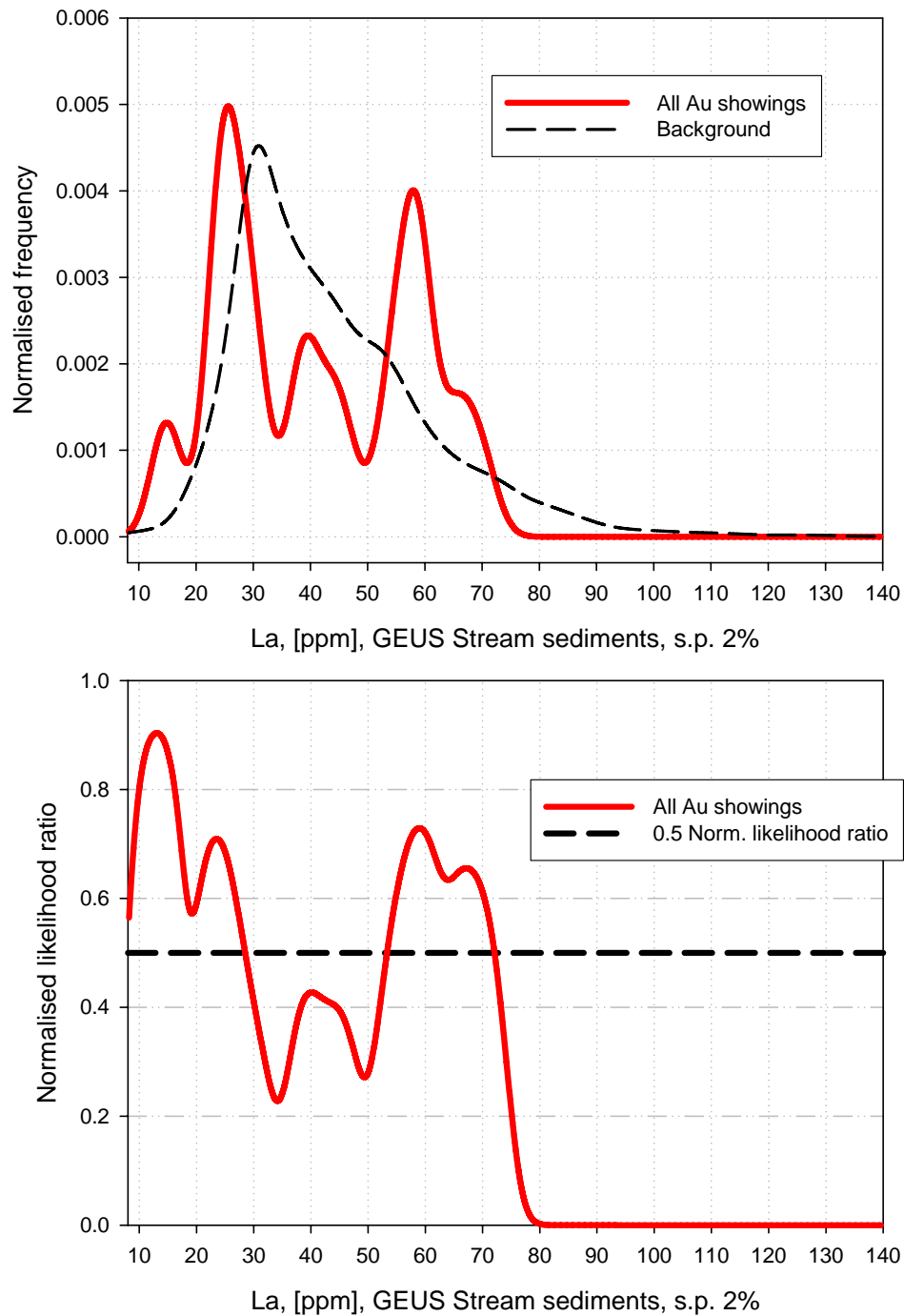


**Figure C23.** La, spread parameter 2% - Regional stream sediment geochemistry from GEUS.

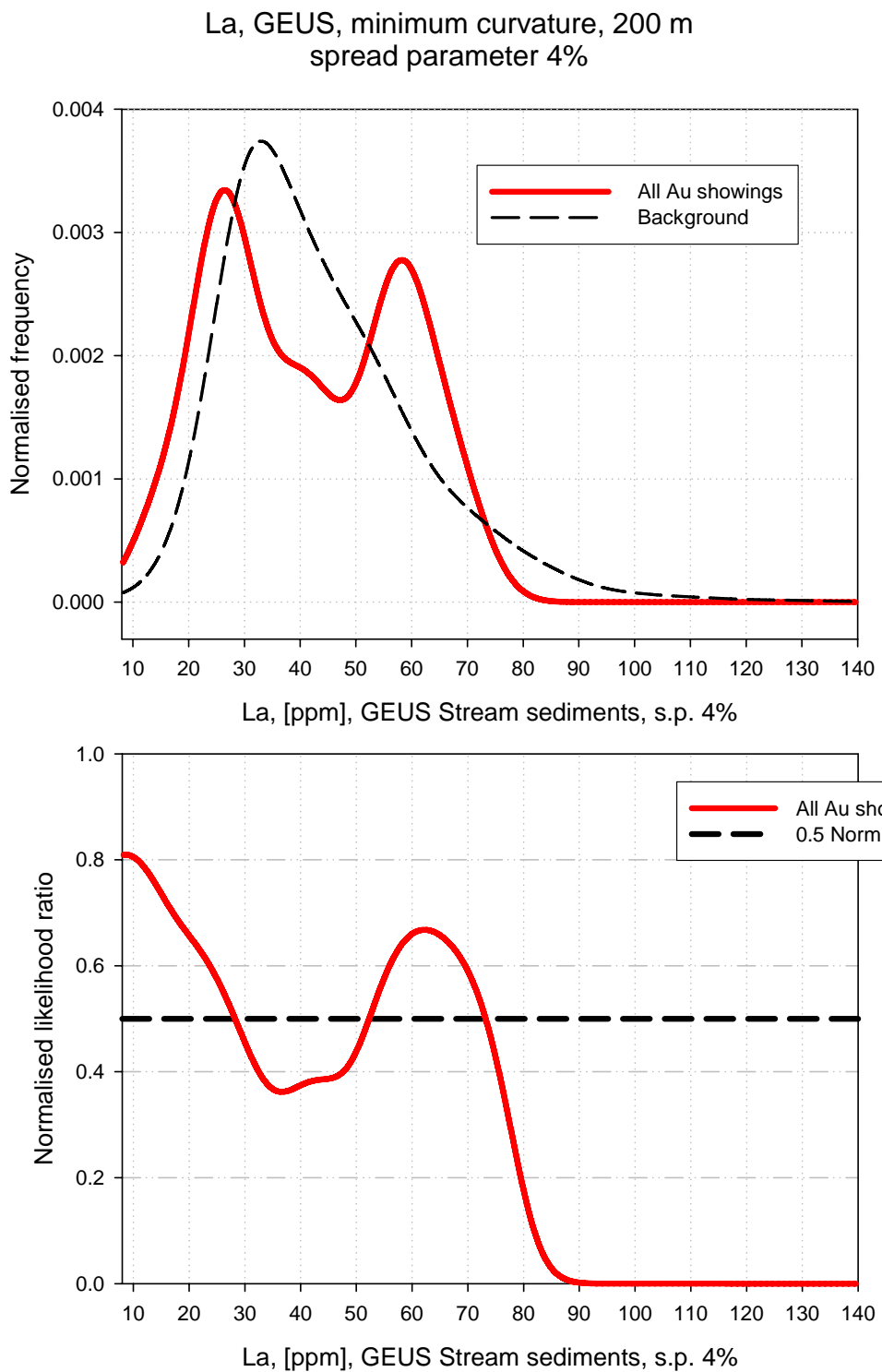


**Figure C24.** La, spread parameter 4% - Regional stream sediment geochemistry from GEUS.

MgO, GEUS, minimum curvature, 200 m  
spread parameter 0.5%

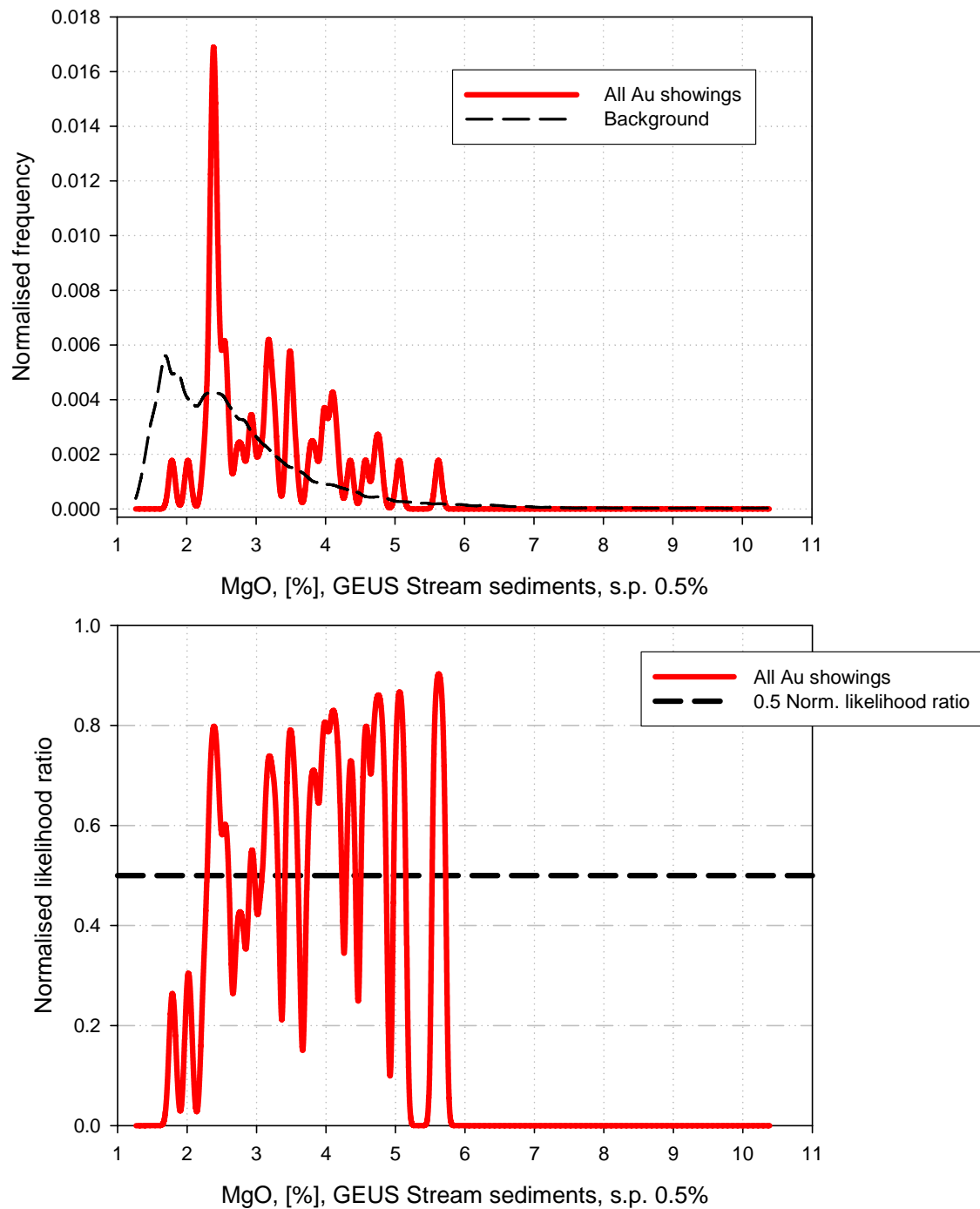


**Figure C25.** MgO, spread parameter 0.5% - Regional stream sediment geochemistry from GEUS.

MgO, GEUS, minimum curvature, 200 m  
spread parameter 2%

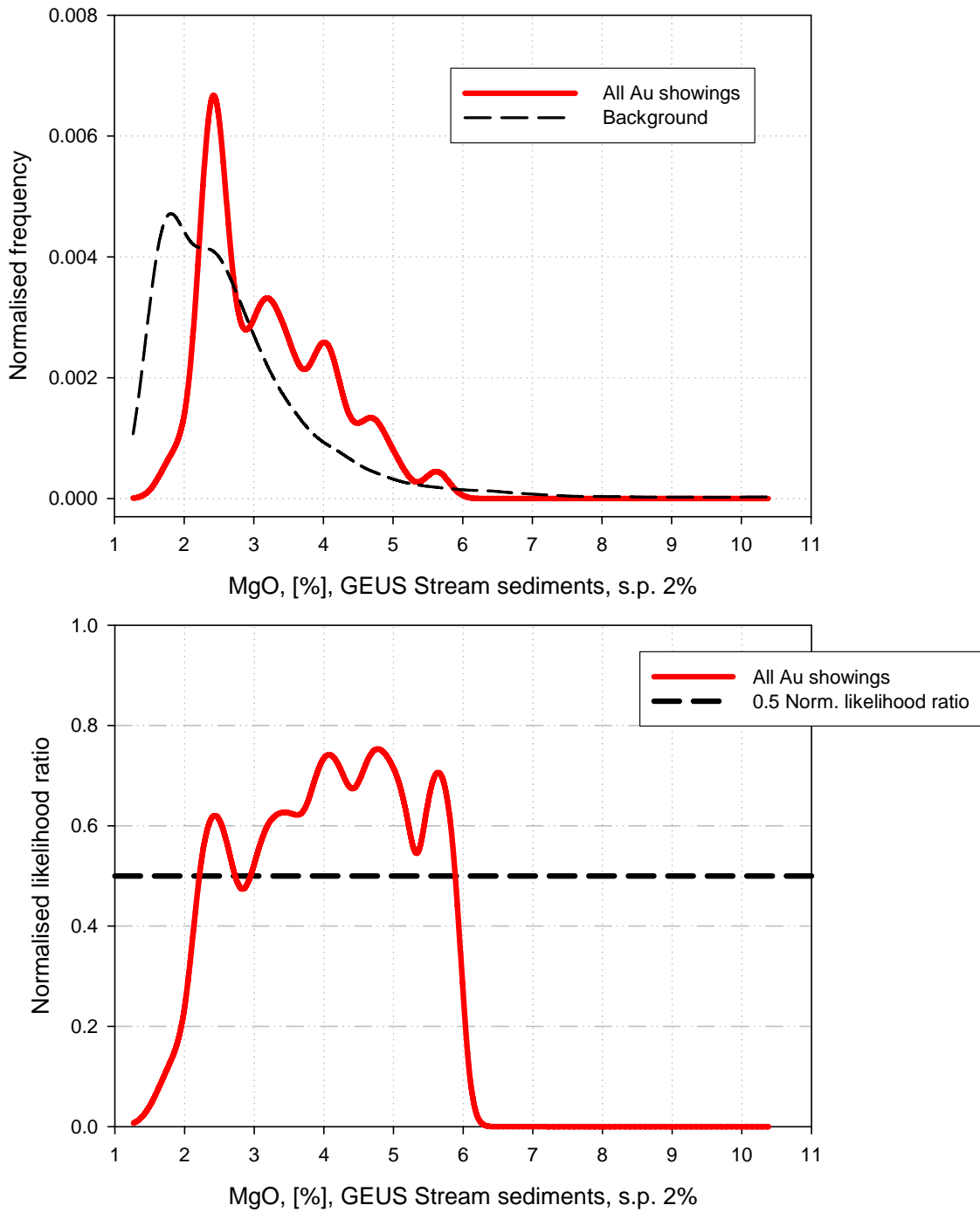


**Figure C26.** MgO, spread parameter 2% - Regional stream sediment geochemistry from GEUS.

MgO, GEUS, minimum curvature, 200 m  
spread parameter 4%

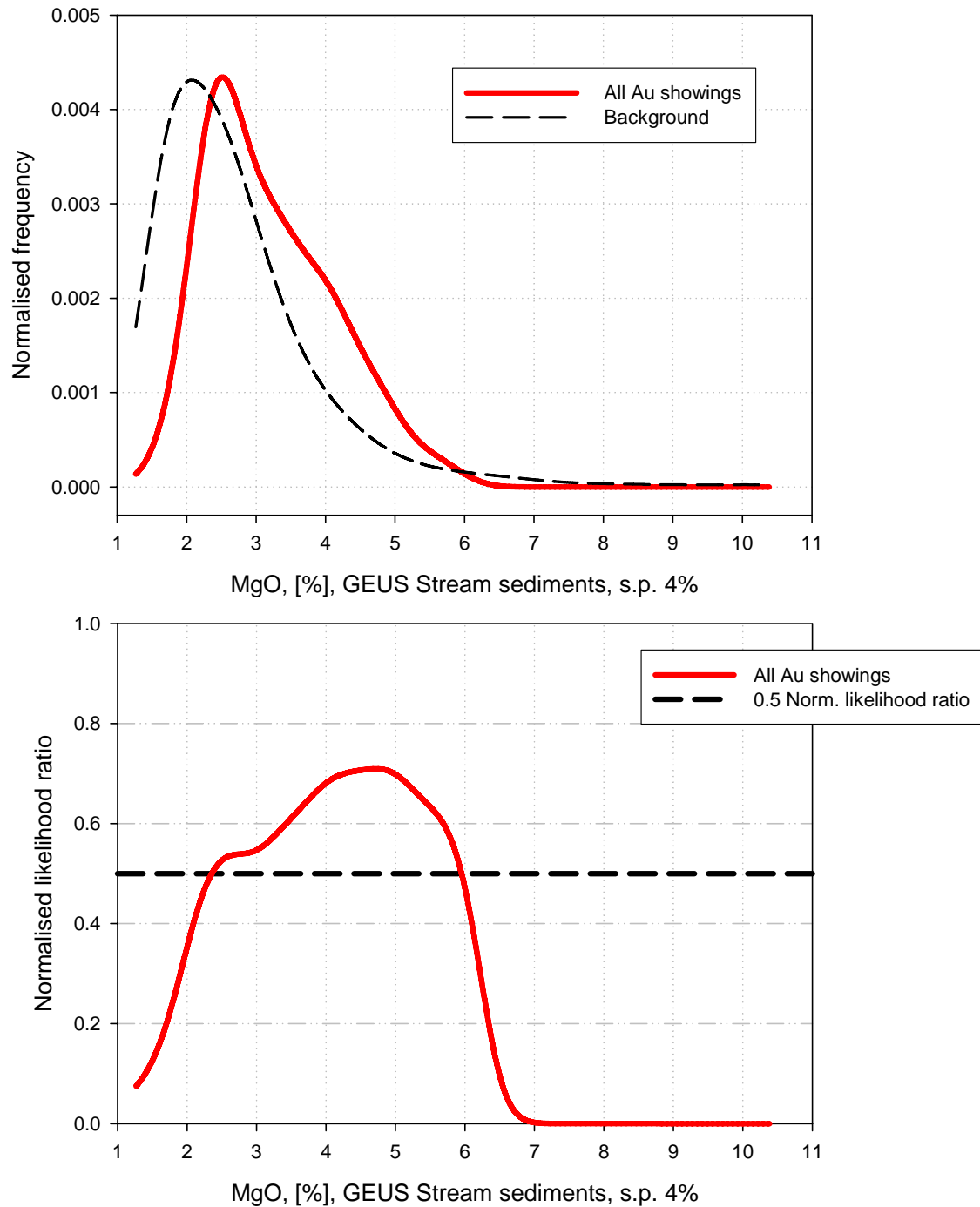


**Figure C27.** MgO, spread parameter 4% - Regional stream sediment geochemistry from GEUS.

$\text{Na}_2\text{O}$ , GEUS, minimum curvature, 200 m  
spread parameter 0.5%

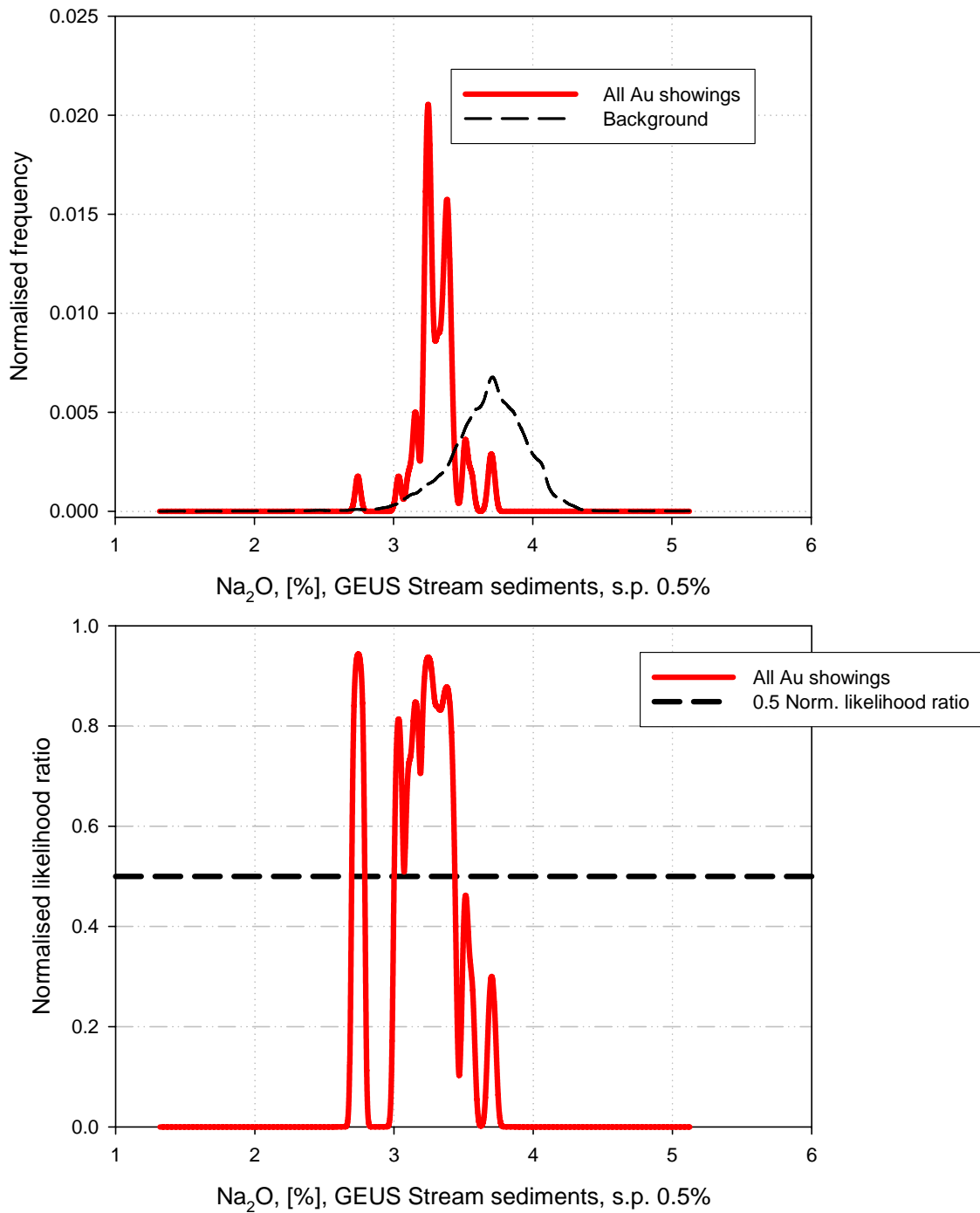


**Figure C28.**  $\text{Na}_2\text{O}$ , spread parameter 0.5% - Regional stream sediment geochemistry from GEUS.

$\text{Na}_2\text{O}$ , GEUS, minimum curvature, 200 m  
spread parameter 2%

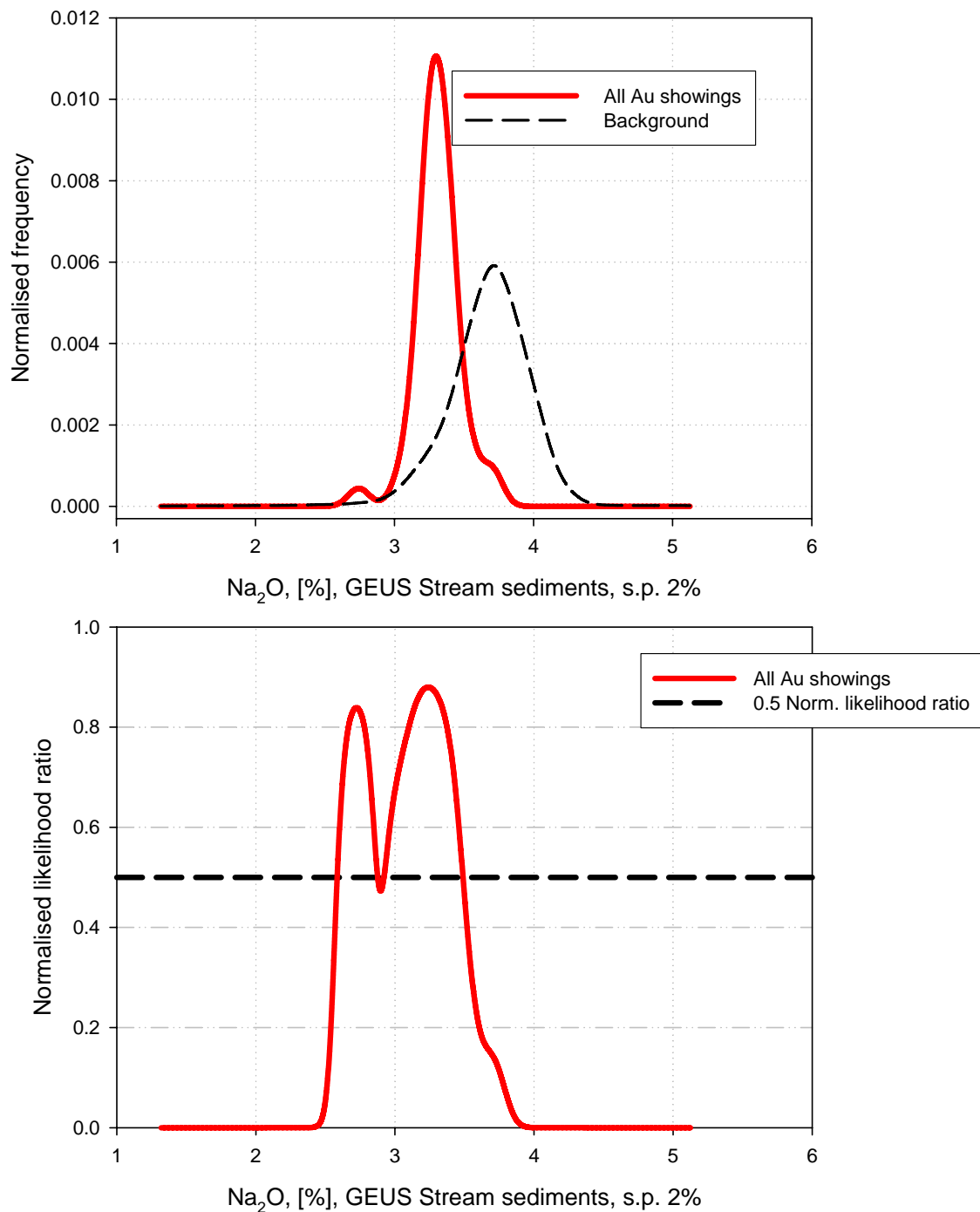


**Figure C29.**  $\text{Na}_2\text{O}$ , spread parameter 2% - Regional stream sediment geochemistry from GEUS.

$\text{Na}_2\text{O}$ , GEUS, minimum curvature, 200 m  
spread parameter 4%

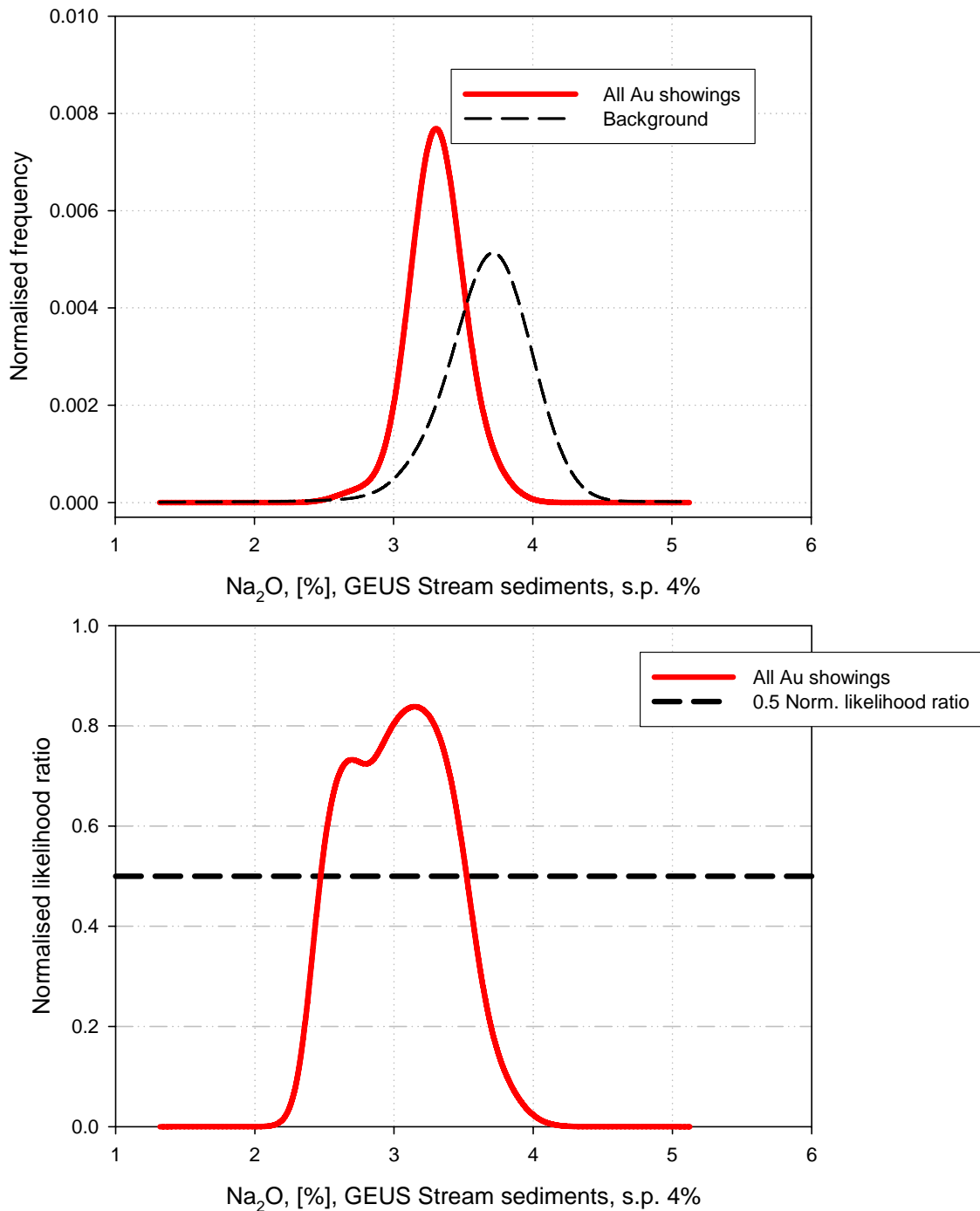
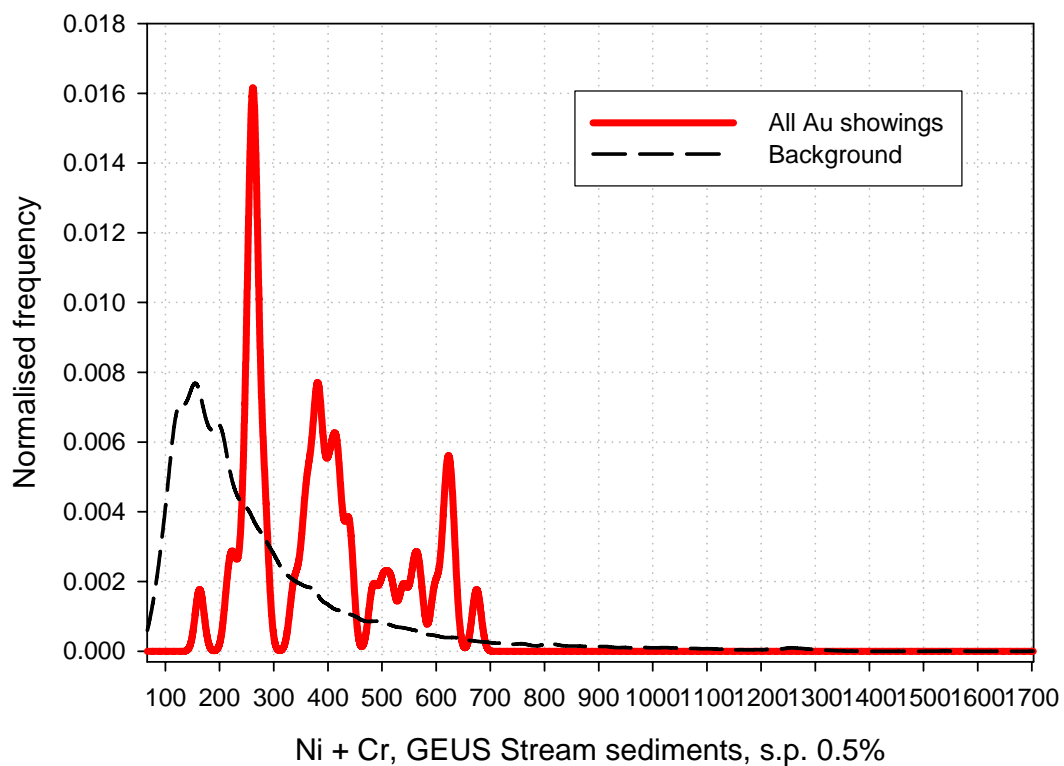
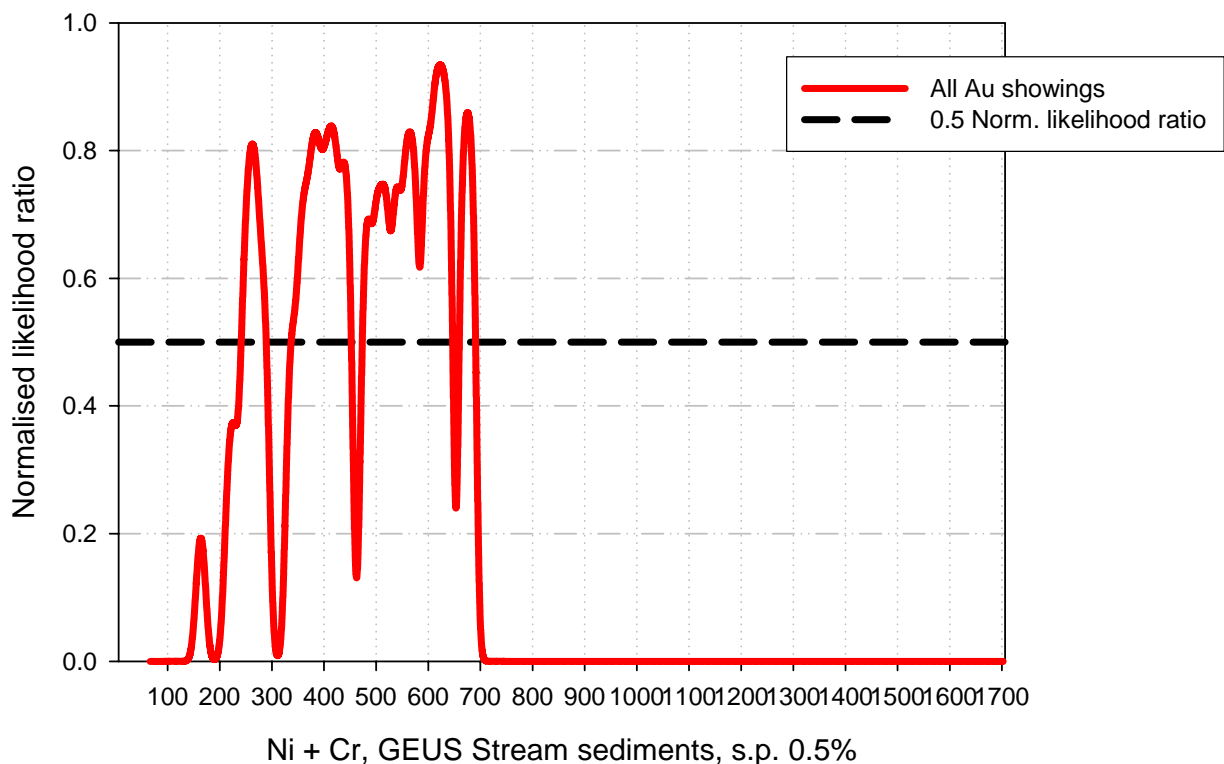


**Figure C30.**  $\text{Na}_2\text{O}$ , spread parameter 4% - Regional stream sediment geochemistry from GEUS.

Ni + Cr, GEUS, minimum curvature, 200 m  
spread parameter 0.5%



Ni + Cr, GEUS Stream sediments, s.p. 0.5%



Ni + Cr, GEUS Stream sediments, s.p. 0.5%

**Figure C31.** Ni + Cr, spread parameter 0.5% - Regional stream sediment geochemistry from GEUS.

Ni + Cr, GEUS, minimum curvature, 200 m  
spread parameter 2%

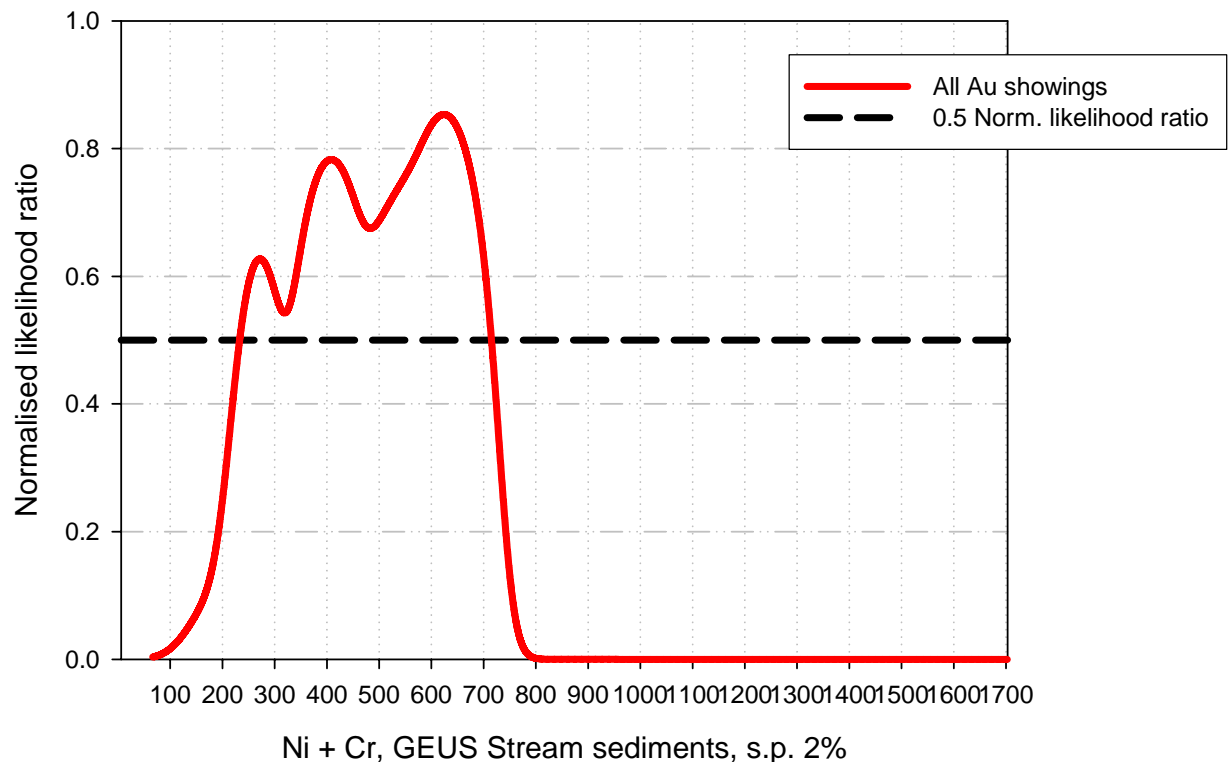
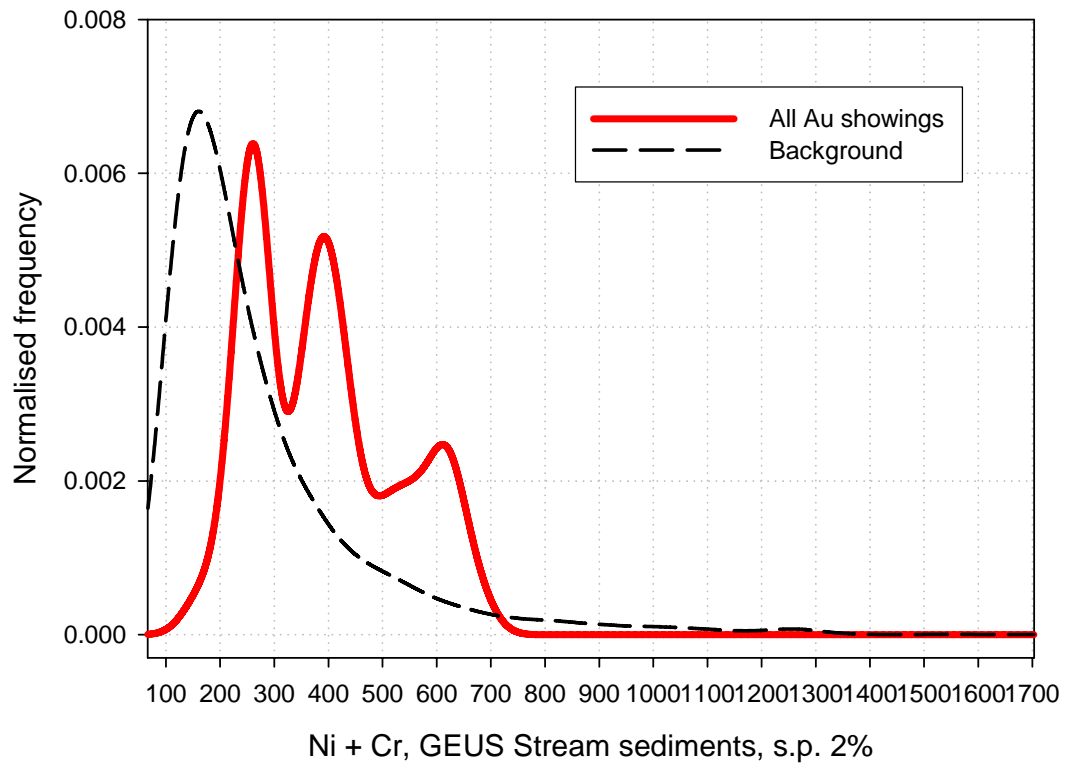
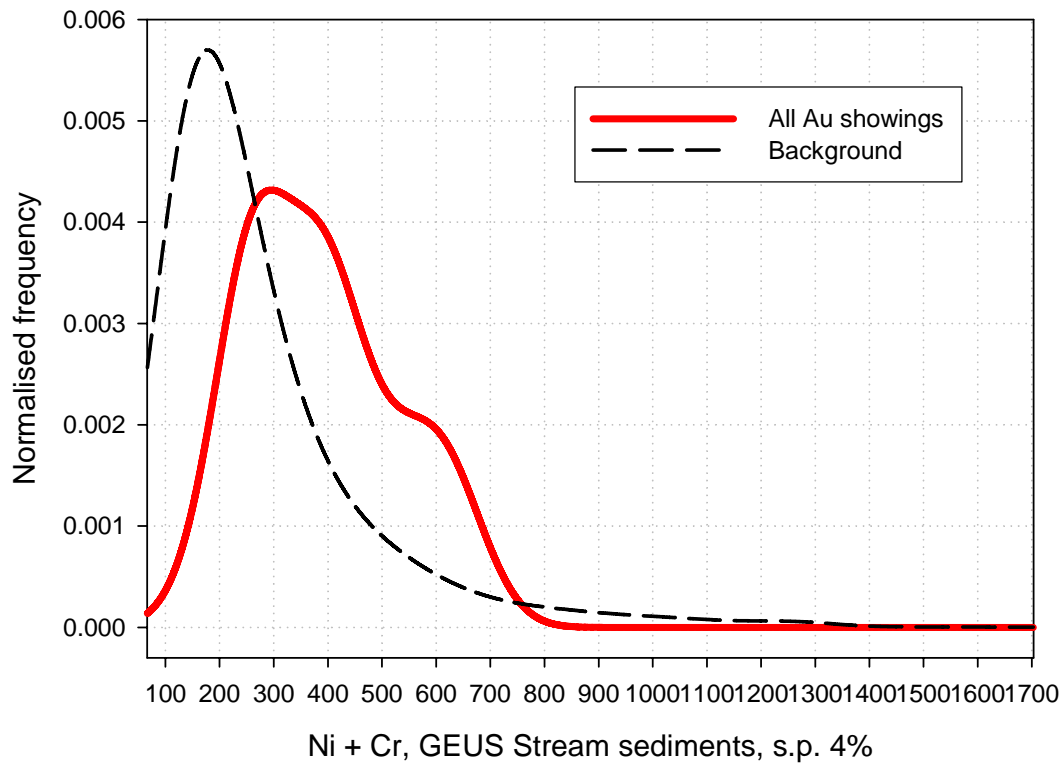
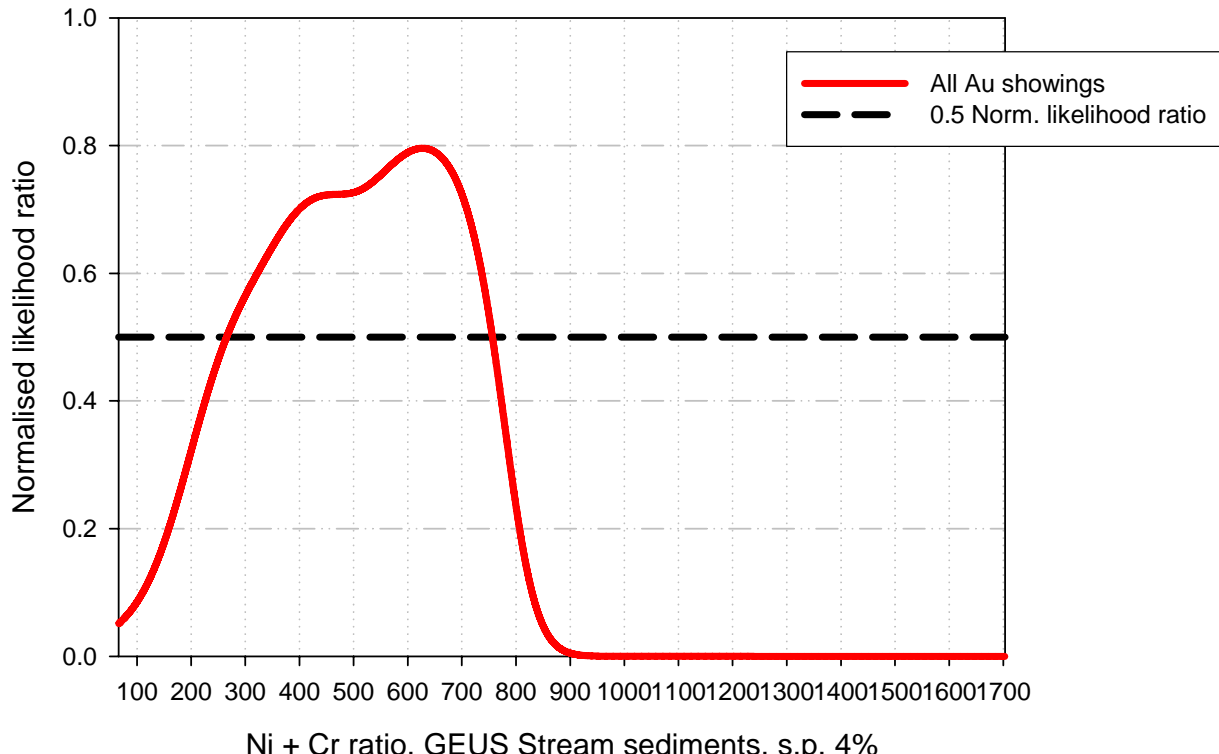


**Figure C32.** Ni + Cr, spread parameter 2% - Regional stream sediment geochemistry from GEUS.

Ni + Cr, GEUS, minimum curvature, 200 m  
spread parameter 4%



Ni + Cr, GEUS Stream sediments, s.p. 4%



Ni + Cr ratio, GEUS Stream sediments, s.p. 4%

Figure C33. Ni + Cr, spread parameter 4% - Regional stream sediment geochemistry from GEUS.

Ni/Mg ratio, GEUS, minimum curvature, 200 m  
spread parameter 0.5%

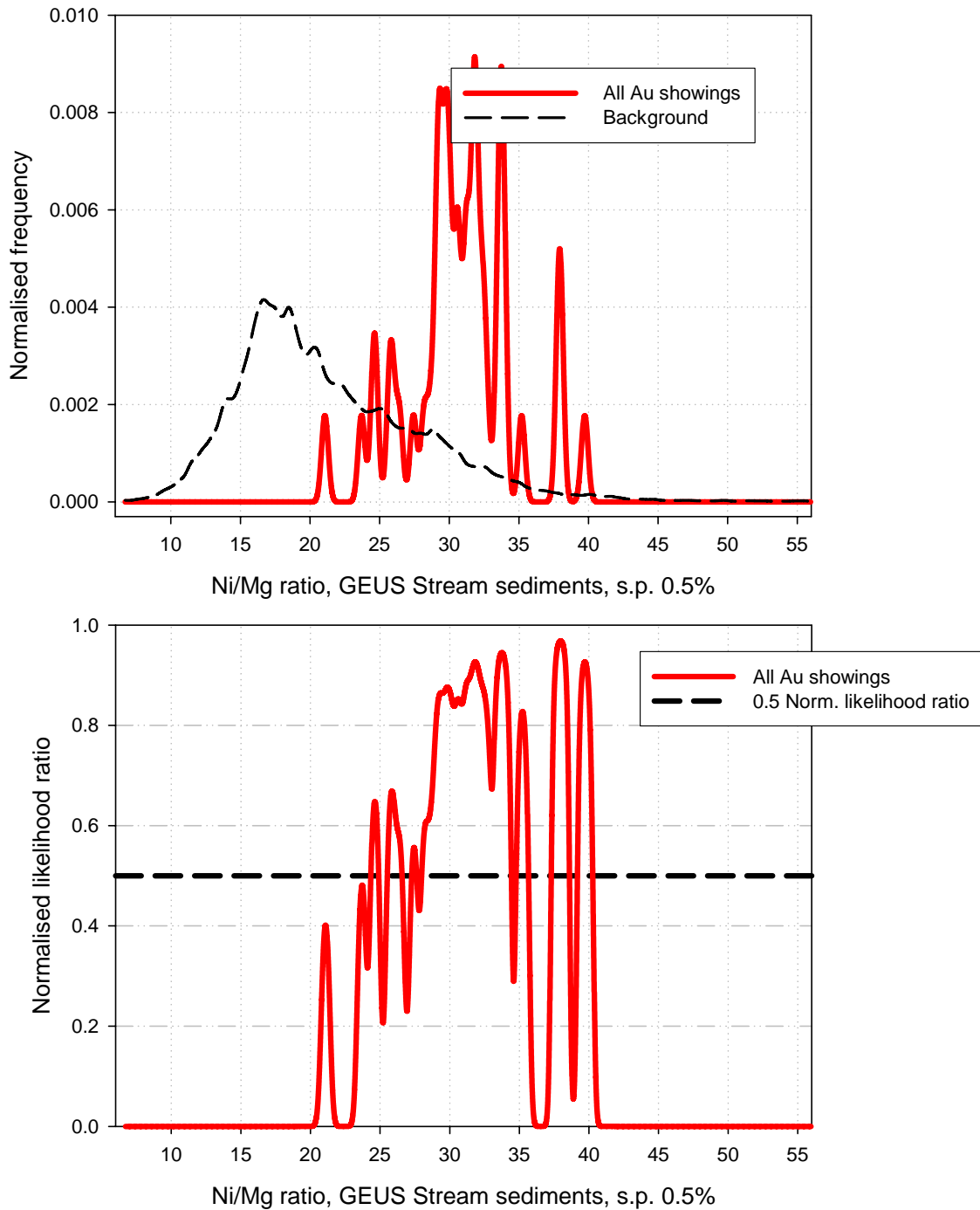


**Figure C34.** Ni/Mg ratio, spread parameter 0.5% - Regional stream sediment geochemistry from GEUS.

Ni/Mg ratio, GEUS, minimum curvature, 200 m  
spread parameter 2%

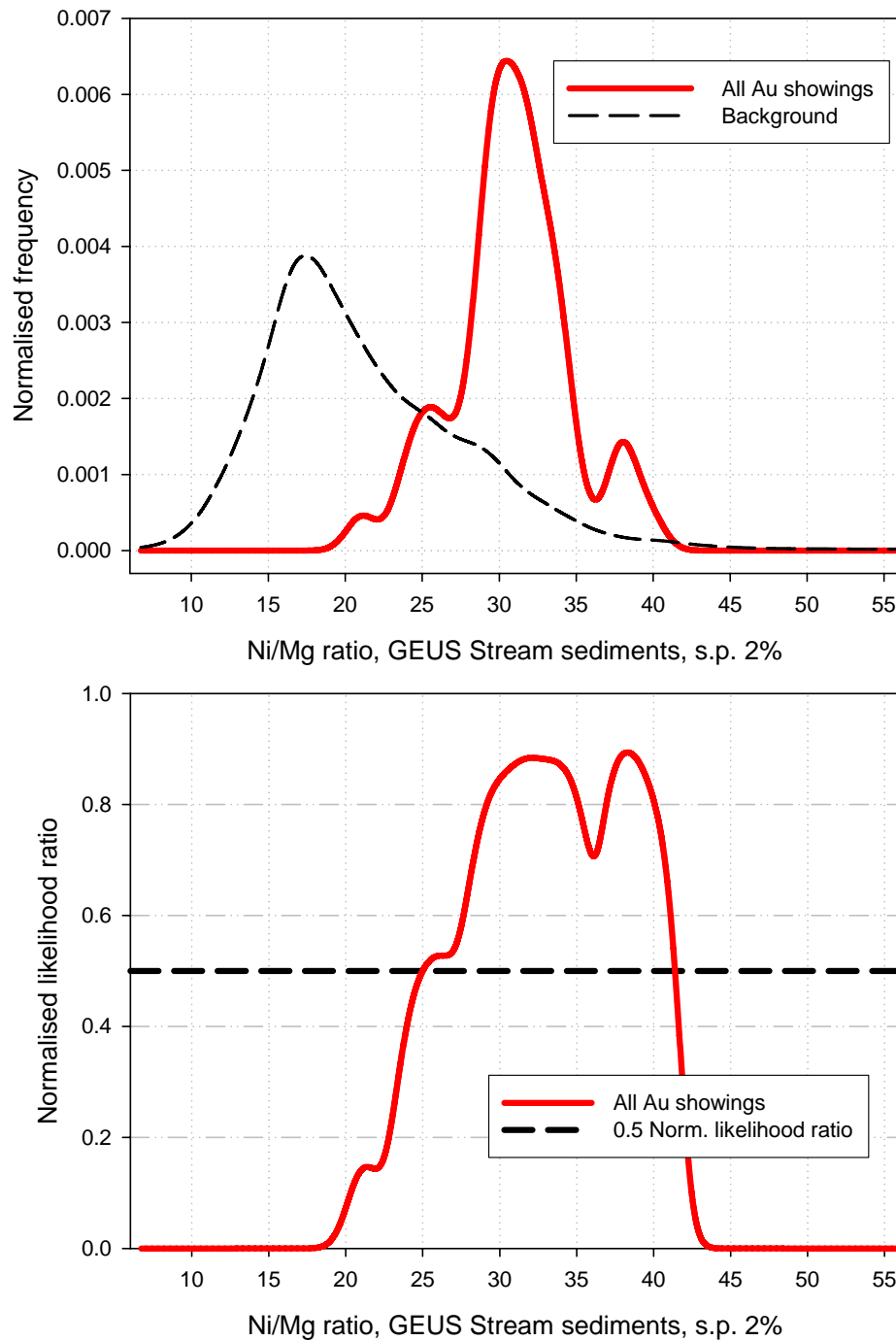


**Figure C35.** Ni/Mg ratio, spread parameter 2% - Regional stream sediment geochemistry from GEUS.

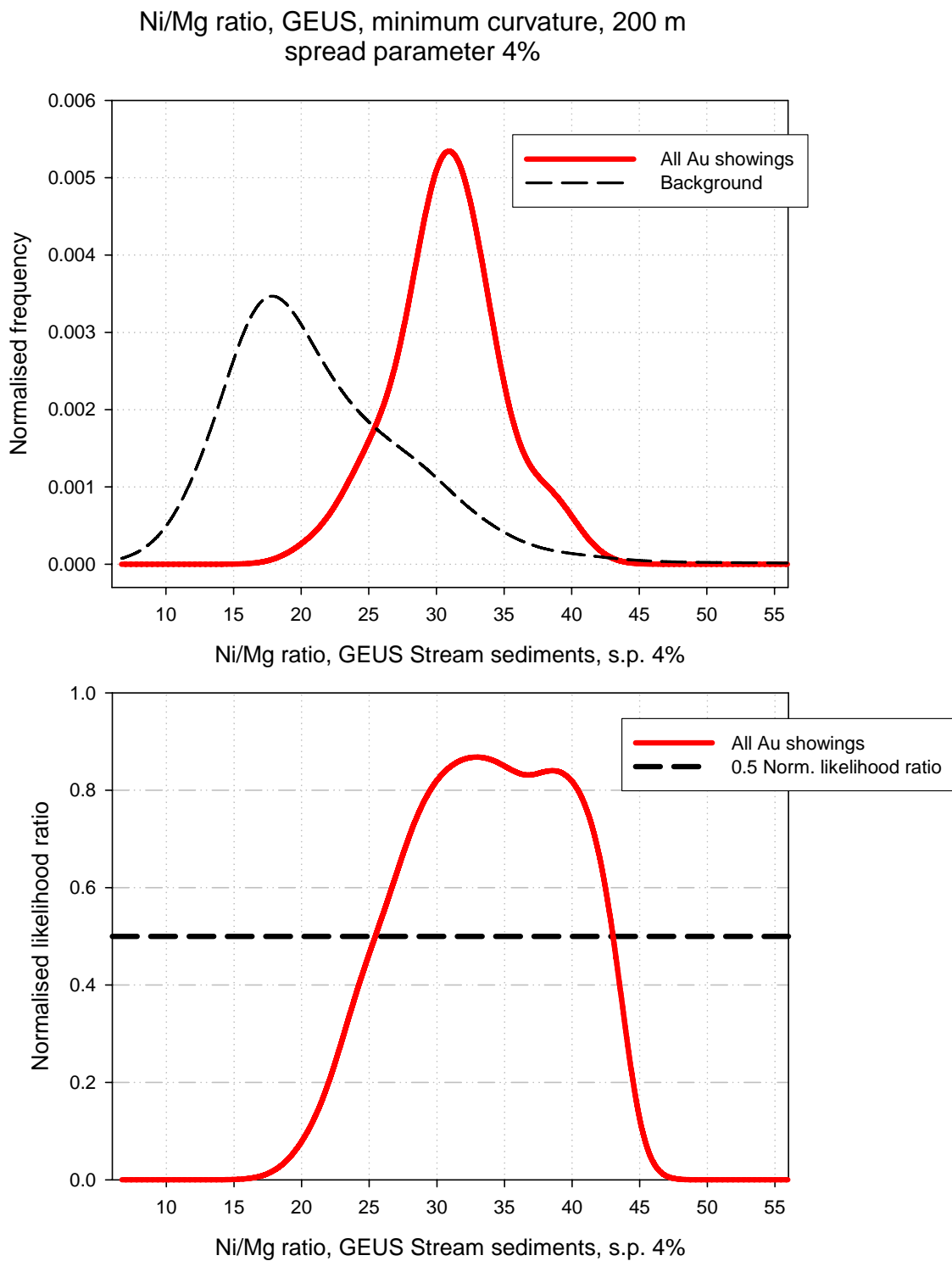


**Figure C36.** Ni/Mg ratio, spread parameter 4% - Regional stream sediment geochemistry from GEUS.

$P_2O_5$ , GEUS, minimum curvature, 200 m  
spread parameter 0.5%

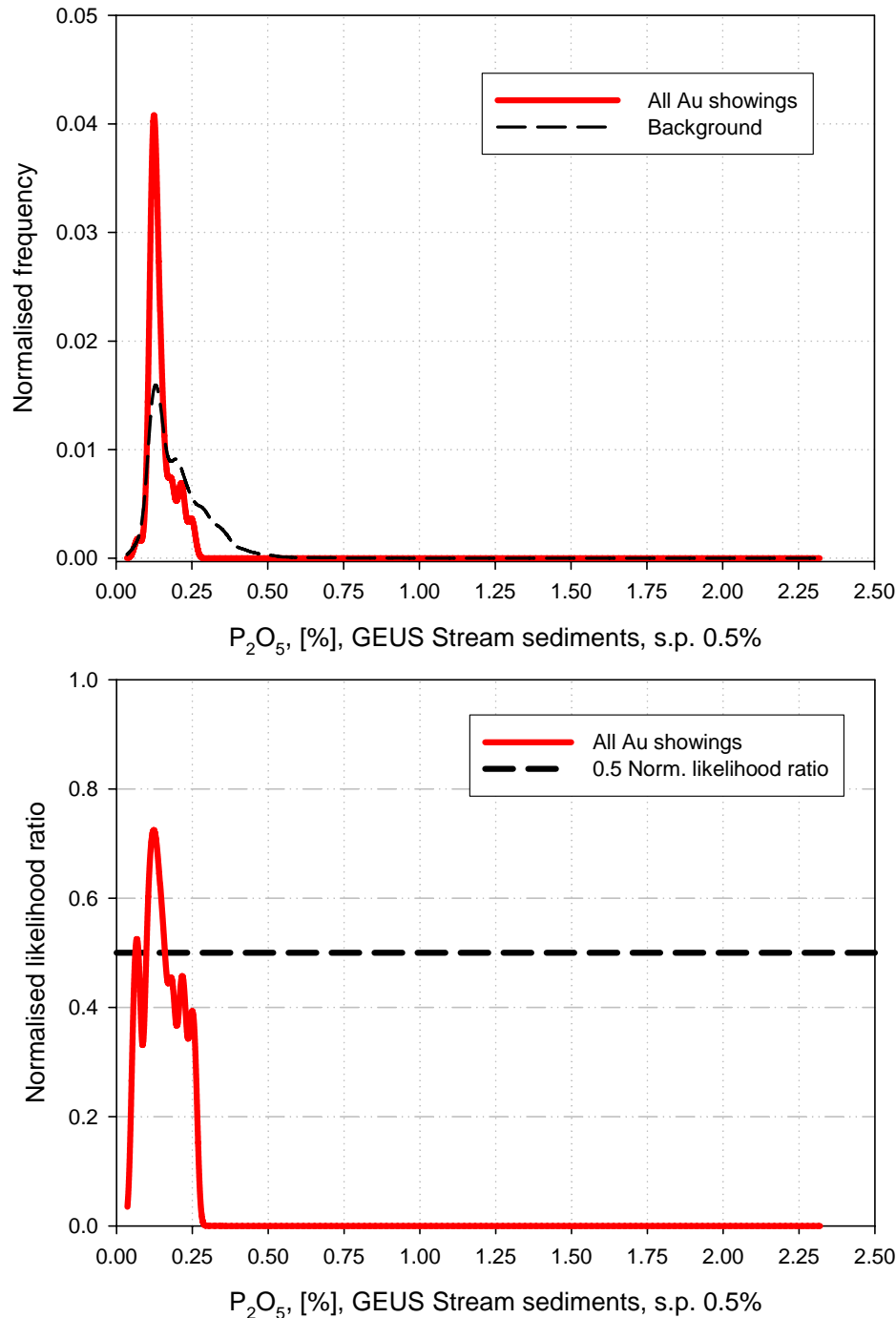


**Figure C37.**  $P_2O_5$ , spread parameter 0.5% - Regional stream sediment geochemistry from GEUS.

$P_2O_5$ , GEUS, minimum curvature, 200 m  
spread parameter 2%

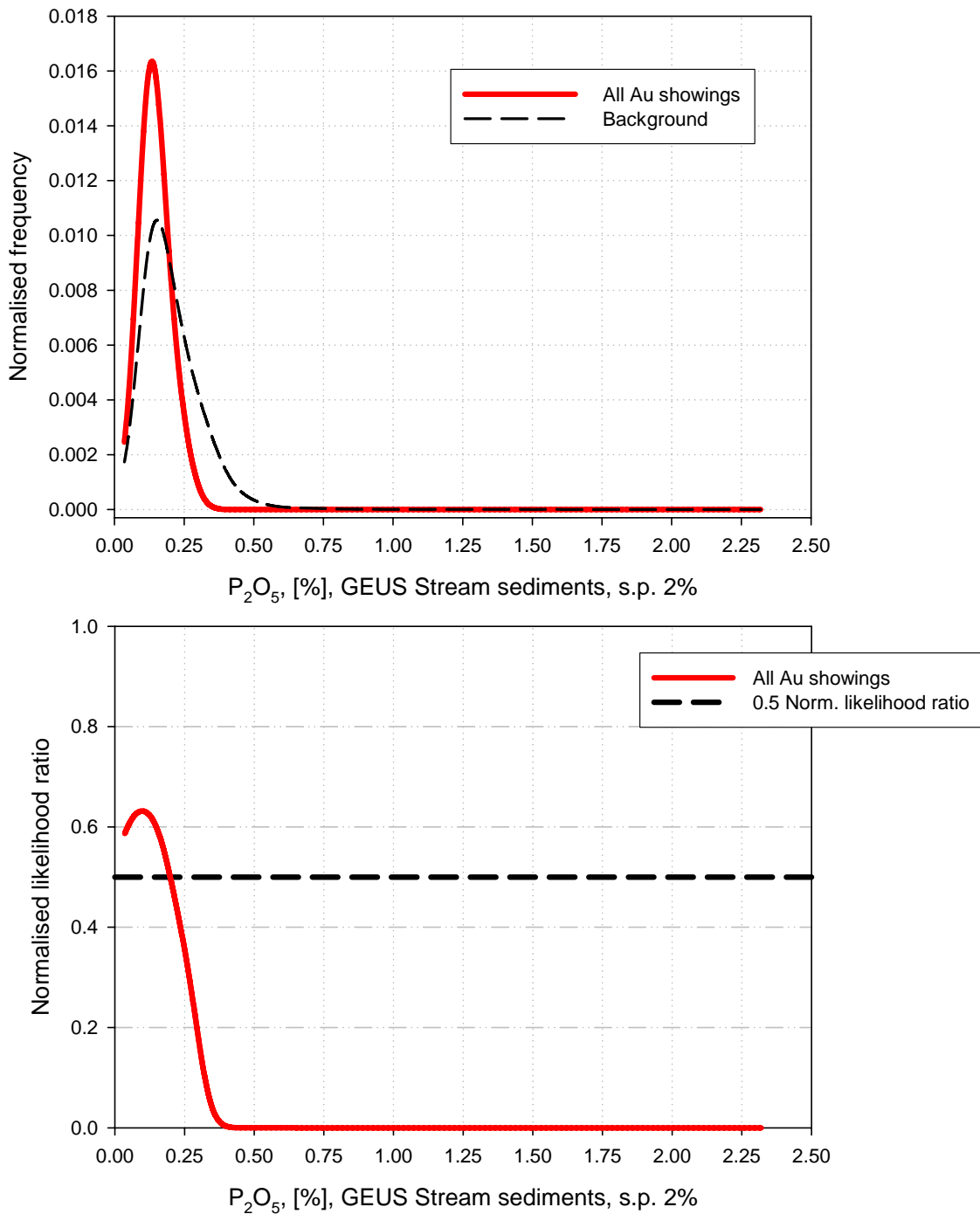


**Figure C38.**  $P_2O_5$ , spread parameter 2% - Regional stream sediment geochemistry from GEUS.

$P_2O_5$ , GEUS, minimum curvature, 200 m  
spread parameter 4%

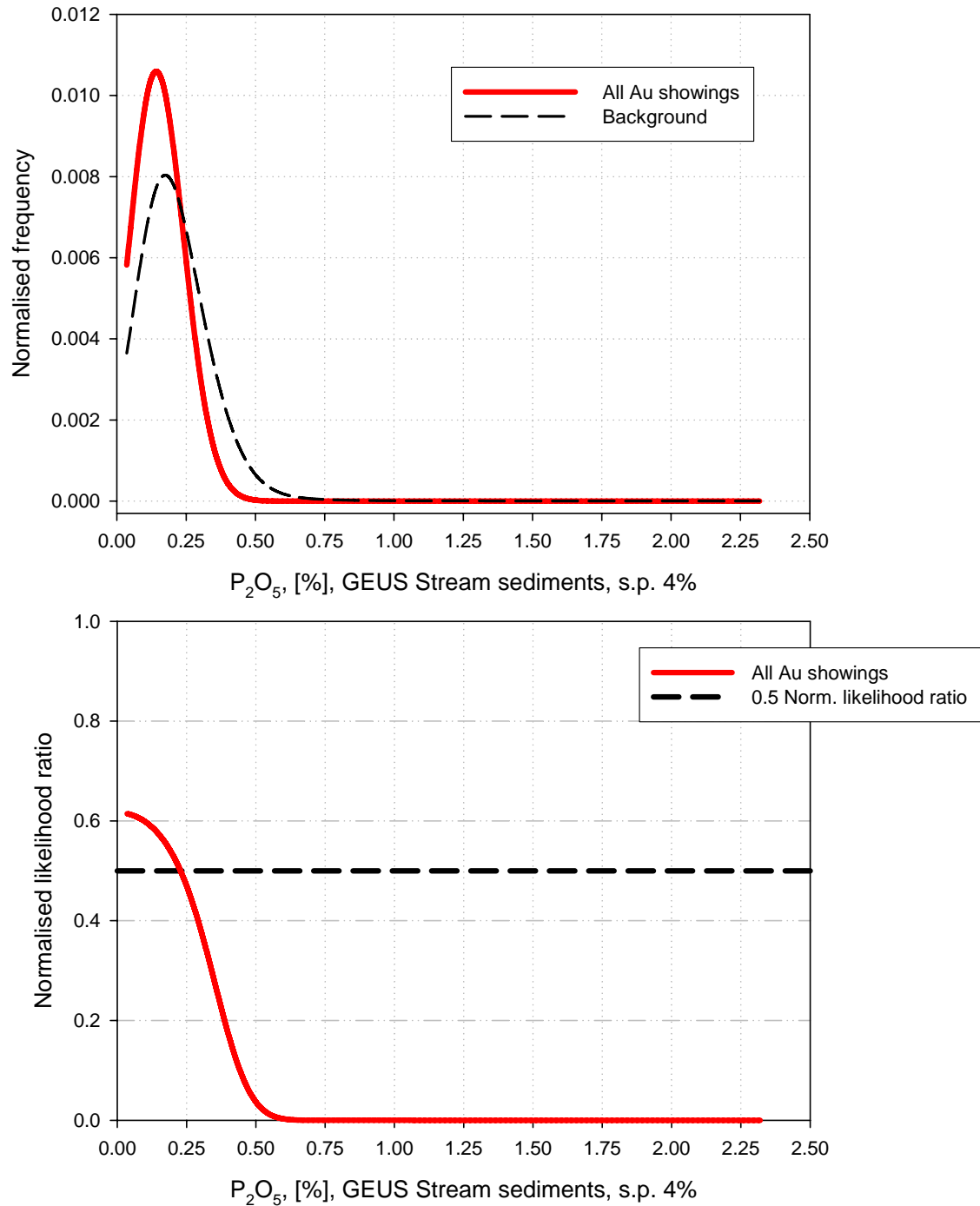


**Figure C39.**  $P_2O_5$ , spread parameter 4% - Regional stream sediment geochemistry from GEUS.

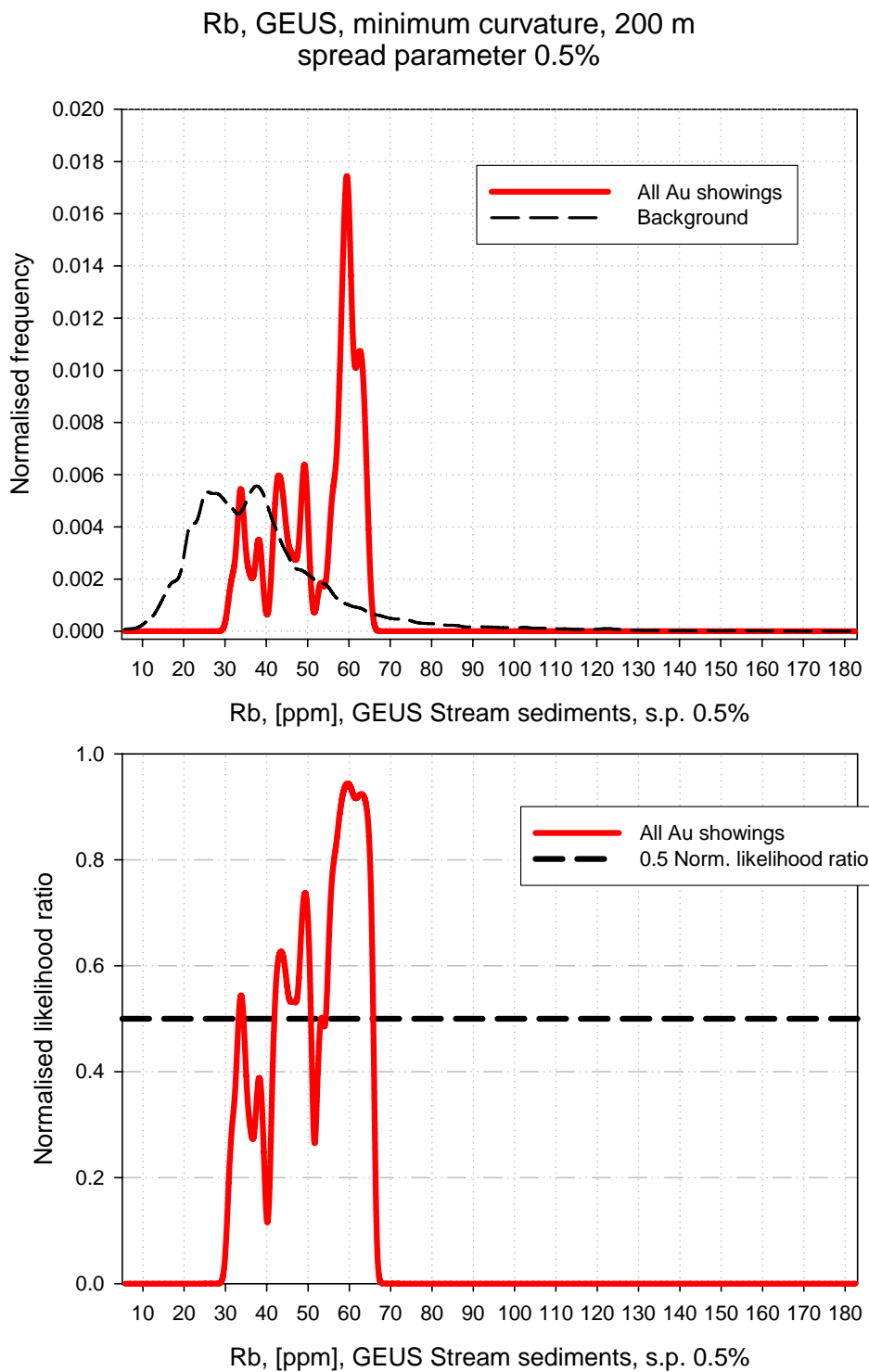


**Figure C40.** *Rb, spread parameter 0.5% - Regional stream sediment geochemistry from GEUS.*

Rb, GEUS, minimum curvature, 200 m  
spread parameter 2%

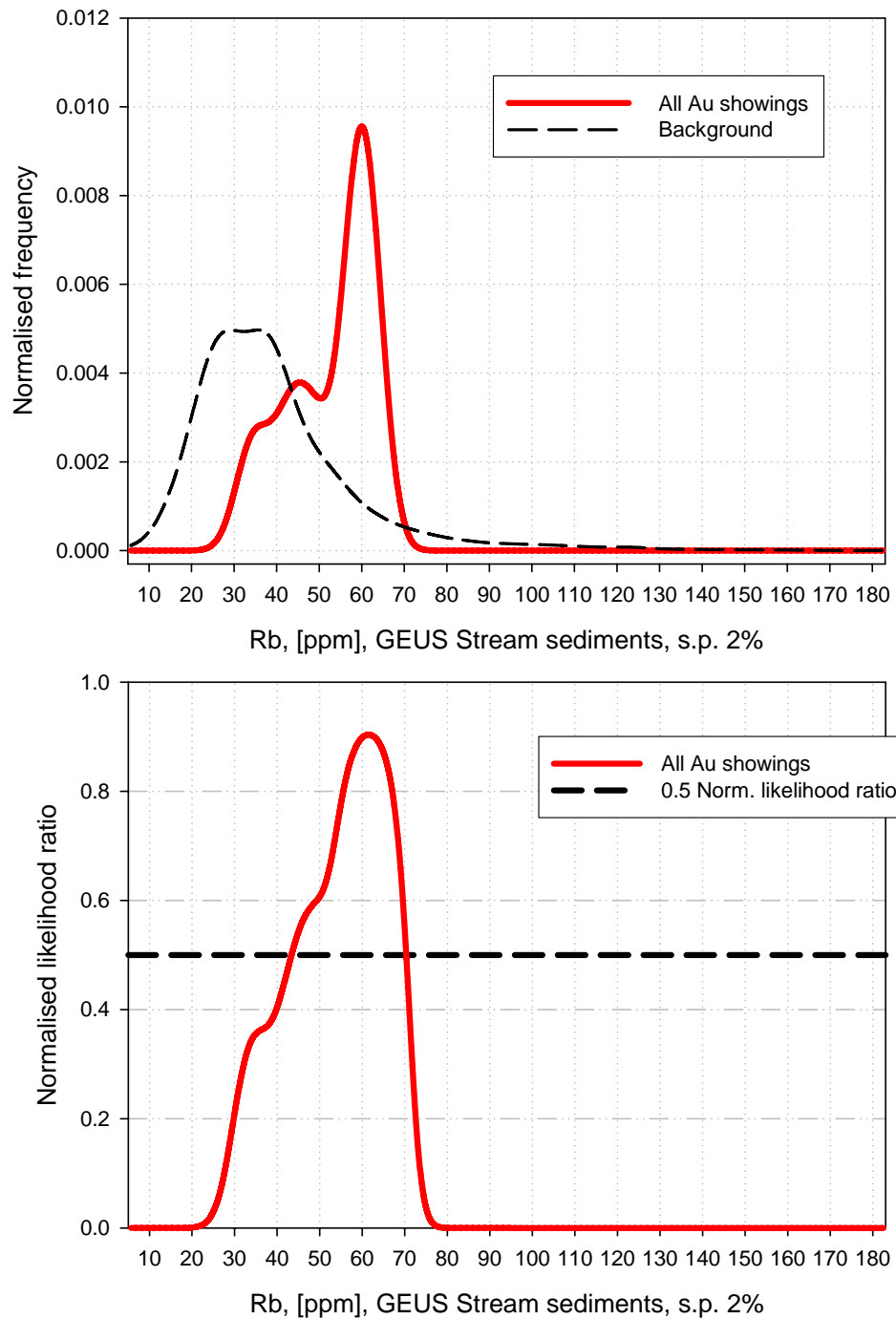


**Figure C41.** *Rb, spread parameter 2% - Regional stream sediment geochemistry from GEUS.*

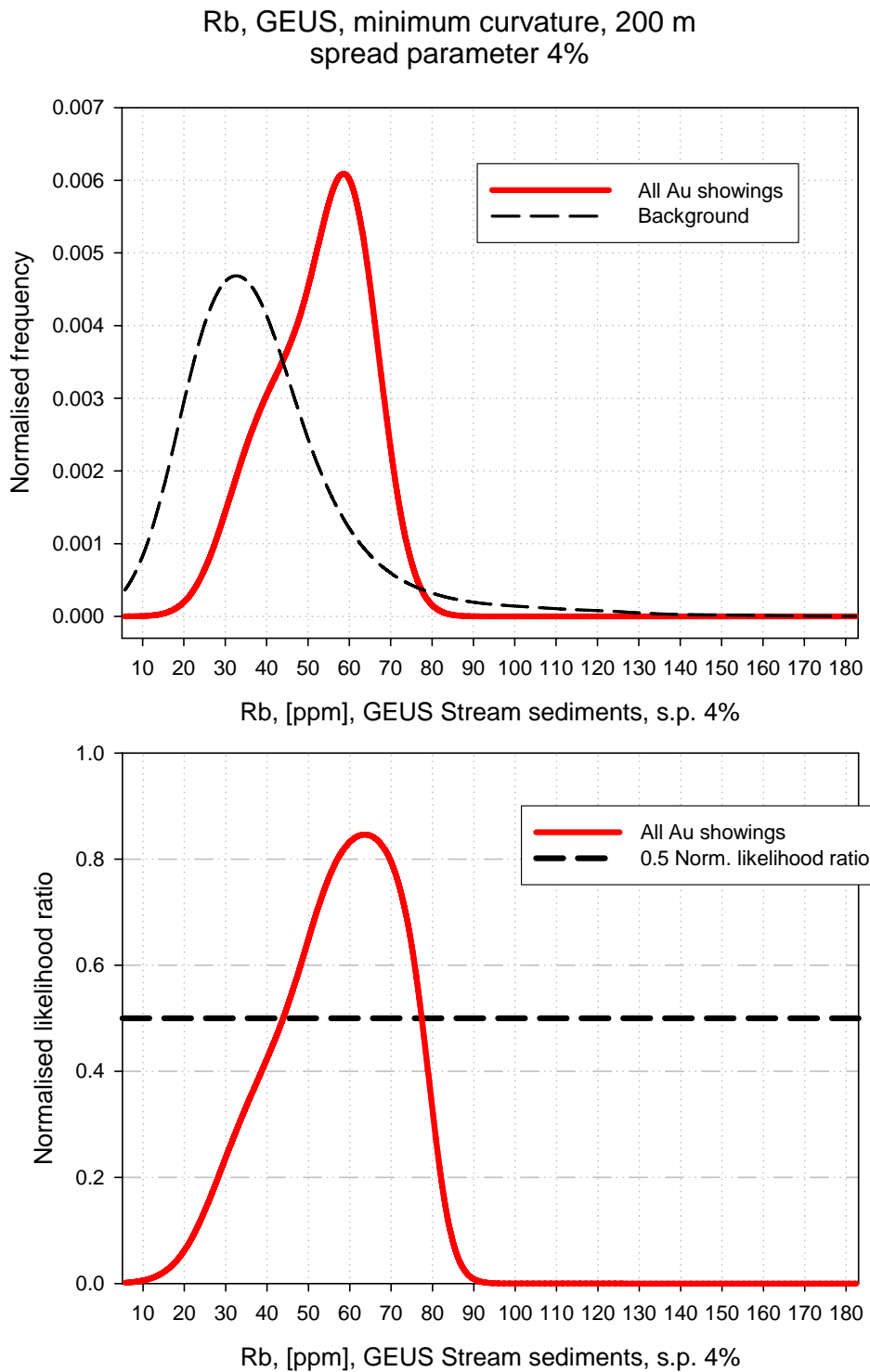
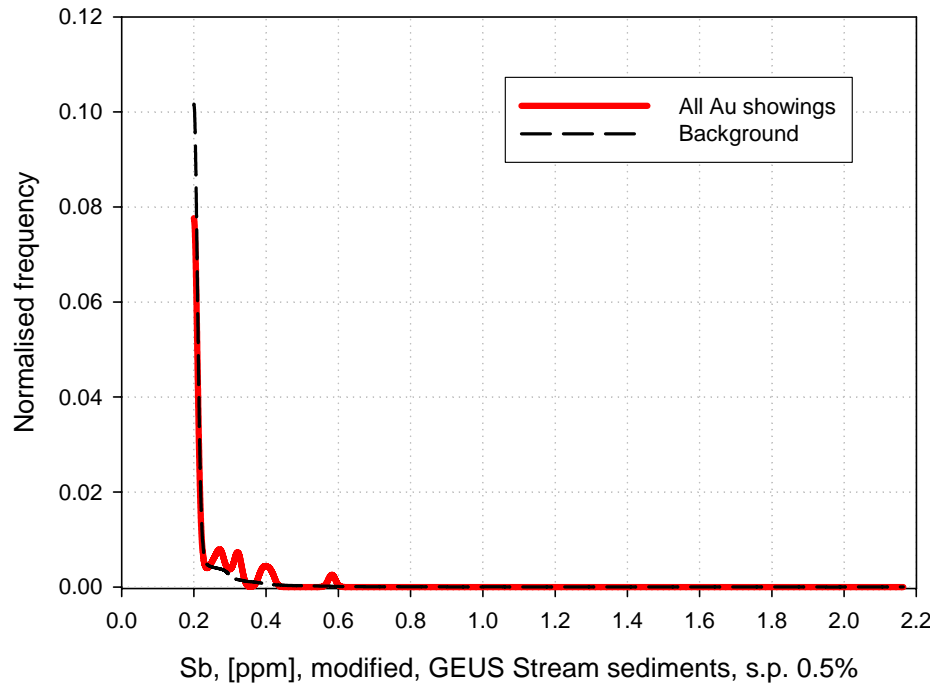
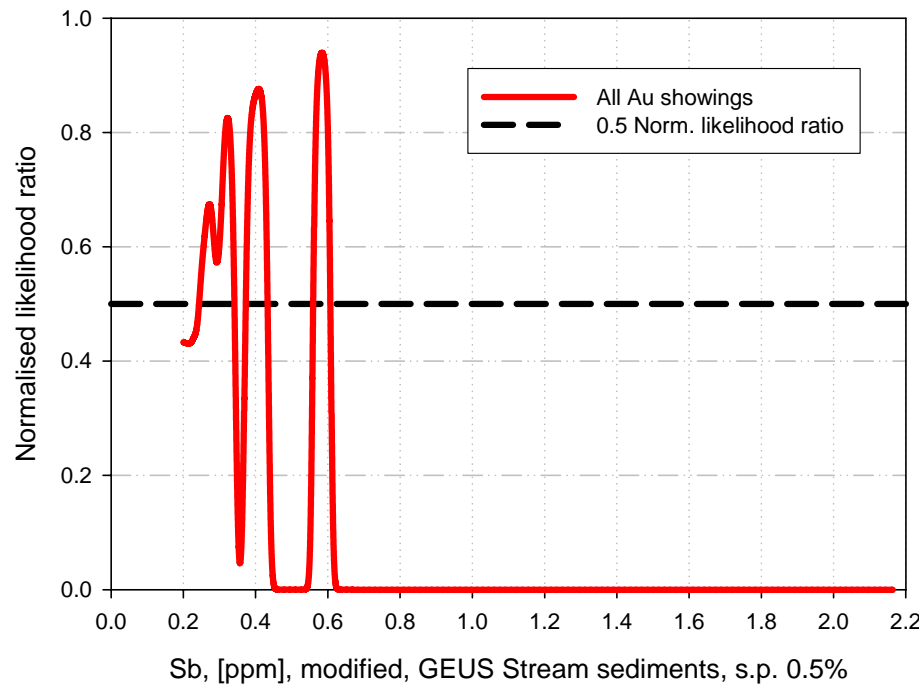


**Figure C42.** *Rb, spread parameter 4% - Regional stream sediment geochemistry from GEUS.*

Sb, GEUS, minimum curvature, modified, 200 m  
spread parameter 0.5%



Sb, [ppm], modified, GEUS Stream sediments, s.p. 0.5%



Sb, [ppm], modified, GEUS Stream sediments, s.p. 0.5%

**Figure C43.** Sb, spread parameter 0.5% - Regional stream sediment geochemistry from GEUS.

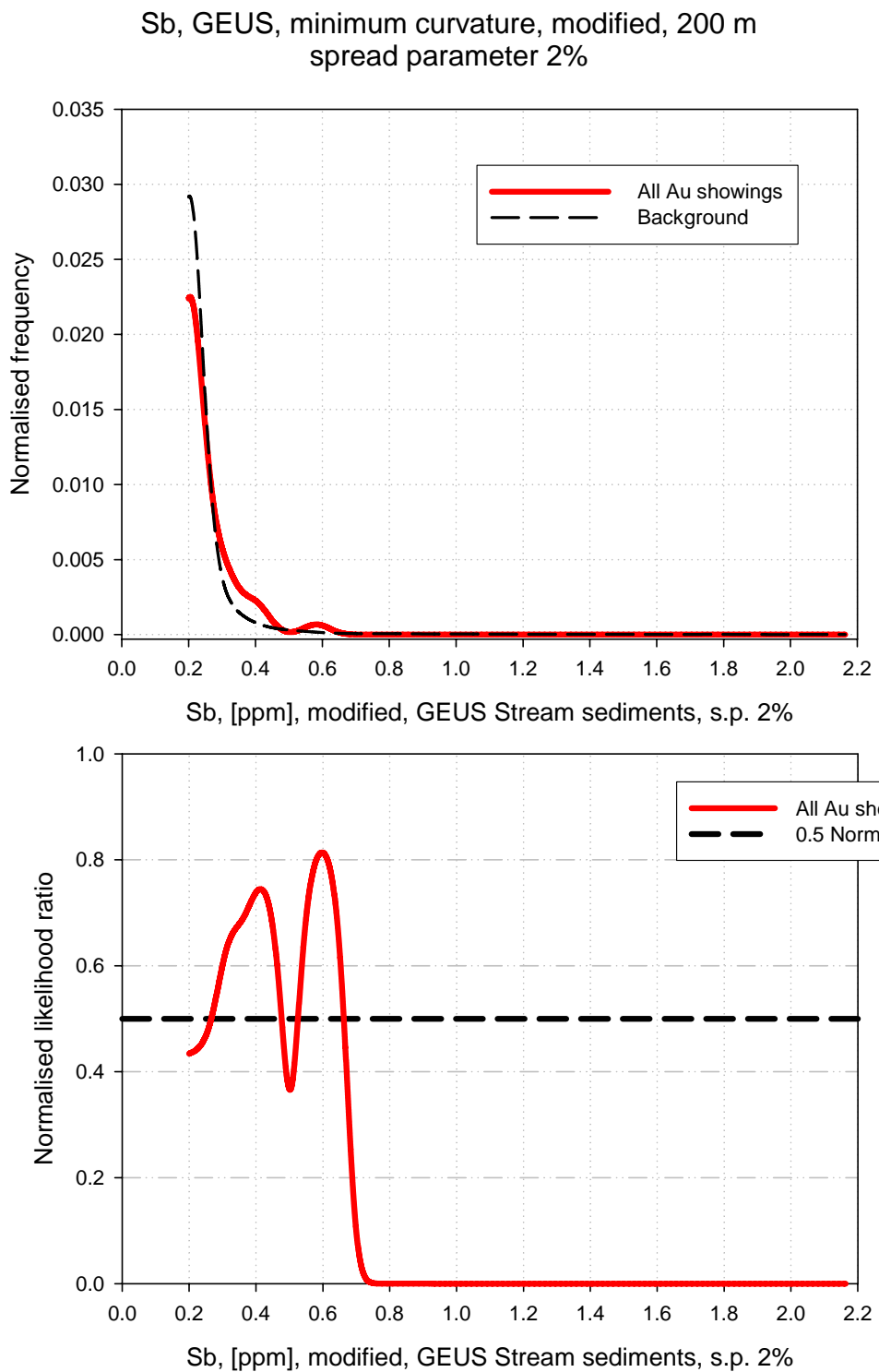


**Figure C44.** Sb, spread parameter 2% - Regional stream sediment geochemistry from GEUS.

Sb, GEUS, minimum curvature, modified, 200 m  
spread parameter 4%

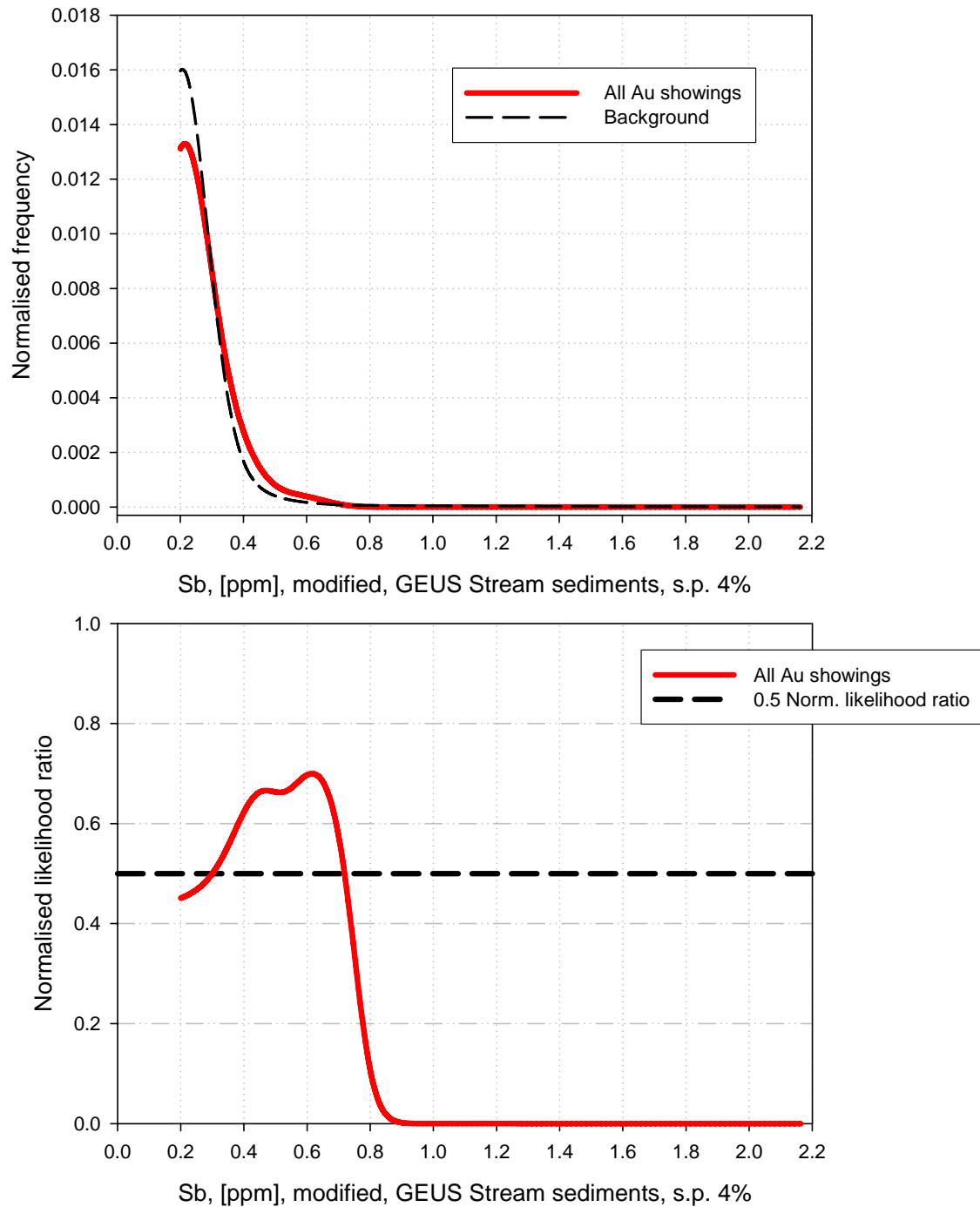


**Figure C45.** Sb, spread parameter 4% - Regional stream sediment geochemistry from GEUS.

$\text{SiO}_2$ , GEUS, minimum curvature, 200 m  
spread parameter 0.5%

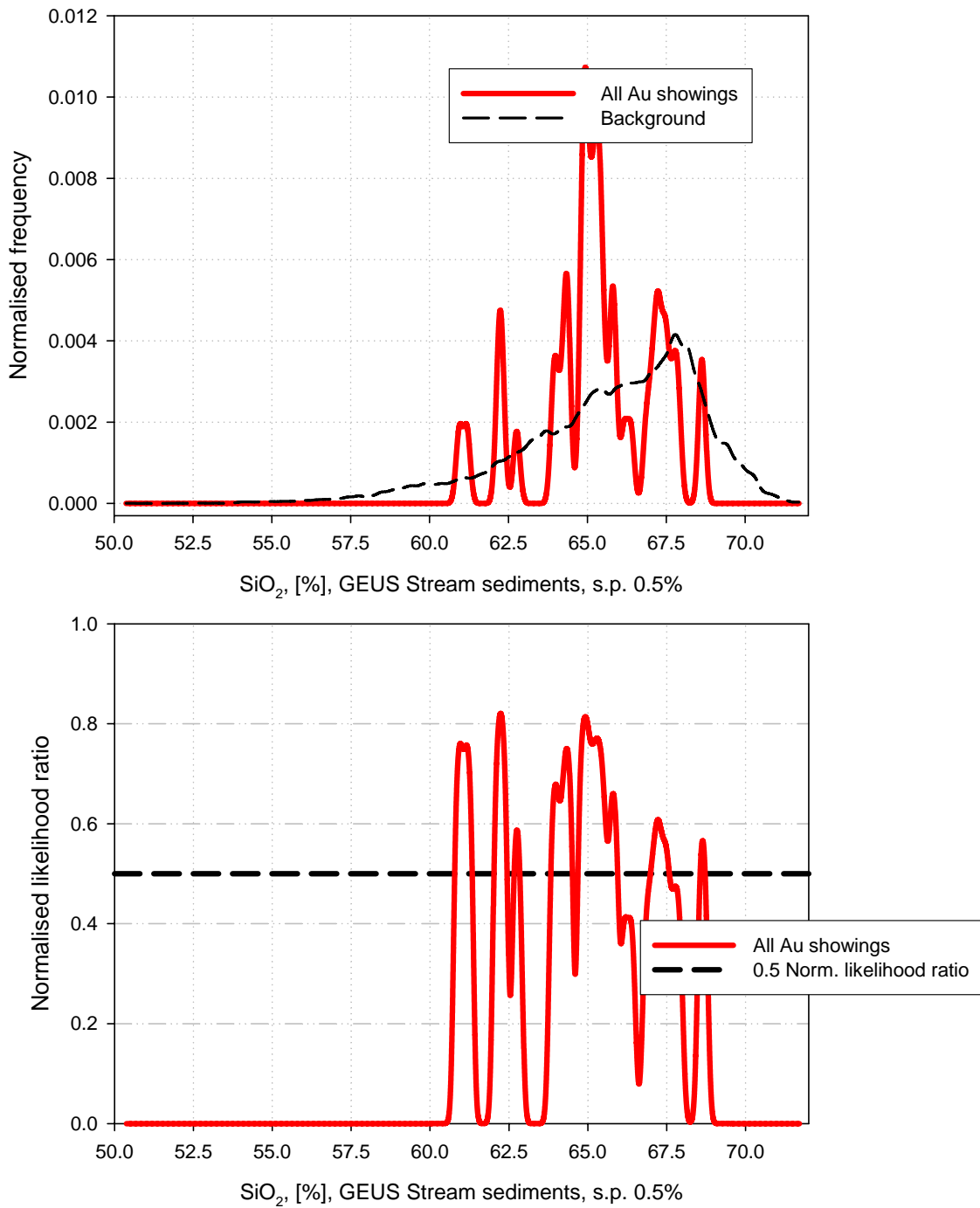


**Figure C46.**  $\text{SiO}_2$ , spread parameter 0.5% - Regional stream sediment geochemistry from GEUS.

$\text{SiO}_2$ , GEUS, minimum curvature, 200 m  
spread parameter 2%

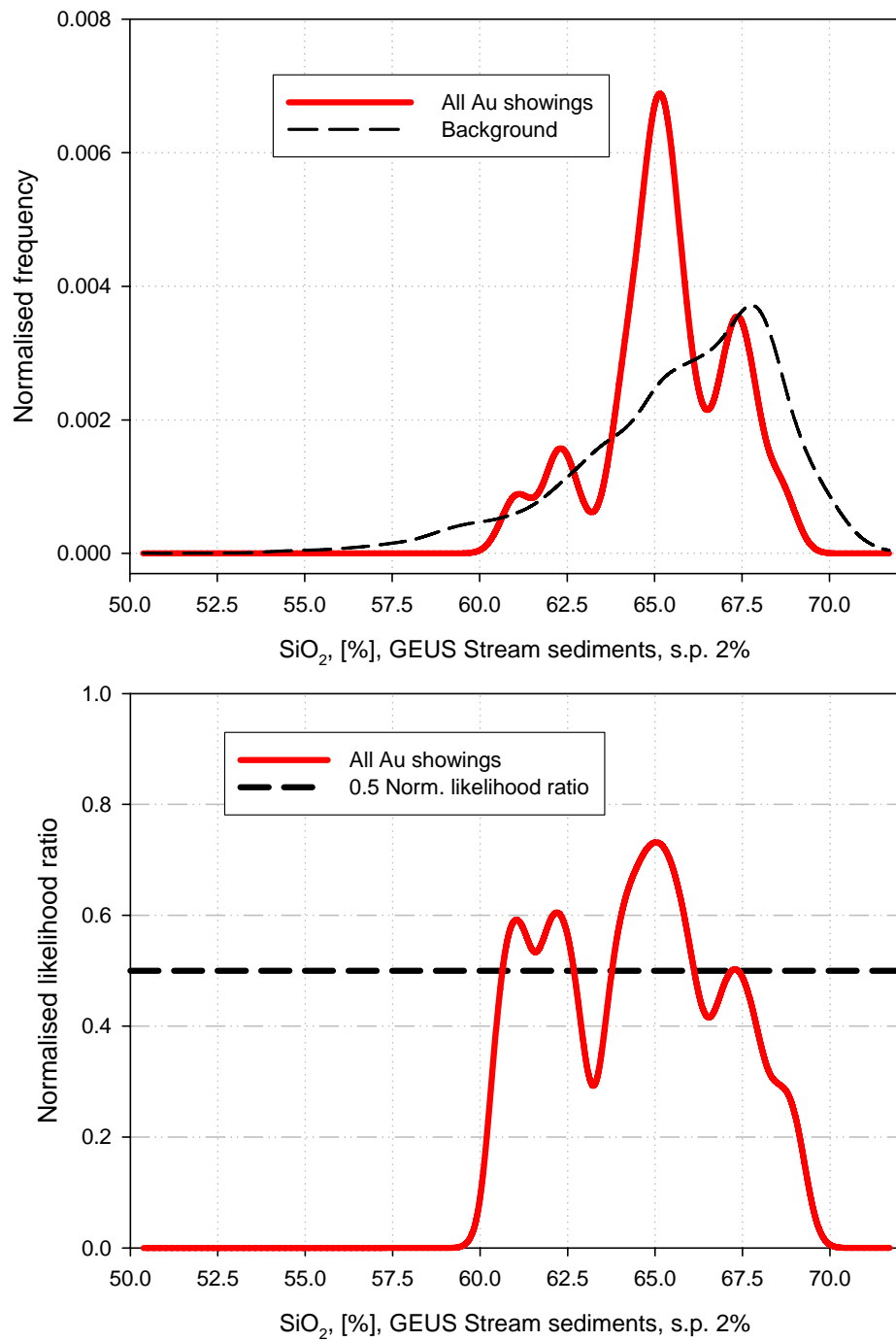


**Figure C47.**  $\text{SiO}_2$ , spread parameter 2% - Regional stream sediment geochemistry from GEUS.

$\text{SiO}_2$ , GEUS, minimum curvature, 200 m  
spread parameter 4%

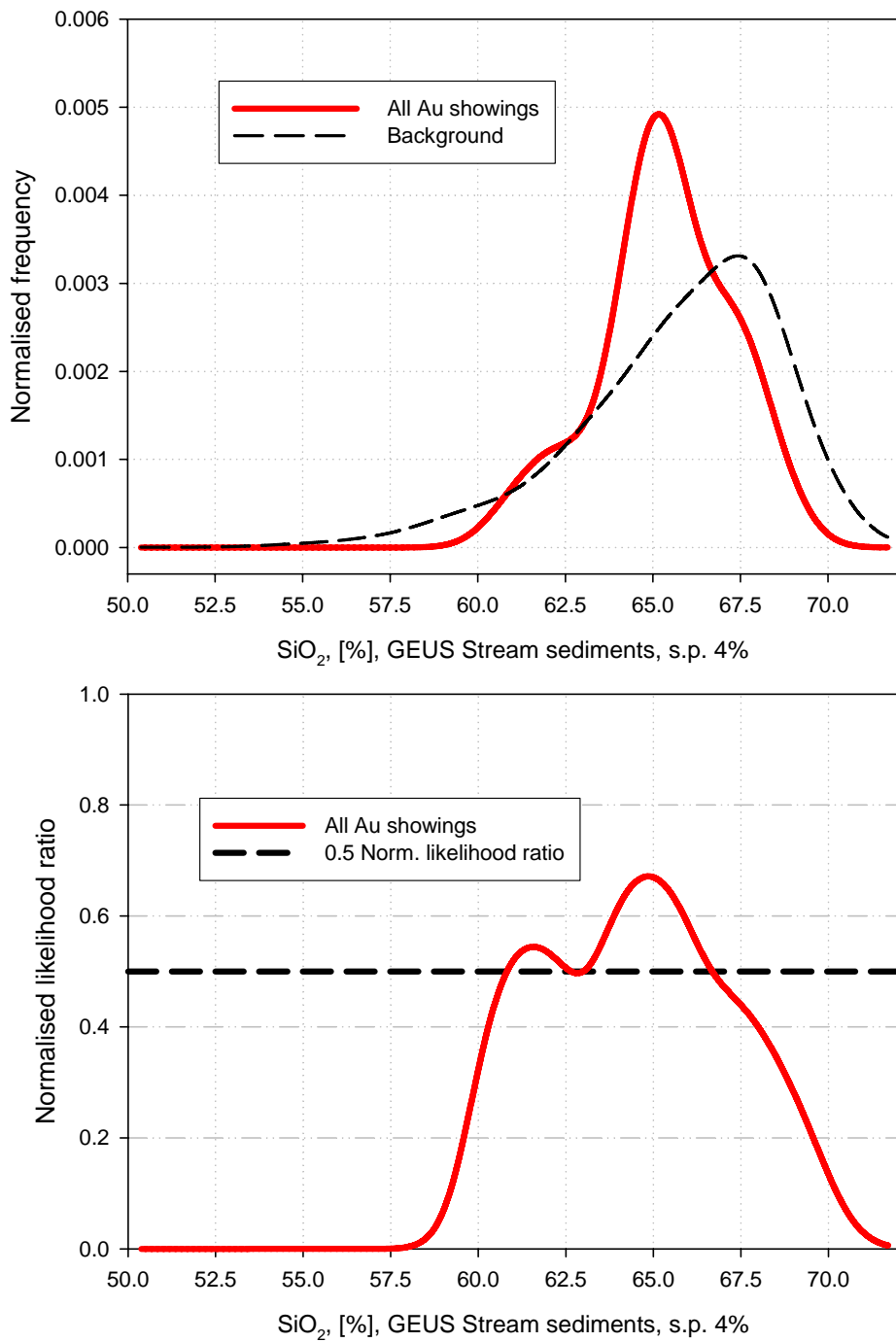


**Figure C48.**  $\text{SiO}_2$ , spread parameter 4% - Regional stream sediment geochemistry from GEUS.

Th, GEUS, minimum curvature, 200 m  
spread parameter 0.5%

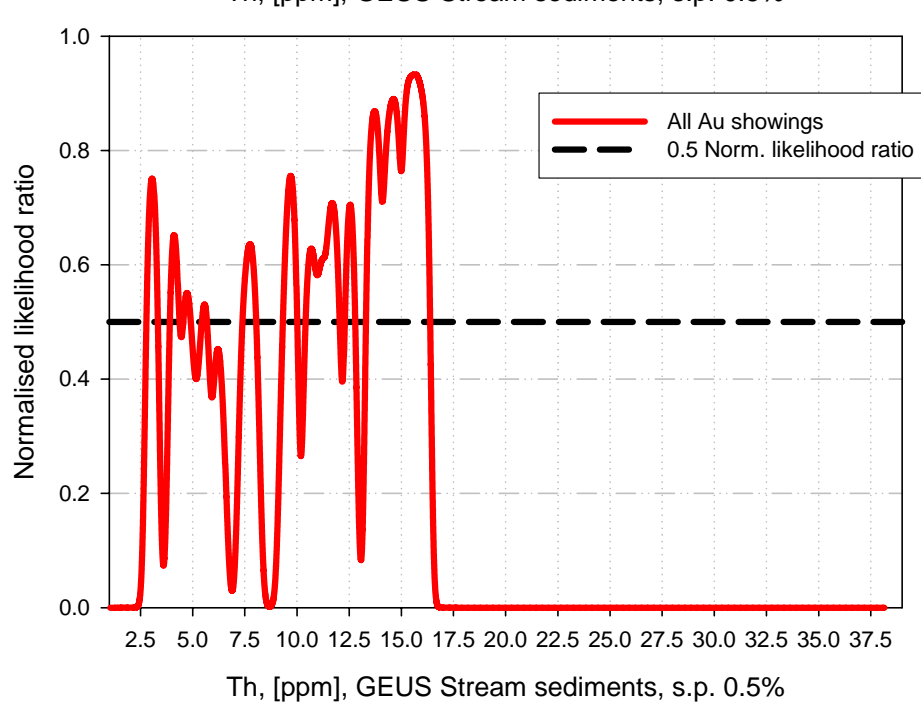
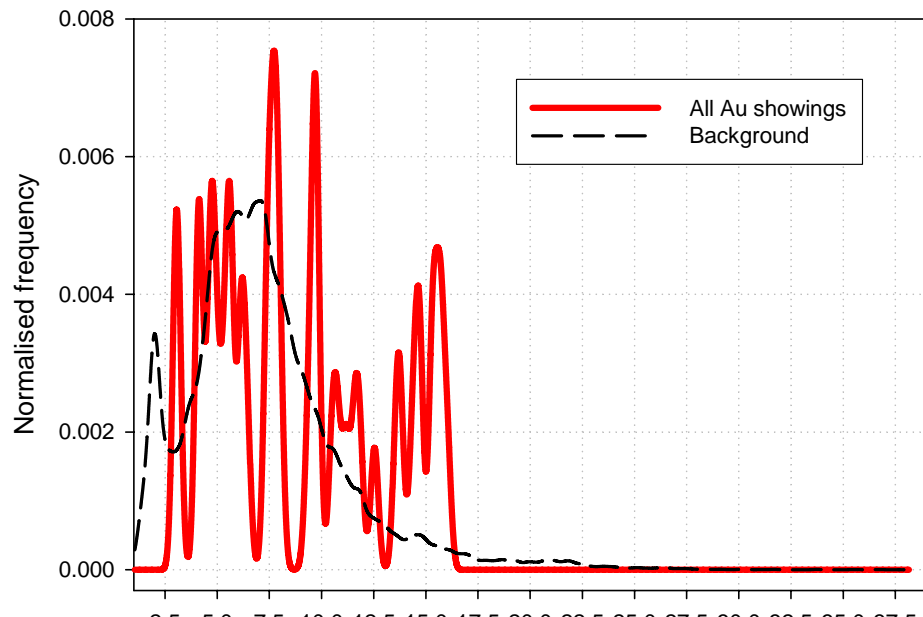


**Figure C49.** *Th, spread parameter 0.5% - Regional stream sediment geochemistry from GEUS.*

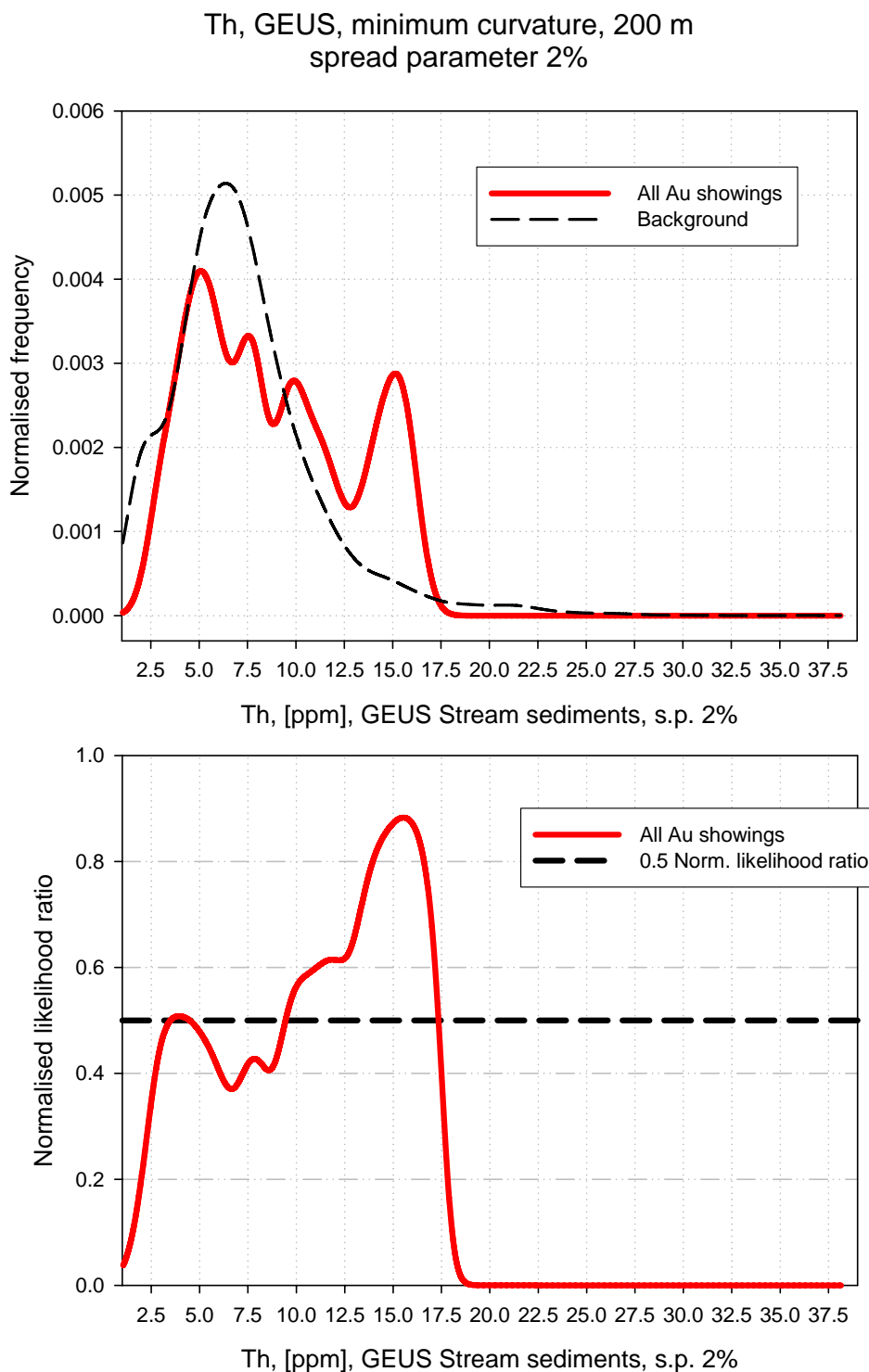
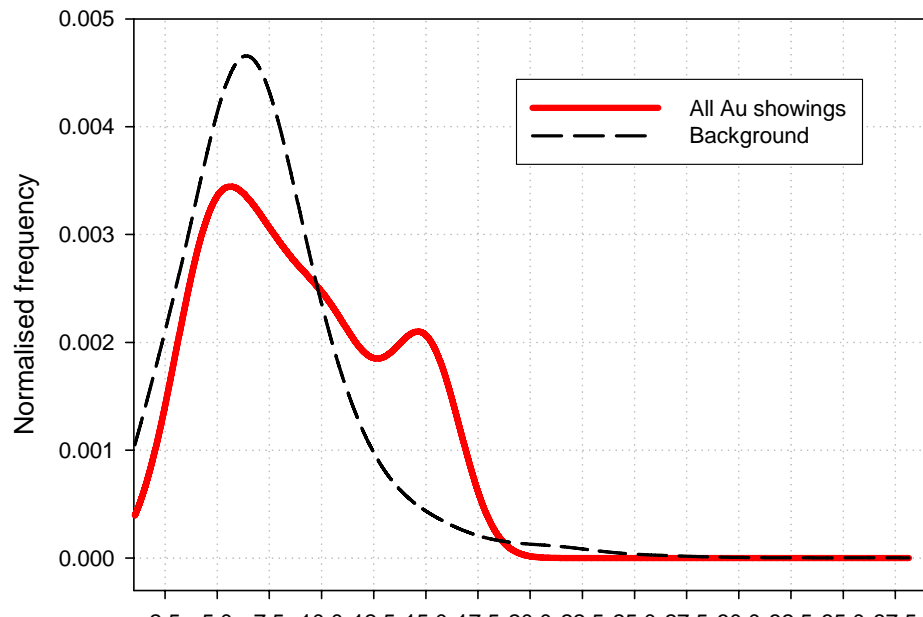


**Figure C50.** *Th, spread parameter 2% - Regional stream sediment geochemistry from GEUS.*

Th, GEUS, minimum curvature, 200 m  
spread parameter 4%



Th, [ppm], GEUS Stream sediments, s.p. 4%

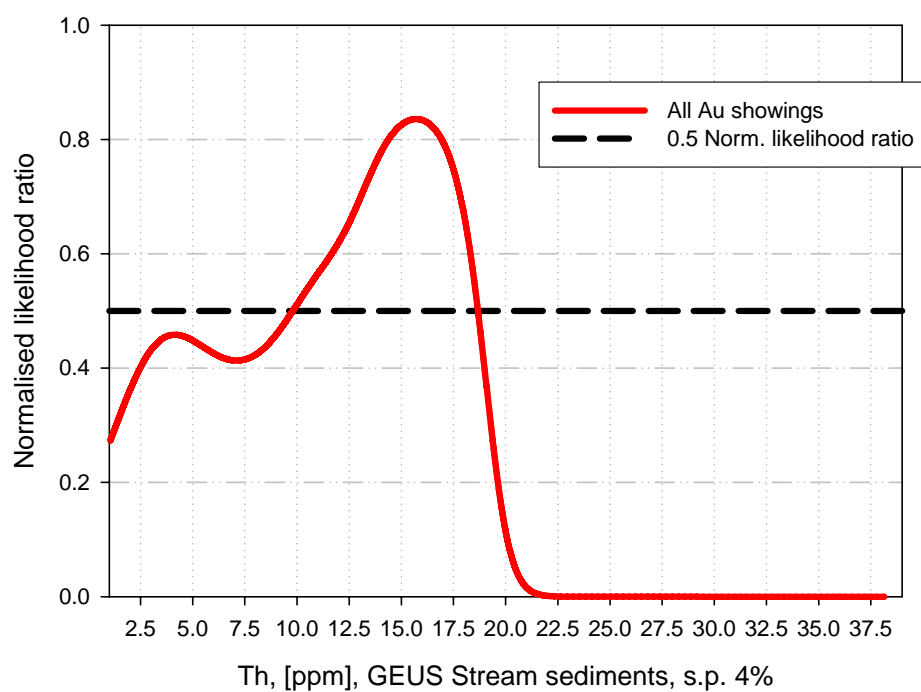


**Figure C51.** *Th, spread parameter 4% - Regional stream sediment geochemistry from GEUS.*

$\text{TiO}_2$ , GEUS, minimum curvature, 200 m  
spread parameter 0.5%

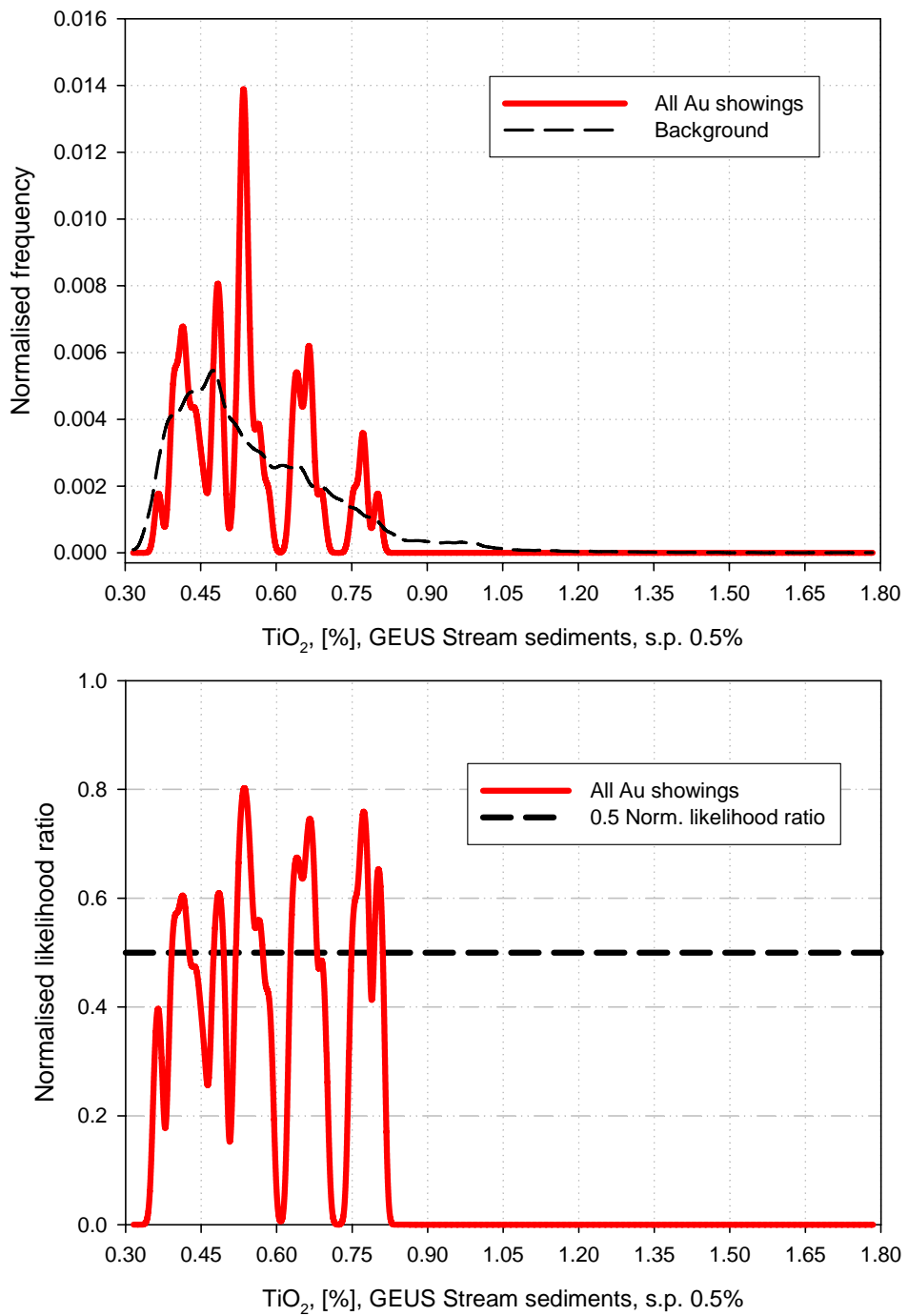


**Figure C52.**  $\text{TiO}_2$ , spread parameter 0.5% - Regional stream sediment geochemistry from GEUS.

$\text{TiO}_2$ , GEUS, minimum curvature, 200 m  
spread parameter 2%

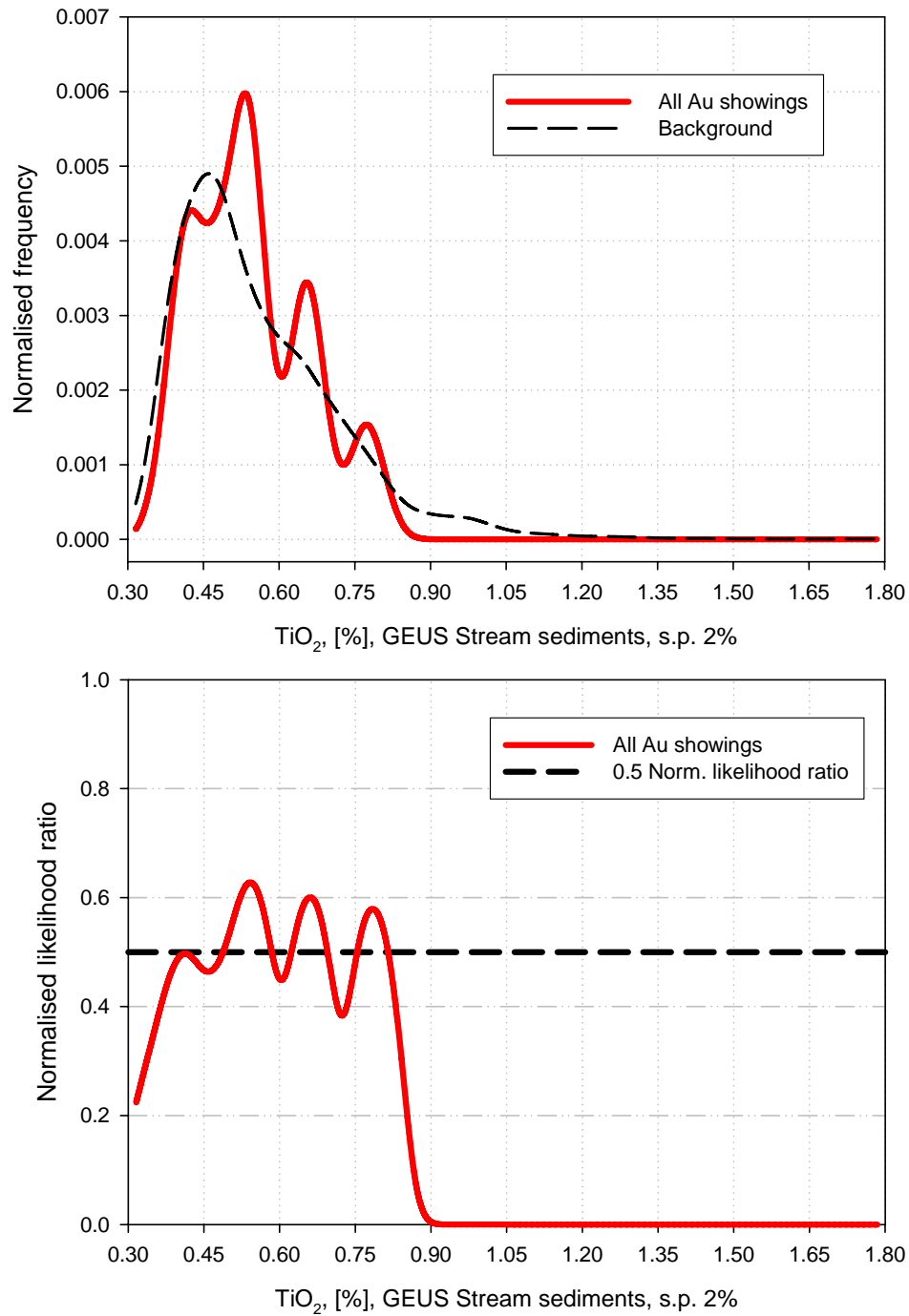


**Figure C53.**  $\text{TiO}_2$ , spread parameter 2% - Regional stream sediment geochemistry from GEUS.

$\text{TiO}_2$ , GEUS, minimum curvature, 200 m  
spread parameter 4%

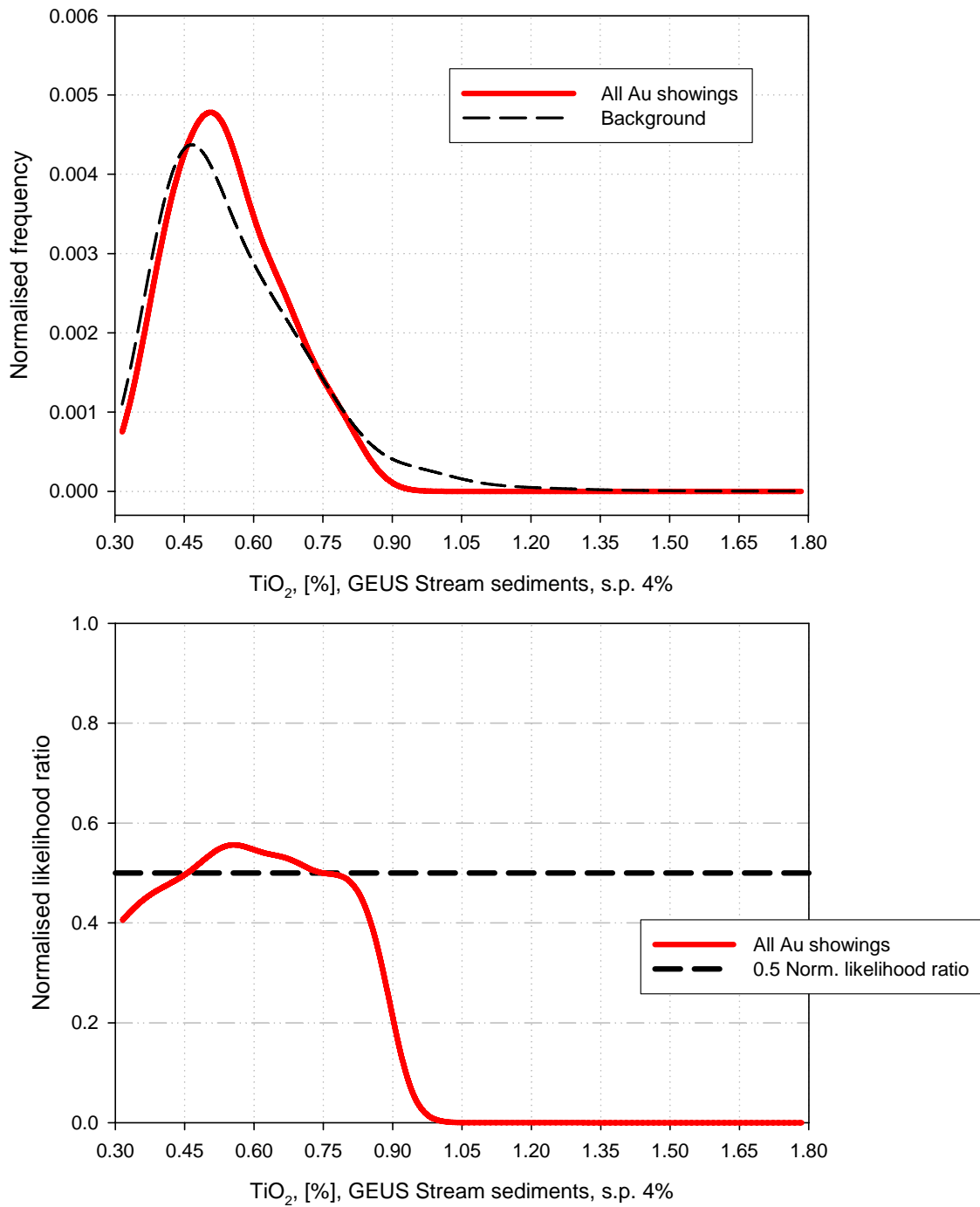
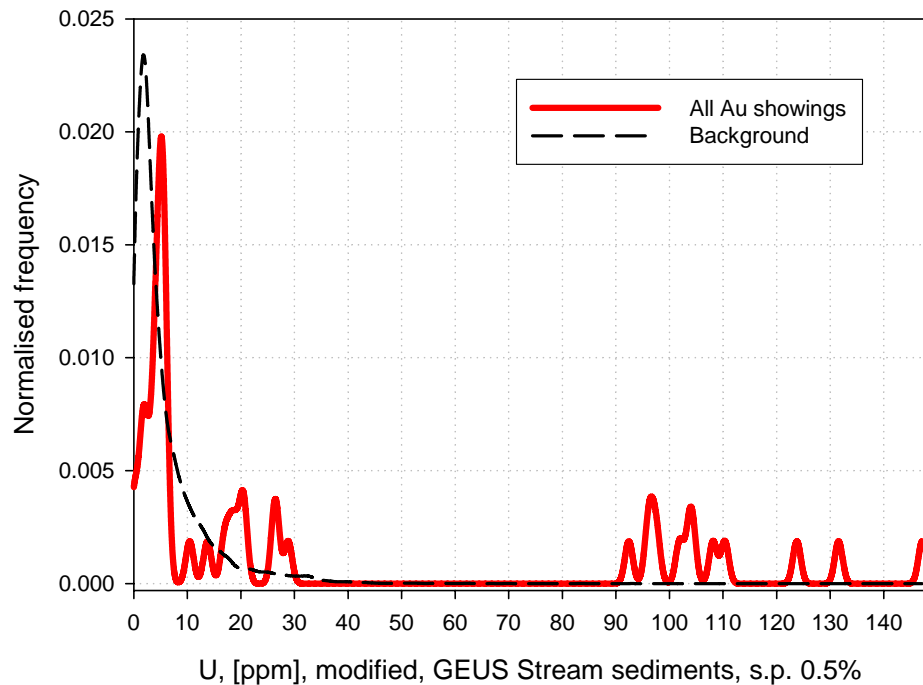
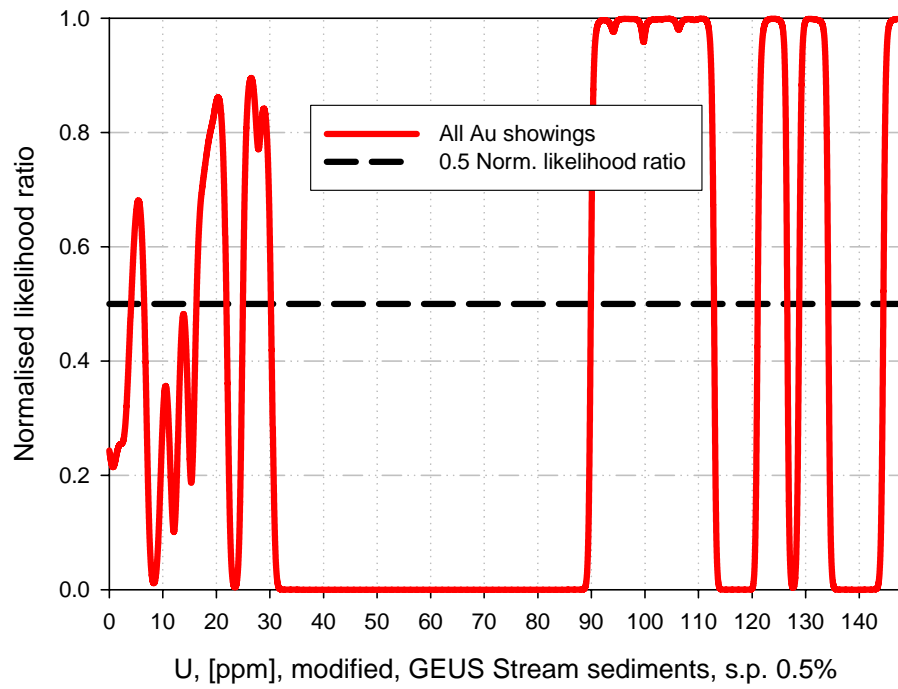


**Figure C54.**  $\text{TiO}_2$ , spread parameter 4% - Regional stream sediment geochemistry from GEUS.

U, GEUS, minimum curvature, modified, 200 m  
spread parameter 0.5%



U, [ppm], modified, GEUS Stream sediments, s.p. 0.5%



U, [ppm], modified, GEUS Stream sediments, s.p. 0.5%

**Figure C55.** *U, spread parameter 0.5% - Regional stream sediment geochemistry from GEUS.*

U, GEUS, minimum curvature, modified, 200 m  
spread parameter 2%

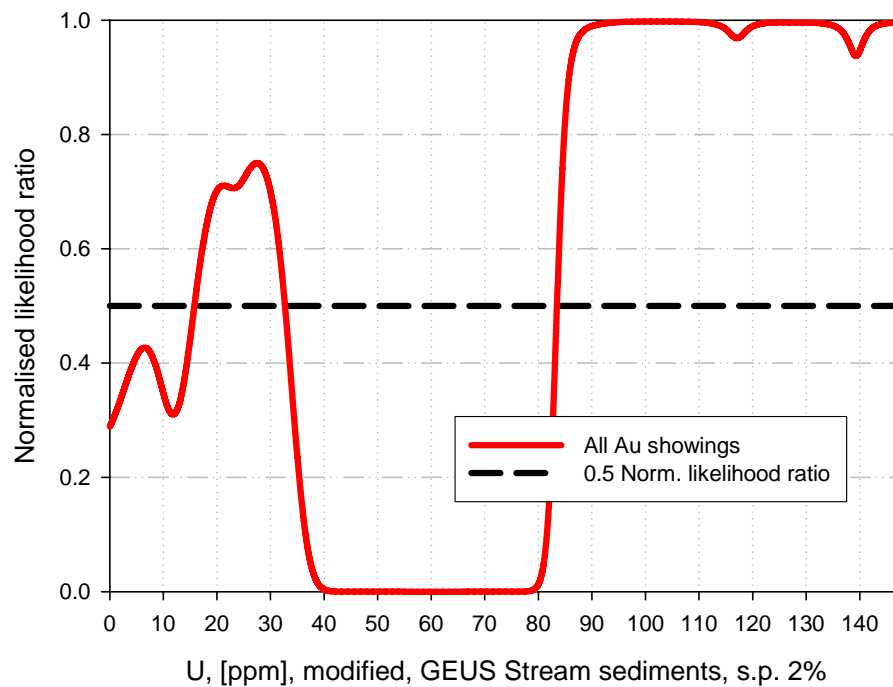
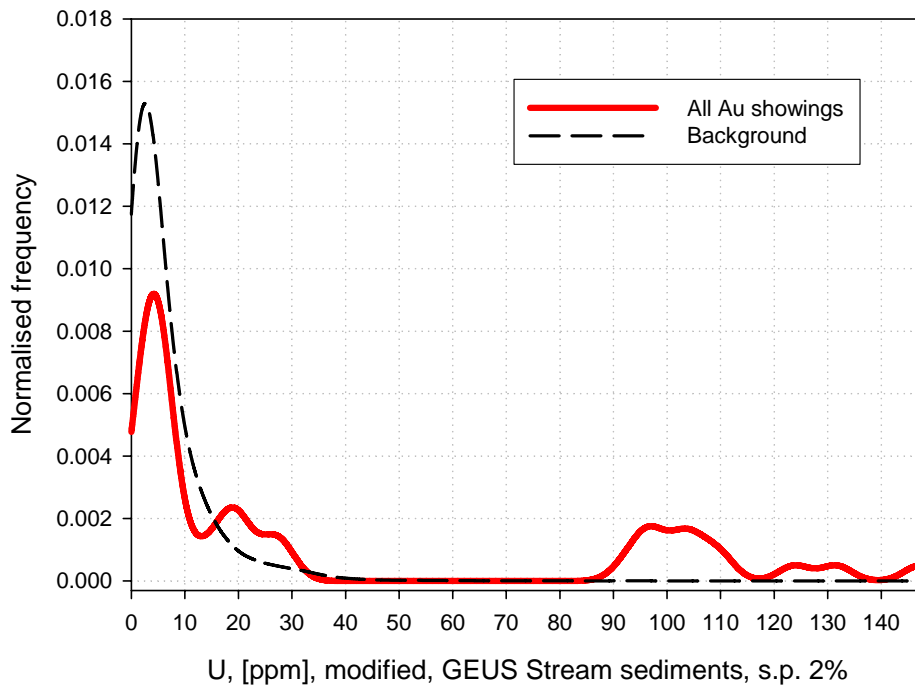


**Figure C56.** *U, spread parameter 2% - Regional stream sediment geochemistry from GEUS.*

U, GEUS, minimum curvature, modified, 200 m  
spread parameter 4%

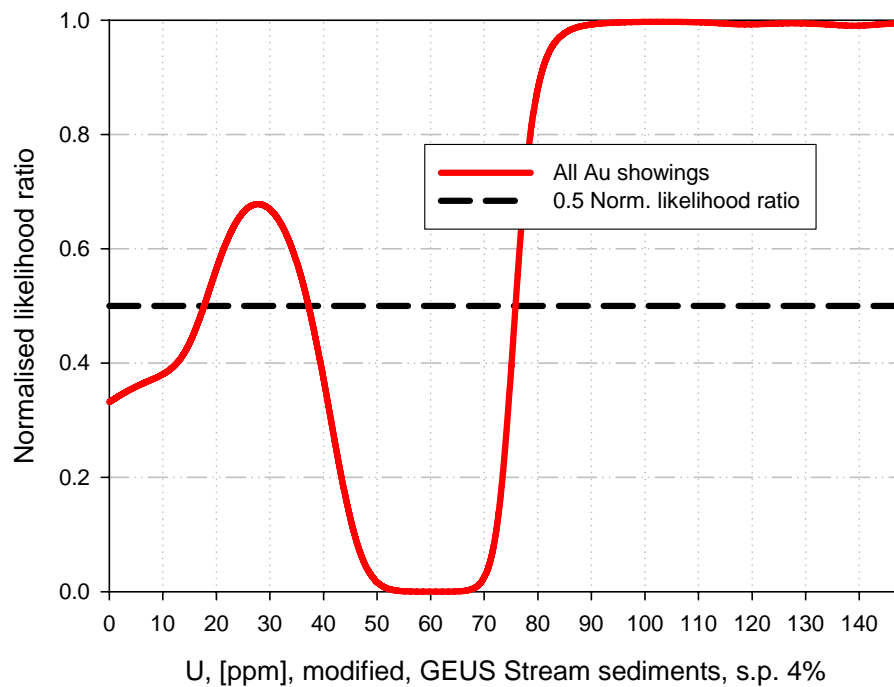
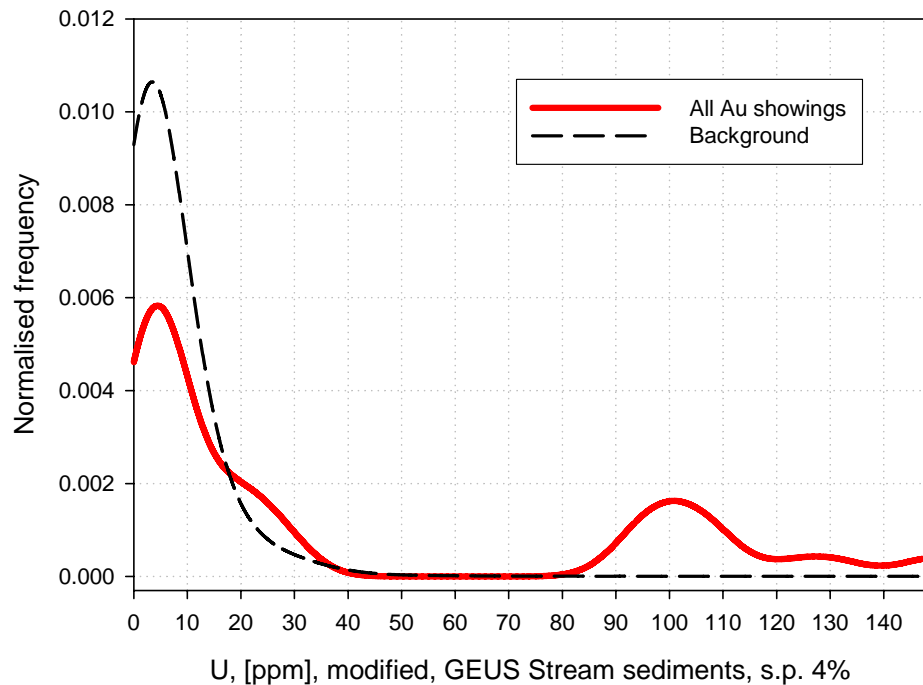


**Figure C57.** U, spread parameter 4% - Regional stream sediment geochemistry from GEUS.

V, GEUS, minimum curvature, 200 m  
spread parameter 0.5%

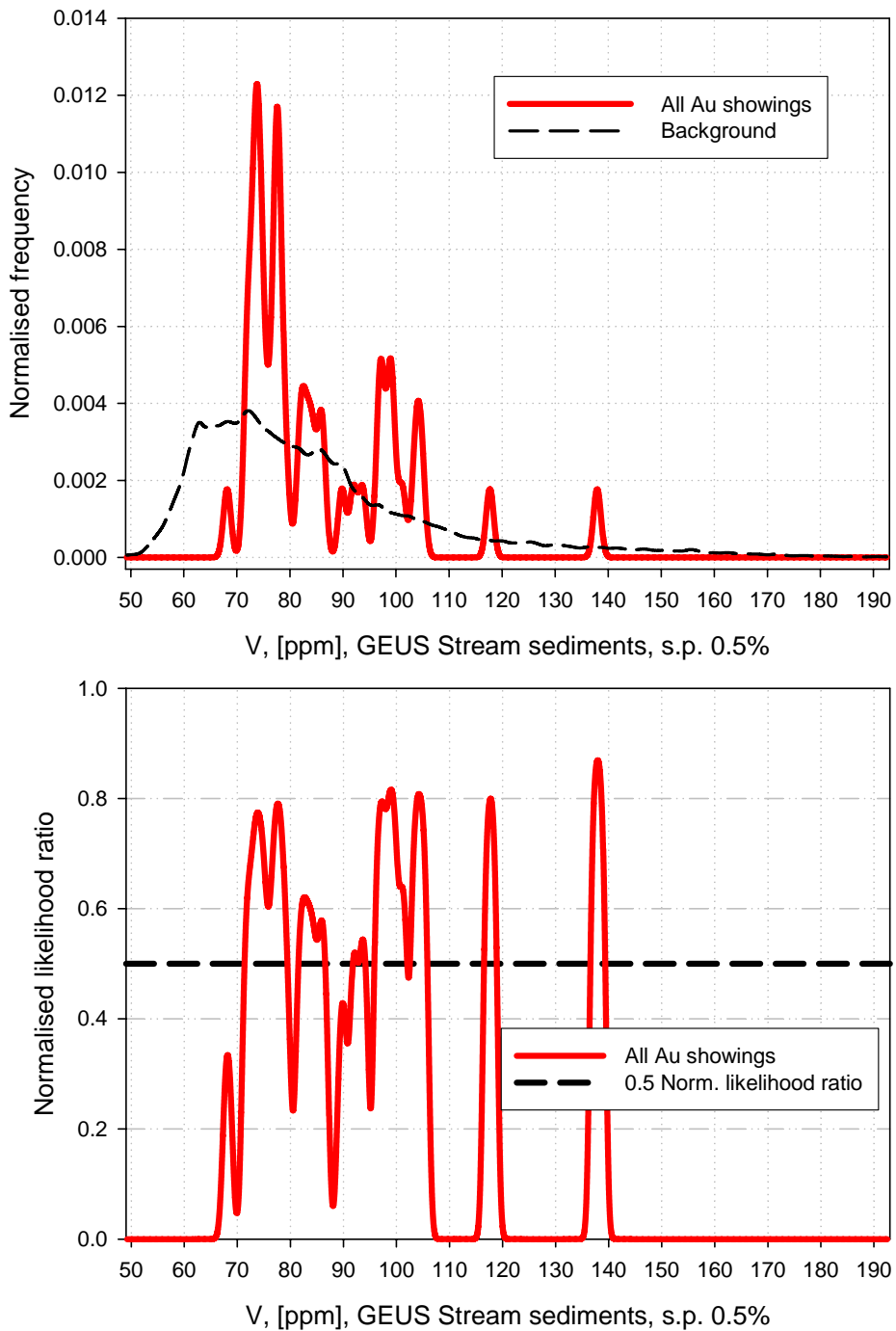


**Figure C58.** V, spread parameter 0.5% - Regional stream sediment geochemistry from GEUS.

V, GEUS, minimum curvature, 200 m  
spread parameter 2%

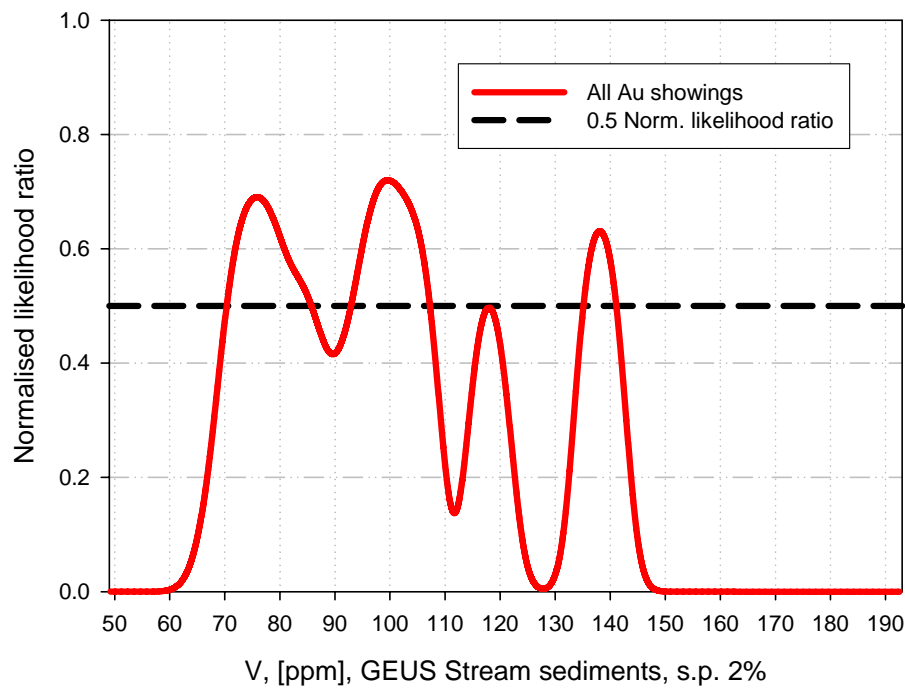
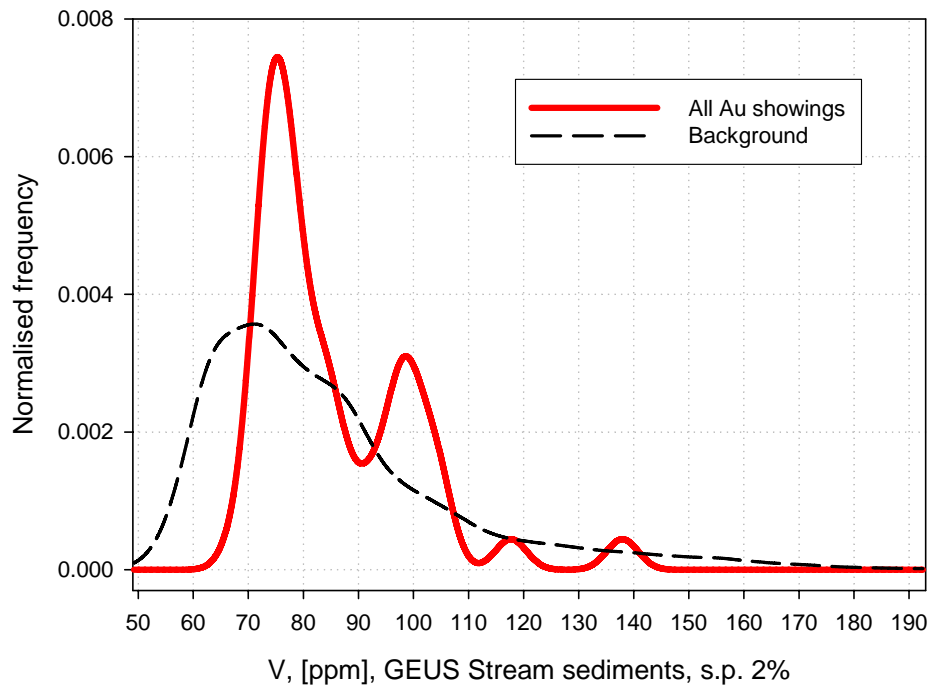


**Figure C59.** V, spread parameter 2% - Regional stream sediment geochemistry from GEUS.

V, GEUS, minimum curvature, 200 m  
spread parameter 4%

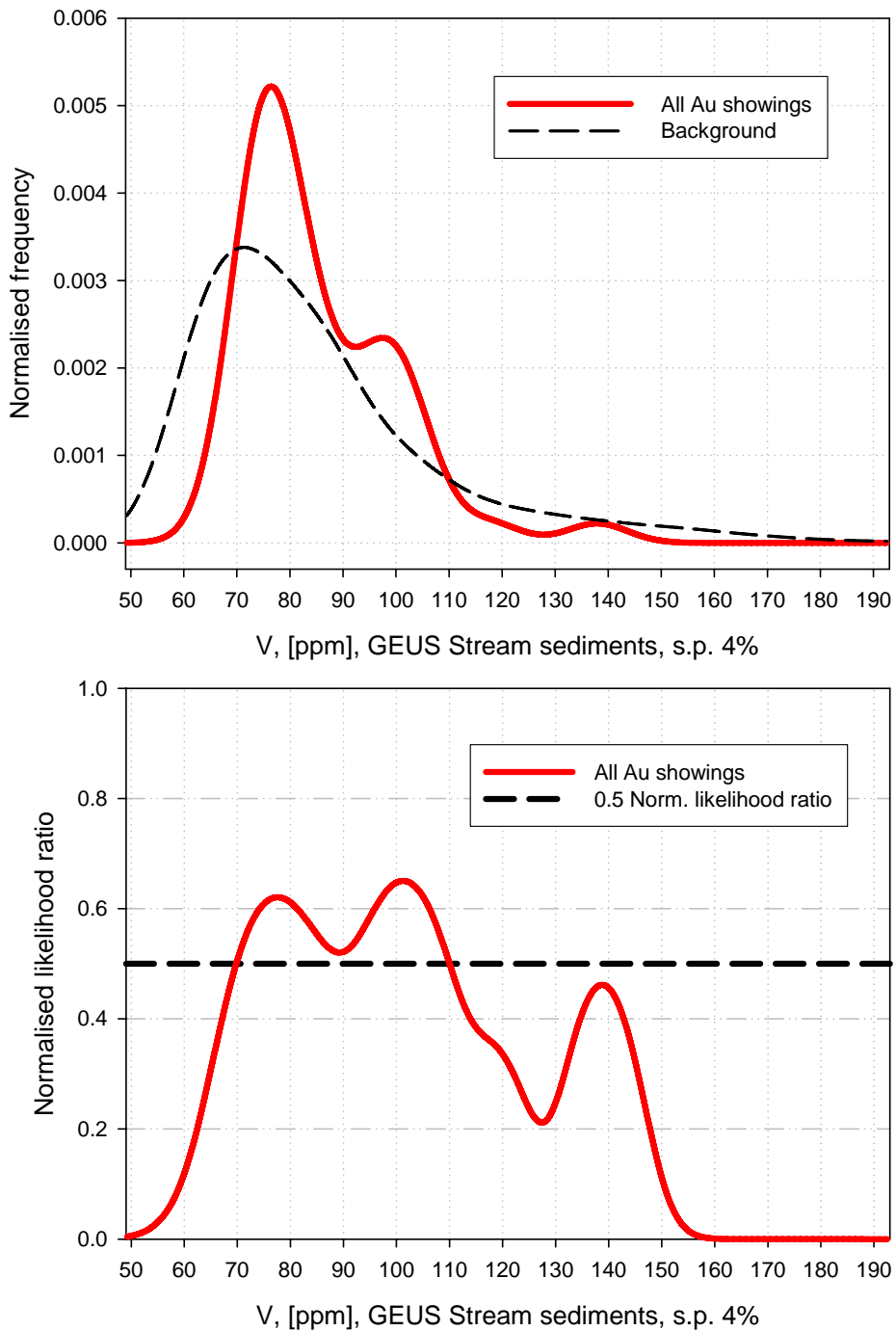


**Figure C60.** V, spread parameter 4% - Regional stream sediment geochemistry from GEUS.

Zn, GEUS, minimum curvature, 200 m  
spread parameter 0.5%

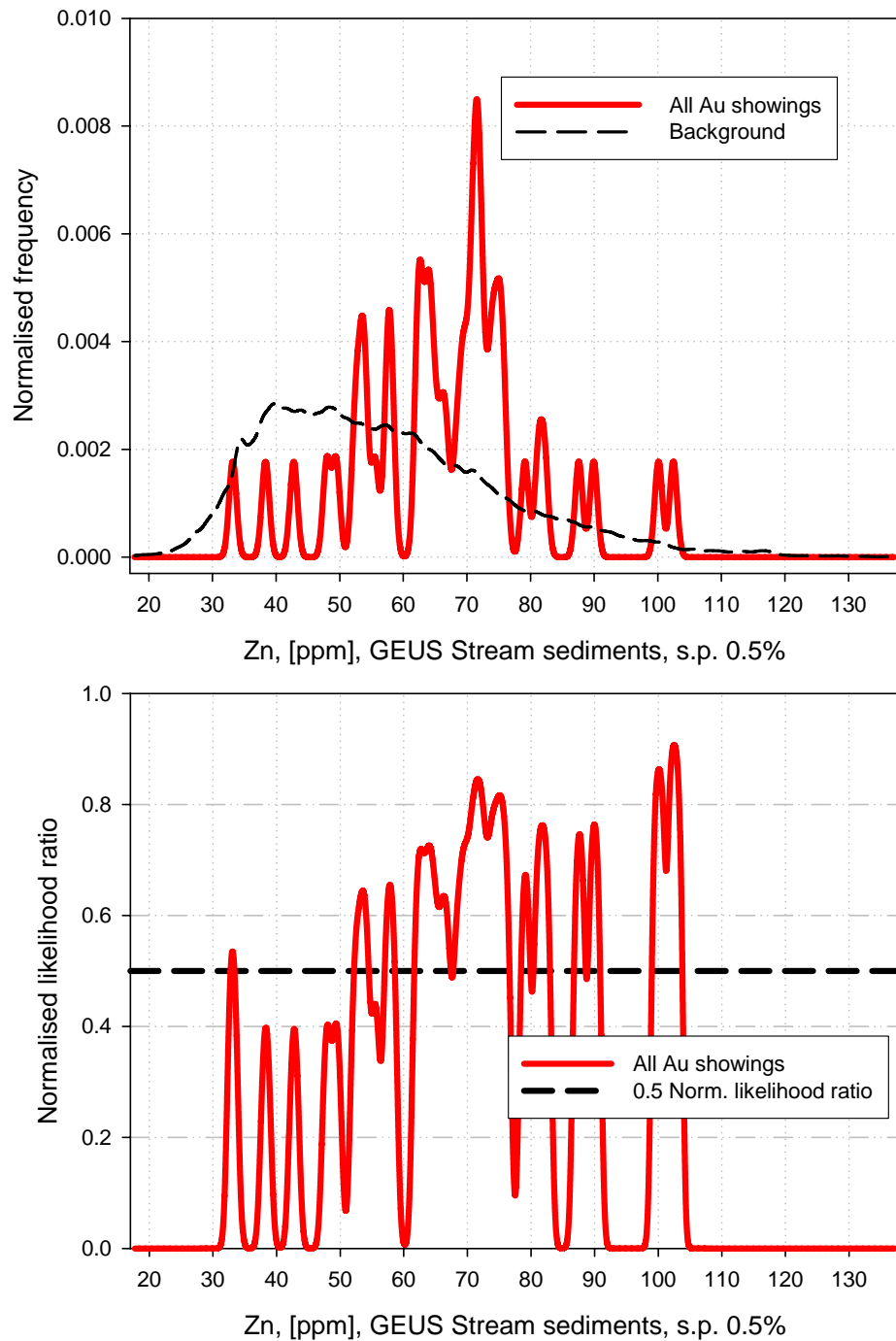


**Figure C61.** Zn, spread parameter 0.5% - Regional stream sediment geochemistry from GEUS.

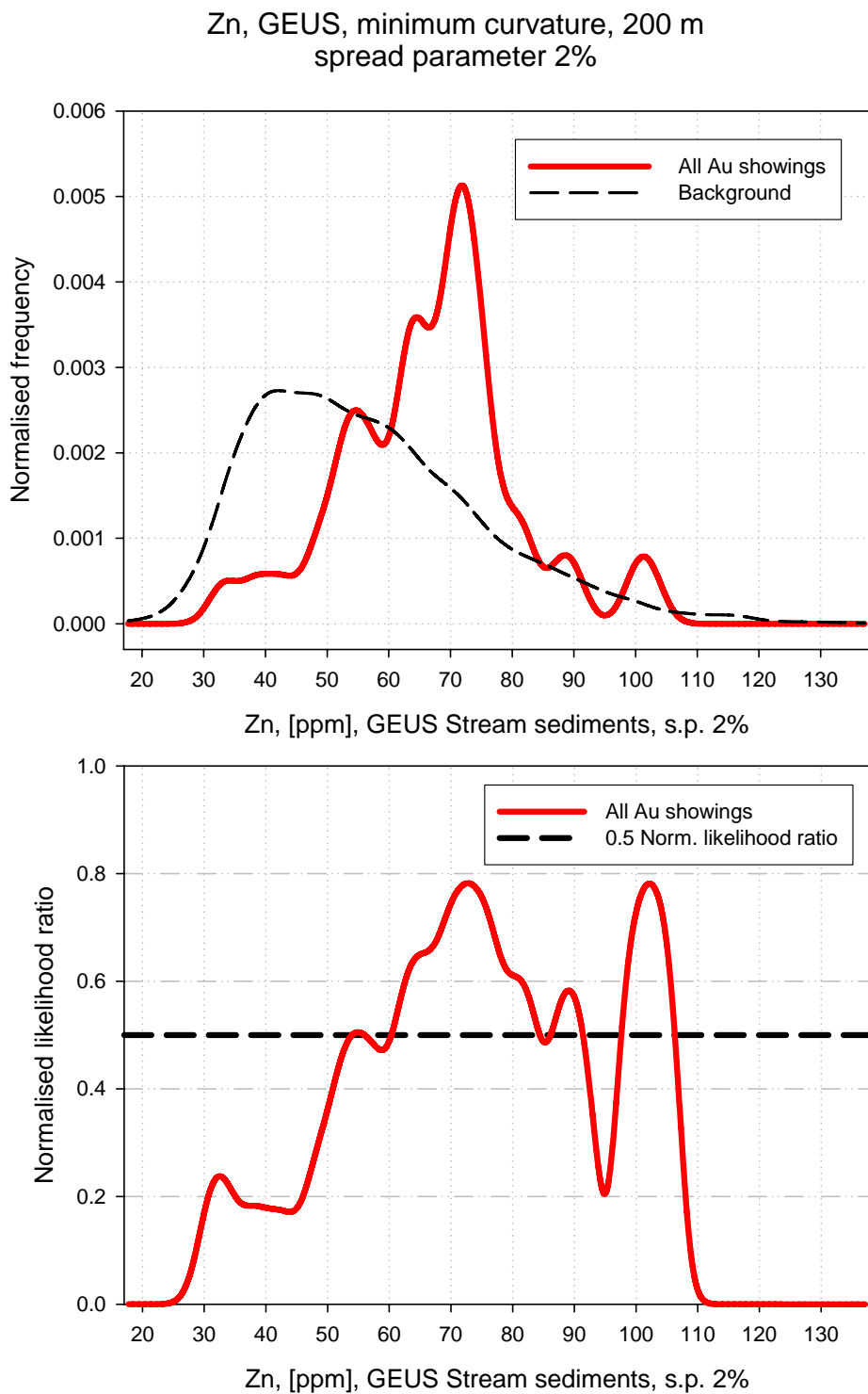


**Figure C62.** Zn, spread parameter 2% - Regional stream sediment geochemistry from GEUS.

Zn, GEUS, minimum curvature, 200 m  
spread parameter 4%

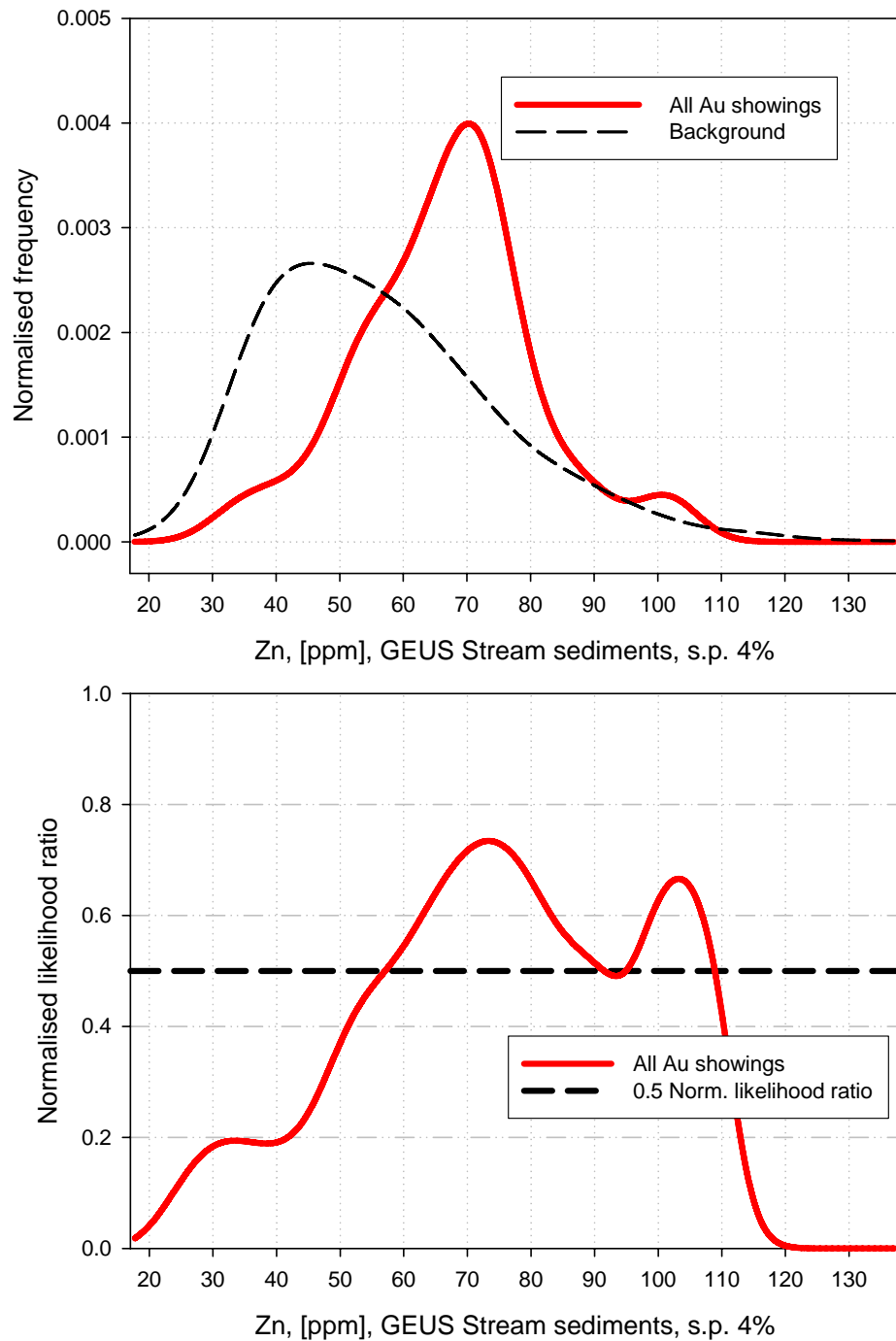


**Figure C63.** Zn, spread parameter 4% - Regional stream sediment geochemistry from GEUS.

Zr, GEUS, minimum curvature, 200 m  
spread parameter 0.5%

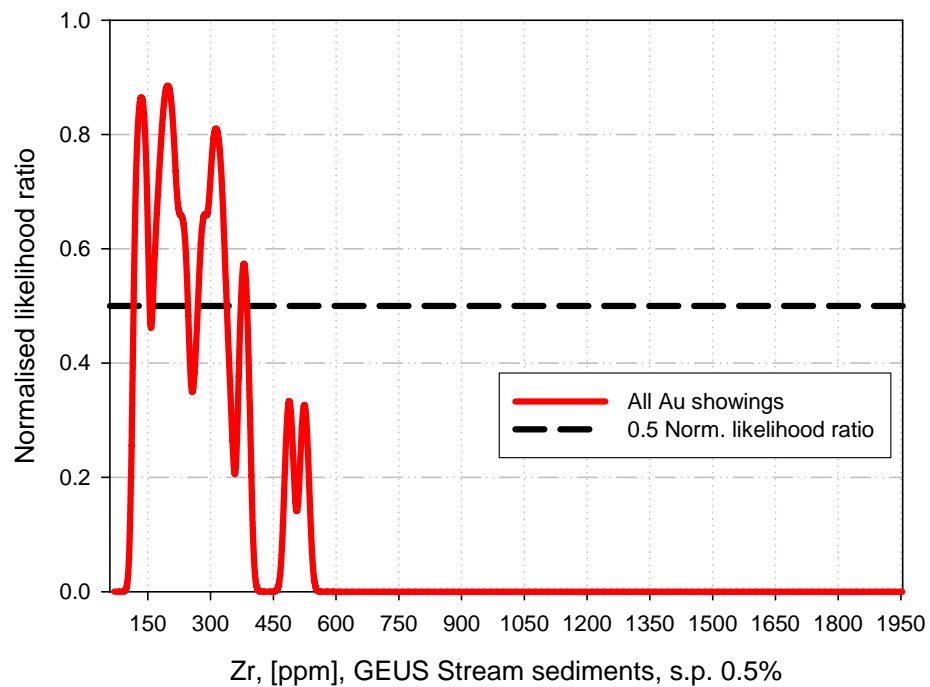
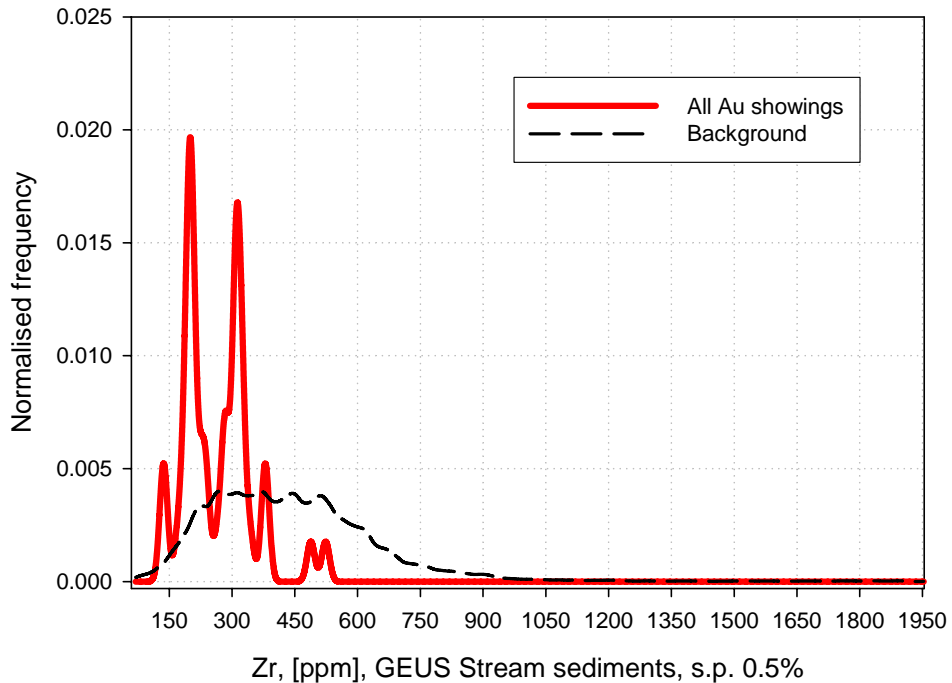


**Figure C64.** Zr, spread parameter 0.5% - Regional stream sediment geochemistry from GEUS.

Zr, GEUS, minimum curvature, 200 m  
spread parameter 2%

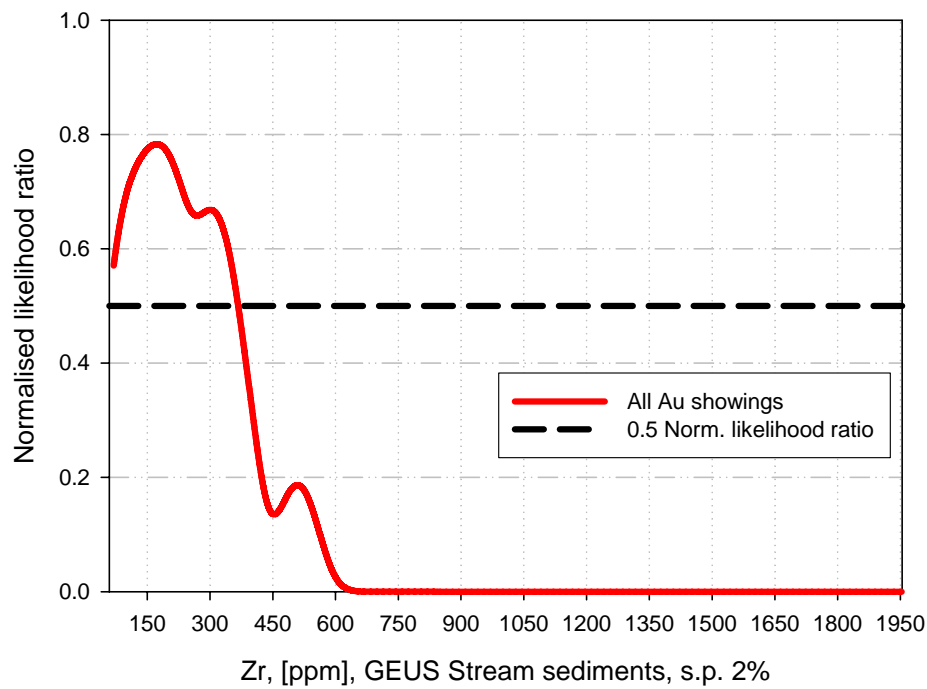
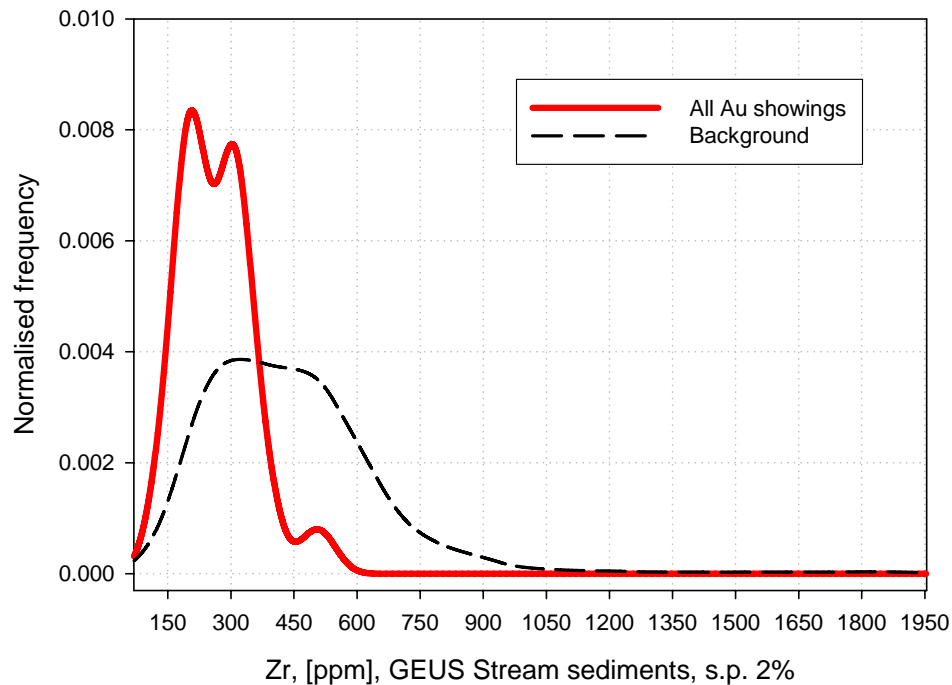


**Figure C65.** Zr, spread parameter 2% - Regional stream sediment geochemistry from GEUS.

Zr, GEUS, minimum curvature, 200 m  
spread parameter 4%

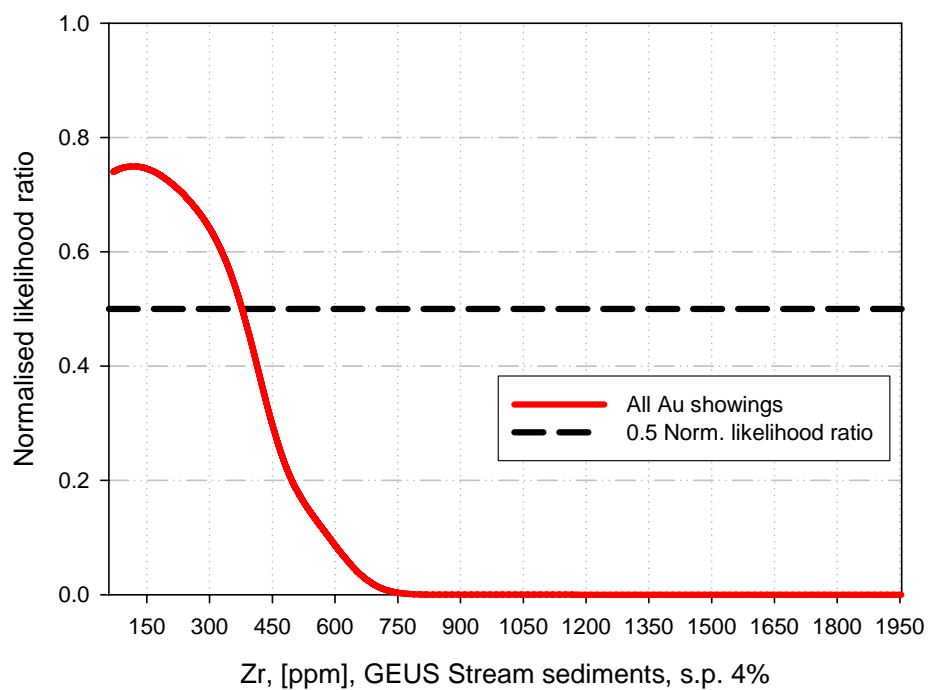
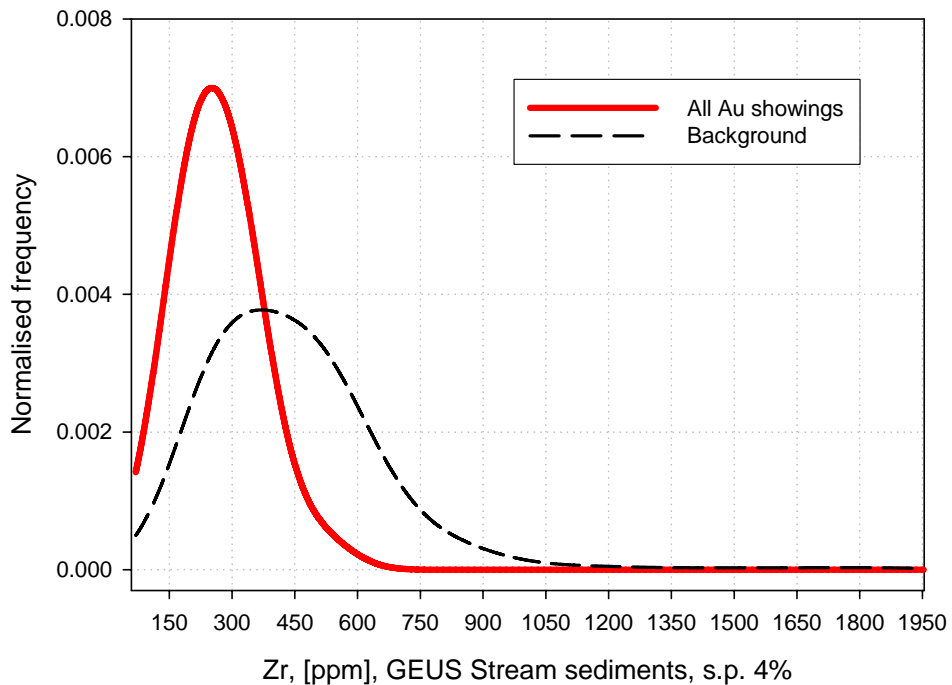
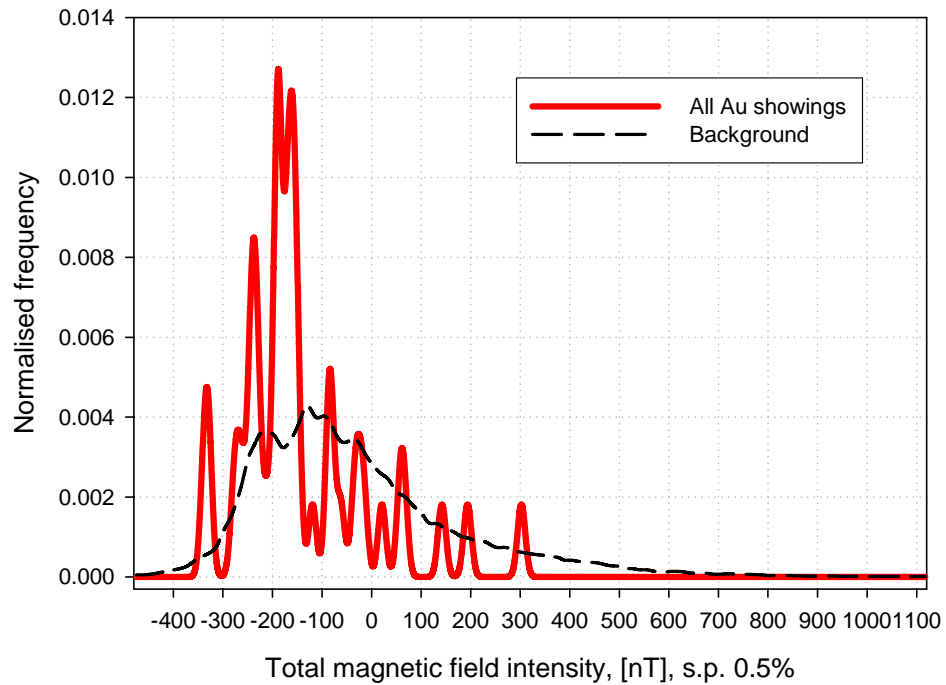
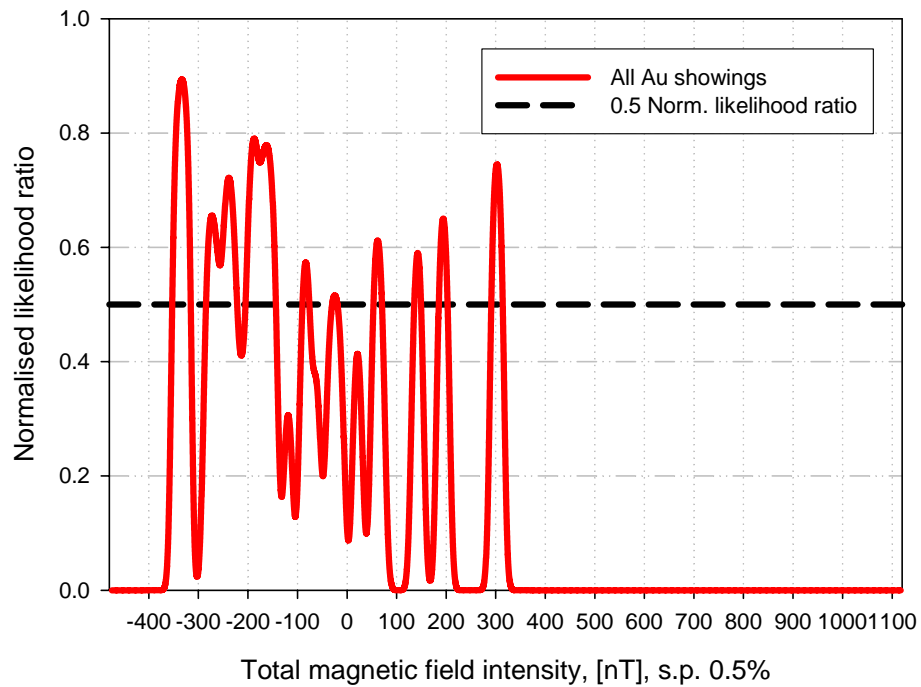


**Figure C66.** Zr, spread parameter 4% - Regional stream sediment geochemistry from GEUS.

Total magnetic field intensity, gridcells 200 m  
spread parameter 0.5%



Total magnetic field intensity, [nT], s.p. 0.5%



Total magnetic field intensity, [nT], s.p. 0.5%

**Figure C67** Total magnetic field intensity (TMI) spread parameter 0.5% – Regional aeromagnetic data from GEUS.

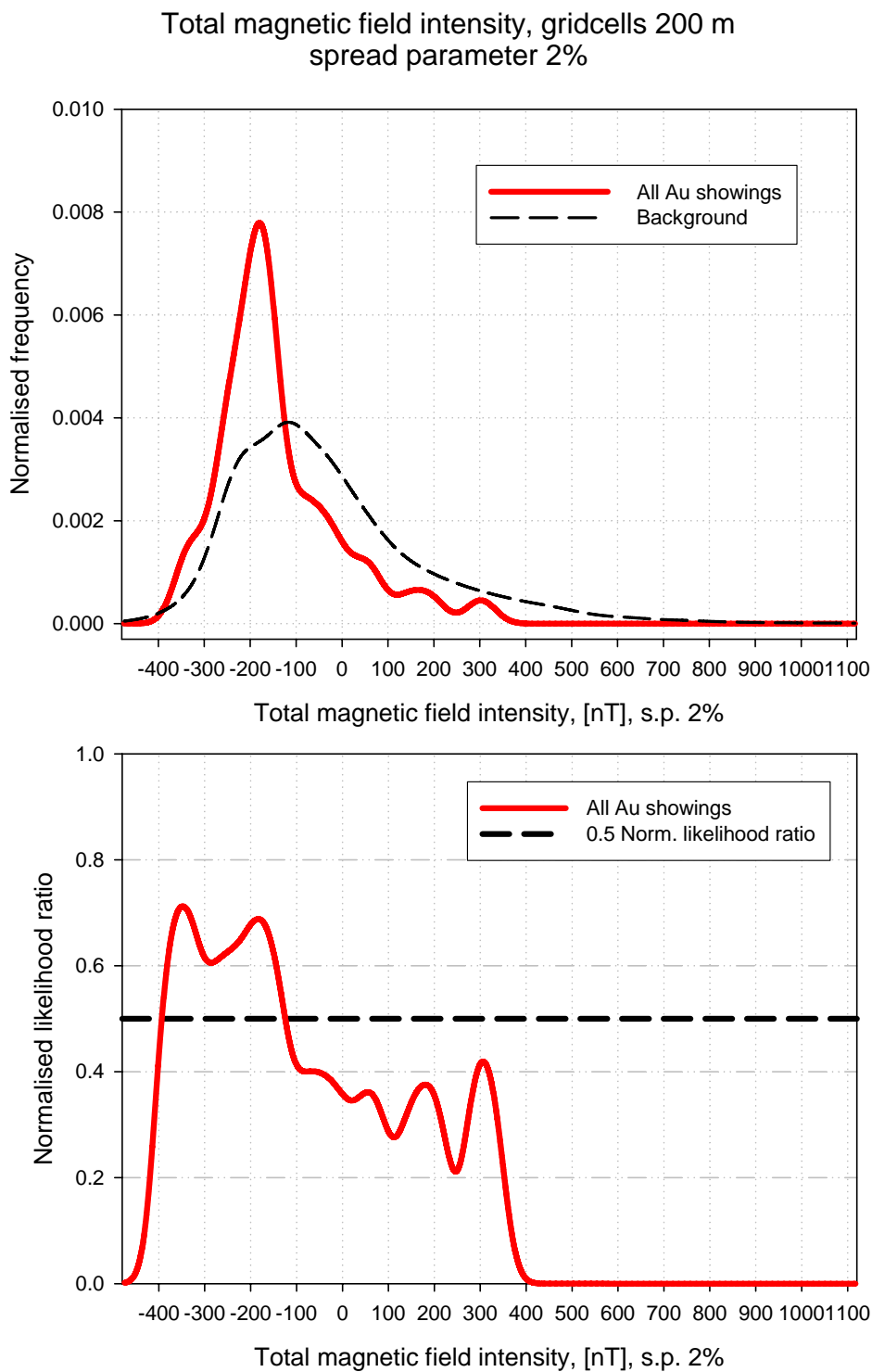


**Figure C68.** Total magnetic field intensity (TMI) spread parameter 2% – Regional aeromagnetic data from GEUS.

Total magnetic field intensity, gridcells 200 m  
spread parameter 4%

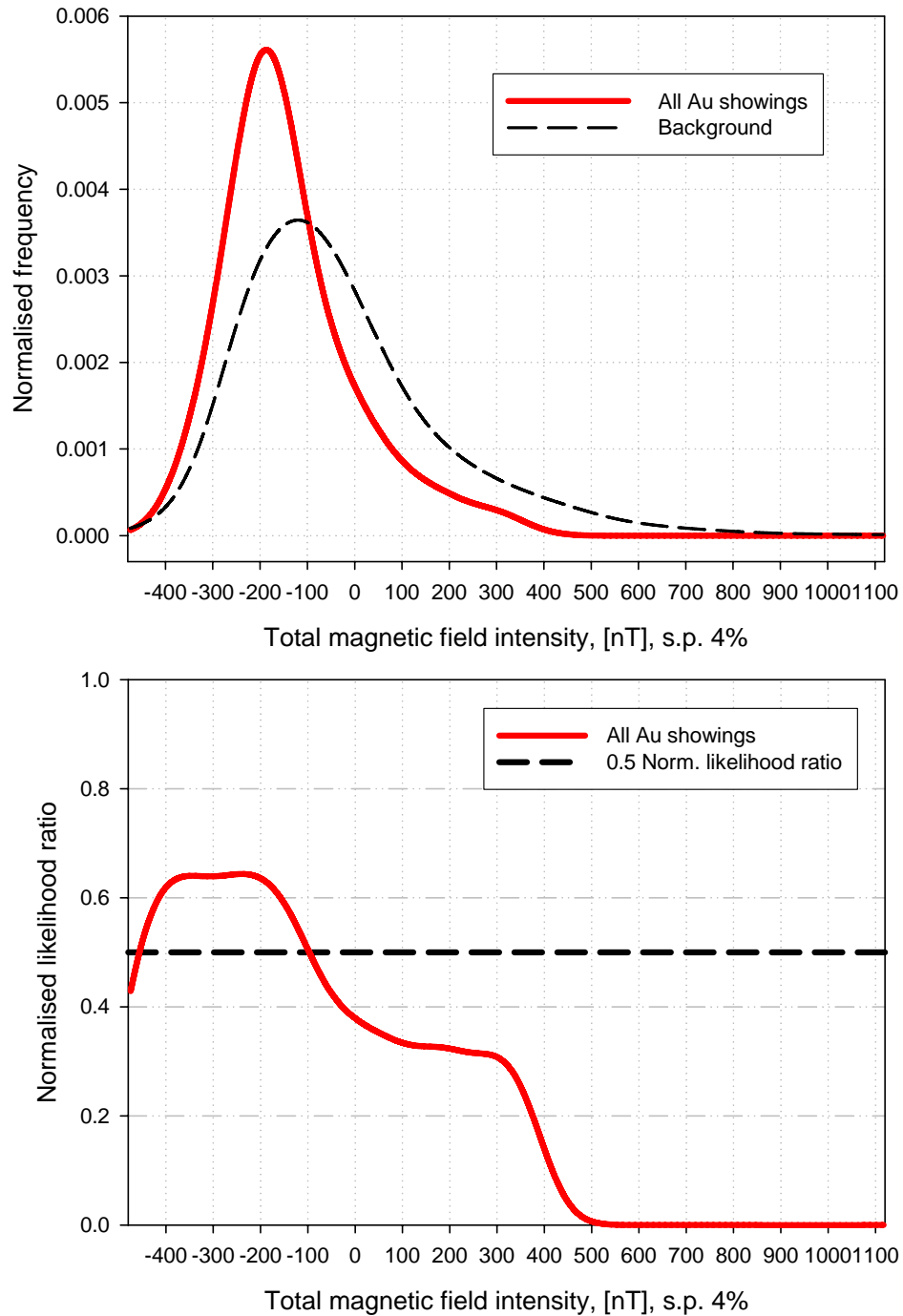


**Figure C69.** Total magnetic field intensity (TMI) spread parameter 4% – Regional aeromagnetic data from GEUS.

Vertical gradient of total magnetic field intensity, gridcells 200 m  
spread parameter 0.5%

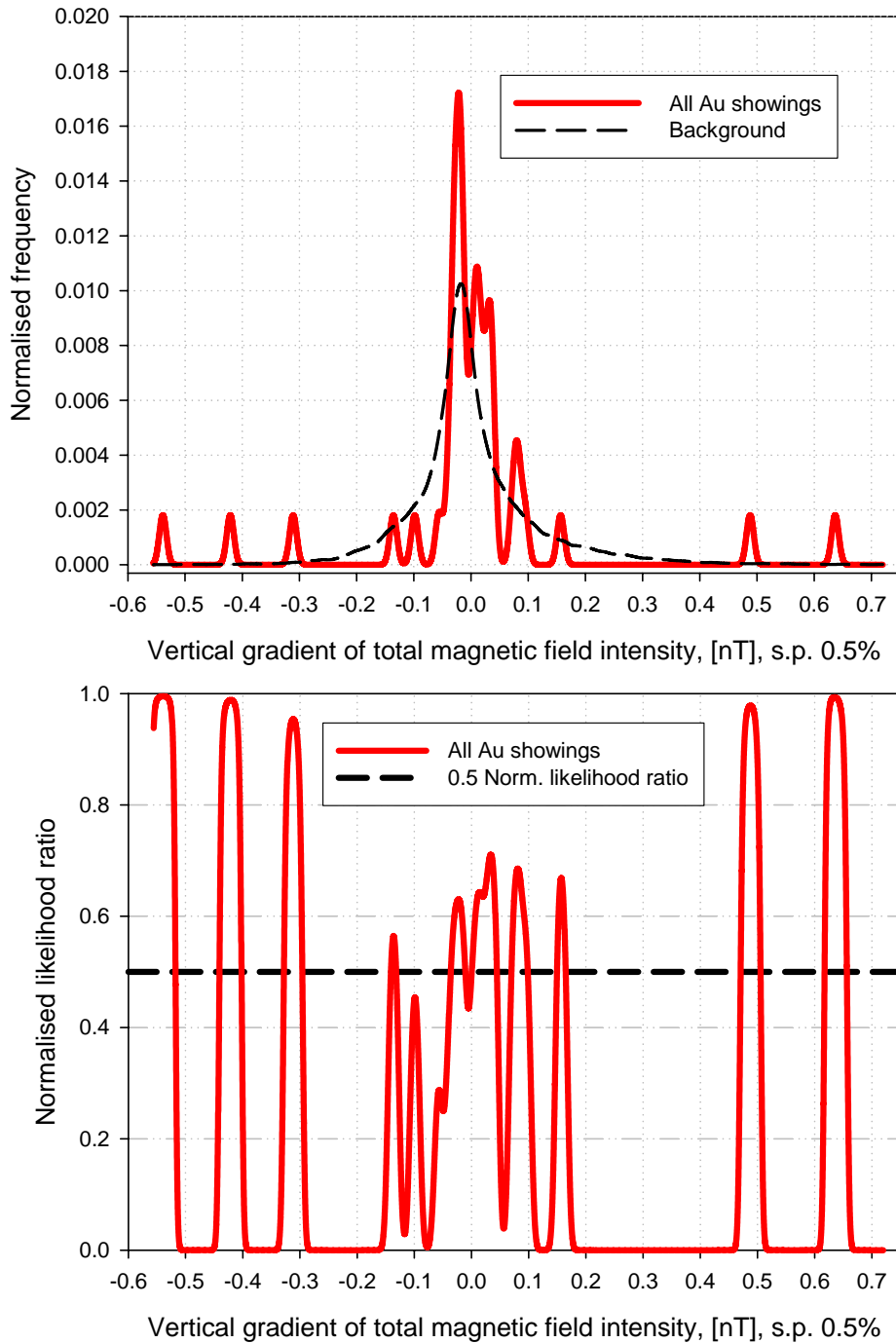


**Figure C70.** Vertical gradient of TMI spread parameter 0.5% – Regional aeromagnetic data from GEUS.

Vertical gradient of total magnetic field intensity, gridcells 200 m  
spread parameter 2%

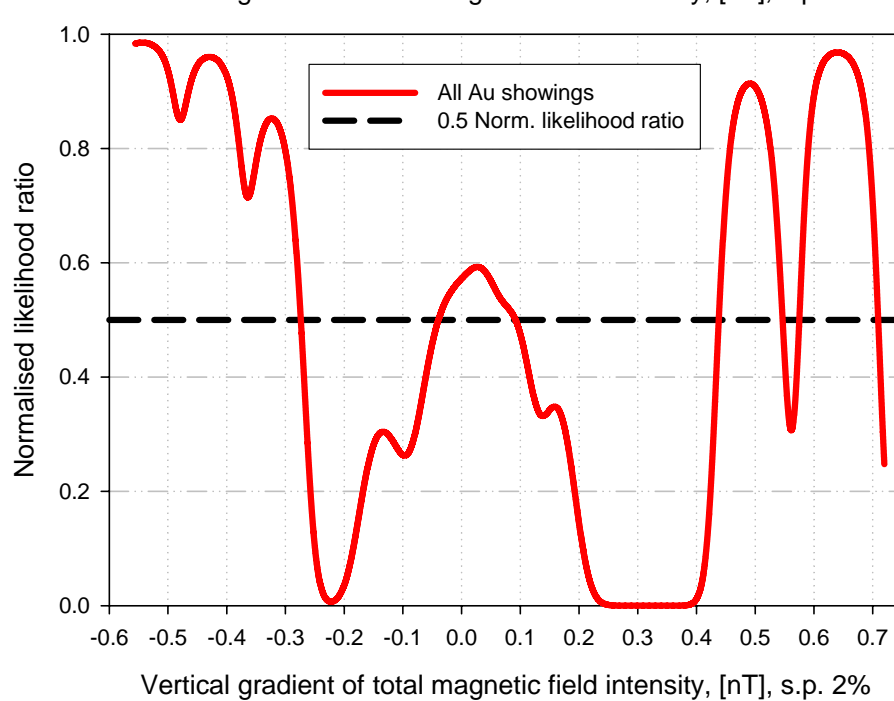
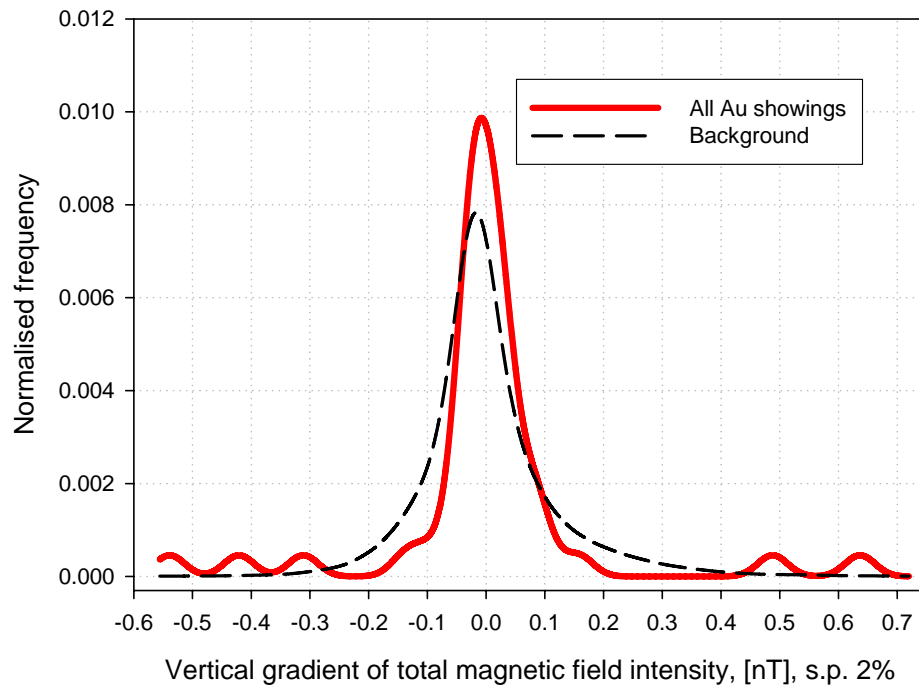


**Figure C71.** Vertical gradient of TMI spread parameter 2% – Regional aeromagnetic data from GEUS.

Vertical gradient of total magnetic field intensity, gridcells 200 m  
spread parameter 4%

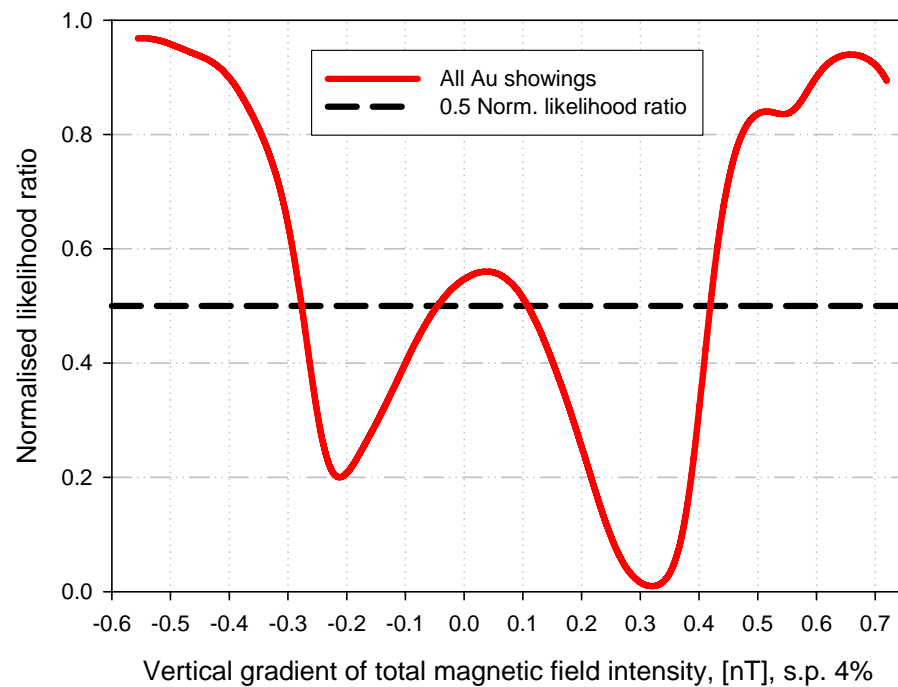
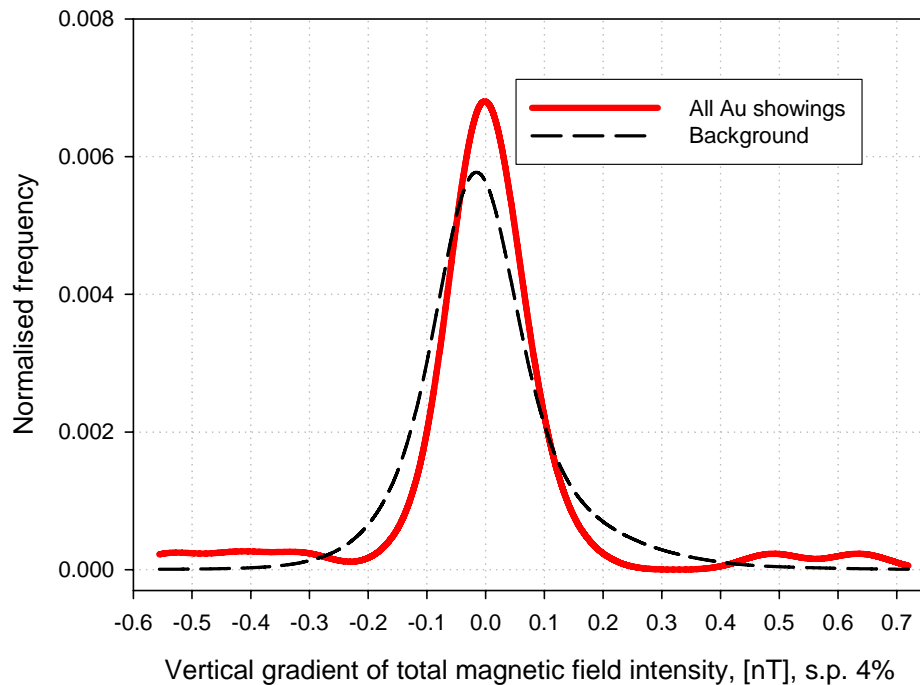


**Figure C72.** Vertical gradient of TMI spread parameter 4% – Regional aeromagnetic data from GEUS.

Amplitude of the horizontal gradient of TMI, gridcells 200 m  
spread parameter 0.5%

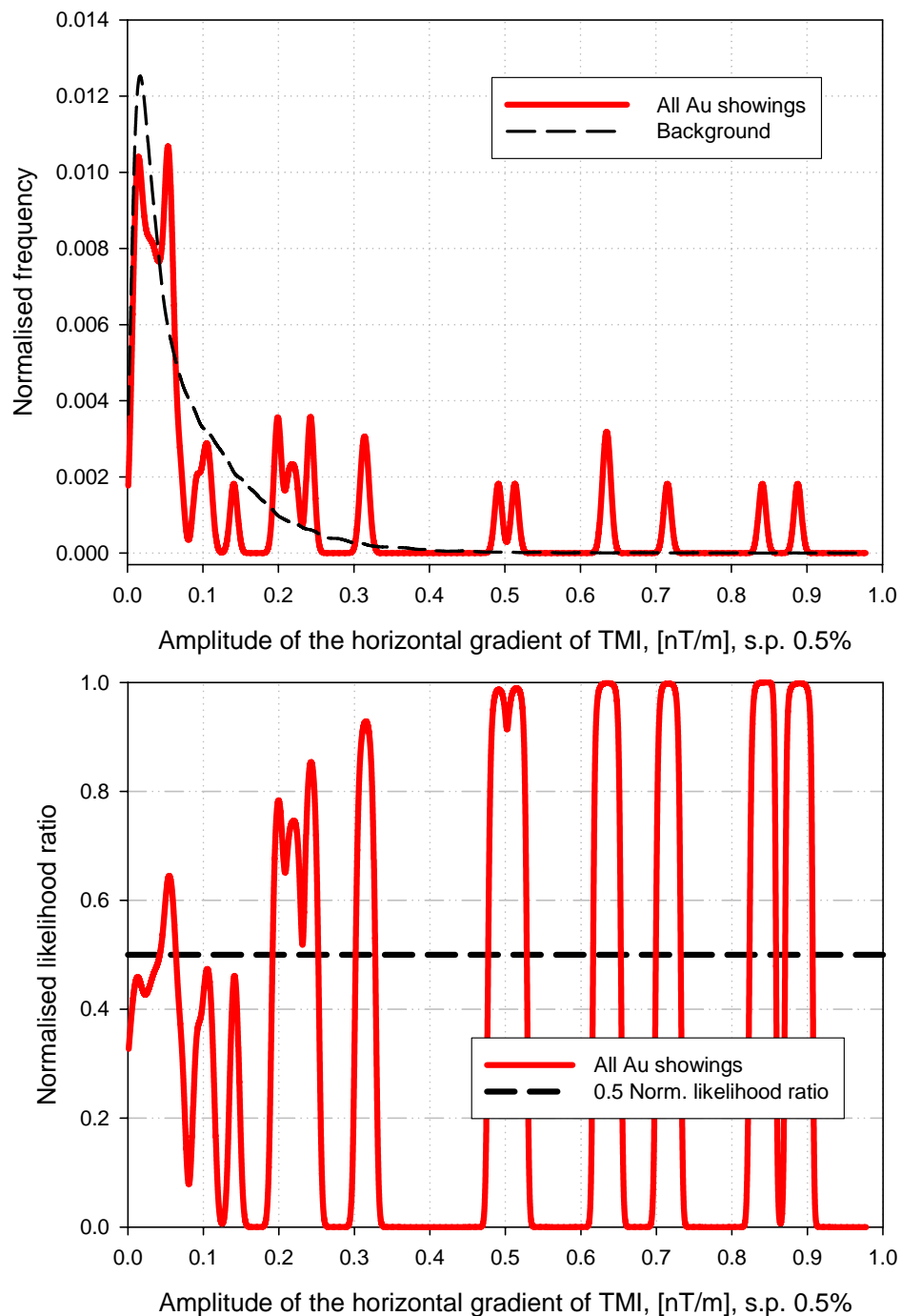


**Figure C73.** Amplitude of horizontal gradient vector of TMI spread parameter 0.5% – Regional aeromagnetic data from GEUS.

Amplitude of the horizontal gradient of TMI, gridcells 200 m  
spread parameter 2%

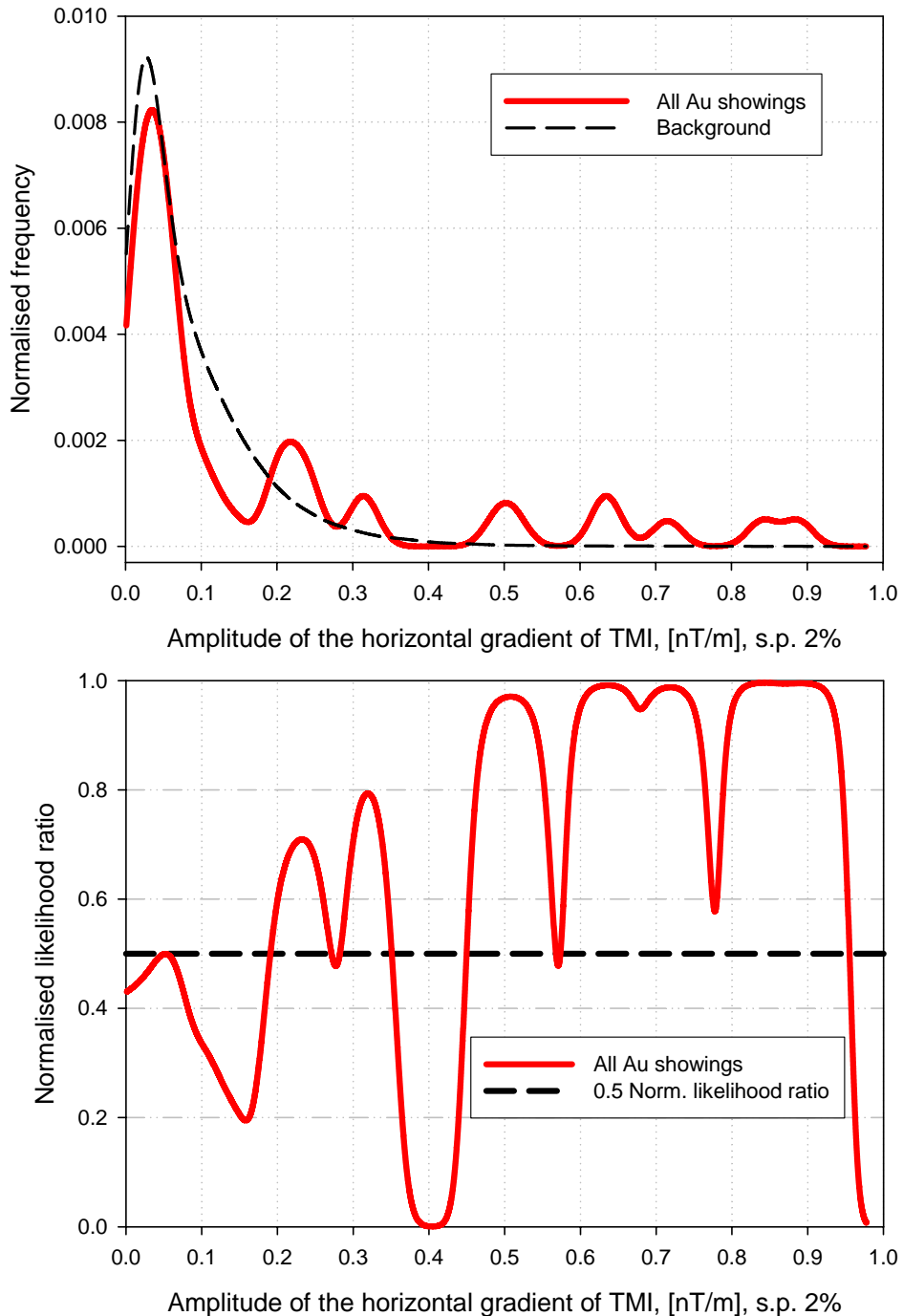


**Figure C74.** Amplitude of horizontal gradient vector of TMI spread parameter 2% – Regional aeromagnetic data from GEUS.

Amplitude of the horizontal gradient of TMI, gridcells 200 m  
spread parameter 4%

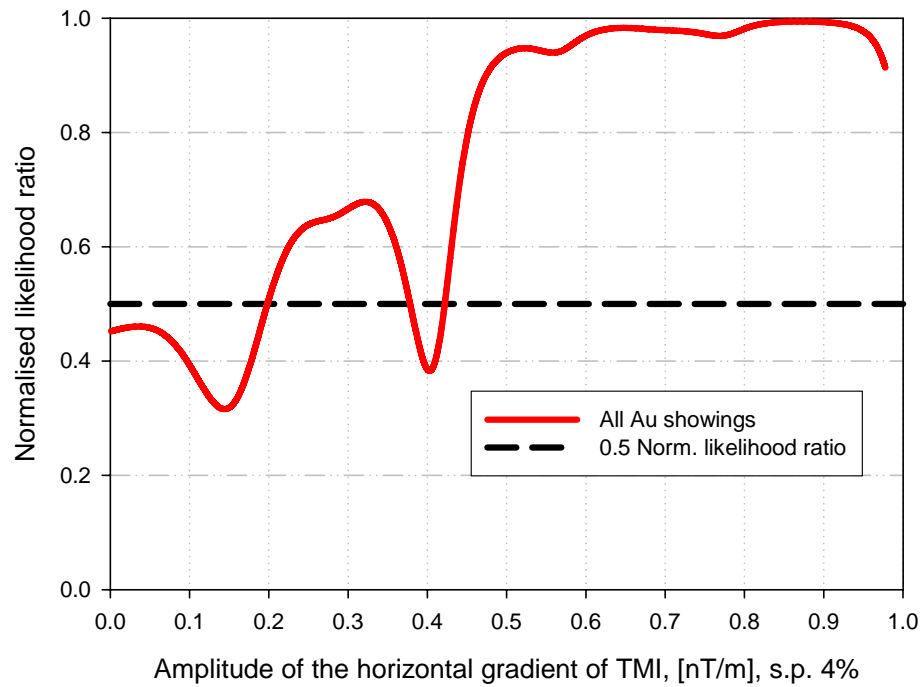
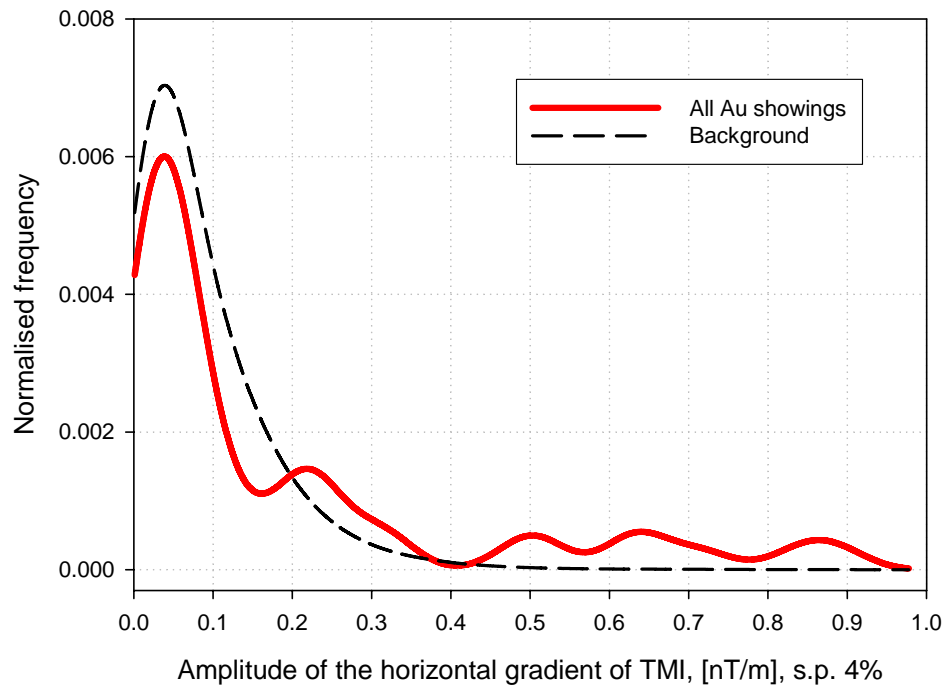


**Figure C75.** Amplitude of horizontal gradient vector of TMI spread parameter 4% – Regional aeromagnetic data from GEUS.

Horizontal gradient of TMI in dir. E, gridcells 200 m  
spread parameter 0.5%

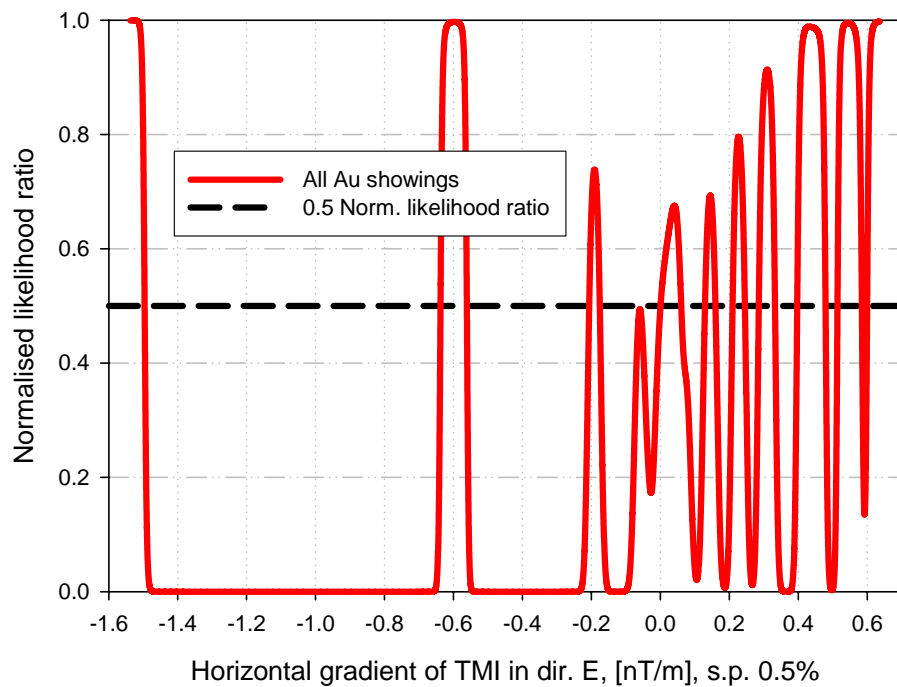
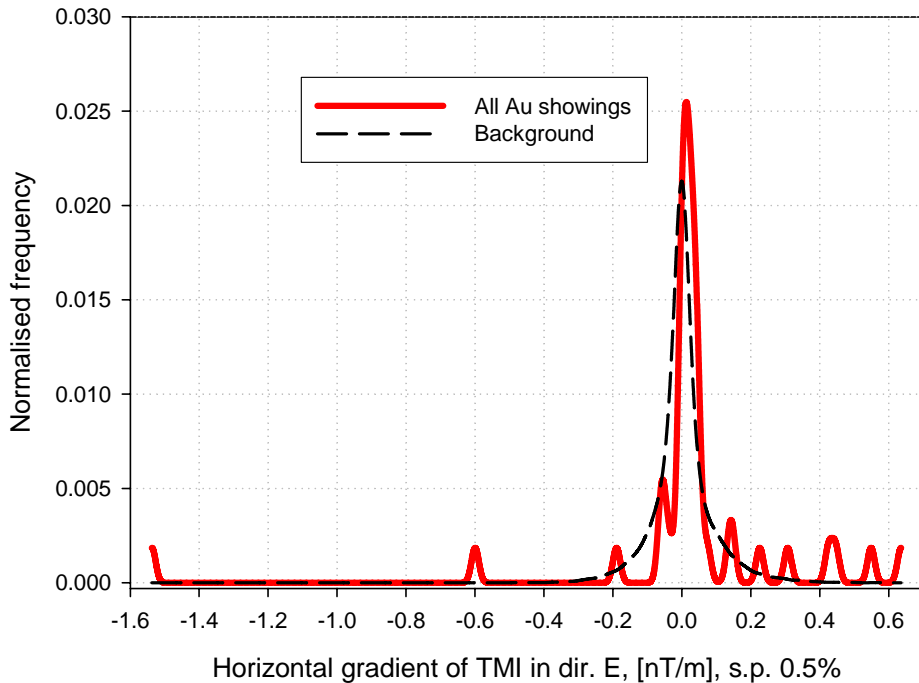


**Figure C76.** Horizontal gradient in east direction of TMI spread parameter 0.5% – Regional aeromagnetic data from GEUS.

Horizontal gradient of TMI in dir. E, gridcells 200 m  
spread parameter 2%

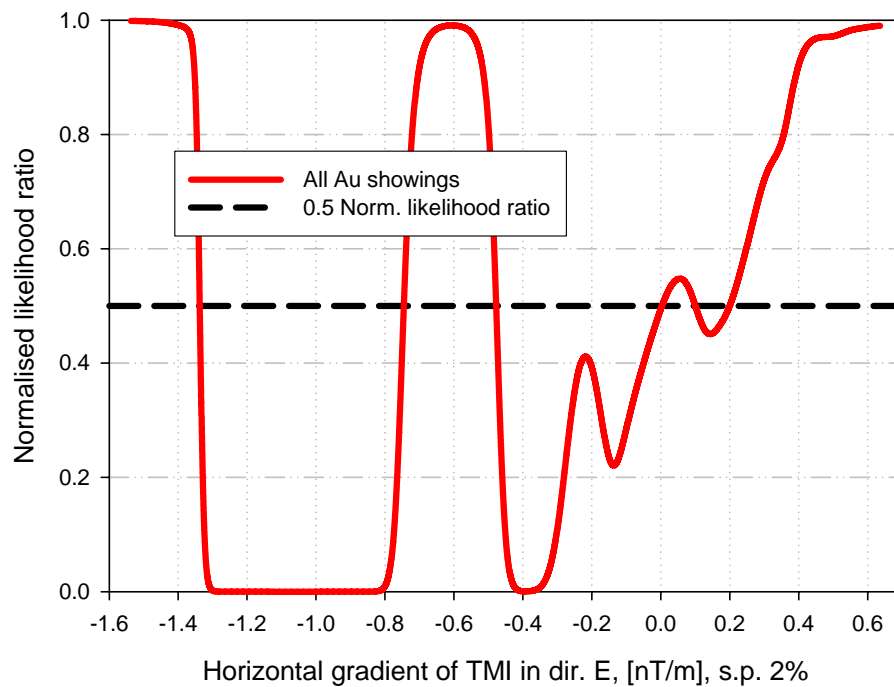
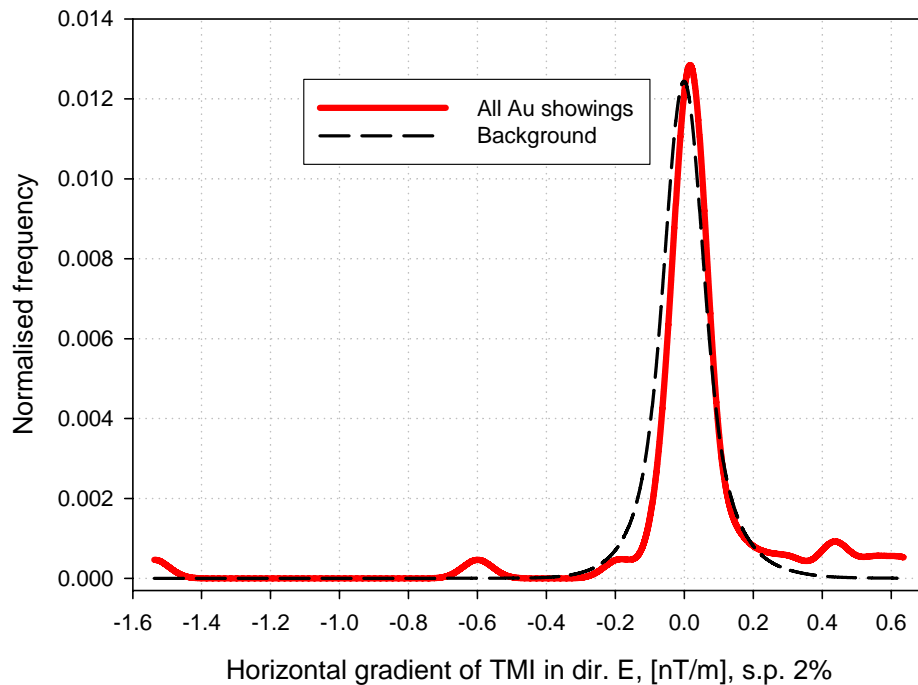


**Figure C77.** Horizontal gradient in east direction of TMI spread parameter 2% – Regional aeromagnetic data from GEUS.

Horizontal gradient of TMI in dir. E, gridcells 200 m  
spread parameter 4%

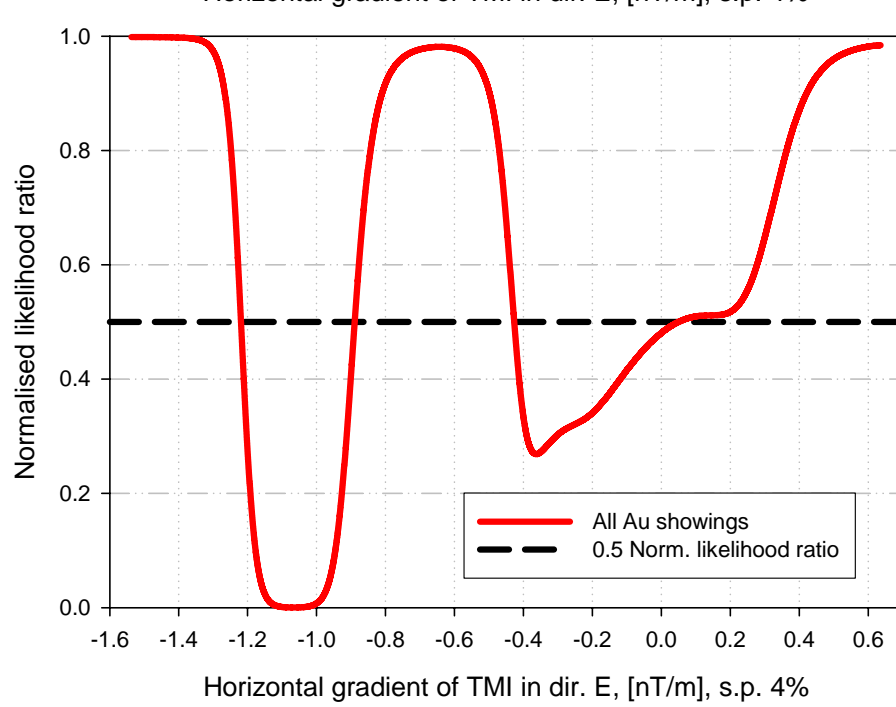
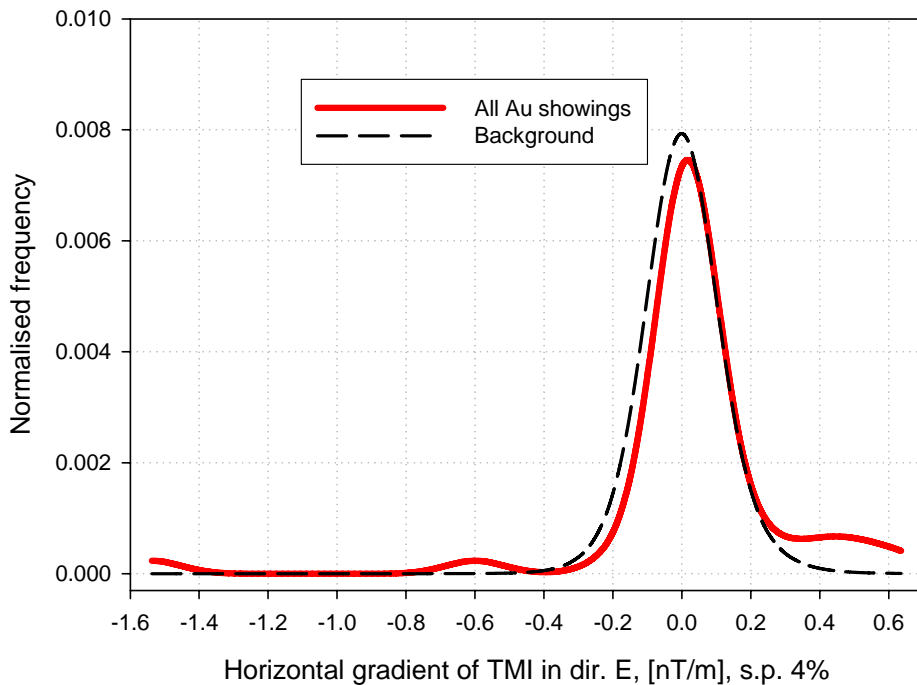
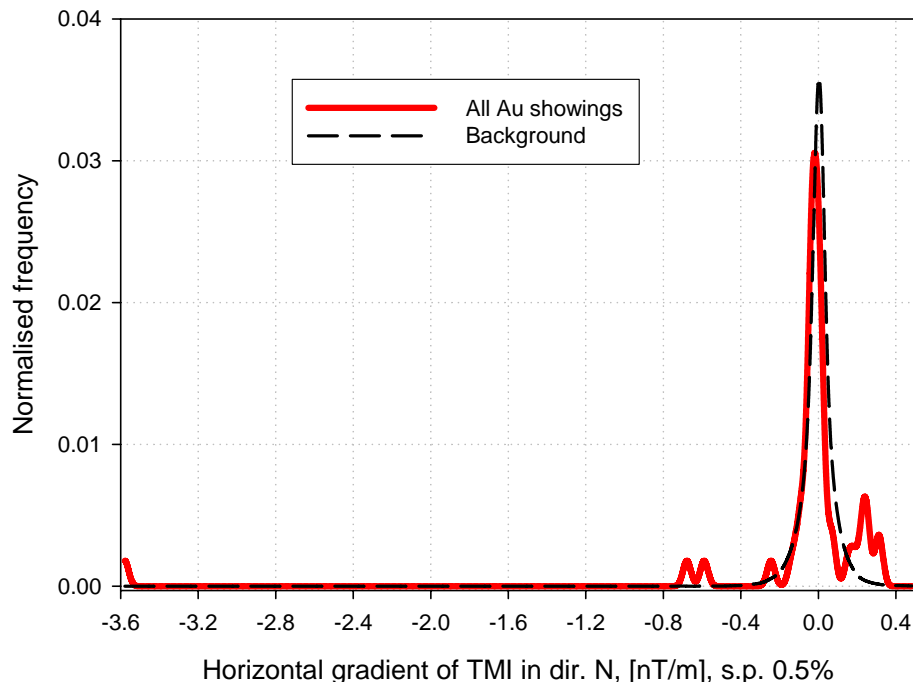
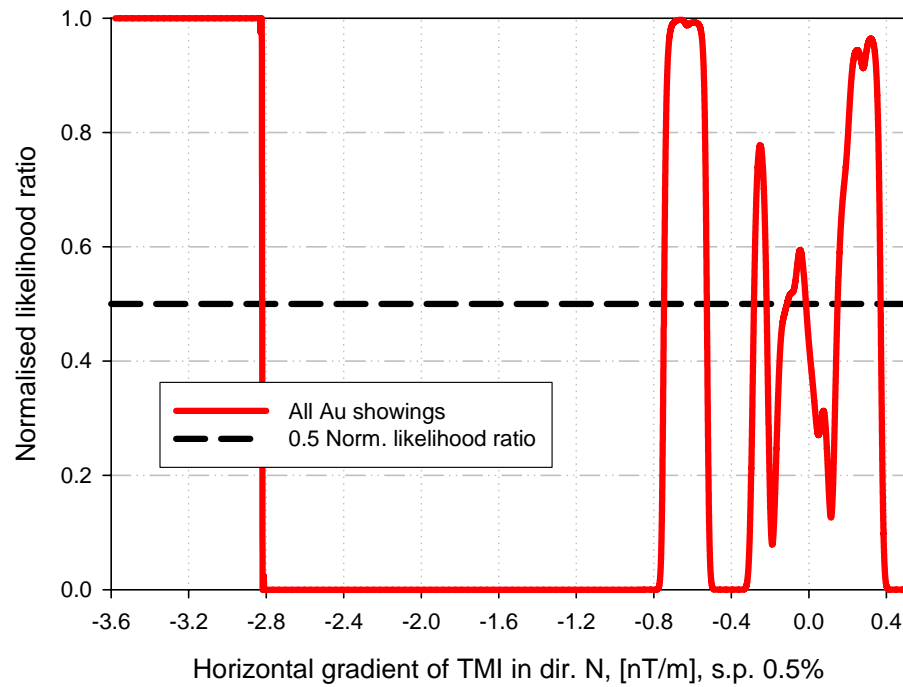


**Figure C78.** Horizontal gradient in east direction of TMI spread parameter 4% – Regional aeromagnetic data from GEUS.

Horizontal gradient of TMI in dir. N, gridcells 200 m  
spread parameter 0.5%



Horizontal gradient of TMI in dir. N, [nT/m], s.p. 0.5%



Horizontal gradient of TMI in dir. N, [nT/m], s.p. 0.5%

**Figure C79.** Horizontal gradient in north direction of TMI spread parameter 0.5% – Regional aeromagnetic data from GEUS.

Horizontal gradient of TMI in dir. N, gridcells 200 m  
spread parameter 2%

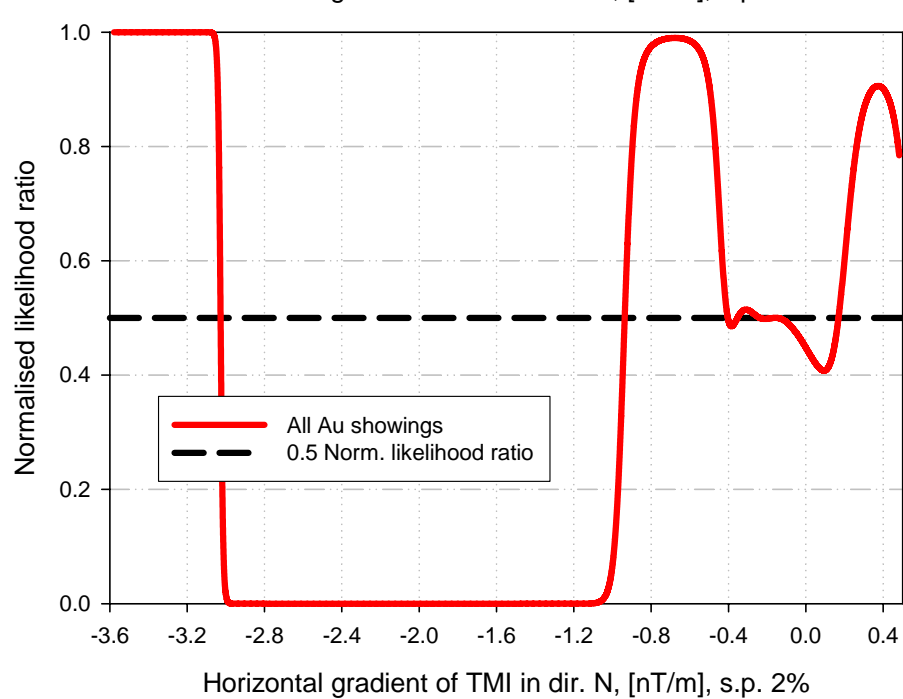
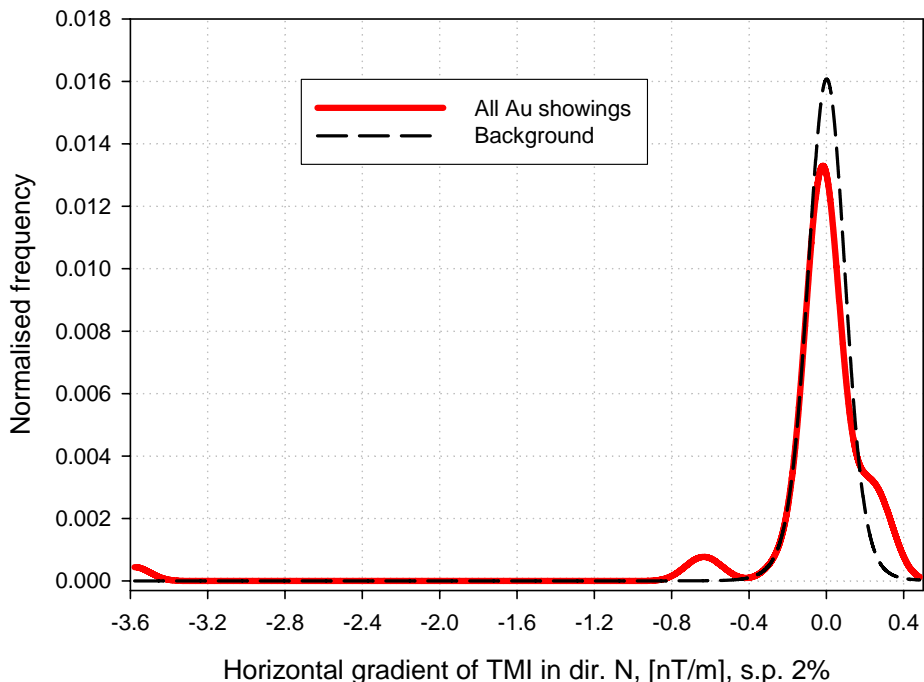


**Figure C80.** Horizontal gradient in north direction of TMI spread parameter 2% – Regional aeromagnetic data from GEUS.

Horizontal gradient of TMI in dir. N, gridcells 200 m  
spread parameter 4%

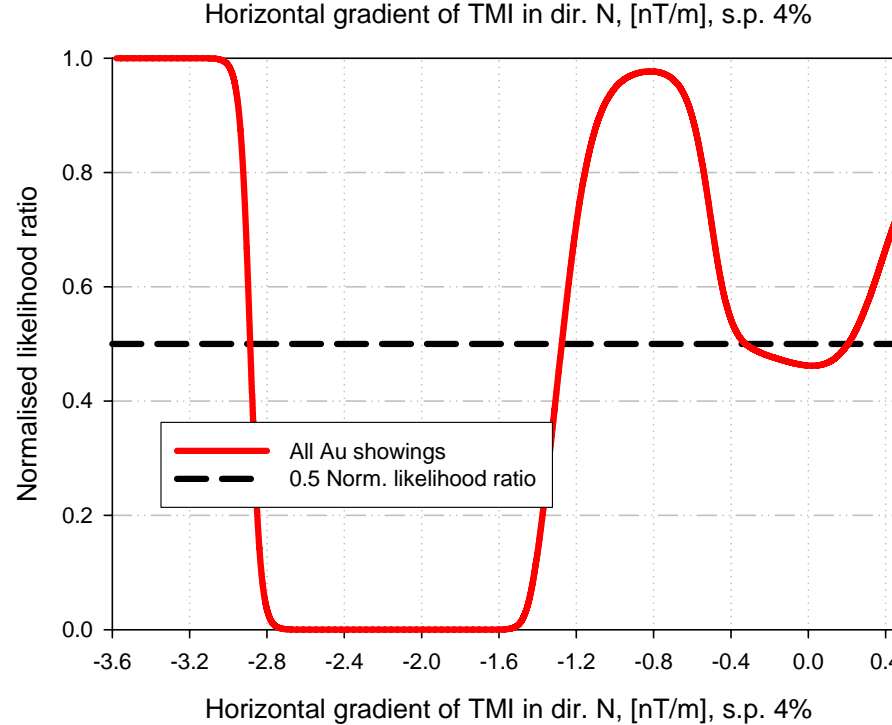
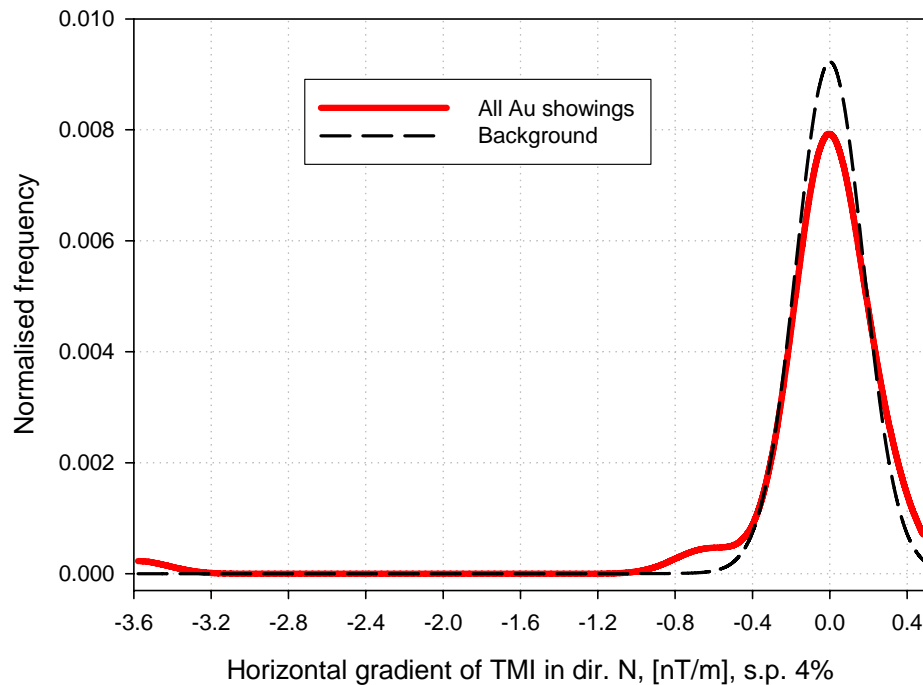


**Figure C81.** Horizontal gradient in north direction of TMI spread parameter 4% – Regional aeromagnetic data from GEUS.

Horizontal gradient of TMI in dir. NW, gridcells 200 m  
spread parameter 0.5%

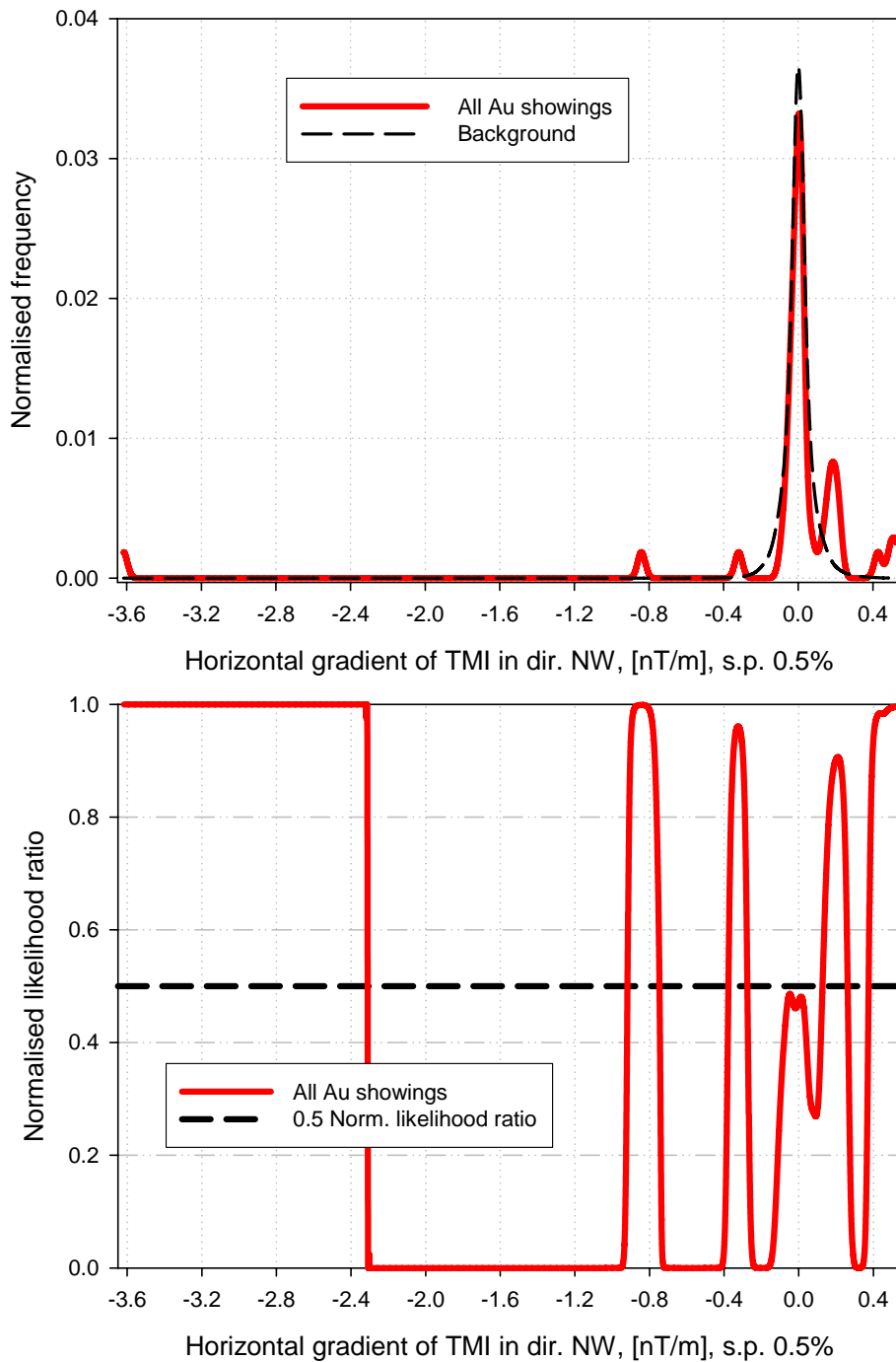


**Figure C82.** Horizontal gradient in northwest direction of TMI spread parameter 0.5% – Regional aeromagnetic data from GEUS.

Horizontal gradient of TMI in dir. NW, gridcells 200 m  
spread parameter 2%

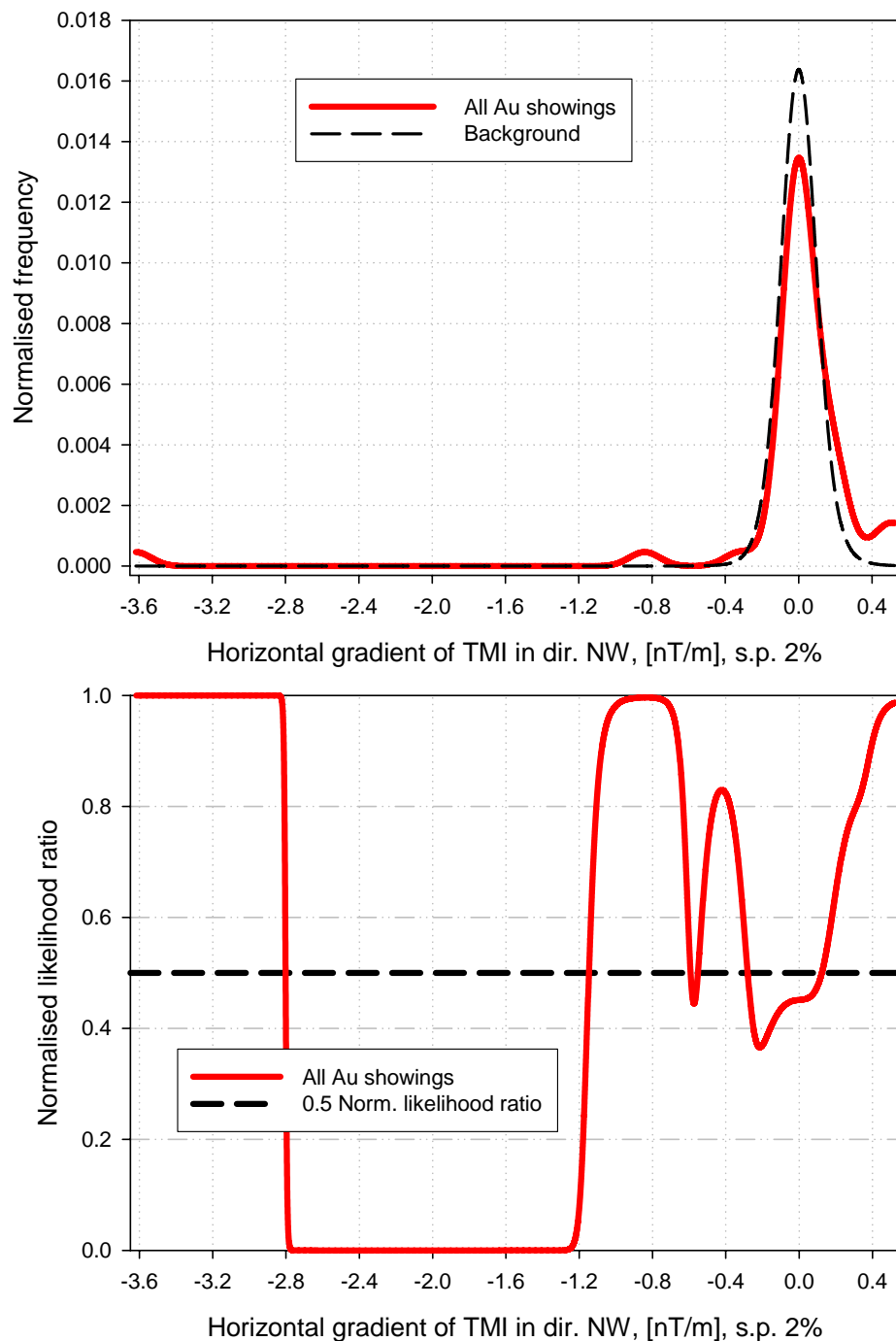


**Figure C83.** Horizontal gradient in northwest direction of TMI spread parameter 2% – Regional aeromagnetic data from GEUS.

Horizontal gradient of TMI in dir. NW, gridcells 200 m  
spread parameter 4%

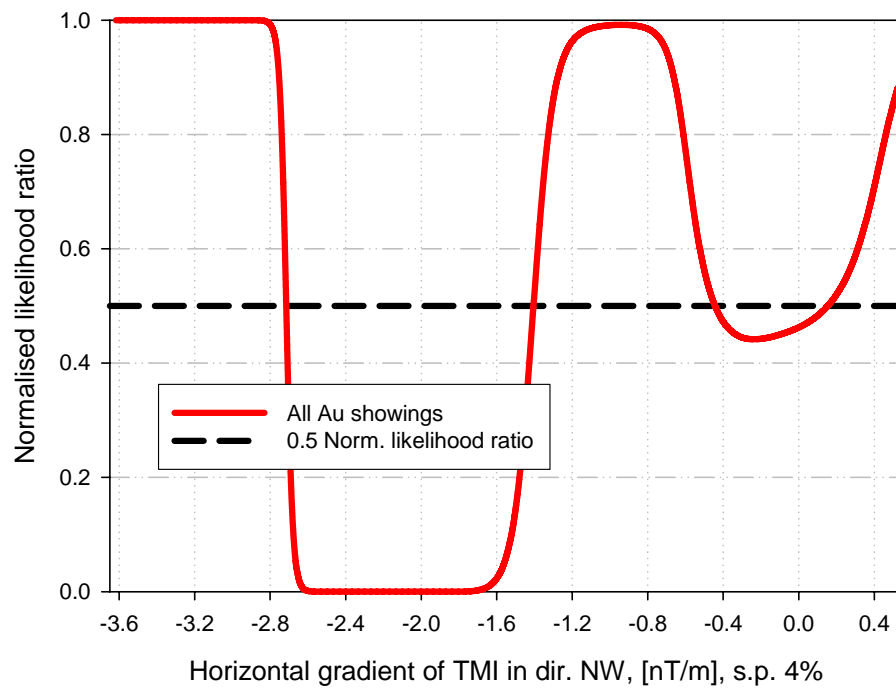
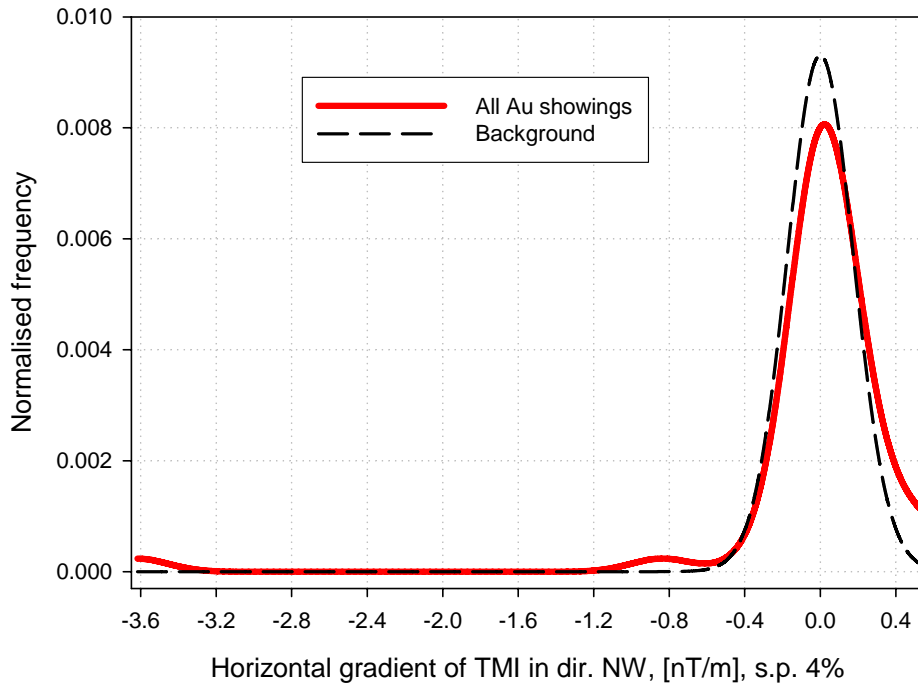


**Figure C84.** Horizontal gradient northwest direction of TMI spread parameter 4% – Regional aeromagnetic data from GEUS.

Horizontal gradient of TMI in dir. SE, gridcells 200 m  
spread parameter 0.5%

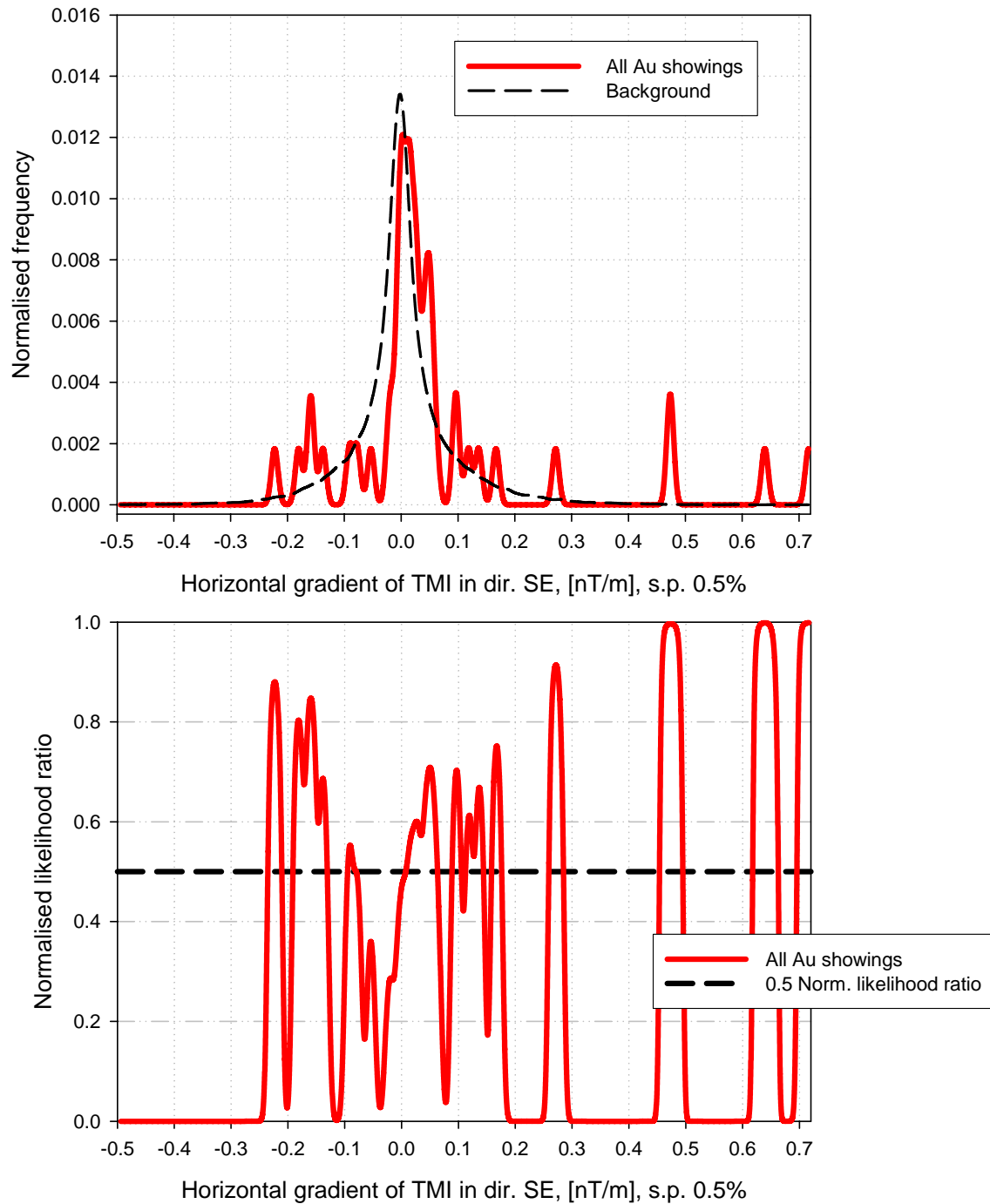


**Figure C85.** Horizontal gradient in southeast direction of TMI spread parameter 0.5% – Regional aeromagnetic data from GEUS.

Horizontal gradient of TMI in dir. SE, gridcells 200 m  
spread parameter 2%

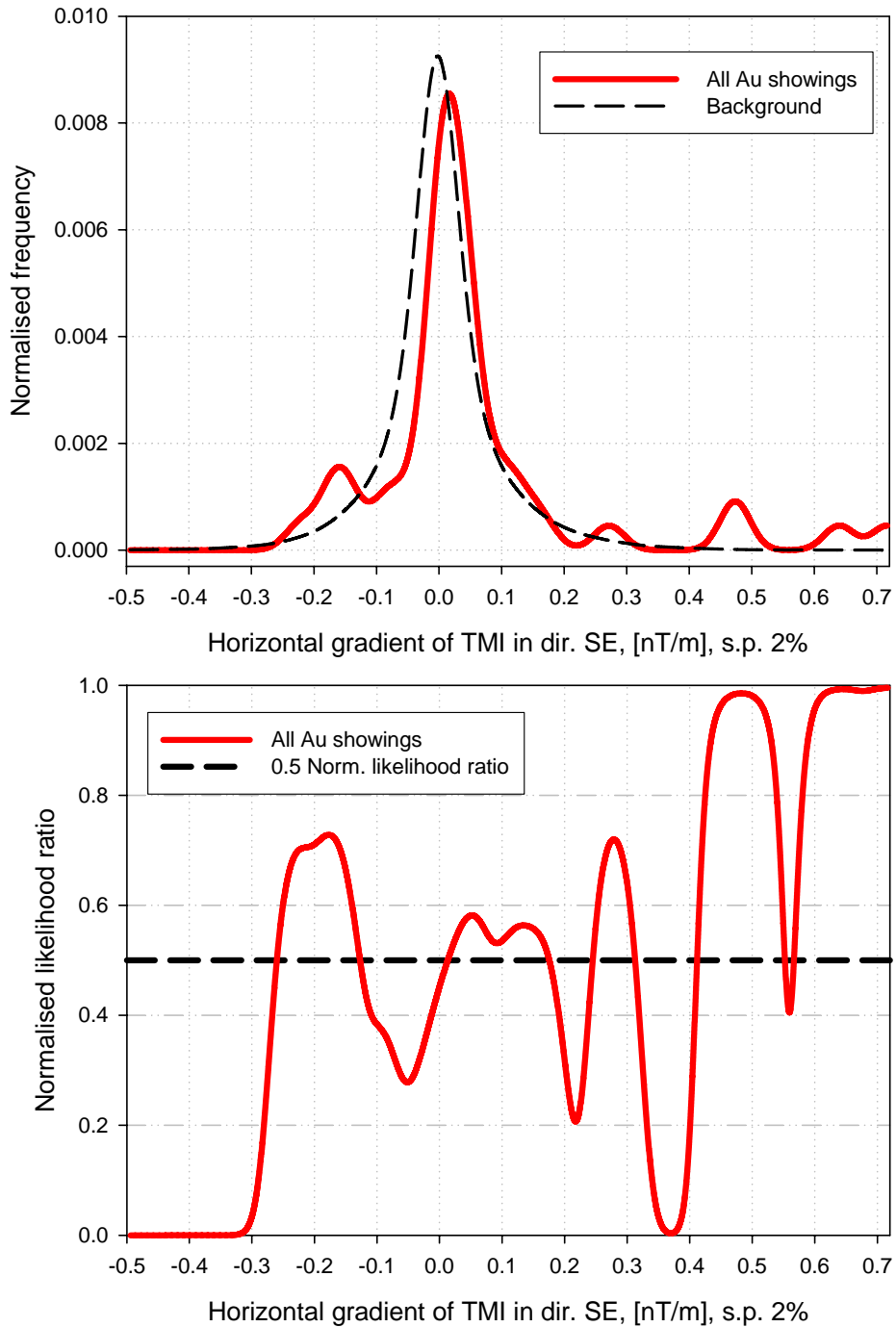


**Figure C86.** Horizontal gradient in southeast direction of TMI spread parameter 2% – Regional aeromagnetic data from GEUS.

Horizontal gradient of TMI in dir. SE, gridcells 200 m  
spread parameter 4%

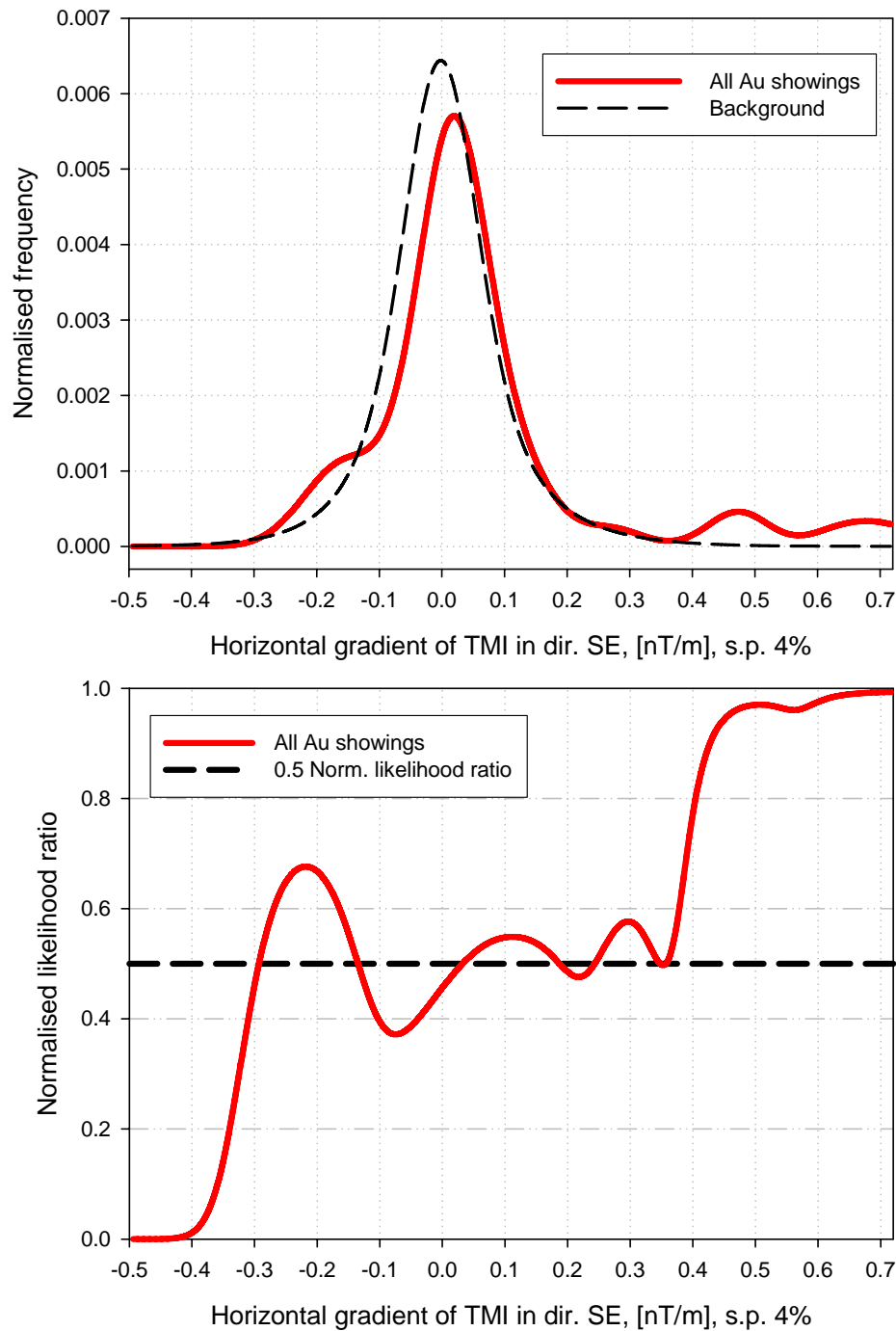


**Figure C87.** Horizontal gradient in southeast direction of TMI spread parameter 4% – Regional aeromagnetic data from GEUS.

## **Appendix D. Predictive potential map for Au showings in the Nuuk region**

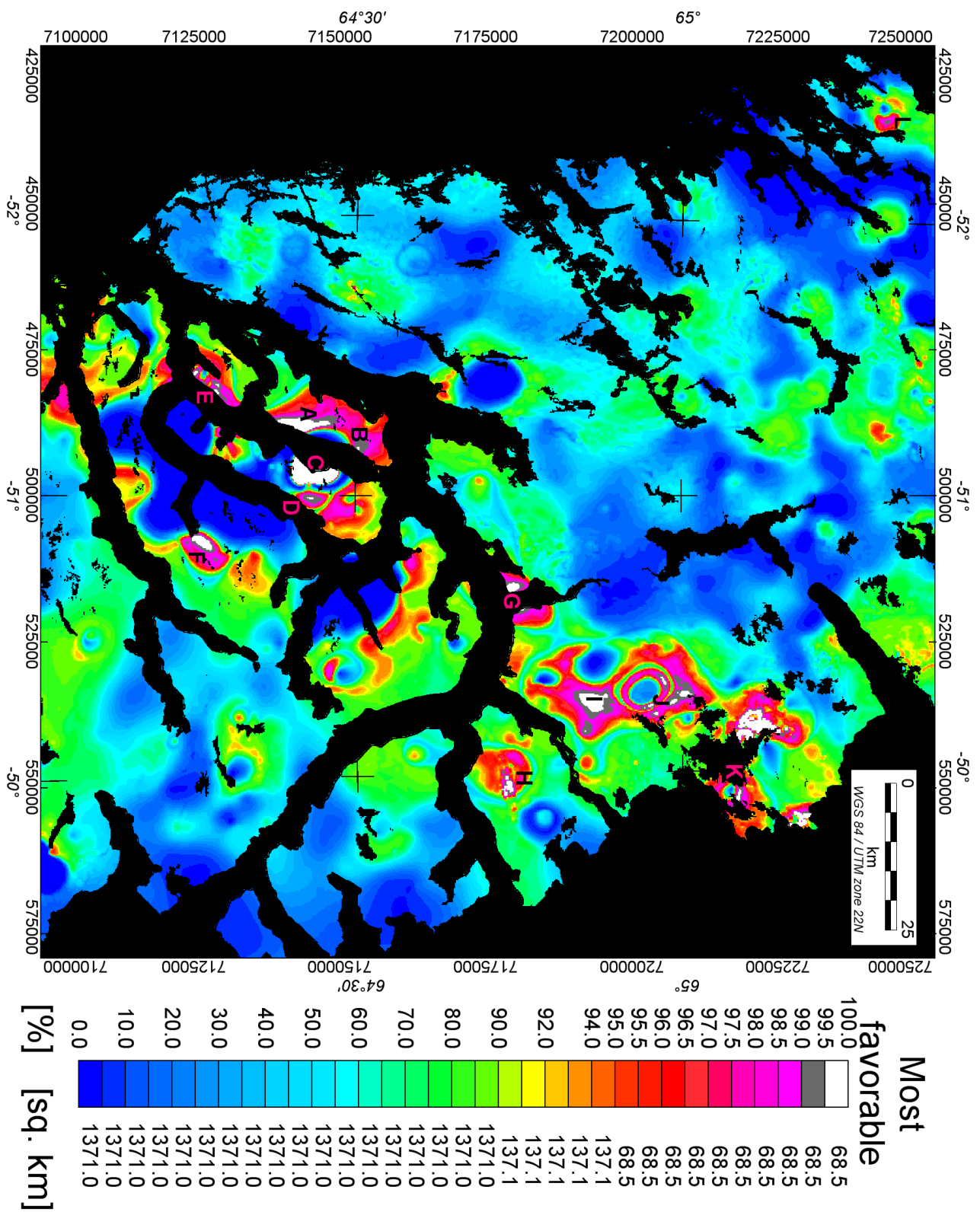


**Figure D1.** Predictive potential map for gold showings in the Nuuk region based on 45 known gold showings and 12 different regional geoscientific data themes: seven geochemical and five geophysical. Individual areas of highest probability for gold (shown in white) are marked with letters. The white areas represent the  $68.5 \text{ km}^2$  most favourable area, grey colouring the next  $68.5 \text{ km}^2$  most favourable area. The letter labels A to L in the figure are referred to in the report.

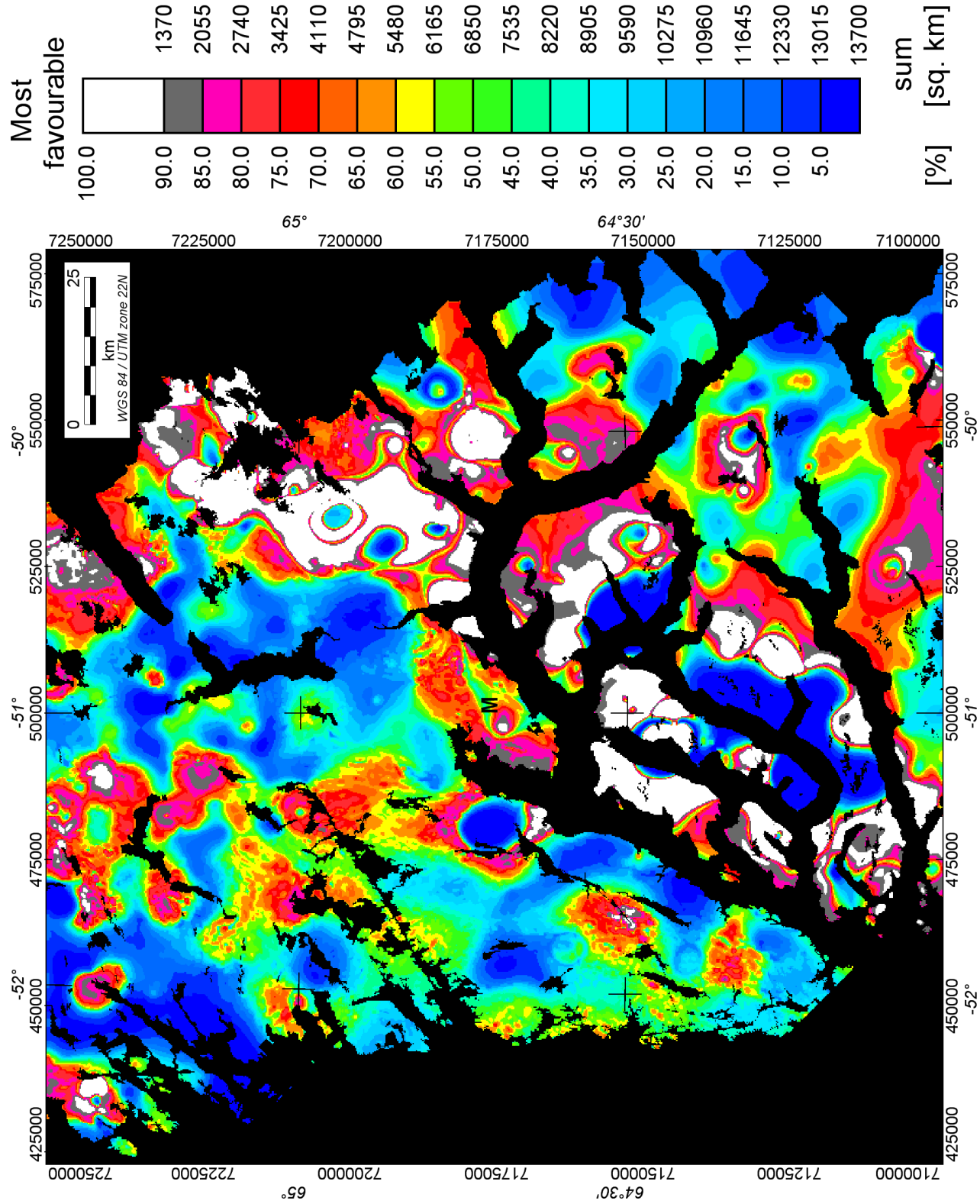


**Figure D2.** Predictive potential map for Au showings in the Nuuk region with the 10% most favourable area ( $1370 \text{ km}^2$ ) in white colour. The map is based on the same data as the map in Fig. D1. The letter label M in the figure is referred to in the report.